Novel Regulators of Prostate Cancer Stem Cells and Tumor Aggressiveness

Eugenio Zoni

Novel Regulators of Prostate Cancer Stem Cells and Tumor Aggressiveness
2016, Eugenio Zoni

ISBN : 978-90-9029652-4

Printing of this thesis was kindly sponsored by Astellas, Sanofi-Aventis and Boehringer Ingelheim.

Cover Image: human prostate cancer cells overexpressing miR-25 (Zoni E. et al., 2015)
Printed by: Gildeprint, Enschede

Novel Regulators of Prostate Cancer Stem Cells and Tumor Aggressiveness

Proefschrift

ter verkrijging van de graad van Doctor aan de Universiteit Leiden, op gezag van Rector Magnificus prof.mr. C.J.J.M. Stolker, volgens besluit van het College voor Promoties te verdedigen op donderdag 2 juni 2016 klokke 13.45 uur

door

Eugenio Zoni

geboren te Monza, Italië
in 1986

Promotores:

Promotor:	Prof. Dr. R.C.M. Pelger
Co-Promotor:	Dr. G. van der Pluijm

Promotiecommissie:

Prof. Dr. R. C. Hoeben

Dr. A-M. Cleton-Jansen

Prof. Dr. G. W. Jenster (EMC, Rotterdam)

Prof. Dr. D. Heymann (University of Sheffield)

The research described in this thesis was performed at the department of Urology of Leiden University Medical Center and was financially supported by the FP7 Marie Curie ITN grant n°264817—BONE-NET and the Dutch Cancer Society under grant agreement UL2015-7599 KWF.

Ignoranti quem portum petat nullus suus ventus est.

Seneca, Letter LXXI, AD 65

To my parents

TABLE OF CONTENTS

1

General Introduction

1. General Properties of Cancer

Cancer is considered one of the leading cause of morbidity and mortality worldwide, with 14 million new cases and 8.2 million cancer-related deaths registered in 2012 (1). The 5 most common cancers diagnosed in women in 2012 were breast, colorectal, lung, cervix and stomach cancer while in men these include lung, prostate, colorectal, stomach and liver cancer.

Carcinogenesis is a complex multi-step process that usually proceeds over several years and starts from one single cell. It progressively drives normal cell evolution into a cell with an increasingly abnormal neoplastic phenotype. This process is the result of a combination of genetic and epigenetic factors determined by individual variability caused by hereditary predisposition, life style and other variables like environmental influences, infectious agents, nutritional factors, hormonal and reproductive factors, and exposure to physical, chemical and biological carcinogens (2). Tumor formation and progression is driven by a sequence of essential alterations in cell physiology, cell homeostasis, randomly occurring mutations and epigenetic alterations of DNA. These events affect genes controlling different processes, such as cell proliferation, differentiation and survival, and bring cancer to acquire different malignant capabilities that together lead to malignant growth. The genetic abnormalities that contribute to cancer pathogenesis generally involve two main mechanisms: the inactivation of negative mediators of cell proliferation (tumor suppressor genes) and the activation of positive mediators of cell proliferation (proto-oncogenes) (3).

The definition of cancer, as established nowadays by the last advances in the tumor biology, includes multiple characteristics and aspects, that surprisingly are already present in the etymology of the word itself. The word “Cancer” originates from the ancient Greek word **“**καρκίνος” (*Karkìnos*, “crab”) credited to the Greek physician Hippocrates (460-370 BC). This word was probably chosen to describe the similarities of solid tumors with swollen veins and spreading projections reminding the shape of a “crab”. Strikingly, this description includes exactly all the elements that the modern biology of tumors ascribe to cancer; a primary tumor mass, the presence of new vessels and the spreading and invasion of the neighboring tissues. Today we learned that the biology of tumors should be investigated not only focusing on the traits of single cancer cells, but also considering the contributions of the tumor microenvironment, the interactions between tumor cells and the supportive stroma, the role of the immune system and the preferential tropism of spreading tumor cells for specific metastatic sites. These interactions are fundamental to understand the mechanisms that lead to the switch from a contained disease to the aggressive spreading and metastatic phase of tumors. These events and characteristics have been systematically outlined in 2000

by Hanahan and Weinberg as “Hallmarks of Cancer” (4) and more recently updated to include the supportive cellular and non-cellular microenvironment (5,6).

1.1. Hallmarks of Cancer

There is a certain series of events that have to occur to drive the transformation from a normal cell to a cancer cell. These events are part of a multistep process and all the steps involved in this process contribute progressively to the generation and development of cancer. The fundamental characteristics of cancer or the hallmarks of cancer represent the set of properties that a cell or a group of cells in general have to acquire to become a tumor and to interact with the surrounding stroma (5,6) (**Fig. 1**):

Sustaining Proliferative Signaling: normal cells are constantly proliferating as part of the physiological turnover present in every normal tissue. However, their proliferation is finely tuned and regulated by multiple growth factors to maintain a proliferative rate appropriate for the maintenance of the homeostasis of the tissues where they home. These growth factors are part of a paracrine signaling and their availability or signaling efficacy depends also on the capability of the “receiving” normal or tumor cells to properly react to these stimuli. In cancer, the tumor cells can instruct the supportive tumor-stroma to supply growth factors (7) or acquire a “self-sustained proliferative signaling” resulting in an autocrine and abnormal proliferative stimulation.

Evading Growth Suppressors: part of the regulation of the maintenance of the homeostasis of cells and tissue is determined by the suppression of the proliferation. Normal cells have to proliferate to generate new tissues and maintain the tissue integrity but also have to stop their growth to prevent abnormal hyper-proliferation. In cancer, tumor cells have to escape these suppressive mechanisms and have to circumvent the programs that negatively regulates cell proliferation. Typical alterations in tumor suppressor genes include the loss of function of critical “gatekeeper” of cell-cycle progression such as pRb (Retinoblastoma 1) and p53 which regulates apoptosis and is a stress responsive sensor.

Resisting to Cell Death: Programmed cell death, apoptosis, is one of the mechanisms in normal physiology that prevents cancer development and the afore mentioned p53 is one of the key player in this process. There are two main circuits that orchestrate apoptosis: one receives and process extracellular death-inducing signals (e.g. Fas and Fas ligand mechanism) and the other sense intracellular signals (intrinsic program). Both the machineries converge on the activation of a cascade of proteolytic cleavage events involving latent and effector caspases. Cancer cells have evolved a variety of

strategies to avoid this programmed death. The most common feature of tumor cells evading apoptosis is the loss of p53; other strategies include the suppression of pro-apoptotic factors (e.g. Bax, Puma, Bim) or the upregulation of anti-apoptotic genes (e.g. Bcl-2, Bcl-X_L).

Enabling Replicative Immortality: normal cells in healthy tissues are capable of pass through only a limited number of division cycles. The mechanisms that limit the number of growth-and-division cycles are essentially two: senescence (nonproliferative but viable state) and crisis (cell death). Both are linked to the length of telomeric DNA that in a cell dictates how many cycles of division are still available before the cell enters in a phase of DNA instability (i.e. crisis). It is a remarkable properties of cancer cells their ability to proliferate indefinitely, escaping from this control. One of the mechanisms that drive immortalization in tumor cells is the presence of telomerase activity, responsible for the integrity of telomeric DNA, detected in up to 90% of spontaneously immortalized cells.

Inducing Angiogenesis: in every normal tissue, nutrients and oxygen are provided by a fully functional network of vessels, responsible also for the elimination of wastes and other products of the metabolism. In normal physiology, in an adult organism these vessels remain mostly stable and quiescent. In malignant tumors, vessel remodelling and new vessel formation occurs after the so-called “angiogenic switch” which cause the normal quiescent vasculature to sprout and produce new branches (neovascularization). This abnormal angiogenesis produces vessels that are histologically different from those formed during the physiological process. Moreover, highly invasive tumor cells can form fluid-conducting channels in a process defined as “vasculogenic mimicry” (8). The new vessels in the tumor have an aberrant morphology and are characterized by abnormal level of endothelial cells proliferation and apoptosis. In addition, the leakiness that characterize these vessels is one of the major effectors for the low efficiency in the delivery of therapies specifically to the tumor.

Activating Invasion and Metastasis: the invasion of the surrounding tissues, the intravasation in blood and lymphatic vessels and the formation of distant metastasis represent one of the critical problem in tumor progression. In this context transformed epithelial cells acquire a motile mesenchymal phenotype in a process referred to as “epithelial to mesenchymal transition” (EMT) (9). However, cancer cell migration is not restricted to singly migrating cells. Different patterns of cell migration include single-cell migration, multicellular streaming and collective cell migration, (reviewed in (10)). The impact of this process during the onset of metastatic spreading and its relevance in the

establishment of therapy resistance will be discussed more in details in the next paragraphs.

Interaction with the tumor stroma: tumor cells do not behave independently from the rich microenvironment where they are localized and that represents an important component during tumor initiation, growth and progression. During cancer progression the stroma co-evolves with the tumor and create a dynamic signaling network of paracrine signals that promotes cancer. The different stromal components involved in this process include: cancer-associated fibroblasts (CAFs), pericytes, endothelial cells, immune cells and the extracellular matrix (reviewed in (6)).

Metabolic reprogramming: In addition to the above mentioned specific characteristics, tumor cells can also adapt their metabolism and switch to the so called “aerobic glycolysis” converging their metabolism largely to glycolysis (i.e. Warburg-effect) (11). This is one of the basis of the non-invasive visualization of tumors based on positron emission tomography (PET) with radiolabelled analog of glucose as reporter. In proliferating (cancer) cells the mitochondrial metabolism is reprogrammed toward macromolecular synthesis to sustain multiple cell divisions, (reviewed in (12)). Moreover, oncogenic mutations in metabolic enzymes such as the cytosolic $NADP^+$-dependent isocitrate dehydrogenase 1 gene (IDH1) and the mitochondrial homolog IDH2 responsible for converting α-ketoglutarate to 2-hydroxyglutarate (2HG), a metabolite found only in reduced amounts in mammalian cells under normal conditions have been reported (12,13). Interestingly this has also effects on epigenetic mechanisms, resulting in altered histone methylation marks, hypermethylation at CpG islands and dysregulated cell differentiation(12).
Moreover, it is important to note the pro-inflammatory and immunosuppressive properties of cancer cells. Inflammation can sustain proliferative signaling and inhibiting cell death, activate extracellular matrix-modifying enzymes and support invasion and angiogenesis (14,15). Tumor cells can also secrete immunosuppressive factors or recruit immunosuppressive cells, blocking the action of cytotoxic lymphocytes or recruit tumor associated macrophages that can enhance tumor progression and metastasis and suppress antitumor immunity (16-18).

All the aspects discussed above depend, to a large extent, on genomic alterations in neoplastic cells. Different cells can gain different alterations and the combination of several alteration together will produce a cancer cell, capable of outgrow and gain a local dominance over other neoplastic and/or normal cells. In this perspective, tumor progression is characterized by the expansion of different heterogeneous clones. In this process, only those clones capable of gaining all the hallmarks of cancer will succeed in

generating a malignant tumor. The issue of intra-tumor and inter-tumor heterogeneity and its impact on resistance to current therapies will be discussed in the next paragraphs.

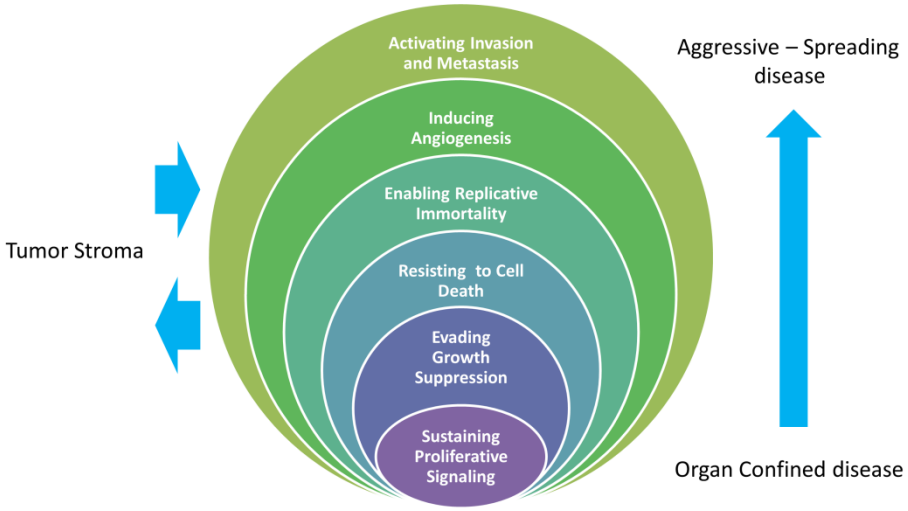

Figure 1. Schematic representation of the hallmarks of cancer, their correlation with cancer progression and reciprocal interaction with the tumor stroma.

1.2. Tumor Heterogeneity

There are two main levels of complexity in tumor heterogeneity. If we consider the tumor mass as an independent entity, one level consists of the differences *between* different cancer types or different patients affected by the same cancer and is defined as *inter-tumor heterogeneity* (**Fig. 2**). Another level of heterogeneity encompasses the cellular differences *within* the same tumor (e.g. multiple cell clones with different properties, dispersed within the same tumor mass of the same patient) and is defined as *intra-tumor heterogeneity* (**Fig. 2**). Despite the fact that, overall, the evolution and progression of these tumor can be similar (e.g. onset of primary tumor, progression from benign to malignant growth, neo-angiogenesis, invasion of surrounding tissues, and formation of distant metastasis) there are intrinsic differences that distinguish one cancer from the other and, within the same cancer family, one cancer subtype to another (e.g. hormone-naïve or androgen-independent prostate cancer). These differences are part of the so-called inter-tumor heterogeneity and reflect the differential responsiveness to specific therapeutics and not to others. Additionally, the tropism for specific metastatic sites (e.g. osteotropism in prostate cancer), is also characteristic of certain malignancies and can be ascribed to the inter-tumor heterogeneity.

The second level of complexity comprises intra-tumor heterogeneity. As already discussed, cancer formation is a multistep process that starts from one single cell; on the other hand, tumors are tissues and therefore are constituted by a variety of different tumor- and other-cell types. As established in the last decade by high-resolution genome-wide studies, the formation and progression of tumors is characterized by a continuous “Darwinian-like” evolution of branches of specific clones (19). This process of “clonal evolution” results also in the construction of a supportive tumor microenvironment, which is continuously being remodelled during the tumor progression. Different cell types contribute to increase the complexity and the heterogeneity of this environment. As previously mentioned, these cell types include, among the others, also non-malignant cells, such as immune and inflammatory cells, endothelial cells, pericytes, and cancer-associated fibroblast. For the purpose of this thesis we will mainly focus on the cancer cells and discuss the different cell types and subpopulation that are represented within the tumor. Macroscopic tumors are constituted of different subpopulation of malignant cells. Depending on environmental stimuli and stochastic processes, or depending on their alterations, such as mutations and epigenetic changes, these clones can acquire a dominant phenotype with clinically relevant characteristics (e.g. resistance to therapy). In this respect, the intra-tumor heterogeneity is one of the relevant problems in the identification of therapeutic strategies capable to eradicate completely all the different cancer cell subpopulations

and clones that maintain the cancer. Similarly, this also has an impact on studies that approach tumor biology without distinguishing the different cell types dispersed within the tumor.

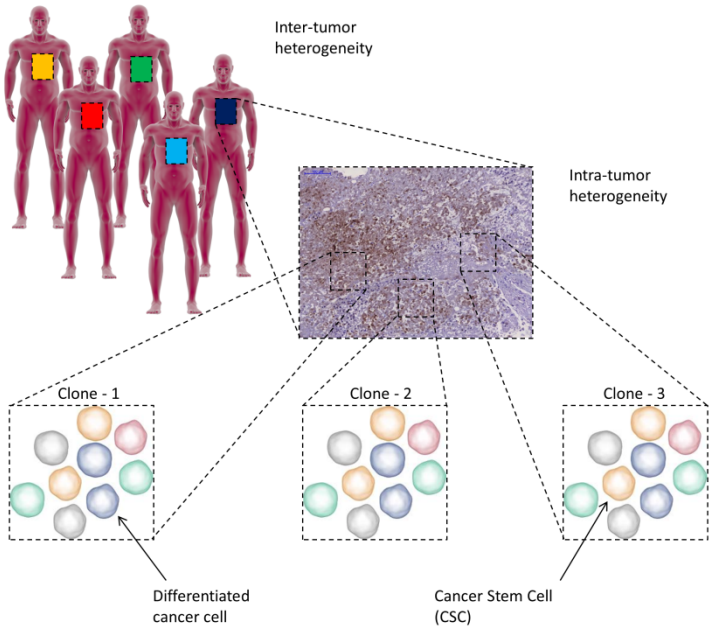

Figure 2. Schematic representation of inter-tumor and intra-tumor heterogeneity. Adapted from [19].

Molecular- and genetic-profiles of cancerous “bulk” tissues indeed cannot discriminate between the aggressive subsets of cancer cells responsible for tumor maintenance, growth & the development of therapy resistance and less aggressive, more differentiated cancer cell subpopulations. This raises the question whether the different clones and subpopulations present in the tumor are properly represented also in a transcriptional analysis between “bulk” tumor and “normal” tissues. One of the aspects of tumor heterogeneity, that has revolutionized the tumor biology in the last years, is indeed the discovery of a subpopulation of cancer cells with tissue stem-like properties, the cancer stem cells (CSCs). The contribution of these cells to the tumor formation and maintenance, metastasis, therapy resistance and their clinical relevance for the identification of new therapeutic strategies will be discussed later.

2. Anatomy of the Prostate

The prostate is a walnut-sized exocrine gland, well encapsulated and positioned in the pelvic cavity inferior of the bladder (it surrounds the first tract of the urethra) and anterior of the rectum (20) (**Fig. 3**). The function of the prostate is to secrete a slightly alkaline milky white fluid, that constitutes about the 30% of the volume of the semen and that contains carbohydrates, phospholipids, and enzymes (e.g. prostate specific acid phosphatase (PAP) and prostate specific antigen (PSA)) (21).

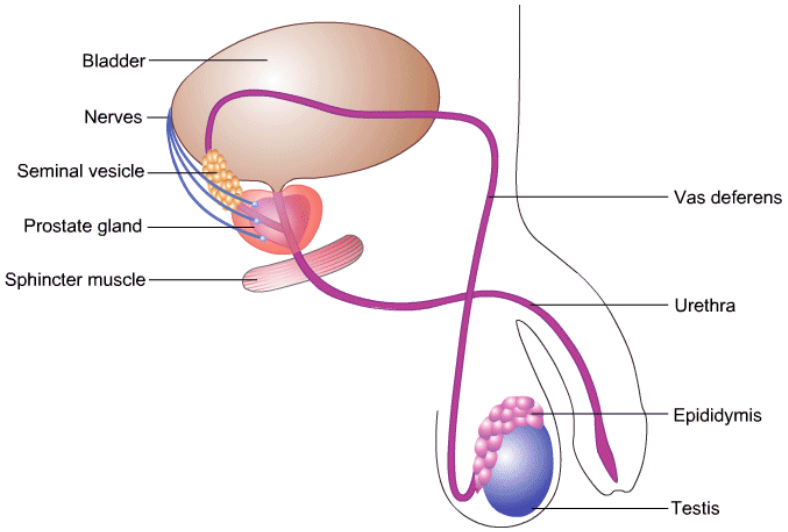

Figure 3. Anatomy of the prostate within the male reproductive system.
Source: http://www.aboutcancer.com/prostate

The prostate can be divided in four "zones" (mainly used in pathology, (22,23)) (**Fig. 4**) or in four lobes (mainly used in anatomy):

1) *Central zone*: it surrounds the ejaculatory ducts and constitutes about 20% of the whole gland and it presents large and irregular ducts. Approximately 1 – 5% of prostate cancer originates from this region and tend to invade the seminal vesicles (24). This part roughly corresponds to the median lobe.
2) *Peripheral zone*: accounts for the majority of the gland and it originates from the mesoderm. Up to 70% of prostate cancer originates from this part. Roughly corresponds to the posterior lobe.
3) *Transition zone*: it surrounds the prostatic urethra and it originates from the endoderm. About 20% of prostate cancer originates from this zone which is also responsible for the formation of benign prostatic hyperplasia (BPH, discussed later (25)). Roughly corresponds to the anterior lobe.
4) *Anterior fibromuscular stroma*: it consists of muscular and fibrous tissue.

The "fourth lobe" is named lateral and spans all zones.

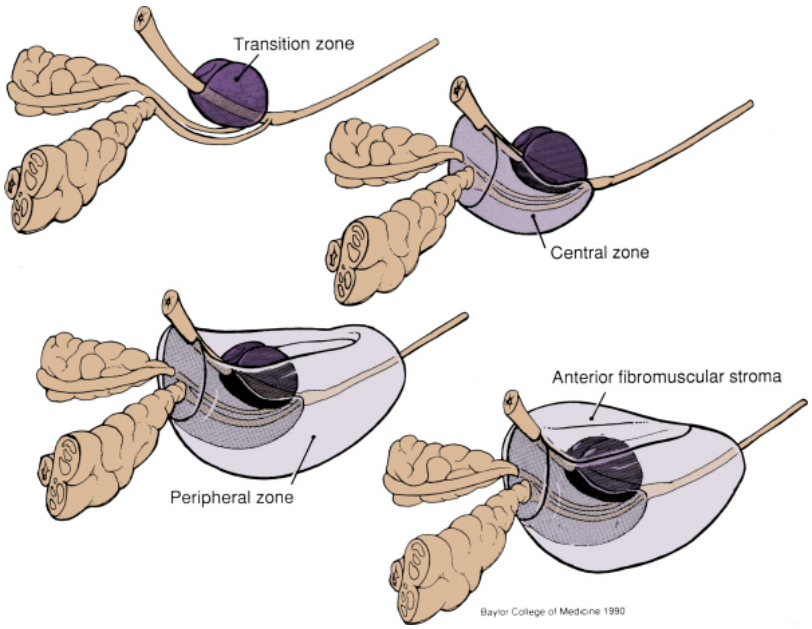

Figure 4. Structure of the prostate. The four zones are indicated: transition zone, central zone, peripheral zone and anterior fibromuscular stroma. From Baylor College of Medicine 1990.

The growth of the prostate is regulated by androgens like testosterone. Testosterone is mainly produced by Leydig cells in the testis and to lower extent in the adrenal cortex

and its synthesis is controlled by luteinizing hormone (LH) and the follicle stimulating hormone (FSH). The secretion of LH from the pituitary gland is regulated by the hypothalamic luteinizing hormone-releasing hormone (LHRH) (26). When testosterone is converted to 5α-dihydrotestosterone (DHT) by 5α-reductase, it can stimulate the growth of the prostate (for example during puberty) (27). DHT in the blood is associated with the sex hormone-binding protein (SHB), responsible for its transportation into the vasculature and to the target cells, where androgens bind and activate the androgen receptor (AR). Activation of the AR by androgens results in the transcription of androgen-responsive genes like PSA or the prostate-specific gene TMPRSS2 (28,29).

2.1. Architecture of the prostate

The prostate has a glandular structure characterized by several ducts constituted by three major cell types: luminal, basal and neuroendocrine cells (30) (**Fig. 5**). These cells are different in morphology, function and significance for tumorigenesis.

Luminal cells: these cells are located along the glandular lumen and have a secretory function. They are terminally differentiated and express specific differentiation markers such as AR and cytokeratin 8/18 (31,32). Additionally, they are androgen regulated and produce PSA and PAP. Cells with self-renewal properties have been identified within the luminal compartment in mice and humans (33,34) and proposed as the cell-of-origin of castration resistant prostate cancer (CRPC, discussed later).

Basal cells: these cells are located between the luminal cells and the basal layer that separates the epithelium from the stroma, which consists of fibroblasts, blood vessels, nerve cells, smooth muscles cells, infiltrating immune cells and connective tissue. The contribution of these cells and components to prostate cancer is crucial, especially during the progression of the disease (35,36). Basal cells are proliferative and characterized by the expression of cytokeratin 5 and 14 (37,38). Experimental evidence have shown the presence of stem-like cells within the basal compartment (39,40) which could maintain basal cells or differentiate into luminal cells and neuroendocrine cells (41,42).

Neuroendocrine cells: these cells are dispersed within the basal layer and are androgen independent; they express different neuropeptides like serotonin and chromogranin A (43). It is hypothesized that their function is to participate in the differentiation of the normal prostate and they also play a role in tumorigenesis (44,45).

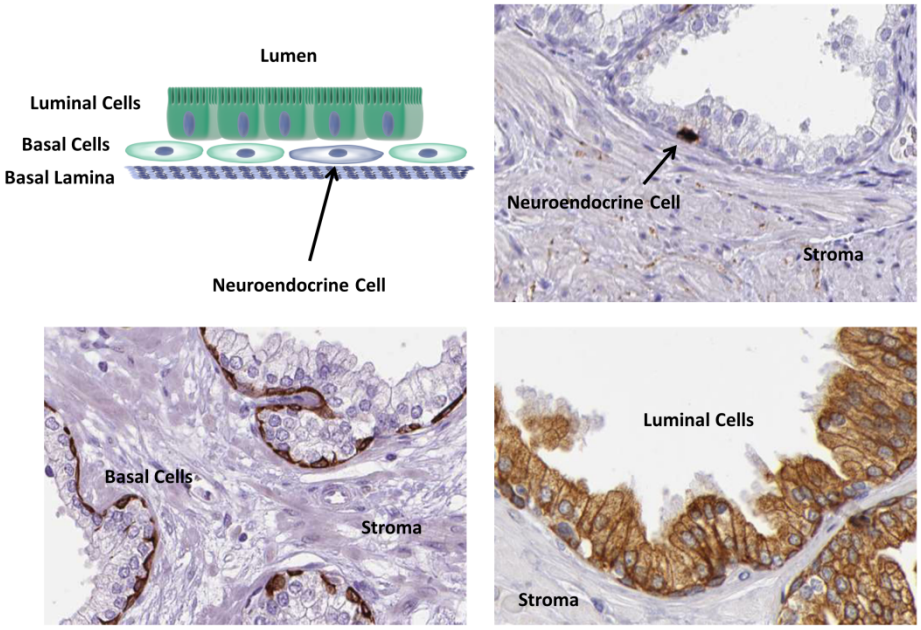

Figure 5. Histology of the prostate. The epithelial layer that characterizes the prostate consists of basal cells (Cytokeratin 5 positive, bottom left), separated from the stroma by the basal lamina; neuroendocrine cells, dispersed within the basal cells (Chromogranin A positive cells, top right) and luminal cells (Cytokeratin 18 positive cells, bottom right). Source: www.proteinatlas.org.

3. Diseases of the Prostate

Due to its high blood perfusion and connection with the urethra, the prostate gland is susceptible to acute and chronic bacterial infection (i.e. prostatitis) typically treated with antibiotics (46). Moreover, during aging, the prostate increases physiologically in size and this can result in benign prostatic hyperplasia (BPH), classified in two types: histologic BPH, characterized by microscopic evidence of epithelial and stromal hyperplasia, and macroscopic BPH, characterized by an enlargement of the prostate (25). Three main theories have been proposed to explain the etiology of BPH (47): 1) the enlargement of the prostate could be caused by a shift in the prostatic androgen metabolism occurring with age, which lead to abnormal accumulation of dihydrotestosterone; 2) changes in epithelial-stromal interaction induce prostatic growth; 3) an expansion in epithelial stem cells. Clinical manifestations of an enlargement of the prostate include lower urinary tracts symptoms such as bladder outlet obstruction and chronic urinary retention which results in additional complications (e.g. infections). Treatment options include pharmacologic agents employed to relax the prostatic smooth muscle (alpha-blockers, 5-alpha reductase

inhibitors) or transurethral resection (48,49). Additionally, there are some similarities between BPH and prostate cancer as both require androgens for growth and development and therefore might respond to antiandrogen treatments (50).

4. Prostate Cancer

4.1. Epidemiology

Prostate cancer is the second leading cause of death from cancer in males in western countries with 220,800 new cases estimated for 2015 (51). The incidence of prostate cancer increases with age (prostate cancer is a rare event in men under the age of 50), and it is higher in the western world compared to less developed countries, due to differences in life-style, eating habits, environmental agents and ethnicity (52). However, there is homogeneity in the age-dependent prevalence of prostate cancer in different countries.

4.2. Prostate Cancer Initiation

Prostate cancer is considered a multifocal disease. The primary tumor often presents multiple histologically independent foci that can be genetically identified for their properties and are relevant for understanding the distinction between latent and clinical disease (30). Although prostate cancer is commonly considered a disease of older men, analysis of specimen collected from younger healthy individuals revealed the presence of histologic foci of prostate cancer also in men in their 20s to 40s, suggesting an early onset of cancer (53). In the majority of the cases, these multifocal lesions will result in a latent disease that will not progress to clinically detectable and relevant prostate cancer. This can be explained by two hypothesis: there is a critical difference between the initiation of the pathogenic program of latent and clinical prostate cancer, or the critical events that are needed to generate a clinical disease do not occur in the latent foci. In the initiation phase, the normal prostate gland present a ductal-acinar histology, characterized by an organized epithelium with luminal secretory cells, basal and neuroendocrine cells and a basal lamina (**Fig. 5**). This organized structure is altered during the “initiation stage”, where histological changes of the luminal epithelium occur and lead to luminal epithelial hyperplasia defined as prostatic intra-epithelial neoplasia (PIN) (54). PIN lesions are classified between low-grade and high-grade, they are multifocal and, at this stage, the cancer is contained by the intact basal layer which prevents the invasion of the surrounding tissues. The morphological integrity of the glandular structures prevents also an increased release of PSA into the blood stream. For this reason PIN lesions are usually detected by biopsy and not by blood test as they don’t produce increased PSA levels (55). High-grade PIN

lesions are characterized by high expression of proliferation markers (56) and by the histological presence of basal cells (30).

A number of genomic alterations such as copy number variations and chromosomal rearrangements (insertions, deletions) associated with prostate cancer and hereditary prostate cancer have been identified with multiple genome analysis studies (30).

Among the most common copy number alterations, those occurring at 8p21 (Nkx3.1), at 10q23 (PTEN) and at 8q24 (MYC) involve key regulatory genes (30,57-59). In addition, genome-wide association studies have shown the involvement of HPC1 and HPC2 (mapped in 1q24-25 and 17p11 respectively) in hereditary prostate cancer (60,61). The down regulation of Nkx3.1 is one of the critical events in prostate cancer initiation and is detected in up to 80% of the prostate tumors (also in PIN lesions and early invasive carcinoma). Nkx3.1 has a critical role in prostate morphogenesis and differentiation and mutant mice for Nkx3.1 develop PIN lesions that resemble closely those detected in human.

Another frequent chromosomal loss detected in a high percentage of prostate cancer cases is represented by PTEN (tumor suppressor gene). Loss of PTEN leads to hyperactive PI3K-AKT-mTOR signaling, which results in aberrant cell proliferation and metabolism (62). Recent studies have shown that the allelic loss of PTEN represents an early event in prostate carcinogenesis and correlates with progression of the disease (59). As for Nkx3.1, also loss of PTEN in mice results in PIN lesions and/or adenocarcinoma (63).

Besides the aforementioned chromosomal losses, genetic studies have identified also gene amplifications in prostate tumors. The oncogene MYC is amplified during initiation of prostate tumors and upregulation of MYC has been registered in PIN lesions (64). Similarly, transgenic mice overexpressing human MYC undergo rapid formation of PIN lesions, followed by progression to invasive adenocarcinoma (65). Another set of genetic alterations is represented by chromosomal rearrangements. Among these, the most common alteration regards the family of transcription factors (ERG, ETV1 and ETV4) and the prostate specific gene TMPRSS2 (66). The most frequent rearrangement produces the fusion gene TMPRSS2-ERG, where the N-terminally truncated ERG protein is expressed under the control of the promoter of the androgen-regulated TMPRSS2 gene (66). This alteration usually occurs in cancer initiation and is also detected as early event during cancer progression.

4.3. Prostate Cancer Detection

The oldest known case of prostate cancer diagnosed reliably by morphological and biochemical techniques dates back to 2,700 years ago (67). Schultz and co-workers

described that a well preserved skeleton of a 40 to 50-year-old Schythian king who lived during the Iron Age in the Southern Siberia (Arzhan) suffered from macroscopically visible osteoblastic and osteolytic lesions throughout the entire skeleton (67). This diagnosis is based on microscopic imaging of the lesions and detection of prostate-specific-antigen (PSA) complexed with α1-antichymotrypsin (PSA/ACT) in the extracellular matrix (ECM) proteins extracted from the compact cortical bone of the skeleton from Arzhan (68,69).

The blood test for PSA, nowadays routinely used in the clinic, has revolutionized the clinical practice over the past four decades and has represented the standard for prostate cancer detection and monitoring. PSA is a glandular kallikrenin-related peptidase produced by the gene KLK3 and its transcription is regulated by androgens which make its expression a main characteristic of the prostate epithelium (70). PSA is continuously produced by the healthy prostate. In the normal prostate, the morphological structure of the glands contains PSA tightly confined and only a reduced amount is released into the blood (0.6 ng/ml in a healthy adult male) where it exits in multiple forms: as pro-protein or mature protein and free or associated with different protease inhibitors (70). In BPH or prostate cancer, the disruption of the normal prostate architecture often results in a massive release of PSA into the blood (>100 ng/ml) that is measured almost exclusively in males with advanced prostate cancer (70). Altered PSA levels in blood are also commonly detected during the occurrence of other alterations of the prostate such as inflammation (prostatitis) and its' levels are also influenced by age. For this reason, PSA is considered as a prostate-specific marker but not a cancer-specific marker. In this perspective, two more specific and clinically-promising markers for prostate cancer detection are represented by the non-coding messenger RNA for the so called Prostate Cancer Antigen 3 (PCA3), identified in 1999 (71) and the fusion gene TMPRSS2-ERG described in 2005 (66). However, although PCA3 and TMPRSS2-ERG (also as combined biomarkers) displayed higher specificity and diagnostic accuracy for prostate cancer outcome, PSA is still the most widely used biomarker in prostate cancer diagnosis (72). Importantly, the expression of KLK3 at molecular level in the prostate epithelium and the increase of PSA level in the blood of men affected by prostate cancer are not directly correlated (73). The detection of augmented PSA level into the blood is indeed determined by an increased release of PSA from the prostatic gland as a consequence of disruption of normal prostate architecture and not by an increase of its transcription. This leads to the documented paradox that during development and progression of prostate cancer, KLK3 expression might slightly decrease (74).

The typical clinical practice for men with high PSA levels schedules biopsy to assess the possible presence of prostate cancer. The prostate tissue collected is then graded according to the Gleason scoring system introduced for the first time in the clinic

in the 1960s and recently updated in 2005 (75-77). The Gleason scale describes the primary and secondary architectural pattern of the tissue obtained from prostate biopsies and classifies tumors according to their differentiation, from 1 to 5, based on the morphological architecture of the prostate (76,78). Briefly, Gleason 1 corresponds to a transformed prostate epithelium that resembles a normal prostatic epithelial tissue; from Gleason 2 to Gleason 4, the infiltration of cells at the margin of the gland is progressively increasing; Gleason 5 corresponds to a cancerous prostate which has completely lost its epithelial structure and is filled with invading mesenchyme-like cancer cells. The final Gleason score is obtained upon mathematical addition of primary and secondary score and can range from 2 to 10 (79). In addition, the status of the primary tumor is also graded, from organ-confined to fully invasive (T1-4), with or without involvement of lymph nodes (N0 or N1) and with or without presence of distant metastasis (M0 or M1 a-c) (80). These together constitute the so called Tumor-Node-Metastasis (TNM) system of grading.

4.4. Treatment of Localized Disease

There are several options for treating prostate cancer patients with localized disease, depending on the stage and the patient condition.

As previously mentioned, due to improved screening methods, prostate cancer can be detected already at the very initial stage. Active surveillance is considered a logical approach for those men with localized prostate cancer and associated low-risk to prevent overtreatment (81-83). The clinical criteria to define an active surveillance strategy are: confined disease with T1-T2 stage, maximum PSA level of 10 ng/mL and Gleason score <7 (84). Additionally, watchful waiting is considered an alternative for old men with less aggressive disease (85).

Surgical approaches like the removal of the entire prostate are applied to men with high life expectancy and localized disease with the aim to completely eradicate the tumor (86). In these patients, given the low risk of lymph node involvement, the removal of pelvic lymph nodes remains controversial (86,87).

Another therapeutic approach for the localized disease is radiotherapy which employs x- and gamma-rays or alpha emitting radio isotopes (88) to kill tumor cells by causing DNA damage. Two applications are possible: external beam radiotherapy and internal radiotherapy (also called brachytherapy, which consists of implantation near the cancerous region of radioactive plugs which will release slowly the radiation). Recently, also image guided intensity-modulated radiotherapy has been developed to deliver high dose particles to specific regions reducing the impact on the surrounding tissues (89). It is important to consider that although surgical removal and radiotherapy produce a

similar outcome, they have a different impact on the quality of life of the patient (e.g. urinary and sexual function) (90).

4.5. Prostate Cancer Progression and Bone metastasis

When the cancer enters into the “progression phase”, the loss of the basal lamina occurs and results in the switch from high-grade PIN to adenocarcinoma with an invasive phenotype, macroscopically characterized by the lack of basal cells as shown by p63 and cytokeratin 5/14 staining (91). However, whether prostate cancer is originated from luminal or basal prostate cancer stem cells is still under debate (33,92). The majority of prostate adenocarcinomas present with an acinar morphology while ductal and mucinous adenocarcinomas are more rare. In less than 2% of the cases the adenocarcinomas are classified as neuroendocrine variants and mainly occur during recurrence after androgen deprivation therapy (93). This can partially be explained by the fact that neuroendocrine cells lacking of AR expression survive ADT and prevail producing relapse (94).

The terminal phase of prostate cancer progression encompasses systemic metastasis, which coincides with the development of therapy resistance, e.g castration and chemotherapy resistance (95). The majority of aggressive prostate cancers is characterized by their osteotropism leading to the development of predominantly osteoblastic/osteosclerotic lesions and, thus, represent one of the major clinical challenges in uro-oncology. The first explanation for the bone tropism of prostate cancer metastasis was provided in 1940 when Oscar Batson suggested that the venous network that drains the prostate and connect the pelvic veins to the paravertebral venous plexus could explain the dissemination (96). However, another study demonstrated that the venous network does not represent the major driver in the dissemination of prostate cancer cells to the bones (97). Alternatively the interactions between cancer cells and the endothelium was also suggested to underlie organ-specific dissemination (98). Furthermore, the interaction between the chemokine (C-X-C motif) receptor (CXCR) 4 (CXCR4) and its ligand stromal derived factor 1 (SFD1, also known as CXCL12) may be critically important (99). Prostate cancer cells express CXCR4 and experimental evidence has shown that neutralization of CXCR4 reduces prostate cancer bone metastasis in preclinical models (100). Moreover, prostate cancer cells also express various integrins, e.g. integrin $\alpha v\beta 3$, which correlates with prostate cancer bone metastasis and is responsible for the interaction with fibronectin, vitronectin and osteopontin (101-104). The notion that molecular factors might be involved in the specific bone tropism of certain cancer cells was for the first time postulated by Sir Stephen Paget who introduced the “Seed and Soil” hypothesis in which he compared the bone metastatic breast cancer cells to the seed of plants, capable of growing only in

a fertile soil, the bone marrow (105). Today we know that the formation of distant metastasis is a complex process, characterized by multiple bi-directional interactions between the tumor cells and the supportive stroma (106). This process starts at the level of the confined primary tumor where factors systemically released contribute to the conditioning of the metastatic "soil" and provide the establishment of the so called "pre-metastatic niche" (107). The "pre-metastatic niche" is defined as a fertile microenvironment induced in the metastatic target organs that facilitates the future invasion, colonization and the proliferation of metastatic tumor cells (107). During the establishment of the "pre-metastatic niche", bone marrow-derived hematopoietic progenitor cells expressing VEGF receptor 1 (VEGFR1) are recruited to metastatic target organs by specific factors released by the primary tumor (108). Among these factors, LOXL enzymes, VEGFA, VEGFC, TNFα and TGF-β produced by the primary tumor stimulate inflammation, attachment and recruitment of, for example, myeloid cells and the expansion of lymphatic vessels in the proximity of the sentinel lymph nodes (109-112). Interestingly it has been proposed that extracellular vesicles and exosomes released from the primary tumor represent the mechanism of communication between the primary cancer cells and the metastatic sites during the induction of the "pre-metastatic niche" (113) also in prostate cancer (114).

Additionally, in primary and metastatic cancers, tumor cells interact with different cell types that constitute the stroma. Such cells include tumor-associated macrophages (TAMs), cancer associated fibroblasts (CAFs), endothelial cells, pericytes and mesenchymal stem cells (MSCs) reviewed in (6,115). Tumor cells produce several factors that "activate" the surrounding stromal cells and induce remodelling of the EMC. These factors include fibroblast growth factor 2 (FGF2), vascular endothelial growth factor (VEGF), platelet-derived growth factor (PDGF), epidermal growth factor (EGF), interleukins colony-stimulating factors and TGF-β (116) and proteolytic enzymes (117) that remodel ECM, enabling cell migration. In the progression and castration resistant phase of prostate cancer, cancerous polarized-epithelial cells localized at the site of the primary tumor undergo biochemical changes and acquire an invasive and often mesenchymal phenotype (118,119) which confers them enhanced migratory ability, invasiveness, resistance to apoptosis and resistance to therapy, which are all properties resulting in a clinically-relevant phenotype (120,121). Together these events result in the invasion of the surrounding stroma and in the intravasation and circulation of cancerous cells in the blood stream. Tumor cells which possess stem cell-like characteristics, that survive in the circulation can extravasate at those distant sites where the "pre-metastatic niche" has previously prepared a fertile "soil" for future colonization. Recent research has highlighted the clinically relevant properties of the so called circulating tumor cells (CTCs) capable of surviving into the blood stream and in

distant metastatic sites (122). Once that these CTCs have colonized the metastatic site (e.g. the bone), they may activate a reverse program of mesenchymal-to-epithelial transition (MET) and remain dormant for years (123). Therefore it appears that these disseminating tumor cells (DTCs) can perpetuate in the bone the malignant progression and establish a “metastatic niche”.

Typically, the “metastatic niche” is located at perivascular locations (124). CTCs and DTCs may, potentially, establish a metastatic niche through competition with hematopoietic stem cells (HSCs) for their niche at a perivascular location (124-127). Moreover it has been hypothesized that tumor cells can also create their own niche (125,128). PCa cells amplify the existing hematopoietic niche and induce de novo an ectopic epithelial tissue-of-origin niche which together with the amplified hematopoietic niche generates a hybrid niche, supportive for cancer cell growth (106) and reviewed in (129). DTCs can survive in the bone microenvironment as non-proliferating (dormant) cells that originate microscopic lesions (classified as micrometastasis) (130,131). The mechanisms that induce exit from dormancy are still largely unknown (131). However, it has been shown that a collagen-I enriched fibrotic environment plays a crucial role in the cytoskeletal reorganization in dormant cells and in their awakening from dormancy (132). Once that these cells escape from dormancy, they induce local inflammation, followed by vascular and bone remodelling and establishment of a distant secondary tumor (bone metastasis) (120,133). Recently, it was revealed that the molecular signature of the stroma response in prostate cancer-induced osteoblastic bone metastasis highlights the amplification of hematopoietic and prostate epithelial stem cell niche (106). This observation supports the notion that angiogenesis and osteogenesis are crucial processes involved in the formation and growth of osteoblastic bone metastasis. Moreover, a recent report described the presence of two different type of microvessels: type “H” ($CD31^{high}$ and $endomucin^{high}$) and type “L” ($CD31^{low}$ and $endomucin^{low}$) (134). Interestingly, angiogenesis and osteogenesis have been coupled to the type “H” vessels, that provide also signals for HSCs and where osteoblasts also reside (135). Moreover, the kinetic of type “H” vessels in mice shows a peak at week 4 and loss of type “H” endothelium during ageing has been documented (134). Together this support the involvement of angiogenesis in the homing of metastatic cells in the bones in preclinical mouse models.

The bone remodelling induced by metastatic cancer cells results in either bone formation (osteoblastic bone metastasis) or bone resorption (osteolytic bone metastasis) and interferes with hematopoiesis (133). In prostate cancer, the bone lesions are typically osteoblastic (133,136), however the co-existence of osteobastic and osteolytic response have been documented (137).

Factors inducing osteoblast recruitment and activity in prostate cancer are: BMP6 (138), and BMP modulators, such as Noggin (NOG) (139); IGF1 (140) VEGFs (141), wnt signaling (142) and modulators of Wnt signaling such as dickkopf (DKK) and Sclerostin (SOST) (139). On the other hand, factors modulating osteoclast recruitment and activity in prostate cancer are: MMP-7, which promotes osteolysis via cleavage of RANKL that stimulates osteoclastogenesis (143); Noggin which antagonizes bone morphogenetic proteins (BMPs) and impairs bone formation (139,144);

It has been hypothesised that osteolytic cancer cells produce PTHrP that stimulates osteoblasts to secrete RANKL. This in turn stimulates ostecolasts progenitor cells and leads to osteoclastogenesis therefore bone resorption. During this process, many factors such as TGF-β, IGF-1 and calcium are released from the mineralised matrix to further feed cancer cell growth, thus perpetuating this "vicious cycle" (133,145). In prostate cancer for example, the expression of the calcium sensing receptor by tumor cells makes them responsive to the release of calcium during bone resorption and leads to increased proliferation and PTHrP release (146,147). However, the inhibition of bone resorption as strategy to impair bone metastasis with agents such as bisphosphonates revealed no effect on cancer cell proliferation in animal studies (148,149) and clinical trials also in prostate cancer (150) suggesting that other mechanisms support tumor cell growth in the bone. In this perspective, the recent identification of the molecular stroma response in osteoblastic prostate cancer (106) supports the coupling of angiogenesis and ostegenesis in bone metastasis (134) and suggest that anti angiogenesis might impact on the growth of osteotropic prostate cancer cells in the bone.

4.6. Treatment of Advanced Disease

As previously described, PSA testing allows an early detection of many cases of the disease when the cancer is still confined and may therefore be successfully resolved by surgery or radiotherapy. However, after local treatment, 20-40% of the cases, biochemical relapse will occur (PSA > 0.2 ng/ml) (**Fig. 6**) (95). Typically these patients will be treated with androgen deprivation therapy (ADT, which consists of chemical or surgical castration and/or treatment with anti-androgens) which will lead to regression of prostate tumors (151).

A strategy consists in the modulation of the testosterone biosynthesis via interference with LH and LHRH. This can be achieved in two ways: employment of LH agonists to produce in the long term a downregulation of the LH receptor thus resulting in a decrease of the testosterone biosynthesis (152); employment of LH antagonists which result in a rapid decrease of testosterone levels (152). Another strategy consists of treatment with anti-androgens such as bicalutamide and enzalutamide (153).

Despite these therapies, 30-70% of the patients treated with androgen deprivation therapy will inevitably display increased PSA levels, acquire resistance to androgen suppression and develop incurable metastatic disease (154). This situation is commonly defined as castration resistant prostate cancer (CRPC) or hormone refractory prostate cancer (HRPC). Although similar, these two terms refer actually to two different clinical situations. Patients who are traditionally identified as HRPC are highly heterogeneous depending on: 1) the clinical status, 2) the level of PSA, 3) the applicability of hormone therapy and 4) the eventual presence of metastasis (95).

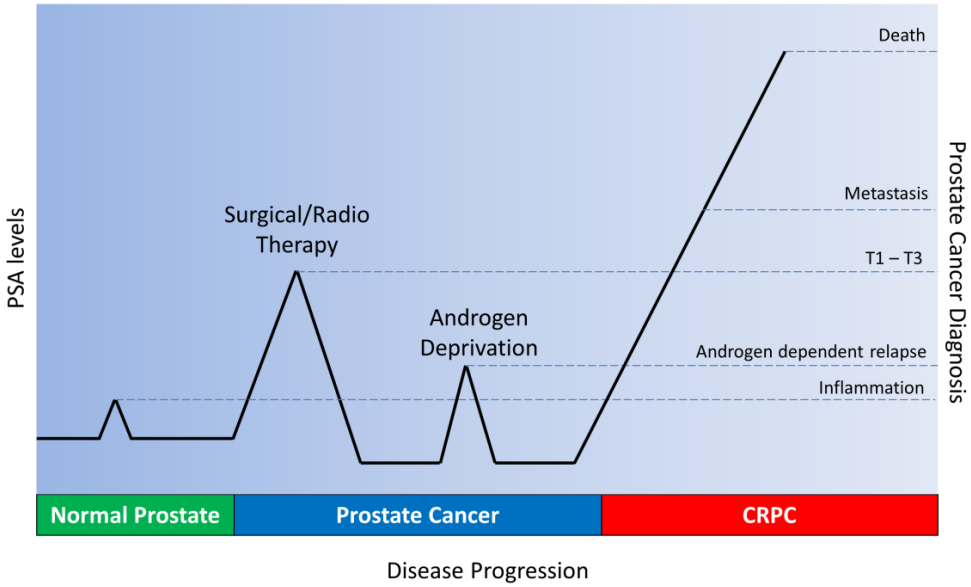

Figure 6. Overview of prostate cancer progression combined with diagnosis and treatment options. Prostate cancer is initially treated with prostatectomy or radiotherapy and in almost 80% of the cases, patients will be cured. In 20-30% of the cases, prostate cancer relapses and these patients will be typically treated with androgen deprivation therapy. However, the development of castration resistance prostate cancer (CRPC) will inevitably occur. Although these patients will be treated with therapies such as docetaxel, cabazitaxel, enzalutamide and abiraterone, the development of incurable metastasis, typically in the bone will occur.

Interestingly, there are documented cases in which the androgen receptor (AR) signaling remains active after androgen deprivation therapy probably through escape mechanisms (30). Such mechanisms include amplification of the AR gene (155-157), gain-of-function mutations of AR (158-162), expression of alternative splice variants (163-165) and endogenous expression of enzymes involved in DHT synthesis by tumor tissue (166-169). For this reason, the term CRPC has been progressively introduced into

the clinic to indicate a condition where response to hormonal therapy is still possible, therefore reveals a different condition from HRPC (95).
Once that tumor acquires resistance to androgen suppression and patients develop metastasis mainly in the bones, treatment options are limited and include symptomatic care with analgesics or radiotherapy to reduce bone pain, treatment with bone-seeking isotopes (e.g. Strontium-89 and the recently FDA-approved Radium-223 chloride) and chemotherapy (170). Typical therapeutic treatments consist of agents targeting the androgen pathway (abiraterone acetate and enzalutamide) and taxanes (docetaxel and cabazitaxel), which target microtubules and result in the arrest of the cell cycle (170-174). Current first-line treatments consist of combination therapy with docetaxel and prednisone, while second line combination treatments are cabazitaxel and prednisone, abiraterone acetate and prednisone and enzalutamide (171-174). Recent studies revealed that simultaneous treatment of ADT and docetaxel significantly increases patient survival (175,176). However, longer follow up of these studies is needed to assess whether this benefit translates also into metastatic-free survival.

4.7. Prostate Cancer Stem Cells

According to what is commonly known as the “cancer stem cell hypothesis”, CSCs appear to be strongly involved in tumor formation, therapy resistance, recurrence and metastasis. As we already mentioned in a previous paragraph, cancer is a disease that originates from a single normal cell after a series of specific genomic and non-genomic alterations. As a result it was hypothesized that cells with self-renewal ability represent good candidates for oncogenic transformation and cancer formation (47). There are two putative sources of cells with self-renewal properties that are believed to generate cancer: adult stem cells (SCs) and non-stem cells that acquire self-renewal properties after de-differentiation and transformation. The majority of prostate cancer have a luminal phenotype and the absence of basal cells is a diagnostic feature of prostate adenocarcinoma (91,177). One could, therefore, speculate that prostate tumors originate from luminal progenitor cells or stem cells within the basal layer that after transformation differentiate into a luminal progeny. However, the histological compartment where the putative cell of origin of prostate cancer resides is still under debate. In hormone-naïve cancer, experimental evidence in rodents and humans support the existence of cells with self-renewal properties and tumorigenic ability in the basal compartment of the prostate ($\alpha_2\beta_1$ integrin^{hi} and CD133^{+} cells (178,179)) (**Fig. 7**). Other common markers include ALDH^{high}, CD44^{+} and CD24^{-} (39,40,180). On the other hand, in CRPC, cells with self-renewal properties exhibit a luminal phenotype. These cells have been identified in castrated mice and are known as castration-resistant Nkx3.1-expressing cells, named CARNS (33) and later the stem-like cells with luminal

phenotype (CARN-like cells) were also identified in humans (34). CARNs are characterized by low AR expression, and display the stem-cell marker ALDH1A1 or NANOG and express the luminal marker NKX3.1 and CK18 (34). Interestingly, the experimental observation in favour of the luminal hypothesis suggest the presence of a residual and dormant subpopulation of cancer cells which are castration-resistant for survival but castration-sensitive for growth (34). Recently the field has been additionally complicated by the experimental evidence that murine luminal (CD49f positive (181)) and basal (CD24 positive (182)) cells and human luminal (CD26 positive (182)) and basal (CD49f positive (182)) cells are capable of generating prostate organoids (183). However, the debate about the localization of the cell of origin of human prostate cancer and its role in the progression to a castration resistant phase is still controversial.

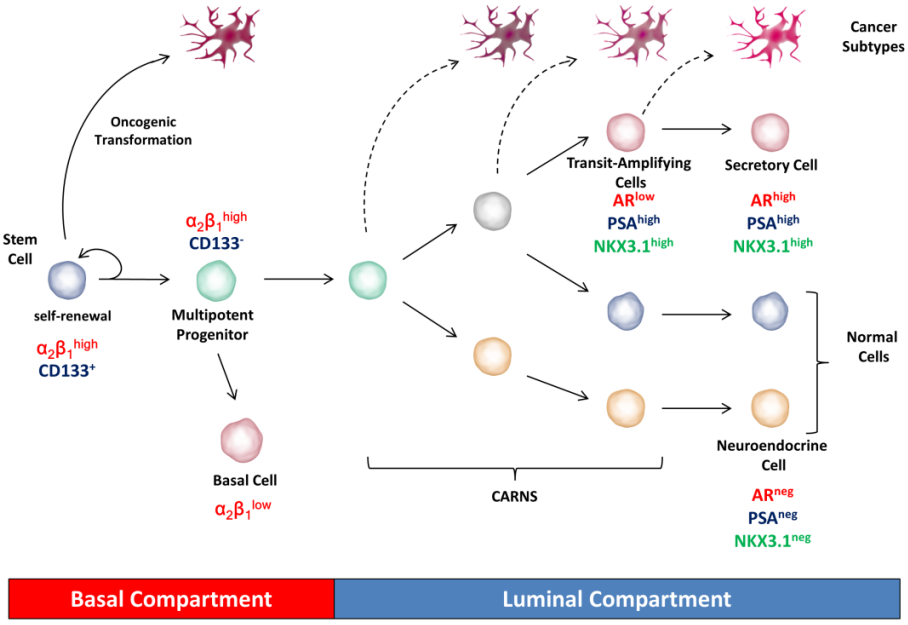

Figure 7. Hierachical model of tumorigenesis: role of normal and transformed tissue stem/progenitor cells. Cells within the different epithelial compartments can be distinguished by their phenotypic characteristics.

In addition to haematological malignancies, the presence of a subpopulation of epithelial cells with self-renewal properties is generally recognized in solid tumors including those of the human prostate. Furthermore accumulating experimental and clinical evidence suggest that such cells are highly tumorigenic and may play a key role in distant metastasis in preclinical models (33,178,183) and in clinical reality (184,185).

The assumed role of CSCs in tumor maintenance represents one of the major problems for the identification of new, targeted therapies capable of eradicating the disease. Current therapies are indeed very effective in the treatment of the primary tumor mass (186). However, the relapse that is commonly observed (even after many years) in patients, suggests the presence of subpopulation of cells, resistant to therapy, which probably remain dormant for long time and that are capable of producing a new tumor (186,187).

5. Pathways Involved in Prostate Cancer Progression and Bone Metastasis

The notion that genes involved in developmental process are also likely to be altered in cancer is known and established. Molecular analysis revealed that a wide range of genes, commonly expressed during prostate organogenesis and developmental processes, are also abnormally expressed in prostate cancer.

Wnt pathway: the Wnt signaling pathway is an evolutionarily conserved pathway that regulates crucial aspects of development and cell behaviour, such as differentiation, migration and cell polarity. The Wnt signaling is characterized by two branches: a canonical pathway (Wnt/β-catenin dependent) and a non-canonical pathway (β-catenin independent).

The **canonical Wnt signaling** is activated upon the interaction between a ligand (Wnt) and its receptor (Frizzled, Fz) and co-receptor (low-density-lipoprotein-related protein 5/6, LRP5 and LRP6) (**Fig. 8A**).

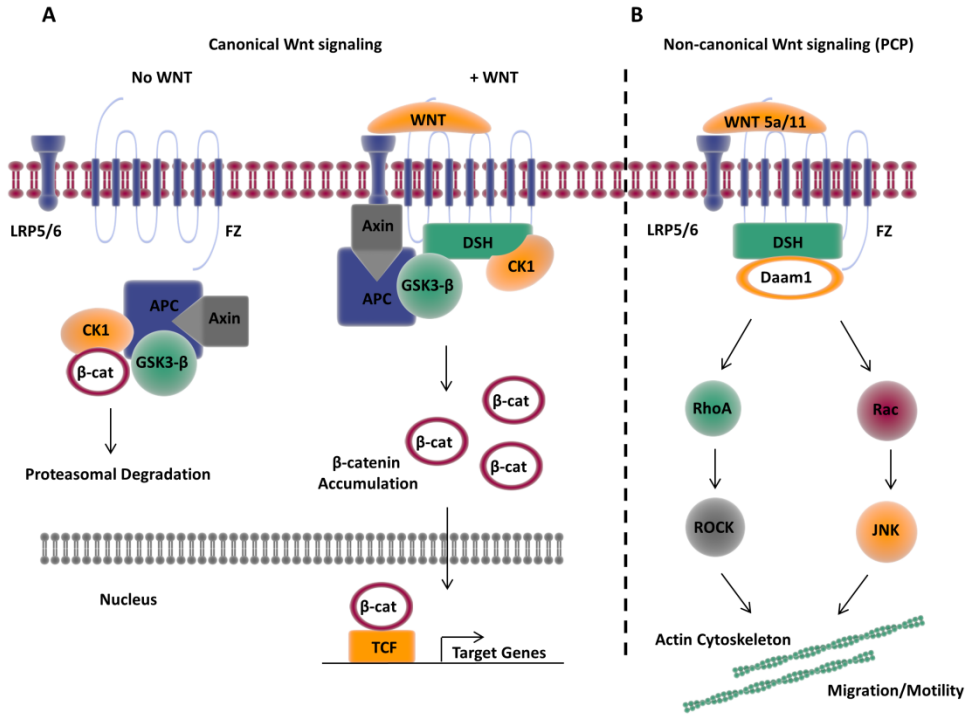

Figure 8. Schematic representation of canonical (A) and non-canonical (B) Wnt signaling.

In the absence of Wnt, a complex of Axin, APC, GSK3-β, CK1 and β-catenin is localized in the cytoplasm. CK1 and GSK3-β phosphorylate β-catenin which is subsequently degraded by the proteasomal machinery. In presence of Wnt, LRP6 is phosphorylated by CK1 and GSK3-β, thus recruiting to the plasma membrane a complex containing Axin and Dishevelled (Dsh), which is sequestered or degraded. This results in stabilization of β-catenin which subsequently translocates into the nucleus and mediates transcription of downstream target genes via interaction with LEF/TCF family members. Canonical Wnt signaling regulates process such as cell fate decision and anteroposterior organization in embryogenesis, as well as important function in organogenesis and stem cell renewal.

Many studies have documented alterations of the Wnt signaling pathway during prostate cancer progression, reviewed in (30,188-191). More specifically, elevated canonical Wnt signaling seems to play a role in the onset of castration resistance in prostate cancer (192). Additionally, alterations or interferences with canonical Wnt signaling, such as modulation of DKK (142) or mutation in sclerostin (SOST), which inhibits LRP5, contribute to disrupt bone formation, a process also regulated by Wnt signaling (193). In addition to the well-established effects of Wnt-signaling on enhanced osteogenesis, Wnt-signaling also induces bone-active factors, such as OPG which prevents the binding of RANKL to RANK thereby inhibiting osteoclast function (194).

The **non-canonical Wnt signaling**, comprise two branches of signaling transduction: the Wnt/Ca^{2+} signaling and the Wnt/planar cell polarity (PCP) pathway (195) (**Fig. 8B**). In Wnt/Ca^{2+} signaling, the interaction between Wnt and Fz activates phospholipase C via G proteins and lead to increase intracellular Ca^{2+}. This can induce, for example, EMT and invasion, therefore promoting cancer progression. In Wnt/PCP, the non-canonical Wnt (Wnt5a and Wnt11) bind their receptor Fz which recruits Dsh at the plasma membrane. This lead to a cascade of interactions which converge on common regulators of cytoskeletal remodelling and actin organization such as RhoA, Rac1 and JNK, which also impact on cell motility.

Wnt/PCP and canonical-Wnt signaling are both part of a negative feedback-loop where Wnt/PCP negatively regulates canonical-Wnt signaling and *vice versa* (196). In cancer, due to aberrant alterations in tumor cells, cancer cells can escape from these control mechanisms and as tumors progress, Wnt/PCP gets activated and promote cell motility, invasion and metastasis (195). Interestingly, β-catenin and GSK3-β have indeed been shown to be decreased in prostate cancer cell lines with high invasive and metastatic potential, such as PC3 (197). Therefore one could speculate that there is a misbalance in these cells between canonical and non-canonical Wnt signaling which results in mesenchymal phenotype and invasive properties.

Notch pathway: the Notch signaling pathways exerts also a crucial role during embryogenesis and organogenesis. In cancer, an aberrant activation of this pathway produces abnormal cell proliferation, increase in self-renewal properties and induction of therapy resistance (198,199). Conversely from Wnt signaling, the Notch signaling pathways requires a direct cell-to-cell contact for its activation. Typically, a signal-sending cell expressing on its plasma membrane the ligand (JAG1/2 or Delta-like 1, 3 and 4, in mammals) stimulates a signal-receiving cell expressing on its membrane the receptor (Notch1/2/3/4). This interaction produces a series of proteolytic cleavages operated by ADAM10 and γ-secretases that convert the full-length transmembrane Notch receptor into a transcriptional activator (Notch intracellular domain, NICD). Subsequently, NICD translocates into the nucleus, where it interacts with RBPjk/CBP transcription factors, resulting in the transcription of downstream target genes (e.g. Hairy and enhancer of split, HES and Hairy/enhancer-of-split related with YRPW motif, HEY) (**Fig. 9**).

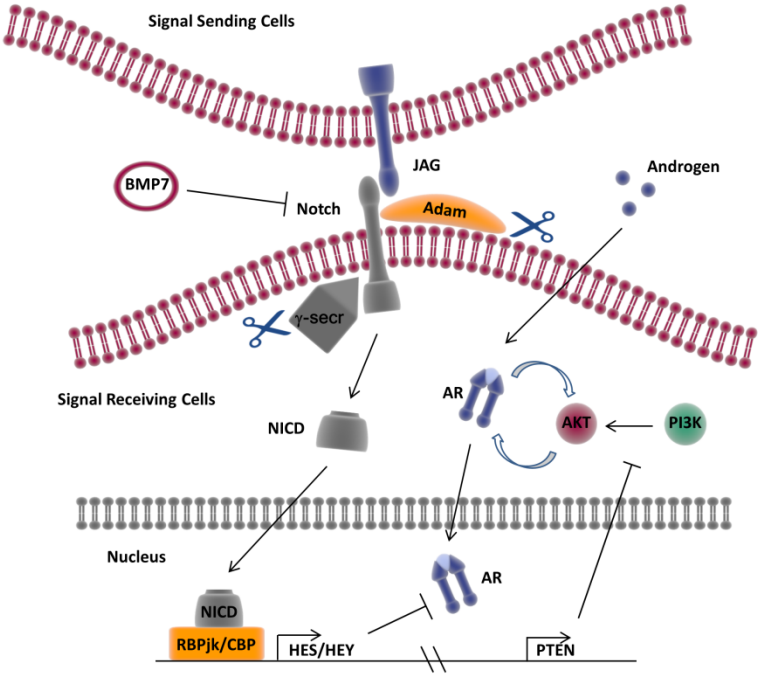

Figure 9. Schematic representation of Notch signaling.

Notably, Notch plays a crucial role during prostate organogenesis and is involved in its regeneration (198). Importantly, and relevant for the purpose of this thesis, the Notch

signaling pathway is characterized by multiple cross-talk with other major signaling pathways involved in prostate cancer progression and bone metastasis formation (e.g. TGF-β, AR and PI3K/AKT) (**Fig. 9**) (200-205). Members of TGF- β superfamily can control Notch signaling: for example, Bone morphogenetic protein 7 (BMP7) can inhibit the branching morphogenesis of the prostate during development via down-regulation of Notch signaling (206). Notch can also suppress AR signaling which is crucially involved in prostate growth and disease. Upon binding of androgen to the AR, the receptor undergoes a homodimerization and traslocates into the nucleus where it can recruit coactivators such as p300/CBP and steroid receptor coactivator 1 (SRC1). The downstream target of Notch, HEY1 can directly bind the N-terminal activation domain of AR thus preventing androgen signaling, supporting a role of Notch in the acquisition of a castration resistant phenotype (204). Finally, Notch can also suppress the PI3K/AKT pathway that is fundamental for prostate growth and cell migration (207). The activation of this pathway triggers a cascade of sequential phosphorylation that can be suppressed by PTEN (198). It appears that NICD contributes to induction of PTEN expression, therefore suppressing indirectly PI3K/AKT pathway (208). This has led to the paradox that Notch signaling (particularly when triggered by Notch1) can exert a tumor suppressive role in the prostate. The complexity of the interaction between the Notch signaling and AR and PI3K/AKT pathways is further increased by a reciprocal feedback mechanism between PI3K/AKT and AR signaling: recently it was indeed demonstrated that inactivation of PI3K/AKT induces activity in AR signaling, while suppression of AR pathway induces increase in PI3K/AKT (209). Given the established increased in PI3K/AKT in advanced prostate cancer (59,210), one could speculate that an increase in Notch signaling (as documented during prostate cancer progression), through its downstream target HEY1, produces a decrease in the AR pathway (castration resistant phase) which results in increased PI3K/AKT signaling (increase migration and metastasis). Notch signaling has also been shown to critically be involved in prostate cancer progression and bone metastasis formation and JAG1 has been found to be elevated in metastatic prostate cancer compared to primary tumor (211). Additionally, in the bone microenvironment, tumour-derived JAG1 activates the Notch pathway in osteoblasts and osteoclasts and the activation of the pathway in osteoblasts results in a growth advantage to bone metastatic tumour cells (212). Interestingly, mechanistic studies showed that the proliferative effect was dependent on osteoblast-secreted IL-6, which was transcriptionally regulated by the Notch signaling in breast cancer (213). The Notch signaling pathways represents a promising target for therapy against tumor growth (214) and bone metastasis (213). However, the presence of studies addressing the possible application of γ-secretase inhibitors in breast but not prostate cancer is remarkable.

TGF-β superfamily signaling pathways: during the early phase of prostate tumor growth, TGF-β acts as tumor suppressor by reducing proliferation and inducing apoptosis (215). However, during tumor progression, TGF-β switch gains a tumor promoter role and facilitates EMT and therefore metastasis (9,216). The transforming growth factor (TGF)-β superfamily of ligands includes more than 30 factors such as Bone morphogenetic proteins (BMPs), Growth and differentiation factors (GDFs), activins, inhibins, nodal and Anti-müllerian hormone (AMH). For the purpose of this thesis we will mainly focus on TGF-β members and BMPs. TGF-β is a pleiotropic cytokine that regulates many biological processes such as tissue growth and morphogenesis, cell proliferation and apoptosis, adhesion, differentiation, migration and metastasis (217). The TGF-β cytokine family consists in different members (TGF-β1, β2 and β3) whose bioactive cytokine molecule is a dimer consisting in a polypeptide chain which is cleaved from a latent precursor into the biologically active product (218).

BMPs include approximately twenty members and these are less homologous compared to the TGF-β isoforms (219). They are functionally involved in skeletal and joint morphogenesis, bone remodeling and in different cellular processes including osteogenesis, cell differentiation, anterior/posterior axis specification, growth, and homeostasis (220). In normal tissues, basal release of TGF-β by local sources is enough for the maintenance of homeostasis. In case of tissue injury, TGF-β is abundantly released by blood platelets and stromal components to prevent aberrant regenerative cell proliferation and inflammation. This occurs also in tumor microenvironment, where TGF-β is frequently present initially as factor to prevent premalignant progression, and eventually as factor that cancer cells may use to their advantage (218).

TGF-β superfamily members bind to type I and type II serine/threonine kinase receptors (**Fig. 10**). In human, seven different human type I receptors have been identified (ALK1-7) and five type II receptors, namely, TGF-β receptor II (TβRII), BMP receptor II (BMPRII), activin receptor II (ActRII), ActRIIB and AMH receptor type II. TGF-β binds TβRII and ALK5 and in endothelial cells it signals also via ALK1. BMP signaling occurs via BMPRII, ActRII and ActRIIB in association with ALK1,2,3 or 6 depending on the molecular context (221-231).

Binding of TGF-β and BMPs to their heterodimeric transmembrane receptors induces phosphorylation of type I receptor threonine/serine kinases. The signal is then transduced via Smad intracellular proteins, which later translocate into the nucleus and regulate transcription. The Smad pathway is also named **canonical signaling pathway**. TGF-β type I receptor propagates the signal by phosphorylating receptor-regulated Smad proteins (R-Smads) Smad-2 and -3. On the other hand, BMPs induce phosphorylation of Smad-1, -5 and -8 (218,232) (**Fig. 10**). This phosphorylation operated

by activated type I receptor occurs at the C-terminal SXS domain that is shared by all Smad proteins and that represent a nuclear localization signal (218,233).

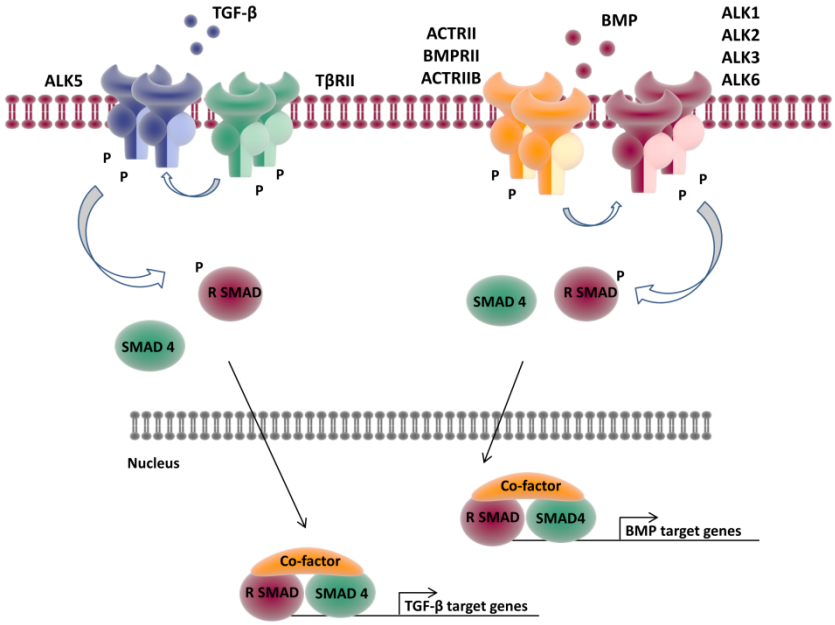

Figure 10. Schematic representation of the TGF-β and BMP signaling.

Depending on their phosphorylation state, Smad-2 and Smad-3 linked to Smad-4 undergo constant nucleo-cytoplasmic shuttling, in a sort of rapid activation-deactivation cycle, determined by repeated cycles of dephosphorylation and rephosphorylation, involving direct interactions with both nuclear pore proteins and importins and exportins, a protein family of transport factors (233).

TGF-β also regulates alternative pathways via Smad-independent signaling (**non-canonical Smad signaling**). These signaling include the extracellular-signal- regulated kinase (ERK1 and ERK2), p38, MAPKs, c-Jun N-terminal Kinase (JNK), PI3K-Akt and small GTPases. The non-canonical Smad signaling pathways have been extensively reviewd in (234-236).

Each step in the TGF-β signaling pathways is controlled by specialized factors. These factors include encapsulation of the extracellular ligand by binding proteins, inhibition of activation of latent TGF-β, receptor-interacting partners (BAMBI, SARA and FKBP12), inhibitory Smads (Smad6 and Smad7) and post-translational modification by E3 ubiquitin ligases, co-repressors and phosphatases, reviewed in (237).

Integrins: integrins belong to a family of heterodimeric transmembrane glycoprotein receptors which consist of an α and a β subunit and which play important roles in tissue development and cancer (238,239). To date 18 α and 8 β subunits have been identified from which 24 different functional heterodimers can be generated (240). Integrins regulate many processes such as cell adhesion, migration, proliferation, neo angiogenesis (241) and have been shown to undergo changes in their expression during the transition to neoplastic phase (242,243). Integrins establish the connection between the cell and the extracellular environment (mostly the extracellular matrix molecules) and the cytoskeleton and transduce signals from the outside and into the cells and vice versa (reviewed in (238,240,244-246)) (**Fig. 11**). In addition, integrins can modulate the signaling cascade of multiple growth factor receptors via RasGTP, such as the epidermal growth factor (EGF), platelet-derived growth factor (PDGF) and fibroblast growth factor (FGF) receptors, thereby lowering the threshold level in different signaling pathways (247). Moreover, ligation and clustering of integrins can lead to the activation of focal adhesion kinase (FAK) and extracellular signal-related kinase kinase (MEK) (248) which have been implicated in prostate cancer progression and metastasis (249,250). Previous studies have shown that specific integrins (such as αvβ3 (101,102)) correlate with poor survival and are involved in the formation of bone metastasis (251-254). Furthermore, targeting of α_v integrin (knockdown or selective drug targeting) in human prostate cancer cells, abolished the formation of bone metastasis in preclinical mouse model (255,256).

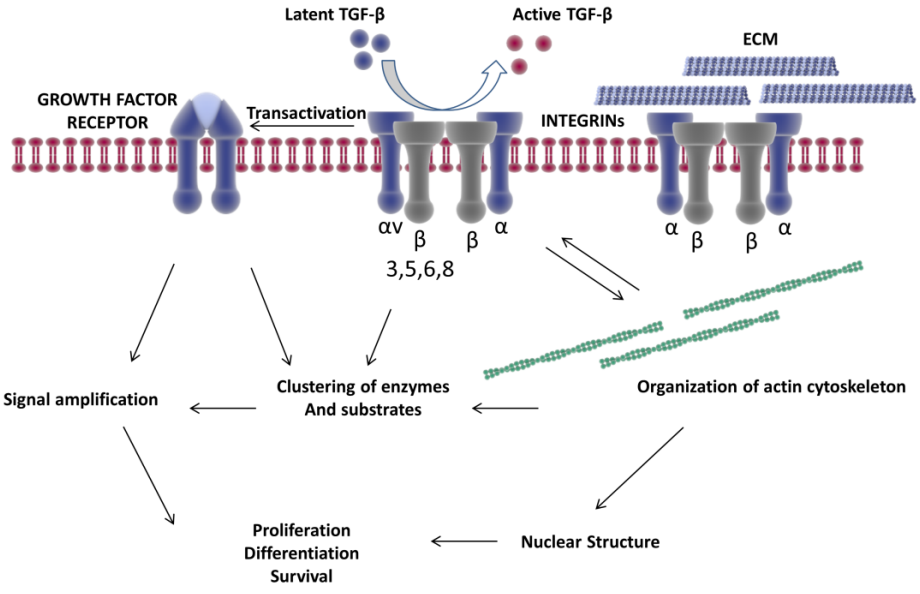

Figure 11. Schematic representation of the multiple roles of integrins.

Additionally, α_v integrins appear to be up-regulated in tumor- and metastasis-initiating prostate cancer cells ($ALDH^{high}$ (39,257)) and these integrins are involved in the activation of latent TGF-β, thereby modulating TGF-β signaling (and *vice versa* in a feedforward loop (244,258-260)) (**Fig. 8**). As previously outlined, high bone turnover provides a significant contribution to the development and the relapse of bone metastasis (261). Interestingly, it has been reporter that increased expression of integrin alpha-v enhanced the TGF-β mediated osteoclastogenesis (262). Therefore it appears that changes in integrin expression play an important role in malignat disease and impact not only on primary tumor growth and invasion but also on the bone microenvironment.

Cripto pathway: Cripto (TDGF1, CRIPTO-1) is a small, GPI-anchored/secreted fetal-oncoprotein that plays important roles in regulating stem cell differentiation, embryogenesis, tissue growth and remodelling (263). An essential mediator for the Cripto signaling is the Glucose-regulated protein 78 (GRP78) (264). As for Wnt and Notch, Cripto represents one of those embryonic signaling pathways that when corrupted can drive tumor initiation and progression. The Cripto pathway modulates the signaling of multiple TGF-β ligand that transduce the signal via Smad2 and 3 such as Nodal, GDF1 and GDF3 (265-267) (**Fig. 12**). Interestingly, Cripto has also been shown to negatively regulate the activation of Smad by Activin-A (268,269), Activin-B (270) and TGFβ-1 (269,271) leading to suppression of the cytostatic effect of these ligands (271,272). These cross-talk with the TGFβ pathway, also crucially involved in prostate cancer bone metastasis, highlight the interest of elucidating the role of Cripto signaling in the contest of bone metastasis. Additionally, even though the soluble vs. secreted effects regulated by Cripto are not yet been entirely elucidated (273), Cripto has also signaling activities that are independent from the TGF-β pathway. Relevant for the purpose of this thesis, soluble Cripto can activate and promote signaling routes of extreme relevance in prostate cancer formation and progression, such as the already discussed PI3K/AKT. In this context, blockade of Cripto binding to cell surface GRP78 inhibits oncogenic Cripto signaling via MAPK/PI3K and Smad2/3 signaling routes (270). Moreover, Cripto is also known to modulate Wnt and Notch signaling pathways (274-277). The interaction between Cripto and PI3K/AKT pathway is mediated via Glypican-1, a GPI-anchored heparan sulphate proteoglycan, that activates a cascade of phosphorylation in which MAP Kinase are involved. This lead to the subsequent activation of PI3K/AKT pathway which promotes proliferation and motility (278). Cripto has also been shown to cross-talk with Wnt signaling; it can bind LRP5/6 facilitating the interaction with Wnt3a, therefore stimulating Wnt pathway through cytoplasmic stabilization of β-catenin (279). Cripto is also involved in the processing of the Notch receptors by enhancing its

cleavage from the plasma membrane, thereby potentiating Notch signaling (277). Finally, Notch signaling can also modulate the expression of Nodal, further complicating the cross-talk between Notch and Cripto /Nodal signaling (280). As we previously mentioned, one of the key processes that characterize the switch from non-invasive to invasive disease in prostate cancer is represented by EMT. Interestingly, Cripto exerts an important role in this process in prostate cancer, where its overexpression produces increase in the mesenchymal marker Vimentine, decrease in the epithelial marker E-Cadherin and augment PI3K/AKT and FGFR1 activity, thus inducing migration (281).

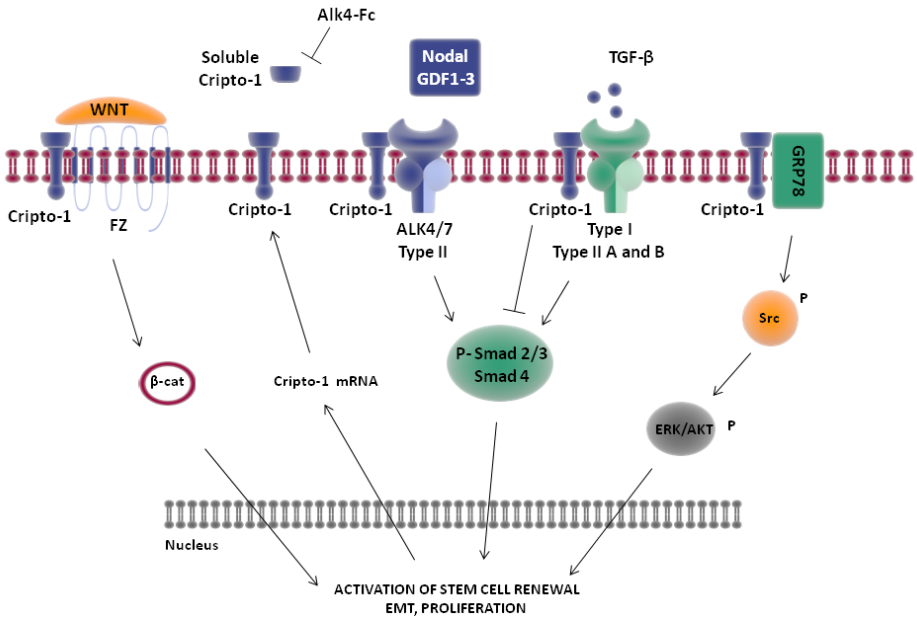

Figure 12. Schematic representation of the multiple interactions of Cripto signaling.

The genetic alterations and the signaling pathways discussed in this paragraph obviously do not cover the entire complexity of aberrant genetic events and abnormalities that characterize multiple pathways and molecules from the onset to the progression of prostate cancer. Among these, we have focused our interest on the alteration and the role of a class of small non coding RNA, namely microRNA, that regulate gene expression. The properties of these molecules, the mechanism of action and their functional relevance in the maintenance of aggressive subpopulation of

cancer cells during prostate cancer progression and metastasis are presented in the next paragraphs.

5.1. The involvement of microRNA in prostate cancer

microRNAs (miRs) are a class of small non-coding RNAs that derive from larger precursor (pri-miRNA) folded into a stem-loop configuration. miRs are transcribed by RNA polymerase II (Pol II) and subsequently processed into the ~70-nucleotide precursors (pre-miR) (282,283). The pre-miR is then cleaved to generate a ~21-25-nucleotide mature miR. miRs localized within Alu-repetitive element, can be transcribed by RNA polymerase III (284). miRs can be positioned at different genomic locations; for example, they can map within introns of both protein-coding or non-coding genes (285). These are transcriptionally regulated through the promoters of these genes (286,287). The transcription of miRs held in the same cluster is regulated by the same promoter and all the miRs from that cluster are transcribed at the same time.

The processing of miR is catalyzed by different multiprotein complexes (**Fig. 13**) (reviewed in (288)). A complex localized in the nucleus and composed by an RNase III enzyme Drosha and the double-stranded RNA-binding domain (dsRBD) protein DGCR8/Pasha, process the pri-miR (289). This enzymatic reaction produces a 2-nucleotide-long 3' overhangs at the cleavage site. The processing of the pri-miR into ~70-bp pre-miRs by Drosha depends on the terminal loop size and the flanking sequence of the Drosha cleavage site. Shortening of the terminal loop, disruption of complementariety within the sequence, or mutations of flanking sequence at the Drosha cleavage site, can significantly reduce, if not abolish the processing of the pri-miR.

After the pri-miR is cleaved by Drosha, the resuting pre-miR is exported from the nucleus into the cytoplasm by Exportin 5 (Exp5), a nucleo/cytoplasmic cargo transporter Ran-GTP dependent (290-292). In the cytoplasm, another RNase III enzyme (Dicer) cleaves the hairpin into a small imperfect dsRNA duplex that contains both the mature miR strand and its complementary strand (293-295). The ability of Dicer to recognize the pre-miR molecules is due to the presence of a PAZ (Piwi-Argonaute-Zwille) domain that allows a low-affinity interaction with the 3' end of ssRNAs (296-298). For this reason, the pre-miR that presents 2-nucleotide 3' overhangs resulting from Drosha cleavage, can be easily recognized and processed by Dicer.

Dicer cleavage generates mature miRs ~21-25-nucleotide long. After the dsRNA duplex is formed, the target specificity and the functional efficiency of a miR, requires that the mature miR strand is incorporated into the RNA-induced silencing complex (RISC) (reviewed in (288)). In human cells, transactivating response (TAR) RNA-binding protein (TRBP), recruits the Argonaute protein Ago2 and together with Dicer they form a trimeric complex that initiates the assembly of the RISC complex (reviewed in (288)).

The mechanism by which the RISC complex incorporates the mature miR strand of the dsRNA duplex is driven by the different stability of the miR duplex. Potentially the

mature miR strand can reside on either strand of the hairpin, but, because of thermodynamic reasons, it mostly derives from the strand with the less stable 5'.

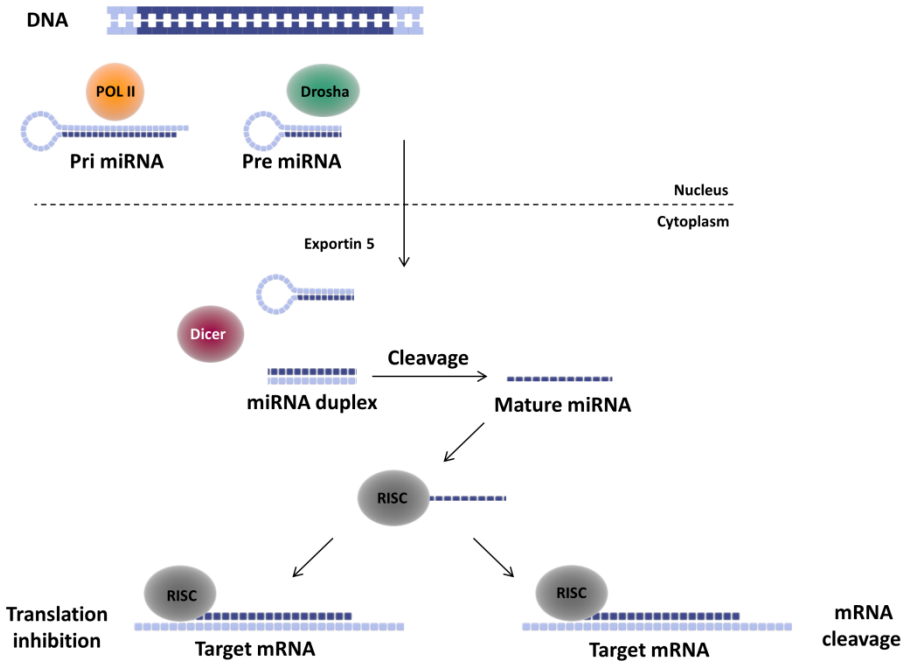

Figure 13. Schematic representation of the microRNA processing pathway.

The detection of microRNA in blood and urines represent an interesting and non-invasive approach to diagnose prostate cancer (299). Independent studies have shown that miR-141 and miR-375 are significantly elevated in the blood of prostate cancer patients with bone metastasis and in the respective exosomes (300,301). Interestingly elevated levels of the two microRNAs are also associated with higher Gleason score, positive lymph nodes and were also detected in the urine of prostate cancer patients (302,303). miR-375 has also been identified as prognostic marker in castration-resistance prostate cancer together with miR-1290 in exosomes (304). Additional microRNA that have been measured in the urine and associated with prostate cancer are miR-107, miR-574-3p and miR-200b (303). Interestingly, the last has also been associated by an independent study with docetaxel resistance (305). In the same study, miR-429, miR-200a, miR-21, miR-200c, miR-375, miR-132 and miR-20 have been associated with lower survival (305). A recent report investigated the expression of microRNAs in patient-derived stem like cells ($CD133^{+}$, $\alpha 2\beta 1$ $integrin^{high}$) enriched from

benign prostatic hyperplasia, Gleason 7 treatment-naive prostate cancer, and CRPC and identified miR-548c-3p as functional biomarker involved in prostate cancer progression (306).

5.2. Mechanisms of microRNA Post-Transcriptional Repression

After incorporation into the RISC complex, the miR interact with its target mRNA by base-pairing interactions. If mRNA/miR complementarity is perfect or near-perfect, the target mRNA can be cleaved and degraded; otherwise the translation is repressed (294).

The target complementarity is determined by base-pairing of nucleotides in the so called “seed sequence” of the miR (307). This sequence is essential for the binding of the miR to the mRNA. The seed sequence is an heptametrical sequence located at positions 2-7 from the miR 5´-end and has to be perfectly complementary to the target mRNA complementary sequence. The miR seed sequence is exploited to develop computational approaches for target prediction.

The microRNA target site is positioned at the 3’UTR region, probably because the movement of ribosomes that occur during translation will contrast RISC binding and interaction (308). Different and “non-canonical” miR-mediated mechanisms of mRNA expression modulation are also emerging. In fact some miRs can bind to the open reading frame (ORF) sequences or to the 5’UTR region of the target genes, determining gene activation rather than repression (309). The RISC action on target mRNA is modulated by the Ago protein that is incorporated in the complex and by the grade of complementarity between the miR strand and its mRNA target. Ago2, for example, is able to cleave RNA, but this event requires extensive base pairing between the miR strand and the mRNA target (310,311).

To date, six models have been proposed for the miR translational repression:

1) the RISC complex induces de-adenylation determining a decrease of translational efficiency by blocking target mRNA circularization (312);
2) RISC complex blocks cap function by interacting with both the cap or eIF4E (313);
3) Argonaute proteins recruit eIF6, which blocks the recruitment of 60s ribosomal subunit (314);
4) RISC complex blocks the translation elongation or promotes premature dissociation of ribosomes (ribosome drop-off) (315);
5) RISC complex induces the proteolysis of nascent peptides during translation (in this model the translation is not inhibited) (316);

6) RISC complex recruits target mRNAs to processing bodies, where the mRNA is degraded or stored in an inactive state for translation (317,318).

5.3. microRNA and Cancer Stem Cells

microRNAs regulate multiple biological process, such development and cell growth and have been proposed as one of the important players during pathogenesis and cancer. In human prostate cancer, several studies in patient samples and xenografts have revealed their characteristic pattern in benign vs. aggressive disease and highlighted their role in castration-resistant prostate cancer and their implication in bone metastasis formation (see microRNAs described in paragraph 3 and reviewed in (299,300,302)).

However, the number of studies addressing the role of specific miRs in the regulation of stem-like properties in bulk prostate cancer cells lines is limited. Remarkably, there is an even lower number of studies, that investigated the expression of miRs directly in selected subpopulation of cells, characterized by stem-like properties and capable of maintaining the tumor and producing metastasis. In these studies new miRs have been identified using expression profiling of subpopulation of cells enriched for cancer stem cells isolated from bulk prostate cancer cell lines. For example, prostaspheres from PC3 cells have been compared to adherent PC3 cells and miR-143 has been identified as promoter of prostate cancer metastasis (319). In other approaches, a fraction of prostate cancer stem cells (PCSCs, described as $CD44^+/CD133^+$) has been isolated by viable cell sorting from culturedLNCaP cells and miR-101 has been found to inhibit cell growth and promote apoptosis in PCSCs (320). With a similar approach, miR-409-3p/5p has been identified in embryonic stem cells and then studied in prostate cancer, where it was found to promote bone metastasis (321). Other studies have also employed cell sorting of various stem/progenitor cell population, including $CD44^+$, $CD133^+$, integrin $\alpha2\beta1^+$ and side population of cells isolate from bulk cell lines and found multiple tumor-suppressive microRNA down-regulated, including miR34a, let-7, miR-106a and miR141 (322). Interestingly, a 'near-patient' approach highlights that a population of $CD44^+$ cells isolated from xenografts led to the identification of miR-34a as master regulator of metastasis (323) and, as a consequence, this was subsequently validated in $CD44^+$ cells isolated from primary prostate tumors. Moreover, in patient-derived stem like cells ($CD133^+$, $\alpha2\beta1^{high}$), it was recently found that miR-548c-3p can be considered as functional biomarker involved in prostate cancer progression (306) as enforced overexpression of this miR in differentiated cells induced stem-like properties and radioresistance. Finally other studies have used Hoechst 33342-based flow cytometry to isolate a CSC-like side population and confirmed the tumor suppressive role of miR-34a and additionally identified miR-200c as mediator of chemoresistance.

Strikingly, there is lack of microRNA expression profiles of cancer-stem like/progenitor cells obtained from clinical prostate cancer specimens. The molecular characterization of this subpopulation of highly tumorigenic cells, could indeed provide novel insights in tumor progression and facilitate the identification of new therapeutic targets and strategies.

6. Outline of the thesis

Cancer is a heterogeneous disease and the presence of multiple genetically distinct foci in the primary prostate cancer supports this notion. The identification of the molecular properties of highly aggressive and metastatic subclones might facilitate the identification of new targets for therapy and putative markers for monitoring the progression of the disease.

In **Chapter 2** of this thesis, we established a microRNA signature common to three key signaling pathways in prostate cancer progression and bone metastasis formation (i.e. TGF-β, Wnt and Notch). With this approach we identified a signature of validated microRNA targeting the process of epithelial-to-mesenchymal transition (EMT) that may be critically involved in the spreading of many aggressive cells from the primary tumor and the formation of distant metastases.

Chapter 3 is focused on a candidate tumor suppressor microRNA that is downregulated in highly metastatic, stem-like $ALDH^{high}$ cells vs. non-metastatic, more differentiated $ALDH^{low}$ prostate cancer cells. We studied the functional role of miR-25 in the maintenance of aggressive behaviour of $ALDH^{high}$ compared to $ALDH^{low}$ subpopulation of cells *in vitro* and *in vivo*. Our analysis revealed that miR-25 represents an important player in the regulation of invasiveness in human prostate cancer through the interaction with at least three signaling pathways.

Chapter 4 describes a follow-up study for the regulatory role of miR-25 in human prostate cancer biology, in particular its role in the cross-talk between the TGF-β and Wnt signalling in prostate carcinogenesis and progression.

In **Chapter 5** we show that the soluble chimeric protein ALK1Fc reduces BMP-9 induced activation of Notch signaling and proliferation in human prostate cancer cells. Alk1Fc is capable of reducing tumor growth in an orthotopic model of human prostate cancer *in vivo*.

Chapter 6 contains a study about the role of Cripto and GRP78 in the maintenance of an aggressive behaviour in human prostate cancer cells *in vitro* and their role in metastatic dissemination in two different preclinical models of prostate cancer invasion and metastasis *in vivo*. The general conclusions are included in **Chapter 7**, the general discussion of this thesis.

REFERENCES

1. 2012 Cancer Statistics. <http://www.cancerresearchuk.org/health-professional/cancer-statistics/worldwide-cancer#heading-Zero>.
2. Marahatta SB, Sharma N, Koju R, Makaju RK, Petmitr P, Petmitr S. Cancer: determinants and progression. Nepal Med Coll J 2005;7(1):65-71.
3. Coleman WB, Tsongalis GJ. Molecular mechanisms of human carcinogenesis. EXS 2006(96):321-49.
4. Hanahan D, Weinberg RA. The hallmarks of cancer. Cell 2000;100(1):57-70.
5. Hanahan D, Weinberg RA. Hallmarks of cancer: the next generation. Cell 2011;144(5):646-74.
6. Pietras K, Ostman A. Hallmarks of cancer: interactions with the tumor stroma. Exp Cell Res 2010;316(8):1324-31.
7. Bhowmick NA, Neilson EG, Moses HL. Stromal fibroblasts in cancer initiation and progression. Nature 2004;432(7015):332-7.
8. Folberg R, Maniotis AJ. Vasculogenic mimicry. APMIS 2004;112(7-8):508-25.
9. Thiery JP, Acloque H, Huang RY, Nieto MA. Epithelial-mesenchymal transitions in development and disease. Cell 2009;139(5):871-90.
10. Friedl P, Locker J, Sahai E, Segall JE. Classifying collective cancer cell invasion. Nat Cell Biol 2012;14(8):777-83.
11. Warburg O. On respiratory impairment in cancer cells. Science 1956;124(3215):269-70.
12. Ward PS, Thompson CB. Metabolic reprogramming: a cancer hallmark even warburg did not anticipate. Cancer Cell 2012;21(3):297-308.
13. Dang L, White DW, Gross S, Bennett BD, Bittinger MA, Driggers EM, et al. Cancer-associated IDH1 mutations produce 2-hydroxyglutarate. Nature 2010;465(7300):966.
14. DeNardo DG, Andreu P, Coussens LM. Interactions between lymphocytes and myeloid cells regulate pro- versus anti-tumor immunity. Cancer Metastasis Rev 2010;29(2):309-16.
15. Grivennikov SI, Greten FR, Karin M. Immunity, inflammation, and cancer. Cell 2010;140(6):883-99.
16. Mougiakakos D, Choudhury A, Lladser A, Kiessling R, Johansson CC. Regulatory T cells in cancer. Adv Cancer Res 2010;107:57-117.
17. Ostrand-Rosenberg S, Sinha P. Myeloid-derived suppressor cells: linking inflammation and cancer. J Immunol 2009;182(8):4499-506.
18. Qian BZ, Pollard JW. Macrophage diversity enhances tumor progression and metastasis. Cell 2010;141(1):39-51.
19. Marusyk A, Almendro V, Polyak K. Intra-tumour heterogeneity: a looking glass for cancer? Nat Rev Cancer 2012;12(5):323-34.
20. Leissner KH, Tisell LE. The weight of the human prostate. Scand J Urol Nephrol 1979;13(2):137-42.
21. Owen DH, Katz DF. A review of the physical and chemical properties of human semen and the formulation of a semen simulant. J Androl 2005;26(4):459-69.
22. McNeal JE. Normal and pathologic anatomy of prostate. Urology 1981;17(Suppl 3):11-6.
23. McNeal JE. The zonal anatomy of the prostate. Prostate 1981;2(1):35-49.
24. Cohen RJ, Shannon BA, Phillips M, Moorin RE, Wheeler TM, Garrett KL. Central zone carcinoma of the prostate gland: a distinct tumor type with poor prognostic features. J Urol 2008;179(5):1762-7; discussion 67.
25. Lepor H. Pathophysiology, epidemiology, and natural history of benign prostatic hyperplasia. Rev Urol 2004;6 Suppl 9:S3-S10.
26. In: Liverman CT, Blazer DG, editors. Testosterone and Aging: Clinical Research Directions. Washington (DC)2004.
27. Marchetti PM, Barth JH. Clinical biochemistry of dihydrotestosterone. Ann Clin Biochem 2013;50(Pt 2):95-107.

28. Powell SM, Christiaens V, Voulgaraki D, Waxman J, Claessens F, Bevan CL. Mechanisms of androgen receptor signalling via steroid receptor coactivator-1 in prostate. Endocr Relat Cancer 2004;11(1):117-30.
29. Heinlein CA, Chang C. Androgen receptor (AR) coregulators: an overview. Endocr Rev 2002;23(2):175-200.
30. Shen MM, Abate-Shen C. Molecular genetics of prostate cancer: new prospects for old challenges. Genes Dev 2010;24(18):1967-2000.
31. Brawer MK, Peehl DM, Stamey TA, Bostwick DG. Keratin immunoreactivity in the benign and neoplastic human prostate. Cancer Res 1985;45(8):3663-7.
32. Hudson DL, Guy AT, Fry P, O'Hare MJ, Watt FM, Masters JR. Epithelial cell differentiation pathways in the human prostate: identification of intermediate phenotypes by keratin expression. J Histochem Cytochem 2001;49(2):271-8.
33. Wang X, Kruithof-de Julio M, Economides KD, Walker D, Yu H, Halili MV, et al. A luminal epithelial stem cell that is a cell of origin for prostate cancer. Nature 2009;461(7263):495-500.
34. Germann M, Wetterwald A, Guzman-Ramirez N, van der Pluijm G, Culig Z, Cecchini MG, et al. Stem-like cells with luminal progenitor phenotype survive castration in human prostate cancer. Stem Cells 2012;30(6):1076-86.
35. Arnold JT, Isaacs JT. Mechanisms involved in the progression of androgen-independent prostate cancers: it is not only the cancer cell's fault. Endocr Relat Cancer 2002;9(1):61-73.
36. Tuxhorn JA, Ayala GE, Smith MJ, Smith VC, Dang TD, Rowley DR. Reactive stroma in human prostate cancer: induction of myofibroblast phenotype and extracellular matrix remodeling. Clin Cancer Res 2002;8(9):2912-23.
37. Nagle RB, Ahmann FR, McDaniel KM, Paquin ML, Clark VA, Celniker A. Cytokeratin characterization of human prostatic carcinoma and its derived cell lines. Cancer Res 1987;47(1):281-6.
38. Bonkhoff H, Stein U, Remberger K. The proliferative function of basal cells in the normal and hyperplastic human prostate. Prostate 1994;24(3):114-8.
39. van den Hoogen C, van der Horst G, Cheung H, Buijs JT, Lippitt JM, Guzman-Ramirez N, et al. High aldehyde dehydrogenase activity identifies tumor-initiating and metastasis-initiating cells in human prostate cancer. Cancer Res 2010;70(12):5163-73.
40. Collins AT, Berry PA, Hyde C, Stower MJ, Maitland NJ. Prospective identification of tumorigenic prostate cancer stem cells. Cancer Res 2005;65(23):10946-51.
41. Lawson DA, Witte ON. Stem cells in prostate cancer initiation and progression. J Clin Invest 2007;117(8):2044-50.
42. Taylor RA, Cowin PA, Cunha GR, Pera M, Trounson AO, Pedersen J, et al. Formation of human prostate tissue from embryonic stem cells. Nat Methods 2006;3(3):179-81.
43. Noordzij MA, van Steenbrugge GJ, van der Kwast TH, Schroder FH. Neuroendocrine cells in the normal, hyperplastic and neoplastic prostate. Urol Res 1995;22(6):333-41.
44. Sciarra A, Mariotti G, Gentile V, Voria G, Pastore A, Monti S, et al. Neuroendocrine differentiation in human prostate tissue: is it detectable and treatable? BJU Int 2003;91(5):438-45.
45. di Sant'Agnese PA. Neuroendocrine differentiation in prostatic carcinoma: an update on recent developments. Ann Oncol 2001;12 Suppl 2:S135-40.
46. Potts JM. The four categories of prostatitis: a practical approach to treatment. Cleve Clin J Med 2001;68(5):389-90, 92-3, 97.
47. Isaacs JT, Coffey DS. Etiology and disease process of benign prostatic hyperplasia. Prostate Suppl 1989;2:33-50.
48. Lepor H. Medical therapy for benign prostatic hyperplasia. Urology 1993;42(5):483-501.
49. Elterman DS, Barkin J, Kaplan SA. Optimizing the management of benign prostatic hyperplasia. Ther Adv Urol 2012;4(2):77-83.

50. Bostwick DG, Cooner WH, Denis L, Jones GW, Scardino PT, Murphy GP. The association of benign prostatic hyperplasia and cancer of the prostate. Cancer 1992;70(1 Suppl):291-301.
51. SEER Stat Fact Sheets: Prostate Cancer. <http://seer.cancer.gov/statfacts/html/prost.html>.
52. Jemal A, Siegel R, Xu J, Ward E. Cancer statistics, 2010. CA Cancer J Clin 2010;60(5):277-300.
53. Yatani R, Kusano I, Shiraishi T, Hayashi T, Stemmermann GN. Latent prostatic carcinoma: pathological and epidemiological aspects. Jpn J Clin Oncol 1989;19(4):319-26.
54. McNeal JE, Bostwick DG. Intraductal dysplasia: a premalignant lesion of the prostate. Hum Pathol 1986;17(1):64-71.
55. Haggman MJ, Macoska JA, Wojno KJ, Oesterling JE. The relationship between prostatic intraepithelial neoplasia and prostate cancer: critical issues. J Urol 1997;158(1):12-22.
56. Bostwick DG. Prostatic intraepithelial neoplasia (PIN). Urology 1989;34(6 Suppl):16-22.
57. Dong JT. Chromosomal deletions and tumor suppressor genes in prostate cancer. Cancer Metastasis Rev 2001;20(3-4):173-93.
58. Lapointe J, Li C, Giacomini CP, Salari K, Huang S, Wang P, et al. Genomic profiling reveals alternative genetic pathways of prostate tumorigenesis. Cancer Res 2007;67(18):8504-10.
59. Taylor BS, Schultz N, Hieronymus H, Gopalan A, Xiao Y, Carver BS, et al. Integrative genomic profiling of human prostate cancer. Cancer Cell 2010;18(1):11-22.
60. Xu J, Zheng SL, Carpten JD, Nupponen NN, Robbins CM, Mestre J, et al. Evaluation of linkage and association of HPC2/ELAC2 in patients with familial or sporadic prostate cancer. Am J Hum Genet 2001;68(4):901-11.
61. Xu J, Zheng SL, Chang B, Smith JR, Carpten JD, Stine OC, et al. Linkage of prostate cancer susceptibility loci to chromosome 1. Hum Genet 2001;108(4):335-45.
62. Carracedo A, Pandolfi PP. The PTEN-PI3K pathway: of feedbacks and cross-talks. Oncogene 2008;27(41):5527-41.
63. Di Cristofano A, Pesce B, Cordon-Cardo C, Pandolfi PP. Pten is essential for embryonic development and tumour suppression. Nat Genet 1998;19(4):348-55.
64. Gurel B, Iwata T, Koh CM, Jenkins RB, Lan F, Van Dang C, et al. Nuclear MYC protein overexpression is an early alteration in human prostate carcinogenesis. Mod Pathol 2008;21(9):1156-67.
65. Ellwood-Yen K, Graeber TG, Wongvipat J, Iruela-Arispe ML, Zhang J, Matusik R, et al. Myc-driven murine prostate cancer shares molecular features with human prostate tumors. Cancer Cell 2003;4(3):223-38.
66. Tomlins SA, Rhodes DR, Perner S, Dhanasekaran SM, Mehra R, Sun XW, et al. Recurrent fusion of TMPRSS2 and ETS transcription factor genes in prostate cancer. Science 2005;310(5748):644-8.
67. Schultz M, Parzinger H, Posdnjakov DV, Chikisheva TA, Schmidt-Schultz TH. Oldest known case of metastasizing prostate carcinoma diagnosed in the skeleton of a 2,700-year-old Scythian king from Arzhan (Siberia, Russia). Int J Cancer 2007;121(12):2591-5.
68. Schmidt-Schultz TH, Schultz M. Bone protects proteins over thousands of years: extraction, analysis, and interpretation of extracellular matrix proteins in archeological skeletal remains. Am J Phys Anthropol 2004;123(1):30-9.
69. Schmidt-Schultz TH, Schultz M. Intact growth factors are conserved in the extracellular matrix of ancient human bone and teeth: a storehouse for the study of human evolution in health and disease. Biol Chem 2005;386(8):767-76.
70. Lilja H, Ulmert D, Vickers AJ. Prostate-specific antigen and prostate cancer: prediction, detection and monitoring. Nat Rev Cancer 2008;8(4):268-78.
71. Bussemakers MJ, van Bokhoven A, Verhaegh GW, Smit FP, Karthaus HF, Schalken JA, et al. DD3: a new prostate-specific gene, highly overexpressed in prostate cancer. Cancer Res 1999;59(23):5975-9.
72. Dijkstra S, Mulders PF, Schalken JA. Clinical use of novel urine and blood based prostate cancer biomarkers: a review. Clin Biochem 2014;47(10-11):889-96.

73. Savblom C, Malm J, Giwercman A, Nilsson JA, Berglund G, Lilja H. Blood levels of free-PSA but not complex-PSA significantly correlates to prostate release of PSA in semen in young men, while blood levels of complex-PSA, but not free-PSA increase with age. Prostate 2005;65(1):66-72.
74. Qiu SD, Young CY, Bilhartz DL, Prescott JL, Farrow GM, He WW, et al. In situ hybridization of prostate-specific antigen mRNA in human prostate. J Urol 1990;144(6):1550-6.
75. Epstein JI, Allsbrook WC, Jr., Amin MB, Egevad LL, Committee IG. The 2005 International Society of Urological Pathology (ISUP) Consensus Conference on Gleason Grading of Prostatic Carcinoma. Am J Surg Pathol 2005;29(9):1228-42.
76. Mellinger GT, Gleason D, Bailar J, 3rd. The histology and prognosis of prostatic cancer. J Urol 1967;97(2):331-7.
77. Gleason DF, Mellinger GT. Prediction of prognosis for prostatic adenocarcinoma by combined histological grading and clinical staging. J Urol 1974;111(1):58-64.
78. Epstein JI. Update on the Gleason grading system. Ann Pathol 2011;31(5 Suppl):S20-6.
79. Humphrey PA. Gleason grading and prognostic factors in carcinoma of the prostate. Mod Pathol 2004;17(3):292-306.
80. Ohori M, Wheeler TM, Scardino PT. The New American Joint Committee on Cancer and International Union Against Cancer TNM classification of prostate cancer. Clinicopathologic correlations. Cancer 1994;74(1):104-14.
81. Godtman RA, Holmberg E, Khatami A, Stranne J, Hugosson J. Outcome following active surveillance of men with screen-detected prostate cancer. Results from the Goteborg randomised population-based prostate cancer screening trial. Eur Urol 2013;63(1):101-7.
82. Hayes JH, Ollendorf DA, Pearson SD, Barry MJ, Kantoff PW, Lee PA, et al. Observation versus initial treatment for men with localized, low-risk prostate cancer: a cost-effectiveness analysis. Ann Intern Med 2013;158(12):853-60.
83. Lund L, Svolgaard N, Poulsen MH. Prostate cancer: a review of active surveillance. Res Rep Urol 2014;6:107-12.
84. Cooperberg MR, Carroll PR, Klotz L. Active surveillance for prostate cancer: progress and promise. J Clin Oncol 2011;29(27):3669-76.
85. Adolfsson J. Watchful waiting and active surveillance: the current position. BJU Int 2008;102(1):10-4.
86. Bianco FJ, Jr., Scardino PT, Eastham JA. Radical prostatectomy: long-term cancer control and recovery of sexual and urinary function ("trifecta"). Urology 2005;66(5 Suppl):83-94.
87. Heidenreich A, Bastian PJ, Bellmunt J, Bolla M, Joniau S, van der Kwast T, et al. EAU guidelines on prostate cancer. part 1: screening, diagnosis, and local treatment with curative intent-update 2013. Eur Urol 2014;65(1):124-37.
88. Allen B. Systemic targeted alpha radiotherapy for cancer. J Biomed Phys Eng 2013;3(3):67-80.
89. Bauman G, Rumble RB, Chen J, Loblaw A, Warde P, Members of the IIEP. Intensity-modulated radiotherapy in the treatment of prostate cancer. Clin Oncol (R Coll Radiol) 2012;24(7):461-73.
90. Eton DT, Lepore SJ, Helgeson VS. Early quality of life in patients with localized prostate carcinoma: an examination of treatment-related, demographic, and psychosocial factors. Cancer 2001;92(6):1451-9.
91. Humphrey PA. Diagnosis of adenocarcinoma in prostate needle biopsy tissue. J Clin Pathol 2007;60(1):35-42.
92. Taylor RA, Toivanen R, Frydenberg M, Pedersen J, Harewood L, Australian Prostate Cancer B, et al. Human epithelial basal cells are cells of origin of prostate cancer, independent of CD133 status. Stem Cells 2012;30(6):1087-96.
93. Hirano D, Okada Y, Minei S, Takimoto Y, Nemoto N. Neuroendocrine differentiation in hormone refractory prostate cancer following androgen deprivation therapy. Eur Urol 2004;45(5):586-92; discussion 92.

94. Kokubo H, Yamada Y, Nishio Y, Fukatsu H, Honda N, Nakagawa A, et al. Immunohistochemical study of chromogranin A in Stage D2 prostate cancer. Urology 2005;66(1):135-40.
95. Carles J, Castellano D, Climent MA, Maroto P, Medina R, Alcaraz A. Castration-resistant metastatic prostate cancer: current status and treatment possibilities. Clin Transl Oncol 2012;14(3):169-76.
96. Nathoo N, Caris EC, Wiener JA, Mendel E. History of the vertebral venous plexus and the significant contributions of Breschet and Batson. Neurosurgery 2011;69(5):1007-14; discussion 14.
97. Dodds PR, Caride VJ, Lytton B. The role of vertebral veins in the dissemination of prostatic carcinoma. J Urol 1981;126(6):753-5.
98. Honn KV, Tang DG. Adhesion molecules and tumor cell interaction with endothelium and subendothelial matrix. Cancer Metastasis Rev 1992;11(3-4):353-75.
99. Wang J, Loberg R, Taichman RS. The pivotal role of CXCL12 (SDF-1)/CXCR4 axis in bone metastasis. Cancer Metastasis Rev 2006;25(4):573-87.
100. Sun YX, Schneider A, Jung Y, Wang J, Dai J, Wang J, et al. Skeletal localization and neutralization of the SDF-1(CXCL12)/CXCR4 axis blocks prostate cancer metastasis and growth in osseous sites in vivo. J Bone Miner Res 2005;20(2):318-29.
101. Schneider JG, Amend SR, Weilbaecher KN. Integrins and bone metastasis: integrating tumor cell and stromal cell interactions. Bone 2011;48(1):54-65.
102. Farias E, Lu M, Li X, Schnapp LM. Integrin alpha8beta1-fibronectin interactions promote cell survival via PI3 kinase pathway. Biochem Biophys Res Commun 2005;329(1):305-11.
103. Weilbaecher KN, Guise TA, McCauley LK. Cancer to bone: a fatal attraction. Nat Rev Cancer 2011;11(6):411-25.
104. Ghotra VP, He S, van der Horst G, Nijhoff S, de Bont H, Lekkerkerker A, et al. SYK is a candidate kinase target for the treatment of advanced prostate cancer. Cancer Res 2015;75(1):230-40.
105. Paget S. The distribution of secondary growths in cancer of the breast. 1889. Cancer Metastasis Rev 1989;8(2):98-101.
106. Ozdemir BC, Hensel J, Secondini C, Wetterwald A, Schwaninger R, Fleischmann A, et al. The molecular signature of the stroma response in prostate cancer-induced osteoblastic bone metastasis highlights expansion of hematopoietic and prostate epithelial stem cell niches. PLoS One 2014;9(12):e114530.
107. Kaplan RN, Rafii S, Lyden D. Preparing the "soil": the premetastatic niche. Cancer Res 2006;66(23):11089-93.
108. Kaplan RN, Psaila B, Lyden D. Bone marrow cells in the 'pre-metastatic niche': within bone and beyond. Cancer Metastasis Rev 2006;25(4):521-9.
109. Hiratsuka S, Watanabe A, Aburatani H, Maru Y. Tumour-mediated upregulation of chemoattractants and recruitment of myeloid cells predetermines lung metastasis. Nat Cell Biol 2006;8(12):1369-75.
110. Kitamura T, Qian BZ, Pollard JW. Immune cell promotion of metastasis. Nat Rev Immunol 2015;15(2):73-86.
111. Erler JT, Bennewith KL, Cox TR, Lang G, Bird D, Koong A, et al. Hypoxia-induced lysyl oxidase is a critical mediator of bone marrow cell recruitment to form the premetastatic niche. Cancer Cell 2009;15(1):35-44.
112. Hirakawa S, Brown LF, Kodama S, Paavonen K, Alitalo K, Detmar M. VEGF-C-induced lymphangiogenesis in sentinel lymph nodes promotes tumor metastasis to distant sites. Blood 2007;109(3):1010-7.
113. Alderton GK. Metastasis. Exosomes drive premetastatic niche formation. Nat Rev Cancer 2012;12(7):447.
114. Sanchez CA, Andahur EI, Valenzuela R, Castellon EA, Fulla JA, Ramos CG, et al. Exosomes from bulk and stem cells from human prostate cancer have a differential microRNA content that contributes cooperatively over local and pre-metastatic niche. Oncotarget 2015.

115. Torsvik A, Bjerkvig R. Mesenchymal stem cell signaling in cancer progression. Cancer Treat Rev 2013;39(2):180-8.
116. Mueller MM, Fusenig NE. Friends or foes - bipolar effects of the tumour stroma in cancer. Nat Rev Cancer 2004;4(11):839-49.
117. Stetler-Stevenson WG, Yu AE. Proteases in invasion: matrix metalloproteinases. Semin Cancer Biol 2001;11(2):143-52.
118. Zhu ML, Kyprianou N. Role of androgens and the androgen receptor in epithelial-mesenchymal transition and invasion of prostate cancer cells. FASEB J 2010;24(3):769-77.
119. Sun Y, Wang BE, Leong KG, Yue P, Li L, Jhunjhunwala S, et al. Androgen deprivation causes epithelial-mesenchymal transition in the prostate: implications for androgen-deprivation therapy. Cancer Res 2012;72(2):527-36.
120. van der Pluijm G. Epithelial plasticity, cancer stem cells and bone metastasis formation. Bone 2011;48(1):37-43.
121. Puhr M, Hoefer J, Schafer G, Erb HH, Oh SJ, Klocker H, et al. Epithelial-to-mesenchymal transition leads to docetaxel resistance in prostate cancer and is mediated by reduced expression of miR-200c and miR-205. Am J Pathol 2012;181(6):2188-201.
122. Bonnomet A, Brysse A, Tachsidis A, Waltham M, Thompson EW, Polette M, et al. Epithelial-to-mesenchymal transitions and circulating tumor cells. J Mammary Gland Biol Neoplasia 2010;15(2):261-73.
123. Brabletz T. To differentiate or not--routes towards metastasis. Nat Rev Cancer 2012;12(6):425-36.
124. Kienast Y, von Baumgarten L, Fuhrmann M, Klinkert WE, Goldbrunner R, Herms J, et al. Real-time imaging reveals the single steps of brain metastasis formation. Nat Med 2010;16(1):116-22.
125. Psaila B, Lyden D. The metastatic niche: adapting the foreign soil. Nat Rev Cancer 2009;9(4):285-93.
126. Sleeman JP. The metastatic niche and stromal progression. Cancer Metastasis Rev 2012;31(3-4):429-40.
127. Shiozawa Y, Pedersen EA, Havens AM, Jung Y, Mishra A, Joseph J, et al. Human prostate cancer metastases target the hematopoietic stem cell niche to establish footholds in mouse bone marrow. J Clin Invest 2011;121(4):1298-312.
128. Sneddon JB, Werb Z. Location, location, location: the cancer stem cell niche. Cell Stem Cell 2007;1(6):607-11.
129. Hensel J, Thalmann GN. Biology of Bone Metastases in Prostate Cancer. Urology 2016.
130. Sosa MS, Bragado P, Aguirre-Ghiso JA. Mechanisms of disseminated cancer cell dormancy: an awakening field. Nat Rev Cancer 2014;14(9):611-22.
131. Aguirre-Ghiso JA. Models, mechanisms and clinical evidence for cancer dormancy. Nat Rev Cancer 2007;7(11):834-46.
132. Barkan D, El Touny LH, Michalowski AM, Smith JA, Chu I, Davis AS, et al. Metastatic growth from dormant cells induced by a col-I-enriched fibrotic environment. Cancer Res 2010;70(14):5706-16.
133. Mundy GR. Metastasis to bone: causes, consequences and therapeutic opportunities. Nat Rev Cancer 2002;2(8):584-93.
134. Kusumbe AP, Ramasamy SK, Adams RH. Coupling of angiogenesis and osteogenesis by a specific vessel subtype in bone. Nature 2014;507(7492):323-8.
135. Wang L, Benedito R, Bixel MG, Zeuschner D, Stehling M, Savendahl L, et al. Identification of a clonally expanding haematopoietic compartment in bone marrow. EMBO J 2013;32(2):219-30.
136. Logothetis CJ, Lin SH. Osteoblasts in prostate cancer metastasis to bone. Nat Rev Cancer 2005;5(1):21-8.
137. Theriault RL, Theriault RL. Biology of bone metastases. Cancer Control 2012;19(2):92-101.

138. Dai J, Keller J, Zhang J, Lu Y, Yao Z, Keller ET. Bone morphogenetic protein-6 promotes osteoblastic prostate cancer bone metastases through a dual mechanism. Cancer Res 2005;65(18):8274-85.
139. Schwaninger R, Rentsch CA, Wetterwald A, van der Horst G, van Bezooijen RL, van der Pluijm G, et al. Lack of noggin expression by cancer cells is a determinant of the osteoblast response in bone metastases. Am J Pathol 2007;170(1):160-75.
140. Rubin J, Chung LW, Fan X, Zhu L, Murphy TC, Nanes MS, et al. Prostate carcinoma cells that have resided in bone have an upregulated IGF-I axis. Prostate 2004;58(1):41-9.
141. Yang YQ, Tan YY, Wong R, Wenden A, Zhang LK, Rabie AB. The role of vascular endothelial growth factor in ossification. Int J Oral Sci 2012;4(2):64-8.
142. Milat F, Ng KW. Is Wnt signalling the final common pathway leading to bone formation? Mol Cell Endocrinol 2009;310(1-2):52-62.
143. Lynch CC, Hikosaka A, Acuff HB, Martin MD, Kawai N, Singh RK, et al. MMP-7 promotes prostate cancer-induced osteolysis via the solubilization of RANKL. Cancer Cell 2005;7(5):485-96.
144. Secondini C, Wetterwald A, Schwaninger R, Thalmann GN, Cecchini MG. The role of the BMP signaling antagonist noggin in the development of prostate cancer osteolytic bone metastasis. PLoS One 2011;6(1):e16078.
145. Roodman GD. Mechanisms of bone metastasis. N Engl J Med 2004;350(16):1655-64.
146. Liao J, Schneider A, Datta NS, McCauley LK. Extracellular calcium as a candidate mediator of prostate cancer skeletal metastasis. Cancer Res 2006;66(18):9065-73.
147. Sanders JL, Chattopadhyay N, Kifor O, Yamaguchi T, Butters RR, Brown EM. Extracellular calcium-sensing receptor expression and its potential role in regulating parathyroid hormone-related peptide secretion in human breast cancer cell lines. Endocrinology 2000;141(12):4357-64.
148. Sasaki A, Boyce BF, Story B, Wright KR, Chapman M, Boyce R, et al. Bisphosphonate risedronate reduces metastatic human breast cancer burden in bone in nude mice. Cancer Res 1995;55(16):3551-7.
149. van der Pluijm G, Que I, Sijmons B, Buijs JT, Lowik CW, Wetterwald A, et al. Interference with the microenvironmental support impairs the de novo formation of bone metastases in vivo. Cancer Res 2005;65(17):7682-90.
150. Yuen KK, Shelley M, Sze WM, Wilt T, Mason MD. Bisphosphonates for advanced prostate cancer. Cochrane Database Syst Rev 2006(4):CD006250.
151. Huggins C, Hodges CV. Studies on prostatic cancer. I. The effect of castration, of estrogen and androgen injection on serum phosphatases in metastatic carcinoma of the prostate. CA Cancer J Clin 1972;22(4):232-40.
152. Heidenreich A, Bastian PJ, Bellmunt J, Bolla M, Joniau S, van der Kwast T, et al. EAU guidelines on prostate cancer. Part II: Treatment of advanced, relapsing, and castration-resistant prostate cancer. Eur Urol 2014;65(2):467-79.
153. Tran C, Ouk S, Clegg NJ, Chen Y, Watson PA, Arora V, et al. Development of a second-generation antiandrogen for treatment of advanced prostate cancer. Science 2009;324(5928):787-90.
154. Uchio EM, Aslan M, Wells CK, Calderone J, Concato J. Impact of biochemical recurrence in prostate cancer among US veterans. Arch Intern Med 2010;170(15):1390-5.
155. Visakorpi T, Hyytinen E, Koivisto P, Tanner M, Keinanen R, Palmberg C, et al. In vivo amplification of the androgen receptor gene and progression of human prostate cancer. Nat Genet 1995;9(4):401-6.
156. Koivisto P, Kononen J, Palmberg C, Tammela T, Hyytinen E, Isola J, et al. Androgen receptor gene amplification: a possible molecular mechanism for androgen deprivation therapy failure in prostate cancer. Cancer Res 1997;57(2):314-9.

157. Linja MJ, Savinainen KJ, Saramaki OR, Tammela TL, Vessella RL, Visakorpi T. Amplification and overexpression of androgen receptor gene in hormone-refractory prostate cancer. Cancer Res 2001;61(9):3550-5.
158. Taplin ME, Bubley GJ, Shuster TD, Frantz ME, Spooner AE, Ogata GK, et al. Mutation of the androgen-receptor gene in metastatic androgen-independent prostate cancer. N Engl J Med 1995;332(21):1393-8.
159. Zhao XY, Malloy PJ, Krishnan AV, Swami S, Navone NM, Peehl DM, et al. Glucocorticoids can promote androgen-independent growth of prostate cancer cells through a mutated androgen receptor. Nat Med 2000;6(6):703-6.
160. Robzyk K, Oen H, Buchanan G, Butler LM, Tilley WD, Mandal AK, et al. Uncoupling of hormone-dependence from chaperone-dependence in the L701H mutation of the androgen receptor. Mol Cell Endocrinol 2007;268(1-2):67-74.
161. Brooke GN, Parker MG, Bevan CL. Mechanisms of androgen receptor activation in advanced prostate cancer: differential co-activator recruitment and gene expression. Oncogene 2008;27(21):2941-50.
162. Steinkamp MP, O'Mahony OA, Brogley M, Rehman H, Lapensee EW, Dhanasekaran S, et al. Treatment-dependent androgen receptor mutations in prostate cancer exploit multiple mechanisms to evade therapy. Cancer Res 2009;69(10):4434-42.
163. Dehm SM, Schmidt LJ, Heemers HV, Vessella RL, Tindall DJ. Splicing of a novel androgen receptor exon generates a constitutively active androgen receptor that mediates prostate cancer therapy resistance. Cancer Res 2008;68(13):5469-77.
164. Guo Z, Yang X, Sun F, Jiang R, Linn DE, Chen H, et al. A novel androgen receptor splice variant is up-regulated during prostate cancer progression and promotes androgen depletion-resistant growth. Cancer Res 2009;69(6):2305-13.
165. Hu R, Dunn TA, Wei S, Isharwal S, Veltri RW, Humphreys E, et al. Ligand-independent androgen receptor variants derived from splicing of cryptic exons signify hormone-refractory prostate cancer. Cancer Res 2009;69(1):16-22.
166. Titus MA, Schell MJ, Lih FB, Tomer KB, Mohler JL. Testosterone and dihydrotestosterone tissue levels in recurrent prostate cancer. Clin Cancer Res 2005;11(13):4653-7.
167. Stanbrough M, Bubley GJ, Ross K, Golub TR, Rubin MA, Penning TM, et al. Increased expression of genes converting adrenal androgens to testosterone in androgen-independent prostate cancer. Cancer Res 2006;66(5):2815-25.
168. Locke JA, Guns ES, Lubik AA, Adomat HH, Hendy SC, Wood CA, et al. Androgen levels increase by intratumoral de novo steroidogenesis during progression of castration-resistant prostate cancer. Cancer Res 2008;68(15):6407-15.
169. Montgomery RB, Mostaghel EA, Vessella R, Hess DL, Kalhorn TF, Higano CS, et al. Maintenance of intratumoral androgens in metastatic prostate cancer: a mechanism for castration-resistant tumor growth. Cancer Res 2008;68(11):4447-54.
170. Tannock IF, de Wit R, Berry WR, Horti J, Pluzanska A, Chi KN, et al. Docetaxel plus prednisone or mitoxantrone plus prednisone for advanced prostate cancer. N Engl J Med 2004;351(15):1502-12.
171. de Bono JS, Oudard S, Ozguroglu M, Hansen S, Machiels JP, Kocak I, et al. Prednisone plus cabazitaxel or mitoxantrone for metastatic castration-resistant prostate cancer progressing after docetaxel treatment: a randomised open-label trial. Lancet 2010;376(9747):1147-54.
172. de Bono JS, Logothetis CJ, Molina A, Fizazi K, North S, Chu L, et al. Abiraterone and increased survival in metastatic prostate cancer. N Engl J Med 2011;364(21):1995-2005.
173. Fizazi K, Scher HI, Molina A, Logothetis CJ, Chi KN, Jones RJ, et al. Abiraterone acetate for treatment of metastatic castration-resistant prostate cancer: final overall survival analysis of the COU-AA-301 randomised, double-blind, placebo-controlled phase 3 study. Lancet Oncol 2012;13(10):983-92.

174. Scher HI, Fizazi K, Saad F, Taplin ME, Sternberg CN, Miller K, et al. Increased survival with enzalutamide in prostate cancer after chemotherapy. N Engl J Med 2012;367(13):1187-97.
175. van Soest RJ, de Wit R. Irrefutable evidence for the use of docetaxel in newly diagnosed metastatic prostate cancer: results from the STAMPEDE and CHAARTED trials. BMC Med 2015;13(1):304.
176. Fizazi K, Faivre L, Lesaunier F, Delva R, Gravis G, Rolland F, et al. Androgen deprivation therapy plus docetaxel and estramustine versus androgen deprivation therapy alone for high-risk localised prostate cancer (GETUG 12): a phase 3 randomised controlled trial. Lancet Oncol 2015;16(7):787-94.
177. Grisanzio C, Signoretti S. p63 in prostate biology and pathology. J Cell Biochem 2008;103(5):1354-68.
178. Richardson GD, Robson CN, Lang SH, Neal DE, Maitland NJ, Collins AT. CD133, a novel marker for human prostatic epithelial stem cells. J Cell Sci 2004;117(Pt 16):3539-45.
179. Maitland NJ, Frame FM, Polson ES, Lewis JL, Collins AT. Prostate cancer stem cells: do they have a basal or luminal phenotype? Horm Cancer 2011;2(1):47-61.
180. Hurt EM, Kawasaki BT, Klarmann GJ, Thomas SB, Farrar WL. CD44+ CD24(-) prostate cells are early cancer progenitor/stem cells that provide a model for patients with poor prognosis. Br J Cancer 2008;98(4):756-65.
181. Goldstein AS, Lawson DA, Cheng D, Sun W, Garraway IP, Witte ON. Trop2 identifies a subpopulation of murine and human prostate basal cells with stem cell characteristics. Proc Natl Acad Sci U S A 2008;105(52):20882-7.
182. Liu AY, Roudier MP, True LD. Heterogeneity in primary and metastatic prostate cancer as defined by cell surface CD profile. Am J Pathol 2004;165(5):1543-56.
183. Karthaus WR, Iaquinta PJ, Drost J, Gracanin A, van Boxtel R, Wongvipat J, et al. Identification of multipotent luminal progenitor cells in human prostate organoid cultures. Cell 2014;159(1):163-75.
184. Eaton CL, Colombel M, van der Pluijm G, Cecchini M, Wetterwald A, Lippitt J, et al. Evaluation of the frequency of putative prostate cancer stem cells in primary and metastatic prostate cancer. Prostate 2010;70(8):875-82.
185. Colombel M, Eaton CL, Hamdy F, Ricci E, van der Pluijm G, Cecchini M, et al. Increased expression of putative cancer stem cell markers in primary prostate cancer is associated with progression of bone metastases. Prostate 2012;72(7):713-20.
186. Maitland NJ, Collins AT. Prostate cancer stem cells: a new target for therapy. J Clin Oncol 2008;26(17):2862-70.
187. Dean M, Fojo T, Bates S. Tumour stem cells and drug resistance. Nat Rev Cancer 2005;5(4):275-84.
188. Kypta RM, Waxman J. Wnt/beta-catenin signalling in prostate cancer. Nat Rev Urol 2012;9(8):418-28.
189. Verras M, Sun Z. Roles and regulation of Wnt signaling and beta-catenin in prostate cancer. Cancer Lett 2006;237(1):22-32.
190. Terry S, Yang X, Chen MW, Vacherot F, Buttyan R. Multifaceted interaction between the androgen and Wnt signaling pathways and the implication for prostate cancer. J Cell Biochem 2006;99(2):402-10.
191. Robinson DR, Zylstra CR, Williams BO. Wnt signaling and prostate cancer. Curr Drug Targets 2008;9(7):571-80.
192. Wang G, Wang J, Sadar MD. Crosstalk between the androgen receptor and beta-catenin in castrate-resistant prostate cancer. Cancer Res 2008;68(23):9918-27.
193. Semenov M, Tamai K, He X. SOST is a ligand for LRP5/LRP6 and a Wnt signaling inhibitor. J Biol Chem 2005;280(29):26770-5.

194. Rentsch CA, Cecchini MG, Thalmann GN. Loss of inhibition over master pathways of bone mass regulation results in osteosclerotic bone metastases in prostate cancer. Swiss Med Wkly 2009;139(15-16):220-5.
195. Wang Y. Wnt/Planar cell polarity signaling: a new paradigm for cancer therapy. Mol Cancer Ther 2009;8(8):2103-9.
196. Veeman MT, Axelrod JD, Moon RT. A second canon. Functions and mechanisms of beta-catenin-independent Wnt signaling. Dev Cell 2003;5(3):367-77.
197. Davies G, Jiang WG, Mason MD. Cell-cell adhesion molecules and signaling intermediates and their role in the invasive potential of prostate cancer cells. J Urol 2000;163(3):985-92.
198. Carvalho FL, Simons BW, Eberhart CG, Berman DM. Notch signaling in prostate cancer: a moving target. Prostate 2014;74(9):933-45.
199. Domingo-Domenech J, Vidal SJ, Rodriguez-Bravo V, Castillo-Martin M, Quinn SA, Rodriguez-Barrueco R, et al. Suppression of acquired docetaxel resistance in prostate cancer through depletion of notch- and hedgehog-dependent tumor-initiating cells. Cancer Cell 2012;22(3):373-88.
200. Zoni E, van der Pluijm G, Gray PC, Kruithof-de Julio M. Epithelial Plasticity in Cancer: Unmasking a MicroRNA Network for TGF-beta-, Notch-, and Wnt-Mediated EMT. J Oncol 2015;2015:198967.
201. Collu GM, Hidalgo-Sastre A, Brennan K. Wnt-Notch signalling crosstalk in development and disease. Cell Mol Life Sci 2014;71(18):3553-67.
202. Han L, Diehl A, Nguyen NK, Korangath P, Teo W, Cho S, et al. The Notch pathway inhibits TGFbeta signaling in breast cancer through HEYL-mediated crosstalk. Cancer Res 2014;74(22):6509-18.
203. Villaronga MA, Bevan CL, Belandia B. Notch signaling: a potential therapeutic target in prostate cancer. Curr Cancer Drug Targets 2008;8(7):566-80.
204. Belandia B, Powell SM, Garcia-Pedrero JM, Walker MM, Bevan CL, Parker MG. Hey1, a mediator of notch signaling, is an androgen receptor corepressor. Mol Cell Biol 2005;25(4):1425-36.
205. Hales EC, Taub JW, Matherly LH. New insights into Notch1 regulation of the PI3K-AKT-mTOR1 signaling axis: targeted therapy of gamma-secretase inhibitor resistant T-cell acute lymphoblastic leukemia. Cell Signal 2014;26(1):149-61.
206. Grishina IB, Kim SY, Ferrara C, Makarenkova HP, Walden PD. BMP7 inhibits branching morphogenesis in the prostate gland and interferes with Notch signaling. Dev Biol 2005;288(2):334-47.
207. Ghosh S, Lau H, Simons BW, Powell JD, Meyers DJ, De Marzo AM, et al. PI3K/mTOR signaling regulates prostatic branching morphogenesis. Dev Biol 2011;360(2):329-42.
208. Whelan JT, Kellogg A, Shewchuk BM, Hewan-Lowe K, Bertrand FE. Notch-1 signaling is lost in prostate adenocarcinoma and promotes PTEN gene expression. J Cell Biochem 2009;107(5):992-1001.
209. Carver BS, Chapinski C, Wongvipat J, Hieronymus H, Chen Y, Chandarlapaty S, et al. Reciprocal feedback regulation of PI3K and androgen receptor signaling in PTEN-deficient prostate cancer. Cancer Cell 2011;19(5):575-86.
210. Pourmand G, Ziaee AA, Abedi AR, Mehrsai A, Alavi HA, Ahmadi A, et al. Role of PTEN gene in progression of prostate cancer. Urol J 2007;4(2):95-100.
211. Santagata S, Demichelis F, Riva A, Varambally S, Hofer MD, Kutok JL, et al. JAGGED1 expression is associated with prostate cancer metastasis and recurrence. Cancer Res 2004;64(19):6854-7.
212. Sethi N, Kang Y. Notch signalling in cancer progression and bone metastasis. Br J Cancer 2011;105(12):1805-10.
213. Sethi N, Dai X, Winter CG, Kang Y. Tumor-derived JAGGED1 promotes osteolytic bone metastasis of breast cancer by engaging notch signaling in bone cells. Cancer Cell 2011;19(2):192-205.

214. Cui D, Dai J, Keller JM, Mizokami A, Xia S, Keller ET. Notch Pathway Inhibition Using PF-03084014, a gamma-Secretase Inhibitor (GSI), Enhances the Antitumor Effect of Docetaxel in Prostate Cancer. Clin Cancer Res 2015;21(20):4619-29.
215. Jones E, Pu H, Kyprianou N. Targeting TGF-beta in prostate cancer: therapeutic possibilities during tumor progression. Expert Opin Ther Targets 2009;13(2):227-34.
216. Kalluri R, Weinberg RA. The basics of epithelial-mesenchymal transition. J Clin Invest 2009;119(6):1420-8.
217. Massague J, Blain SW, Lo RS. TGFbeta signaling in growth control, cancer, and heritable disorders. Cell 2000;103(2):295-309.
218. Massague J. TGFbeta in Cancer. Cell 2008;134(2):215-30.
219. Wu MY, Hill CS. Tgf-beta superfamily signaling in embryonic development and homeostasis. Dev Cell 2009;16(3):329-43.
220. Chen D, Zhao M, Mundy GR. Bone morphogenetic proteins. Growth Factors 2004;22(4):233-41.
221. Franzen P, ten Dijke P, Ichijo H, Yamashita H, Schulz P, Heldin CH, et al. Cloning of a TGF beta type I receptor that forms a heteromeric complex with the TGF beta type II receptor. Cell 1993;75(4):681-92.
222. ten Dijke P, Ichijo H, Franzen P, Schulz P, Saras J, Toyoshima H, et al. Activin receptor-like kinases: a novel subclass of cell-surface receptors with predicted serine/threonine kinase activity. Oncogene 1993;8(10):2879-87.
223. ten Dijke P, Yamashita H, Sampath TK, Reddi AH, Estevez M, Riddle DL, et al. Identification of type I receptors for osteogenic protein-1 and bone morphogenetic protein-4. J Biol Chem 1994;269(25):16985-8.
224. Yamashita H, ten Dijke P, Huylebroeck D, Sampath TK, Andries M, Smith JC, et al. Osteogenic protein-1 binds to activin type II receptors and induces certain activin-like effects. J Cell Biol 1995;130(1):217-26.
225. Liu F, Ventura F, Doody J, Massague J. Human type II receptor for bone morphogenic proteins (BMPs): extension of the two-kinase receptor model to the BMPs. Mol Cell Biol 1995;15(7):3479-86.
226. Nohno T, Ishikawa T, Saito T, Hosokawa K, Noji S, Wolsing DH, et al. Identification of a human type II receptor for bone morphogenetic protein-4 that forms differential heteromeric complexes with bone morphogenetic protein type I receptors. J Biol Chem 1995;270(38):22522-6.
227. Ebisawa T, Tada K, Kitajima I, Tojo K, Sampath TK, Kawabata M, et al. Characterization of bone morphogenetic protein-6 signaling pathways in osteoblast differentiation. J Cell Sci 1999;112 (Pt 20):3519-27.
228. Aoki H, Fujii M, Imamura T, Yagi K, Takehara K, Kato M, et al. Synergistic effects of different bone morphogenetic protein type I receptors on alkaline phosphatase induction. J Cell Sci 2001;114(Pt 8):1483-9.
229. Rosenzweig BL, Imamura T, Okadome T, Cox GN, Yamashita H, ten Dijke P, et al. Cloning and characterization of a human type II receptor for bone morphogenetic proteins. Proc Natl Acad Sci U S A 1995;92(17):7632-6.
230. Scharpfenecker M, van Dinther M, Liu Z, van Bezooijen RL, Zhao Q, Pukac L, et al. BMP-9 signals via ALK1 and inhibits bFGF-induced endothelial cell proliferation and VEGF-stimulated angiogenesis. J Cell Sci 2007;120(Pt 6):964-72.
231. David L, Mallet C, Mazerbourg S, Feige JJ, Bailly S. Identification of BMP9 and BMP10 as functional activators of the orphan activin receptor-like kinase 1 (ALK1) in endothelial cells. Blood 2007;109(5):1953-61.
232. Wu Y, Zhou BP. New insights of epithelial-mesenchymal transition in cancer metastasis. Acta Biochim Biophys Sin (Shanghai) 2008;40(7):643-50.
233. Shi Y, Massague J. Mechanisms of TGF-beta signaling from cell membrane to the nucleus. Cell 2003;113(6):685-700.

234. Moustakas A, Heldin CH. Non-Smad TGF-beta signals. J Cell Sci 2005;118(Pt 16):3573-84.
235. Pardali K, Moustakas A. Actions of TGF-beta as tumor suppressor and pro-metastatic factor in human cancer. Biochim Biophys Acta 2007;1775(1):21-62.
236. Zhang YE. Non-Smad pathways in TGF-beta signaling. Cell Res 2009;19(1):128-39.
237. Lonn P, Moren A, Raja E, Dahl M, Moustakas A. Regulating the stability of TGFbeta receptors and Smads. Cell Res 2009;19(1):21-35.
238. Danen EH, Sonnenberg A. Integrins in regulation of tissue development and function. J Pathol 2003;200(4):471-80.
239. Danen EH. Integrins: regulators of tissue function and cancer progression. Curr Pharm Des 2005;11(7):881-91.
240. Hynes RO. Integrins: bidirectional, allosteric signaling machines. Cell 2002;110(6):673-87.
241. Pontes-Junior J, Reis ST, Dall'Oglio M, Neves de Oliveira LC, Cury J, Carvalho PA, et al. Evaluation of the expression of integrins and cell adhesion molecules through tissue microarray in lymph node metastases of prostate cancer. J Carcinog 2009;8:3.
242. Kikkawa H, Kaihou M, Horaguchi N, Uchida T, Imafuku H, Takiguchi A, et al. Role of integrin alpha(v)beta3 in the early phase of liver metastasis: PET and IVM analyses. Clin Exp Metastasis 2002;19(8):717-25.
243. Enns A, Korb T, Schluter K, Gassmann P, Spiegel HU, Senninger N, et al. Alphavbeta5-integrins mediate early steps of metastasis formation. Eur J Cancer 2005;41(7):1065-72.
244. Margadant C, Sonnenberg A. Integrin-TGF-beta crosstalk in fibrosis, cancer and wound healing. EMBO Rep 2010;11(2):97-105.
245. Xiong J, Balcioglu HE, Danen EH. Integrin signaling in control of tumor growth and progression. Int J Biochem Cell Biol 2013;45(5):1012-5.
246. Truong H, Danen EH. Integrin switching modulates adhesion dynamics and cell migration. Cell Adh Migr 2009;3(2):179-81.
247. Yamada KM, Even-Ram S. Integrin regulation of growth factor receptors. Nat Cell Biol 2002;4(4):E75-6.
248. Chen Q, Lin TH, Der CJ, Juliano RL. Integrin-mediated activation of MEK and mitogen-activated protein kinase is independent of Ras [corrected]. J Biol Chem 1996;271(30):18122-7.
249. Figel S, Gelman IH. Focal adhesion kinase controls prostate cancer progression via intrinsic kinase and scaffolding functions. Anticancer Agents Med Chem 2011;11(7):607-16.
250. Keller ET, Fu Z, Yeung K, Brennan M. Raf kinase inhibitor protein: a prostate cancer metastasis suppressor gene. Cancer Lett 2004;207(2):131-7.
251. Fornaro M, Manes T, Languino LR. Integrins and prostate cancer metastases. Cancer Metastasis Rev 2001;20(3-4):321-31.
252. Ren B, Yu YP, Tseng GC, Wu C, Chen K, Rao UN, et al. Analysis of integrin alpha7 mutations in prostate cancer, liver cancer, glioblastoma multiforme, and leiomyosarcoma. J Natl Cancer Inst 2007;99(11):868-80.
253. Bonkhoff H, Stein U, Remberger K. Differential expression of alpha 6 and alpha 2 very late antigen integrins in the normal, hyperplastic, and neoplastic prostate: simultaneous demonstration of cell surface receptors and their extracellular ligands. Hum Pathol 1993;24(3):243-8.
254. King TE, Pawar SC, Majuta L, Sroka IC, Wynn D, Demetriou MC, et al. The role of alpha 6 integrin in prostate cancer migration and bone pain in a novel xenograft model. PLoS One 2008;3(10):e3535.
255. van den Hoogen C, van der Horst G, Cheung H, Buijs JT, Pelger RC, van der Pluijm G. Integrin alphav expression is required for the acquisition of a metastatic stem/progenitor cell phenotype in human prostate cancer. Am J Pathol 2011;179(5):2559-68.
256. van der Horst G, van den Hoogen C, Buijs JT, Cheung H, Bloys H, Pelger RC, et al. Targeting of alpha(v)-integrins in stem/progenitor cells and supportive microenvironment impairs bone metastasis in human prostate cancer. Neoplasia 2011;13(6):516-25.

257. Zoni E, van der Horst G, van de Merbel AF, Chen L, Rane JK, Pelger RC, et al. miR-25 Modulates Invasiveness and Dissemination of Human Prostate Cancer Cells via Regulation of alphav- and alpha6-Integrin Expression. Cancer Res 2015;75(11):2326-36.
258. Pechkovsky DV, Scaffidi AK, Hackett TL, Ballard J, Shaheen F, Thompson PJ, et al. Transforming growth factor beta1 induces alphavbeta3 integrin expression in human lung fibroblasts via a beta3 integrin-, c-Src-, and p38 MAPK-dependent pathway. J Biol Chem 2008;283(19):12898-908.
259. Munger JS, Huang X, Kawakatsu H, Griffiths MJ, Dalton SL, Wu J, et al. The integrin alpha v beta 6 binds and activates latent TGF beta 1: a mechanism for regulating pulmonary inflammation and fibrosis. Cell 1999;96(3):319-28.
260. Sun H, Hu K, Wu M, Xiong J, Yuan L, Tang Y, et al. Contact by melanoma cells causes malignant transformation of human epithelial-like stem cells via alpha V integrin activation of transforming growth factor beta1 signaling. Exp Biol Med (Maywood) 2011;236(3):352-65.
261. Coleman RE, Major P, Lipton A, Brown JE, Lee KA, Smith M, et al. Predictive value of bone resorption and formation markers in cancer patients with bone metastases receiving the bisphosphonate zoledronic acid. J Clin Oncol 2005;23(22):4925-35.
262. Chin SL, Johnson SA, Quinn J, Mirosavljevic D, Price JT, Dudley AC, et al. A role for alphaV integrin subunit in TGF-beta-stimulated osteoclastogenesis. Biochem Biophys Res Commun 2003;307(4):1051-8.
263. Klauzinska M, Castro NP, Rangel MC, Spike BT, Gray PC, Bertolette D, et al. The multifaceted role of the embryonic gene Cripto-1 in cancer, stem cells and epithelial-mesenchymal transition. Semin Cancer Biol 2014;29:51-8.
264. Shani G, Fischer WH, Justice NJ, Kelber JA, Vale W, Gray PC. GRP78 and Cripto form a complex at the cell surface and collaborate to inhibit transforming growth factor beta signaling and enhance cell growth. Mol Cell Biol 2008;28(2):666-77.
265. Shen MM. Nodal signaling: developmental roles and regulation. Development 2007;134(6):1023-34.
266. Cheng SK, Olale F, Bennett JT, Brivanlou AH, Schier AF. EGF-CFC proteins are essential coreceptors for the TGF-beta signals Vg1 and GDF1. Genes Dev 2003;17(1):31-6.
267. Chen C, Ware SM, Sato A, Houston-Hawkins DE, Habas R, Matzuk MM, et al. The Vg1-related protein Gdf3 acts in a Nodal signaling pathway in the pre-gastrulation mouse embryo. Development 2006;133(2):319-29.
268. Gray PC, Harrison CA, Vale W. Cripto forms a complex with activin and type II activin receptors and can block activin signaling. Proc Natl Acad Sci U S A 2003;100(9):5193-8.
269. Kelber JA, Shani G, Booker EC, Vale WW, Gray PC. Cripto is a noncompetitive activin antagonist that forms analogous signaling complexes with activin and nodal. J Biol Chem 2008;283(8):4490-500.
270. Kelber JA, Panopoulos AD, Shani G, Booker EC, Belmonte JC, Vale WW, et al. Blockade of Cripto binding to cell surface GRP78 inhibits oncogenic Cripto signaling via MAPK/PI3K and Smad2/3 pathways. Oncogene 2009;28(24):2324-36.
271. Gray PC, Shani G, Aung K, Kelber J, Vale W. Cripto binds transforming growth factor beta (TGF-beta) and inhibits TGF-beta signaling. Mol Cell Biol 2006;26(24):9268-78.
272. Shukla A, Ho Y, Liu X, Ryscavage A, Glick AB. Cripto-1 alters keratinocyte differentiation via blockade of transforming growth factor-beta1 signaling: role in skin carcinogenesis. Mol Cancer Res 2008;6(3):509-16.
273. Yan YT, Liu JJ, Luo Y, E C, Haltiwanger RS, Abate-Shen C, et al. Dual roles of Cripto as a ligand and coreceptor in the nodal signaling pathway. Mol Cell Biol 2002;22(13):4439-49.
274. Nagaoka T, Karasawa H, Castro NP, Rangel MC, Salomon DS, Bianco C. An evolving web of signaling networks regulated by Cripto-1. Growth Factors 2012;30(1):13-21.
275. Strizzi L, Bianco C, Normanno N, Salomon D. Cripto-1: a multifunctional modulator during embryogenesis and oncogenesis. Oncogene 2005;24(37):5731-41.

276. Tao Q, Yokota C, Puck H, Kofron M, Birsoy B, Yan D, et al. Maternal wnt11 activates the canonical wnt signaling pathway required for axis formation in Xenopus embryos. Cell 2005;120(6):857-71.
277. Watanabe K, Nagaoka T, Lee JM, Bianco C, Gonzales M, Castro NP, et al. Enhancement of Notch receptor maturation and signaling sensitivity by Cripto-1. J Cell Biol 2009;187(3):343-53.
278. Bianco C, Strizzi L, Normanno N, Khan N, Salomon DS. Cripto-1: an oncofetal gene with many faces. Curr Top Dev Biol 2005;67:85-133.
279. Nagaoka T, Karasawa H, Turbyville T, Rangel MC, Castro NP, Gonzales M, et al. Cripto-1 enhances the canonical Wnt/beta-catenin signaling pathway by binding to LRP5 and LRP6 co-receptors. Cell Signal 2013;25(1):178-89.
280. Postovit LM, Seftor EA, Seftor RE, Hendrix MJ. Targeting Nodal in malignant melanoma cells. Expert Opin Ther Targets 2007;11(4):497-505.
281. Terry S, El-Sayed IY, Destouches D, Maille P, Nicolaiew N, Ploussard G, et al. CRIPTO overexpression promotes mesenchymal differentiation in prostate carcinoma cells through parallel regulation of AKT and FGFR activities. Oncotarget 2015;6(14):11994-2008.
282. Cai X, Hagedorn CH, Cullen BR. Human microRNAs are processed from capped, polyadenylated transcripts that can also function as mRNAs. RNA 2004;10(12):1957-66.
283. Lee Y, Kim M, Han J, Yeom KH, Lee S, Baek SH, et al. MicroRNA genes are transcribed by RNA polymerase II. EMBO J 2004;23(20):4051-60.
284. Borchert GM, Lanier W, Davidson BL. RNA polymerase III transcribes human microRNAs. Nat Struct Mol Biol 2006;13(12):1097-101.
285. Lee Y, Jeon K, Lee JT, Kim S, Kim VN. MicroRNA maturation: stepwise processing and subcellular localization. EMBO J 2002;21(17):4663-70.
286. Ozsolak F, Poling LL, Wang Z, Liu H, Liu XS, Roeder RG, et al. Chromatin structure analyses identify miRNA promoters. Genes Dev 2008;22(22):3172-83.
287. Monteys AM, Spengler RM, Wan J, Tecedor L, Lennox KA, Xing Y, et al. Structure and activity of putative intronic miRNA promoters. RNA 2010;16(3):495-505.
288. Ha M, Kim VN. Regulation of microRNA biogenesis. Nat Rev Mol Cell Biol 2014;15(8):509-24.
289. Lee Y, Ahn C, Han J, Choi H, Kim J, Yim J, et al. The nuclear RNase III Drosha initiates microRNA processing. Nature 2003;425(6956):415-9.
290. Bohnsack MT, Czaplinski K, Gorlich D. Exportin 5 is a RanGTP-dependent dsRNA-binding protein that mediates nuclear export of pre-miRNAs. RNA 2004;10(2):185-91.
291. Lund E, Guttinger S, Calado A, Dahlberg JE, Kutay U. Nuclear export of microRNA precursors. Science 2004;303(5654):95-8.
292. Yi R, Qin Y, Macara IG, Cullen BR. Exportin-5 mediates the nuclear export of pre-microRNAs and short hairpin RNAs. Genes Dev 2003;17(24):3011-6.
293. Bernstein E, Caudy AA, Hammond SM, Hannon GJ. Role for a bidentate ribonuclease in the initiation step of RNA interference. Nature 2001;409(6818):363-6.
294. Hutvagner G, McLachlan J, Pasquinelli AE, Balint E, Tuschl T, Zamore PD. A cellular function for the RNA-interference enzyme Dicer in the maturation of the let-7 small temporal RNA. Science 2001;293(5531):834-38.
295. Ketting RF, Fischer SE, Bernstein E, Sijen T, Hannon GJ, Plasterk RH. Dicer functions in RNA interference and in synthesis of small RNA involved in developmental timing in C. elegans. Genes Dev 2001;15(20):2654-9.
296. Macrae IJ, Zhou K, Li F, Repic A, Brooks AN, Cande WZ, et al. Structural basis for double-stranded RNA processing by Dicer. Science 2006;311(5758):195-8.
297. Park JE, Heo I, Tian Y, Simanshu DK, Chang H, Jee D, et al. Dicer recognizes the 5' end of RNA for efficient and accurate processing. Nature 2011;475(7355):201-5.
298. Tian Y, Simanshu DK, Ma JB, Park JE, Heo I, Kim VN, et al. A phosphate-binding pocket within the platform-PAZ-connector helix cassette of human Dicer. Mol Cell 2014;53(4):606-16.

299. Hessels D, Schalken JA. Urinary biomarkers for prostate cancer: a review. Asian J Androl 2013;15(3):333-9.
300. Mitchell PS, Parkin RK, Kroh EM, Fritz BR, Wyman SK, Pogosova-Agadjanyan EL, et al. Circulating microRNAs as stable blood-based markers for cancer detection. Proc Natl Acad Sci U S A 2008;105(30):10513-8.
301. Yaman Agaoglu F, Kovancilar M, Dizdar Y, Darendeliler E, Holdenrieder S, Dalay N, et al. Investigation of miR-21, miR-141, and miR-221 in blood circulation of patients with prostate cancer. Tumour Biol 2011;32(3):583-8.
302. Brase JC, Wuttig D, Kuner R, Sultmann H. Serum microRNAs as non-invasive biomarkers for cancer. Mol Cancer 2010;9:306.
303. Bryant RJ, Pawlowski T, Catto JW, Marsden G, Vessella RL, Rhees B, et al. Changes in circulating microRNA levels associated with prostate cancer. Br J Cancer 2012;106(4):768-74.
304. Huang X, Yuan T, Liang M, Du M, Xia S, Dittmar R, et al. Exosomal miR-1290 and miR-375 as prognostic markers in castration-resistant prostate cancer. Eur Urol 2015;67(1):33-41.
305. Lin HM, Castillo L, Mahon KL, Chiam K, Lee BY, Nguyen Q, et al. Circulating microRNAs are associated with docetaxel chemotherapy outcome in castration-resistant prostate cancer. Br J Cancer 2014;110(10):2462-71.
306. Rane JK, Scaravilli M, Ylipaa A, Pellacani D, Mann VM, Simms MS, et al. MicroRNA expression profile of primary prostate cancer stem cells as a source of biomarkers and therapeutic targets. Eur Urol 2015;67(1):7-10.
307. Lewis BP, Burge CB, Bartel DP. Conserved seed pairing, often flanked by adenosines, indicates that thousands of human genes are microRNA targets. Cell 2005;120(1):15-20.
308. Gu S, Jin L, Zhang F, Sarnow P, Kay MA. Biological basis for restriction of microRNA targets to the 3' untranslated region in mammalian mRNAs. Nat Struct Mol Biol 2009;16(2):144-50.
309. Garzon R, Marcucci G, Croce CM. Targeting microRNAs in cancer: rationale, strategies and challenges. Nat Rev Drug Discov 2010;9(10):775-89.
310. Okamura K, Liu N, Lai EC. Distinct mechanisms for microRNA strand selection by Drosophila Argonautes. Mol Cell 2009;36(3):431-44.
311. Hu HY, Yan Z, Xu Y, Hu H, Menzel C, Zhou YH, et al. Sequence features associated with microRNA strand selection in humans and flies. BMC Genomics 2009;10:413.
312. Beilharz TH, Humphreys DT, Clancy JL, Thermann R, Martin DI, Hentze MW, et al. microRNA-mediated messenger RNA deadenylation contributes to translational repression in mammalian cells. PLoS One 2009;4(8):e6783.
313. Mathonnet G, Fabian MR, Svitkin YV, Parsyan A, Huck L, Murata T, et al. MicroRNA inhibition of translation initiation in vitro by targeting the cap-binding complex eIF4F. Science 2007;317(5845):1764-7.
314. Wang B, Yanez A, Novina CD. MicroRNA-repressed mRNAs contain 40S but not 60S components. Proc Natl Acad Sci U S A 2008;105(14):5343-8.
315. Petersen CP, Bordeleau ME, Pelletier J, Sharp PA. Short RNAs repress translation after initiation in mammalian cells. Mol Cell 2006;21(4):533-42.
316. Nottrott S, Simard MJ, Richter JD. Human let-7a miRNA blocks protein production on actively translating polyribosomes. Nat Struct Mol Biol 2006;13(12):1108-14.
317. Liu J, Valencia-Sanchez MA, Hannon GJ, Parker R. MicroRNA-dependent localization of targeted mRNAs to mammalian P-bodies. Nat Cell Biol 2005;7(7):719-23.
318. Eulalio A, Huntzinger E, Izaurralde E. Getting to the root of miRNA-mediated gene silencing. Cell 2008;132(1):9-14.
319. Fan X, Chen X, Deng W, Zhong G, Cai Q, Lin T. Up-regulated microRNA-143 in cancer stem cells differentiation promotes prostate cancer cells metastasis by modulating FNDC3B expression. BMC Cancer 2013;13:61.
320. Li K, Liu C, Zhou B, Bi L, Huang H, Lin T, et al. Role of EZH2 in the growth of prostate cancer stem cells isolated from LNCaP cells. Int J Mol Sci 2013;14(6):11981-93.

321. Josson S, Gururajan M, Hu P, Shao C, Chu GY, Zhau HE, et al. miR-409-3p/-5p promotes tumorigenesis, epithelial-to-mesenchymal transition, and bone metastasis of human prostate cancer. Clin Cancer Res 2014;20(17):4636-46.
322. Liu C, Kelnar K, Vlassov AV, Brown D, Wang J, Tang DG. Distinct microRNA expression profiles in prostate cancer stem/progenitor cells and tumor-suppressive functions of let-7. Cancer Res 2012;72(13):3393-404.
323. Liu C, Kelnar K, Liu B, Chen X, Calhoun-Davis T, Li H, et al. The microRNA miR-34a inhibits prostate cancer stem cells and metastasis by directly repressing CD44. Nat Med 2011;17(2):211-5.

2

Epithelial Plasticity in Cancer: unmasking a microRNA network for TGF-β, Notch- and Wnt-mediated EMT

Eugenio Zoni
Gabri van der Pluijm
Peter C. Gray
Marianna Kruithof-de Julio

Journal of Oncology 2015; 2015:198967

Abstract

Epithelial to mesenchymal transition (EMT) is a reversible process by which cancer cells can switch from a sessile epithelial phenotype to an invasive mesenchymal state. EMT enables tumor cells to become invasive, intravasate, survive in the circulation, extravasate and colonize distant sites. Paracrine heterotypic stroma-derived signals as well as paracrine homotypic or autocrine signals can mediate oncogenic EMT and contribute to the acquisition of stem/progenitor cell properties, expansion of cancer stem cells, development of therapy resistance and often lethal metastatic disease. EMT is regulated by a variety of stimuli that trigger specific intracellular signaling pathways. Altered microRNA (miR) expression and perturbed signaling pathways have been associated with epithelial plasticity, including oncogenic EMT. In this review we analyse and describe the interaction between experimentally-validated miRs and their target genes in TGF-β, Notch and Wnt signaling pathways. Interestingly, in this process, we identified a “signature” of 30 experimentally-validated miRs and a cluster of validated target genes that seem to mediate the cross-talk between TGF-β, Notch and Wnt signaling networks during EMT and reinforce their connection to the regulation of epithelial plasticity in health and disease.

Introduction

In the last decade the amount of data regarding microRNAs (miRs) and their target genes described in the literature has expanded tremendously. The volume of information on this new group of regulators (i.e. miRs) has complicated attempts to integrate this data within existing metabolic and signaling networks. As regulators of gene expression, miRs have indeed added a new level of interaction between different networks. In addition, a single miR can potentially regulate multiple different genes at the same time, leading to complex functional outcomes. However, from another perspective, the identification of groups of genes targeted by the same miR and the clustering of these genes within individual signaling pathways represents a means to understand the cross-talk between multiple signaling networks and their role in a common biological process.

The focus of this review is to summarize the validated groups of miRs functionally linked to the cross-talk between TGF-β, Notch and Wnt signaling during the common biological process of Epithelial-to-Mesenchymal Transition (EMT). In particular, this review will address whether the documented cross-talk between these three important EMT-associated pathways, could be further reinforced by the identification of a "signature" of miRs, already depicted in the literature but not yet "sharpened" or clearly

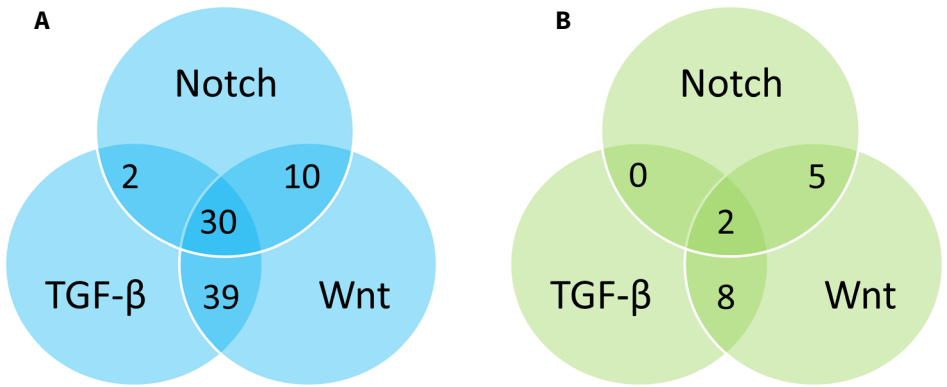

Figure 1. A) Venn diagram showing number of overlapping, experimentally validated miRs targeting KEGG pathway genes from the TGF-β, Wnt and Notch pathways. **B**) Venn diagram showing number of overlapping KEGG pathway genes from the TGF-β, Wnt and Notch pathways.

defined in this role. In the past years, many studies have elegantly described the role of TGF-β, Notch and Wnt pathways in promoting EMT and EMT-associated disorders including fibrosis and metastatic dissemination in cancer (1-6).

Here we identify published and validated interactions between miRs and genes involved in TGF-β, Notch and Wnt signaling. This led to the discovery of a signature of 30 miRs each regulating all three pathways. We then searched for additional validated genes targeted by these 30 miRs and then further clustered these into the TGF-β, Notch and Wnt signaling pathways. Interestingly, in our attempt to identify miRs that were common to all three of these signaling pathways, we found that the 30 miR signature strongly reinforced existing evidence supporting cross-talk between these three pathways during EMT.

Data sources and analysis

In this review we used TarBase v6.0, the largest currently available manually curated miR-target gene database, which includes targets derived from specific and high throughput experiments (7). Using TarBase v6.0 we searched the collection of manually curated, experimentally validated miR-gene interactions for TGF-β (hsa04350), Wnt (hsa04310) and Notch (hsa04330) signaling KEGG pathways in Homo sapiens (8).
Using DIANA-miRPath (9), a miR pathway analysis web-server, we clustered the validated miRs using experimentally validated miR interactions derived from DIANA-TarBase v6.0. Results were merged using a union of genes and analysed with A Priori Analysis Methods (overrepresentation statistical analysis). This statistical analysis identified pathways significantly enriched with targets belonging to a union of genes. A p-value threshold of 0.05 was applied with False Discovery Rate (FDR) correction to the resulting significance levels.

A network of experimentally-validated microRNA highlights the cross-talk between TGF-β, Wnt and Notch signaling in EMT

Using TarBase v6.0 we explored the collection of manually-curated, experimentally-validated miR interactions with genes in the TGF-β, Wnt and Notch KEGG pathways. We identified 84 experimentally validated miRs interacting with genes involved in the TGF-β signaling pathway, 104 miRs in the Wnt pathway and 48 miRs interacting with genes involved in Notch signaling. We clustered the miRs identified in our search in order to obtain a list of experimentally validated miRs shared between all

three pathways focusing first on clusters of two out of three pathways (i.e. experimentally validated miRs shared between only TGF-β and Notch, TGF-β and Wnt or Notch and Wnt) **(Fig. 1)**. We identified 2 experimentally validated miRs shared between the TGF-β and Notch pathways (**Fig. 1** and **Suppl. Table 1**); 10 miRs shared between the Notch and Wnt pathways (**Fig. 1** and **Suppl. Table 2**); 39 miRs shared between the TGF-β and Wnt pathways **(Fig. 1** and **Suppl. Table 3)**. We further identified a signature of 30 experimentally validated miRs targeting all three pathways **(Fig. 1** and **Table 1, 2 and 3).** Within this 30 miR signature, 4 miRs (miR-103a, miR-132, miR-30a and miR-10a) had validated target genes not ascribable to the manually annotated interactions within the KEGG pathways.

DIANA-miRPath was used to collect the complete list of manually-annotated, experimentally-validated and published target genes for the 30 miRs identified. This was done in order to get better insight into the experimental data and understand the functional relevance of our analysis. Of all validated target genes 48 genes could be ascribed to the TGF-β pathway (p-value=6.9e-09), 30 to the Notch pathway (p-value=4.7e-05) and 88 to the Wnt signaling pathway (p-value=5.07e-14). Using the same approach as for the miRs, a cluster of genes was found to be shared between only two of the three pathways (i.e. experimentally validated miR-gene interactions from TGF-β and Notch, TGF-β and Wnt or Notch and Wnt KEGG pathways). With this procedure, we identified 8 manually annotated and validated target genes shared by TGF-β and Wnt KEGG pathways (SMAD2, SMAD3, SMAD4, ROCK2, RHOA, MYC, PPP2R1A and PPP2R1B) and 5 manually annotated and validated target genes shared by Notch and Wnt KEGG pathways (CTBP1, CTBP2, DVL2, DVL3, PSEN1). Interestingly, no genes were shared between TGF-β and Notch KEGG pathways **(Fig. 1B)**. Finally, we determined whether a new cluster of experimentally validated target genes coupled to our signature described above could be connected to a common biological process among TGF-β, Notch and Wnt signaling pathways. Strikingly, only 2 validated target genes, the transcriptional co-activator cAMP-response element-binding protein (CREB)-binding protein (CBP) and the adenovirus E1A-associated cellular p300 transcriptional co-activator protein p300 (EP300), were shared exclusively between the TGF-β, Notch and Wnt signaling KEGG pathways (**Fig. 1B).** These results indicate the relevance of the 30 identified miR signature thus suggesting a possible link between these miRs and cross-talk between TGF-β, Notch and Wnt pathways during EMT.

TABLE 1

miRNA	Gene (TGF-β pathway)	Notch signaling	Wnt signaling
hsa-miR-335-5p	INHBB, **SMAD3**, ID4, ACVR1, ACVR2B, E2F5, **MYC**, BMP2,SP1,GDF5, AMHR2,TGFB2,THBS3,LTBP1,TGFBR2, INHBE	-	**SMAD3, MYC**
hsa-miR-34a-5p	E2F5,**MYC**	-	**MYC**
hsa-miR-1	E2F5,BMP7,THBS1	-	-
hsa-miR-124-3p	ID2, **ROCK2**, ID4,BMP6,**RHOA**,E2F5,SMAD5, ID1,SP1, BMPR1A,ID3,E2F4,**PPP2R1B**	-	**ROCK2,RHOA, PPP2R1B**
hsa-miR-26b-5p	SMAD6,BMP8B,RPS6KB2,ID1,BMP2,**EP300**,IFNG, SMAD7,BMPR2	**EP300**	**EP300**
hsa-miR-155-5p	**SMAD2**,THBS1,**SMAD3**,**RHOA**,SMAD5,SMAD1	-	**SMAD2,SMAD3, RHOA**
hsa-miR-375	CDKN2B,**RHOA**,TGFB2	-	**RHOA**
hsa-miR-21-5p	TGFBR1,THBS1,ZFVYE16,**MYC**,TGFB2,TGFBR2,BMP R2	-	**MYC**
hsa-miR-98	TGFBR1,THBS1,CDKN2B,RPS6KB2,**MYC**,SMAD7,INH BE, RPS6KB1	-	**MYC**
hsa-miR-122-5p	NODAL,SMURF2,**RHOA**	-	**RHOA**
hsa-miR-200c-3p	**EP300**	**EP300**	**EP300**
hsa-miR-9-5p	ID4,**EP300**	**EP300**	**EP300**
hsa-miR-324-3p	**CREBBP**	**CREBBP**	**CREBBP**
hsa-miR-24-3p	**MYC**	-	**MYC**
hsa-miR-194-5p	**EP300**	**EP300**	**EP300**
hsa-miR-92a-3p	THBS1,**SMAD4**,TGFBR2,BMPR2	-	**SMAD4**
hsa-miR-16-5p	SMURF2,**PPP2R1A**,SMAD5,ACVR2A,SP1,SMAD7, SMAD1,RPS6KB1	-	**PPP2R1A**
hsa-miR-93-5p	TGFBR2,BMPR2	-	-
hsa-miR-19a-3p	**SMAD4**,TGFBR2,BMPR2	-	**SMAD4**
hsa-miR-103a-3p	ACVR2B,SMAD7,RPS6KB1	-	-
hsa-miR-132-3p	THBS1	-	-
hsa-miR-30a-5p	THBS1,MAPK1	-	-
hsa-miR-200b-3p	**EP300**	**EP300**	**EP300**
hsa-miR-19b-3p	ACVR1,**SMAD4**,TGFBR2,BMPR2	-	**SMAD4**
hsa-miR-145-5p	**MYC**	-	**MYC**
hsa-miR-31-5p	**RHOA**	-	**RHOA**
hsa-miR-429	**EP300**	**EP300**	**EP300**
hsa-miR-10a-5p	ACVR2A	-	-
hsa-miR-182-5p	**EP300**	**EP300**	**EP300**
Hsa-miR-374a-5p	**EP300**	**EP300**	**EP300**

Table I. List of experimentally validated miRNA-gene interactions for TGf-β signaling pathway. Interaction with Notch and Wnt signaling are also indicated (genes among those in TGf- β pathway).

TABLE 2

miRNA	Gene (Wnt pathway)	Notch signaling	TGF-β signaling
hsa-miR-335-5p	CTNNBIP1,LRP6,TBL1X,WNT10B,CCND2,DKK2,**SMAD 3**,AXIN1,WNT3,FZD8,PPP2R5A,NFAT5,FZD10,**MYC**,V ANGL2,PRKCG,DKK4,FZD1,PRICKLE2,SFRP1,WIF1,DA AM1,WNT7B,WNT9A, PPP3R2	-	**SMAD3**,**MYC**
hsa-miR-34a-5p	WNT1,CCND1,CTNNB1,AXIN2,**MYC**,PPP3R1,LEF1, MAP3K7, CCND3	-	**MYC**
hsa-miR-1	CSNK2A2,CAMK2G,**CTBP1**,**CTBP2**,PPP2R5A,PLCB3, CCND1,DKK1	**CTBP1**,**CTBP2**	-
hsa-miR-124-3p	VANGL1,PORCN,**ROCK2**,**RHOA**,WNT5B,CTNNB1, **PPP2R1B**,NFATC1,**DVL2**	**DVL2**	**ROCK2**,**PPP2R1 B**, **RHOA**
hsa-miR-26b-5p	SFRP4,**DVL3**,FZD5,RUVBL1,VANGL1,GPC4,JUN,CCND 1, VANGL2,PPP3R1,**EP300**,PLCB4,PLCB2	**EP300**,**DVL3**	**EP300**
hsa-miR-155-5p	**GSK3B**,**SMAD2**,APC,VANGL1,WNT5A,**SMAD3**,CSNK1 A1L,**RHOA**,CTNNB1,CSNK1A1,RAC1,**PSEN1**	**PSEN1**	**SMAD2**,**SMAD3**, **RHOA**,
hsa-miR-375	PRKCA,**RHOA**,FZD4,PRKX	-	**RHOA**
hsa-miR-21-5p	TCF4,APC,WNT1,WNT5A,NFAT5,CSNK1A1,**MYC**, PRICKLE2,DAAM1,TBL1XR1	-	**MYC**
hsa-miR-98	VANGL1,WNT10B,SENP2,FZD10,**MYC**	-	**MYC**
hsa-miR-122-5p	**RHOA**,RAC1,TBL1XR1	**RHOA**	**RHOA**
hsa-miR-200c-3p	TCF7L1,**EP300**	**EP300**	**EP300**
hsa-miR-9-5p	WNT8A,WNT6,**EP300**,NFATC3,PLCB4	**EP300**	**EP300**
hsa-miR-324-3p	WNT9B,**CREBBP**,**DVL2**	**CREBBP**,**DVL2**	**CREBBP**
hsa-miR-24-3p	FZD5,CHD8,FZD4,NFAT5,NKD1,**MYC**,PPP3R1	-	**MYC**
hsa-miR-194-5p	**EP300**	**EP300**	**EP300**
hsa-miR-92a-3p	**SMAD4**	-	**SMAD4**
hsa-miR-16-5p	CAMK2G, WNT5A, CCND2, PPP2R5C, JUN,CCND1, AXIN2, **PPP2R1A**, WNT3A,CCND3	-	**PPP2R1A**
hsa-miR-93-5p	MAPK9,CCND1,PRKACB	-	-
hsa-miR-19a-3p	CCND1,**SMAD4**	-	**SMAD4**
hsa-miR-103a-3p	AXIN2,WNT3A,MAP3K7	-	-
hsa-miR-132-3p	WNT3A	-	-
hsa-miR-30a-5p	WNT5A,PPP2R5C,PPP3CA,JUN,CTNNB1,PPP3R1	-	-
hsa-miR-200b-3p	TCF7L1,**EP300**	**EP300**	**EP300**
hsa-miR-19b-3p	DAAM2,TCF4,CCND2,**SMAD4**,PRKACB	-	**SMAD4**
hsa-miR-145-5p	PPP3CA,**MYC**	-	**MYC**
hsa-miR-31-5p	**RHOA**,NFAT5	-	**RHOA**
hsa-miR-429	TCF7L1,**EP300**	**EP300**	**EP300**
hsa-miR-10a-5p	BTRC,MAPK8,MAP3K7	-	-
hsa-miR-182-5p	**EP300**	**EP300**	**EP300**
Hsa-miR-374a-5p	**EP300**	**EP300**	**EP300**

Table II. List of experimentally validated miRNA-gene interactions for Wnt signaling pathway. Interaction with Notch and TGF-β signaling are also indicated (genes among those in Wnt pathway).

TABLE 3

miRNA	Gene (Notch pathway)	Wnt signaling	TGF-β signaling
hsa-miR-335-5p	NUMB,MFNG,LFNG,DLL1,NOTCH3,DTX1,MAML2,JAG2	-	-
hsa-miR-34a-5p	HDAC1,NOTCH2,NOTCH1,DLL1,JAG1	-	-
hsa-miR-1	**CTBP1**,**CTBP2**,NOTCH2,HDAC2,DTX1	**CTBP1**,**CTBP2**	-
hsa-miR-124-3p	RBPJ,**DVL2**,MAML1,JAG2	**DVL2**	-
hsa-miR-26b-5p	**DVL3**,KAT2B,**EP300**	**EP300**,**DVL3**	**EP300**
hsa-miR-155-5p	NOTCH2,PSEN1,RBPJ	-	-
hsa-miR-375	NUMB,JAG1,RBPJ	-	-
hsa-miR-21-5p	JAG1,NCSTN,DTX3L	-	-
hsa-miR-98	DTX4,JAG1	-	-
hsa-miR-122-5p	NUMBL,ADAM17	-	-
hsa-miR-200c-3p	JAG1,**EP300**	**EP300**	**EP300**
hsa-miR-9-5p	NCOR2,**EP300**	**EP300**	**EP300**
hsa-miR-324-3p	**CREBBP**,**DVL2**	**CREBBP**,**DVL2**	**CREBBP**
hsa-miR-24-3p	HDAC1,NOTCH1	-	-
hsa-miR-194-5p	**EP300**	**EP300**	**EP300**
hsa-miR-92a-3p	KAT2B	-	-
hsa-miR-16-5p	NOTCH2	-	-
hsa-miR-93-5p	KAT2B	-	-
hsa-miR-19a-3p	KAT2B	-	-
hsa-miR-103a-3p	NUMB	-	-
hsa-miR-132-3p	LFNG	-	-
hsa-miR-30a-5p	NOTCH1	-	-
hsa-miR-200b-3p	**EP300**	**EP300**	**EP300**
hsa-miR-19b-3p	KAT2B	-	-
hsa-miR-145-5p	APH1A	-	-
hsa-miR-31-5p	NUMB	-	-
hsa-miR-429	**EP300**	**EP300**	**EP300**
hsa-miR-10a-5p	NCOR2	-	-
hsa-miR-182-5p	**EP300**	**EP300**	**EP300**
Hsa-miR-374a-5p	**EP300**	**EP300**	**EP300**

Table III. List of experimentally validated miRNA-gene interactions for Notch signaling pathway. Interaction with Wnt and TGF-β signaling are also indicated (genes among those in Notch pathway).

Identification of a signature of miRs targeting genes linked to TGF-β-, Notch- and Wnt-dependent EMT

1.1. Identification of miRs that regulate canonical and non-canonical TGF-β signaling during EMT

TGF-β signaling plays complex roles during tumor progression and can either inhibit or promote tumor growth depending on the cellular context. The complexity of TGF-β signaling derives in part from the capability of its receptors to activate distinct canonical and non-canonical signaling pathways. In the SMAD-dependent canonical pathway, TGF-β ligands assemble their specific type II and type I transmembrane serine kinase receptors, allowing the constitutively active type II receptor kinase to phosphorylate the type I receptor, thereby activating its kinase.
The active type I receptor then phosphorylates its cognate cytoplasmic SMAD proteins which then enter the nucleus to regulate the transcription of target genes. By contrast, the non-canonical pathway is SMAD-independent and includes TGF-β signaling via the Rho family of GTPases and MAPK/PI3K pathways. In this context, TGF-β has been shown to rapidly activate the Rho-GTPases and its activation of RHOA in epithelial cells leads to induction of stress fibers and acquisition of mesenchymal characteristics, thus promoting EMT (10). Additionally, RHOA is a crucial regulator in the signal transduction events that link activation of latent TGF-β by plasma membrane receptors (e.g. integrins) to the assembly of focal adhesions and sites of F-actin fiber organization (11).

Interestingly, we have identified interactions between RHOA and a group of 5 validated miRs (miR-155, miR-124, miR-375, miR-122 and miR-31) (12-17) **(Fig. 2)**. More specifically, in endothelial cells, miR-155 was shown to block the acquisition of the mesenchymal phenotype induced by TGF-β by directly targeting RHOA (17). Similar observations were made in osteoclast precursor cells, where overexpression of miR-124 decreased RHOA expression and reduced cell migration (18). miR-375 also interferes with cytoskeletal organization by indirectly targeting RHOA during neuronal development (12). Dramatic effects on migration and cytoskeleton disruption have also been reported for miR-122 in hepatocellular carcinoma (HCC). In this context, miR-122 and RHOA interact directly and over-expression of RHOA reverts miR-122-induced mesenchymal to epithelial transition (MET) and inhibition of migration (16). Finally, in breast cancer cells it was demonstrated that overexpression of miR-31 decreases invasion and metastasis via downregulation of RHOA (15) **(Fig. 2)**. Together, these findings highlight the relevance of these miRs in interfering with RHOA mediated EMT.

Modulation of stress fibers and cytoskeletal rearrangements are key events in the acquisition of a mesenchymal phenotype and in the modulation of cellular motility. Two key players in this process are the Rho-serine/threonine kinases ROCK1 and ROCK2 which regulate smooth muscle contraction, formation of stress fibers and focal adhesions (19). ROCK1 and ROCK2 are two major downstream effectors of RHOA that constitute additional important mediators of TGF-β-induced EMT. Interestingly, among the 30 miRs in our signature, we found 2 validated miRs (miR-335 and miR-124) that regulate expression of ROCK1 and ROCK2 (20, 21). Low levels of miR-335 were correlated with poor overall patient survival in neuroblastoma while overexpression of this miR strongly reduced cell migration and impaired F-actin organization (20). Further analysis revealed that miR-335 directly targets ROCK1 providing an explanation for its ability to reduce cell invasion (20). Low levels of miR-124 have been associated with poor prognosis in aggressive HCC while overexpression of miR-124 in HCC cell lines strongly decreased ROCK2 expression and inhibited EMT, formation of stress fibers, filopodia and lamellipodia (21). Taken together these experimental data highlight an important role for miR-335 and miR-124 in SMAD-independent, non-canonical TGF-β effects on cytoskeletal rearrangements via RHOA-dependent signaling pathways **(Fig. 2)**.

TGF-β also induces mesenchymal characteristics via canonical signaling, i.e. via SMAD2 and SMAD3. In the previous paragraph we described the ability of miR-155 to directly decrease RHOA expression and thereby inhibit cell motility and EMT characteristics (17). Interestingly, miR-155 has also been shown to interfere with the canonical TGF-β pathway by directly affecting the formation of the SMAD2/3 signaling complex. Louafi et al. have demonstrated that miR-155 directly targets SMAD2, leading to a reduction of TGF-β-induced SMAD2 phosphorylation and blocking SMAD2-dependent activation of a TGF-β-inducible, SMAD-dependent CAGA reporter plasmid (22). Additionally, miR-155 targets presenilin 1 (PSEN1), a catalytic subunit of the gamma-secretase complex which catalyzes the cleavage of membrane proteins including Notch receptors (23). In this regard, Gudey et al. have shown that PSEN1 plays a crucial role in mediating the interaction between TGF-β and Notch signaling by promoting the association between the TGF-β type I receptor intracellular domain (TβRI-ICD) and the Notch intracellular domain (NICD) which in turn triggers cell-invasive behaviour in prostate cancer (24). Altogether, these data suggest that miR-155 can disrupt both the canonical and non-canonical TGF-β pathways and might represent an interesting modulator of cross-talk between TGF-β and Notch signaling pathways **(Fig. 2).**

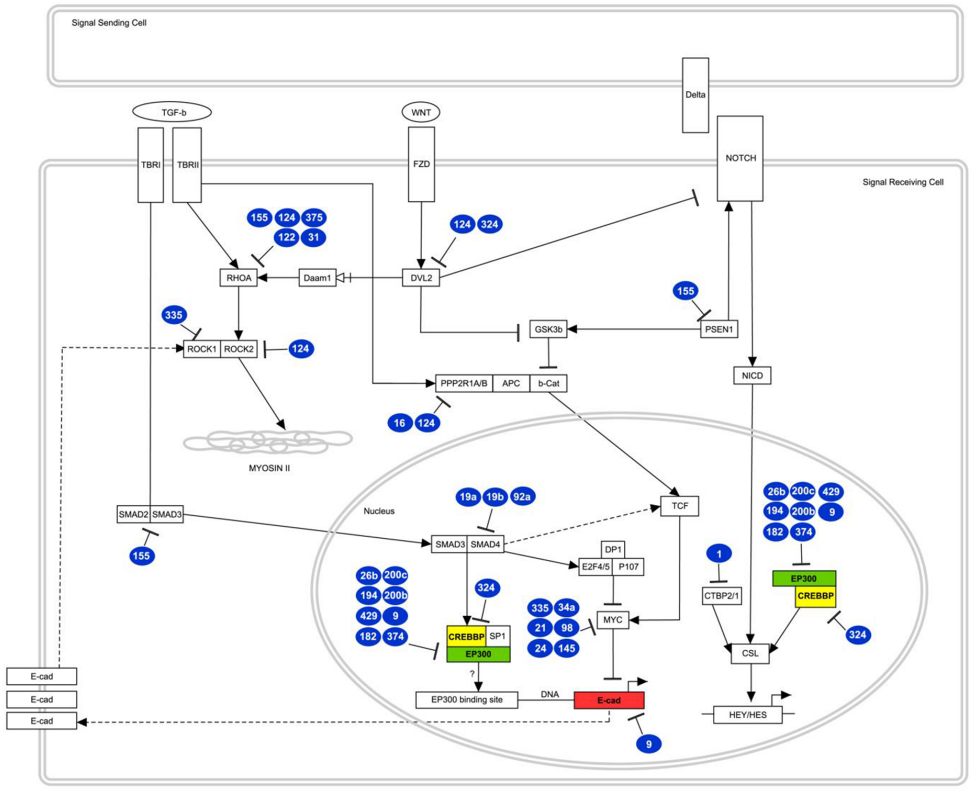

Figure 2. Interaction between miRs from the 30 miR signature and their predicted target genes overlaid on KEGG TGF-β, Notch and Wnt pathways.

1.2. Identification of miRs regulating the cross-talk between TGF-β and Wnt signaling during EMT

The observation that TGF-β alone can be sufficient to induce EMT in epithelial cells (10) while other cell types may not be sensitive to this effect of TGF-β (25) suggests that induction of EMT by TGF-β requires cooperation with other signaling pathways. Indeed, several studies indicate that TGF-β acts together with the Notch and Wnt pathways to promote EMT (4, 6, 26, 27). Remarkably, in our analysis we could not identify any validated miR target genes shared exclusively between the TGF-β and Notch pathways. However, Notch is able to antagonize TGF-β via sequestration of EP300, a factor that in turn acts as transcriptional co-activator for Notch1 (28). The interaction between the cluster of miR target genes ascribable to Notch signaling and their

interactions with miR target genes associated with both TGF-β and Wnt signaling pathways is discussed below.

Concerning Wnt signaling, two interesting genes highlighted in our analysis are PPP2R1A and PPP2R1B. These are the catalytic subunits of the PP2A holoenzyme, a protein phosphatase that reverts the action of protein kinases in many signaling cascades, including Wnt signaling (29). Several reports support the notion that PP2A plays a dual role in Wnt signaling and can act as either a positive or negative regulator of the pathway (30). On one hand, in the absence of Wnt, β-catenin forms a complex with APC, AXIN and GSK3β. This allows GSK3β to phosphorylate β-catenin that is then ubiquitinated and targeted for proteasomal degradation. In this context, different PP2A subunits bind to AXIN and APC, decreasing β-catenin levels and thereby negatively regulating Wnt signaling. On the other hand, in the presence of Wnt, PP2A seems to exert a positive role in β-catenin stabilization (30). In this situation, the complex of APC, AXIN and GSK3β is degraded by Dishevelled (DSH) leading to nuclear β-catenin accumulation and activation of Wnt target genes. Stabilized β-catenin can subsequently localize at plasma membrane in complex with E-Cadherin and PP2A, thus reducing EMT.

Recently, we have demonstrated that activation of Wnt signaling via GSK3β inhibition in metastatic and androgen independent prostate cancer cells (PC3, DU145 and C4-2B) induces dramatic changes in their morphology, blocks their migration, reduces their metastatic growth and strongly affects their mesenchymal phenotype (31). This highlights the ability of Wnt signaling to stabilize E-Cadherin and interfere with EMT in prostate cancer suggesting that PP2A may act as a negative regulator of EMT. Consistent with this possibility, it has been shown that restoring expression of a catalytic subunit of PP2A can revert EMT and suppress tumor growth and metastasis in an orthotopic mouse model of human prostate cancer (32). Interestingly, we identified two miRs in our signature (miR-16 and miR-124) that directly block the expression of catalytic subunits of PP2A (PPP2R1A and PPP2R1B) and that have been positively validated by proteomics and microarray, respectively (13, 23). Strikingly, homozygous deletion (HD) of the miR-16 locus was observed in androgen independent prostate cancer in xenograft models (33). The HD of miR-16 in a subset of androgen independent prostate cancer xenograft might suggest that, in this context, PP2A is present and stable. In turn, this might also suggest that activation of Wnt signaling in androgen independent prostate cancer cells could act synergistically with PP2A to promote stabilization of β-catenin and E-Cadherin leading to reduced EMT. Taken together, these data might identify a subset of androgen independent prostate cancers in which restoration of Wnt signaling reduces the aggressiveness of tumor cells and abolishes their mesenchymal phenotype.

The involvement of miR-16 in EMT in the context of prostate cancer is further reinforced by an interesting observation regarding its role in the tumor-supportive capacity of stromal cells. Musumeci et al. have shown that miR-16 is downregulated in fibroblasts surrounding prostate tumors in patients (34). Additionally, they have demonstrated that miR-16 restoration considerably impairs the tumor-supportive capability of stromal cells *in vitro* and *in vivo* (34). From this perspective, it is important to note that the prostate tumor microenvironment is rich in TGF-β superfamily members including TGF-βs, bone morphogenetic proteins (BMPs), growth/differentiation factors (GDFs), activins, inhibins, Nodal and anti-müllerian hormone (AMH) (35). Among them, miR-16 has been suggested to regulate activin/Nodal signaling via direct interaction with teratocarcinoma-derived growth factor 1 (Cripto, TDGF1). Chen et. al. have indeed shown using luciferase reporter assays that miR-16 (together with miR-15a) directly interacts with the 3'UTR of Cripto (36).

Cripto is a small, GPI-anchored protein that functions as a secreted growth factor and as an obligatory cell surface co-receptor for a subset of TGF-β superfamily ligands including Nodal (37). Cripto regulates both cell movement and EMT during embryonic development and cancer (38) and, strikingly, Nodal, which has been implicated in enhancing tumor cell plasticity and aggressiveness, is expressed in cancerous but not normal human prostate specimens (39). Although it is required for Nodal signaling, Cripto suppresses TGF-beta signaling in multiple cell types (40), reinforcing the inclusion of miR-16 in our signature. Therefore, the reduced expression of miR-16 in the tumor microenvironment in prostate cancer is predicted to facilitate Cripto-dependent Nodal signaling which together with Cripto's other tumor promoting effects could trigger invasiveness, bone metastasis and EMT.

Similar to miR-16, overexpression of miR-124 in androgen independent prostate cancer cell lines (DU145) strongly reduces aggressiveness and invasion (41). This further supports the hypothesis that the increased PP2A stability caused by low levels of miR-16 and miR-124 in a subset of androgen independent prostate cancer cell lines could explain reduced cell migration and invasion, an effect that we also documented upon GSK3β inhibition (31). miR-124 is also likely to be an important player in Wnt signal transduction since proteomics and microarray analyses have revealed that it interacts with DVL2 (a member of DSH protein family) (13, 42). DVL2 binds the cytoplasmic C-terminus of the frizzled family of Wnt receptors and transduces the Wnt signal to down-stream effectors. Interestingly, DVL2 also interacts with insulin receptor substrates (IRS1/2) and thereby promotes canonical Wnt signaling (43). Moreover, IRS1/2 have been identified as key players in the regulation of E-Cadherin expression during EMT (44, 45). IRS1/2 have also been implicated in the progression and etiology of prostate cancer. The IRS1/2 ratio has been shown to be significantly lower in malignant prostate tumors

than in benign prostatic tissue and functional polymorphisms in IRS1 has been associated with a more advanced Gleason score (46, 47). Also reduced migration was documented after miR-124 overexpression in androgen independent prostate cancer suggesting a mechanism in which low levels of miR-124 boost DVL2. This, in turn, would be predicted to lead to GSK3β blockade with subsequent β-catenin and E-Cadherin stabilization. Additionally, low levels of miR-124 strengthen PP2A, which further contribute to stabilize β-catenin and E-Cadherin, therefore reducing EMT.

Another miR in our signature, miR-324, has also been shown to regulated expression of DVL2. Ragan et al. used a luciferase reporter plasmid to demonstrate that miR-324 directly targets DVL2 (48). Interestingly, dysregulation of miR-324 has been linked to macrophage dysfunction in colorectal cancer, where altered Wnt signaling is known to play a pivotal role (49). More specifically, miR-324 was found to be highly expressed in infiltrated macrophages in fresh colon cancer tissues isolated immediately after surgical removal (49). Additionally, in the same work, the oncogene c-Myc was identified as a candidate transcription factor capable of regulating miR-324. This, combined with the identification of miR-324 in our analysis, suggests a fascinating role for miR-324 in the cross-talk between TGF-β and Wnt signaling in EMT and colorectal cancer. The role of TGF-β as a "double edged sword" during colon cancer progression has been extensively documented in the literature. In its tumor suppressive role, TGF-β inhibits progression of the cell cycle by inducing the tumor suppressors p15 (INK4B) and p21 (CDKN1A) and inhibiting expression c-Myc (50). At the same time, c-Myc is also a crucial downstream target of altered Wnt signaling in colon cancer (51) and has been shown to cause loss of E-Cadherin, which is a hallmark of EMT (52). Therefore, miR-324 could be involved in a feedback loop between Wnt, TGF-β and c-Myc. More specifically, altered Wnt signaling during colorectal cancer development could modulate c-Myc levels and therefore miR-324 expression. In turn, abnormal miR-324 levels can interfere with DVL2 expression leading to alteration in the Wnt signaling pathway that further alter c-Myc and E-Cadherin levels **(Fig. 2)**.

We have identified a group of 6 miRs (miR-335, miR-34a, miR-21, miR-98, miR-24 and miR-145) directly linked to c-Myc, reinforcing the role of c-Myc as common downstream target between TGF-β and Wnt mediated EMT. Among them, we have already discussed the role of miR-335 in EMT induced by TGF-β, particularly its interaction with ROCK1 and ROCK2 (20). Interestingly, Tavazoie et al. have shown by microarray that miR-335 also interacts with c-Myc (53), suggesting a more comprehensive role for miR-335 in TGF-β and Wnt mediated EMT. Additionally, Sampson et al. have suggested that miR-98 (from let-7/miR-98 family) might regulate c-Myc expression (54). They have shown that administration of 10058-F4, a compound that

inhibits MYC, strongly increases the expression of miR-98 and other let-7 family members (54). Strikingly, treatment of melanoma cells with 10058-F4 efficiently diminished EMT mediated by TGF-β and S-phase kinase-associated protein 2 (SKP2) (55). Taken together, these data suggest that miR-98 could represent an important mediator in the cross-talk between TGF-β and Wnt and their effect in modulating of EMT.

Deregulated expression of c-Myc has been reported in a wide variety of human cancers and among several key regulators of c-Myc expression, an important role is exerted by p53. Interestingly miR-145 has been reported to repress c-Myc in response to the p53 pathway (56) reinforcing its identification in our EMT signature. Similarly, members of miR-34 family are known to be direct transcriptional targets of p53 and p53-binding sites are localized on the miR-34 gene promoter (57). However, Christoffersen et al. demonstrated that miR-34a is capable of repressing c-Myc in a p53 independent manner (58). This suggests that beside the cross-talk between p53 and c-Myc, there are additional mechanisms that contribute to fine tuning the role of c-Myc in TGF-β and Wnt dependent EMT. From this perspective, a crucial outcome of deregulated MYC signaling is represented by E-Cadherin repression. Lal et al. have shown that miR-24 directly targets MYC, suggesting that this miR could potentially play an interesting role in EMT modulation (59). To support this hypothesis, miR-24 has also been recently shown to regulate the EMT program in response to TGF-β in breast cancer cells. Papadimitriou et al. have demonstrated that miR-24 is capable of modulating TGF-beta-induced breast cancer cell invasiveness through regulation of RhoA-specific guanine nucleotide exchange factor Net1 isoform2 (Net1A), a protein that is necessary for TGF-beta-mediated RhoA activation (60). Together, these findings reinforce the identification of miR-24 in our EMT signature.

The last miR included in the group of those targeting c-Myc is miR-21. Singh et al. have suggested that miR-21 regulates self renewal in mouse embryonic stem (ES) cells and could potentially interact with MYC and other self renewal markers (Oct4, Nanog and Sox2) (61). They have shown that enforced expression of miR-21 in ES cells downregulates renewal markers, including c-Myc (61). This suggests that in specific contexts modulation of miR-21 could potentially affect c-Myc expression and therefore modulate E-Cadherin levels and affect EMT.

Finally, in the previous paragraphs we have described the role of miR-155 as an interesting player capable of disrupting the tumor-promoting effects of SMAD-dependent and SMAD-independent TGF-β signaling (22). Interestingly, in our analysis we identified another group of 4 miRs linked to TGF-β signaling and belonging to the miR-17-92 cluster (i.e. miR-19a, miR-19b and miR-92a) and to its paralog cluster miR-106b-25 (i.e. miR-93). Interestingly, c-Myc has been reported to upregulate the miR-17-92 cluster,

providing further evidence of cross-talk between Wnt and TGF-β signaling (62). Dews et al. performed a detailed study to elucidate the mechanism of interaction between the miR-17-92 cluster and TGF-β signaling, particularly with SMAD4 (63). Using qPCR and microarray analyses they provide evidence suggesting that miR-19a, miR-19b and miR-92a regulate SMAD4 indirectly, i.e. without interacting with the SMAD4 3'UTR (63).

1.3. A group of miRs targeting the CREBBP/EP300 interaction highlight the cross-talk between TGF-β, Wnt and Notch signaling during EMT

As mentioned above, EP300 (p300) and CREBBP (CREB binding protein, CBP) are the only two KEGG pathway genes shared among all three pathways (i.e. TGF-β, Wnt and Notch). EP300 and CREBBP are functionally related transcriptional co-activator proteins that play many important roles in in processes including cell proliferation, differentiation and apoptosis. In the context of Wnt signaling, EP300 has been shown to act synergistically with β-catenin and T cell factor (TCF) during neoplastic transformation (64). Similarly, in the context of TGF-β signaling, it has been reported that phosphorylated Smad3 interacts with the CREBBP/EP300 complex to augment transcriptional activation (65). Additionally, the Notch intracellular domain (NICD) can recruit the complex CREBBP/EP300 to interact with the transcription factor CSL (CBF1/Su(H)/Lag-1) which, in turn, activates the transcription of two known Notch related basic-helix-loop-helix transcription factor families, Hey and Hes (66).

EP300 regulates transcription and remodels chromatin by acting as histone acetyltransferase. It regulates p53 dependent transcription and binds specifically to phosphorylated CREBBP (67). EP300 and CREBBP were originally identified in protein interaction assays through their association with the transcription factor CREB and with the adenoviral-transforming protein E1A respectively (68-70). The roles of CREBBP and EP300 and their interaction during EMT have been extensively studied. However, the large degree of cellular heterogeneity within different organs and tissues makes the role of EP300 in EMT difficult to define with precision (71).

Strikingly, some reports have linked the expression of wild-type EP300 in colorectal and prostate cancer with the degree of intravascular dissemination of cancer cells (probably affected by ongoing EMT) and poor prognosis (72-74). In this context, EP300 seems to promote cancer cells EMT. In support of this, elevated expression of EP300 in hepatocellular carcinomas (HCC) correlates with enhanced vascular invasion, intrahepatic metastasis, shortened survival and, strikingly, low E-Cadherin expression (75). EP300 knockdown strongly increased E-Cadherin expression and significantly decreased migration and invasion in a hepatoma cell line (HLE) that is otherwise highly invasive and poorly differentiated (75).

In the context of cancerous hepatocytes, TGF-β is one factor that plays a major role in the induction of EMT, causing type I collagen induction and formation of liver fibrosis. In this situation, EP300 interacts with Smad3 and function as signal integrator for mediating regulation of collagen synthesis by TGF-β (76). Treatment with HDAC inhibitor strongly decreases EP300 levels and restores E-Cadherin distribution to the hepatocytes cell membrane therefore reducing TGF-β induced EMT (77).

As outlined above, targeting the expression of EP300 and/or CREBBP can simultaneously affect TGF-β, Wnt and Notch pathways. In this regard, miR-9, which is represented in our 30 miR signature, was shown to target EP300 as determined by microarray analysis (78) **(Fig. 2)**. Remarkably, miR-9 has also been shown to be involved in the modulation of E-Cadherin levels via c-Myc. More specifically, Ma et al. have shown that MYC acts as transcriptional activator of miR-9 and that miR-9, in turn, directly targets E-Cadherin (79). Therefore, miR-9 is not only one of the common miRs linking TGF-β, Wnt and Notch signaling it also has the ability to target E-Cadherin which links it directly to EMT. Thus, it appears that miR-9 might represent an interesting regulator of the cross-talk between TGF-β, Wnt and Notch signaling pathways in both normal cells and cancer cells. On one hand, through its effect on E-Cadherin and EP300, miR-9 may maintain the balance between epithelial and mesenchymal cell state in normal cells. On the other hand, in cancer cells that have lost the tumor suppressive effect of TGF-β, the disruption of the TGF-β cytostatic program could cause c-Myc induced up-regulation of miR-9 leading to loss of E-Cadherin and subsequent EMT. Bonev et al. have further shown that in the context of Notch signaling, in addition to its connection with EP300, miR-9 also interacts directly with Hes1 (80). This reinforces the hypothesis that miR-9 represents an interesting regulator of the Notch signaling pathway with a role in the cross-talk between TGF-β, Wnt and Notch.

Regulation of the CREBBP/EP300 complex by miR-9 represents an interesting mechanism of co-regulation of TGF-β, Wnt and Notch signaling pathways. In this regard, it is interesting to note that we identified another group of 5 miRs (miR-26b, miR-194, miR-182, miR-374 and miR-324) that also were shown to interact with EP300 and CREBBP by microarray (81). Among these, notable observations have been reported for miR-26 and miR-324. Cai et al. have shown that miR-26 is strongly downregulated in HT-29 colon cancer cells undergoing TGF-β induced EMT, whereas Ragan et al. have described an interaction between miR-324 and CREBBP by transcriptomic analysis (48, 82). Moreover, interestingly in our analysis we have also identified miR-1, that has been shown to interact with CTBP1/2, two proteins that binds to the C-terminus of adenovirus E1A protein (13) and act as corepressors of Notch target genes (83). **(Fig. 2)**.

As discussed above, there is a connection between miR-324 and DVL2 in the context of Wnt signaling and colon cancer (48, 49). Interactions between TGF-β and Wnt

are important in many biological processes. In particular, in the context of colon cancer, the cascade of events that drives tumor progression is characterized by series of genetic modifications involving components of the Wnt and TGF-β signaling pathways. In colon cancer, the adenoma-carcinoma sequence is initiated by alteration in Wnt signaling (i.e. inactivation of APC). Subsequently, the late stage adenoma shows loss of 18q-arm, where maps the best candidate tumor suppressor gene DPC4/MADH4, which encodes SMAD4, involved in the TGF-β pathway (84). This event drives the progression from the intermediate adenoma stage to late adenoma, resulting in loss of the cytostatic effect of TGF-β. Strikingly, the interaction between β-catenin and the TGF-β pathway depends on the transcriptional co-activator CREBBP as demonstrated by Zhou et al. who used chromatin immune precipitation to show that a complex forms between Smad3, β-catenin and CREBBP (85). These findings together with the identification of EP300 and CREBBP in our analysis suggest that miR-26 and miR-324 may link TGF-β and Wnt signaling with EMT in colon cancer progression.

1.4. Interaction between CREBBP/EP300 and miR-200 family

Recent studies have indicated that the switch in tumor cells from a sessile, epithelial phenotype towards a motile, mesenchymal phenotype is accompanied by the acquisition of stem/progenitor cell characteristics (86). In particular, cells undergoing EMT acquire chemoresistance, a key property attributed to cancer stem cells (CSCs) (86). In this context, the miR-200 family is particularly interesting. The miR-200 family includes miR-200c-3p, miR-200b-3p and miR-429 (all identified in our analysis) and inhibits EMT and cancer cell migration by directly targeting the E-Cadherin transcriptional repressors ZEB1 and ZEB2 (87). Additionally, downregulation of miR-200 family has been described in docetaxel resistant prostate cancer cells, reinforcing the link between EMT and resistance to chemotherapy (88).

Interestingly, our analysis revealed a connection between miR-200 family members and EP300 regulation. Mizuguchi et al. have shown that acetyltransferase EP300 regulates expression of miR-200c-3p overcoming its transcriptional suppression by ZEB1 (89). The same authors showed that treatment with an HDAC inhibitor significantly increased miR-200c-3p levels causing a decrease in Vimentine and ZEB1 and upregulation of E-Cadherin. Strikingly, miR-200c-3p, miR-200b-3p and miR-429 have also been shown to interact with EP300 by microarray and protein analysis (81). These observations enhance the complexity of the regulatory mechanisms governing the interplay between EP300 and E-Cadherin and suggest a positive feedback loop between miR-200 family and EP300. The inhibitory effect of ZEB1 on miR-200 could be attenuated

by EP300 which upregulates miR-200 expression. Furthermore, higher levels of miR-200 could decrease ZEB1, suggesting that the positive effect of EP300 on E-Cadherin expression could also be mediated via miR-200 family **(Fig. 2)**.

Conclusion

In this review, we discussed and summarized the known interactions between miRs and genes involved in TGF-β, Notch and Wnt signaling pathways and highlighted a signature of 30 validated miRs linking these pathways to the process of EMT. Our novel approach led to the identification of cluster of validated and known miRs involved in different pathways in an attempt to reduce the extraordinary volume of information related to the interaction between miRs and different target genes. We believe that the identification of groups of genes targeted by the same miR and the clustering of these genes in different pathways could potentially represent an interesting strategy to better understand the cross-talk between multiple signaling networks, thus facilitating the understanding of their connections and their role in a common biological process.

Acknowledgements:

The research leading to these results has received funding from the FP7 Marie Curie ITN under grant agreement n°264817 - BONE-NET (EZ), Prostate Action UK (EZ, GP) and Clayton Foundation (PG). The authors disclose no potential conflicts of interest.

REFERENCES

1. Thiery, J.P. and J.P. Sleeman, Complex networks orchestrate epithelial-mesenchymal transitions. Nat Rev Mol Cell Biol, 2006. 7(2): p. 131-42.
2. Kalluri, R., EMT: when epithelial cells decide to become mesenchymal-like cells. J Clin Invest, 2009. 119(6): p. 1417-9.
3. Fuxe, J., T. Vincent, and A. Garcia de Herreros, Transcriptional crosstalk between TGF-beta and stem cell pathways in tumor cell invasion: role of EMT promoting Smad complexes. Cell Cycle, 2010. 9(12): p. 2363-74.
4. Timmerman, L.A., et al., Notch promotes epithelial-mesenchymal transition during cardiac development and oncogenic transformation. Genes Dev, 2004. 18(1): p. 99-115.
5. Zavadil, J. and E.P. Bottinger, TGF-beta and epithelial-to-mesenchymal transitions. Oncogene, 2005. 24(37): p. 5764-74.
6. Zavadil, J., et al., Integration of TGF-beta/Smad and Jagged1/Notch signaling in epithelial-to-mesenchymal transition. EMBO J, 2004. 23(5): p. 1155-65.
7. Vergoulis, T., et al., TarBase 6.0: capturing the exponential growth of miRNA targets with experimental support. Nucleic Acids Res, 2012. 40(Database issue): p. D222-9.
8. Kanehisa, M. and S. Goto, KEGG: kyoto encyclopedia of genes and genomes. Nucleic Acids Res, 2000. 28(1): p. 27-30.
9. Vlachos, I.S., et al., DIANA miRPath v.2.0: investigating the combinatorial effect of microRNAs in pathways. Nucleic Acids Res, 2012. 40(Web Server issue): p. W498-504.
10. Bhowmick, N.A., et al., Transforming growth factor-beta1 mediates epithelial to mesenchymal transdifferentiation through a RhoA-dependent mechanism. Mol Biol Cell, 2001. 12(1): p. 27-36.
11. Margadant, C. and A. Sonnenberg, Integrin-TGF-beta crosstalk in fibrosis, cancer and wound healing. EMBO Rep, 2010. 11(2): p. 97-105.
12. Abdelmohsen, K., et al., miR-375 inhibits differentiation of neurites by lowering HuD levels. Mol Cell Biol, 2010. 30(17): p. 4197-210.
13. Baek, D., et al., The impact of microRNAs on protein output. Nature, 2008. 455(7209): p. 64-71.
14. Schmittgen, T.D., miR-31: a master regulator of metastasis? Future Oncol, 2010. 6(1): p. 17-20.
15. Valastyan, S., et al., A pleiotropically acting microRNA, miR-31, inhibits breast cancer metastasis. Cell, 2009. 137(6): p. 1032-46.
16. Wang, S.C., et al., MicroRNA-122 Triggers Mesenchymal-Epithelial Transition and Suppresses Hepatocellular Carcinoma Cell Motility and Invasion by Targeting RhoA. PLoS One, 2014. 9(7): p. e101330.
17. Bijkerk, R., et al., MicroRNA-155 Functions as a Negative Regulator of RhoA Signaling in TGF-beta-induced Endothelial to Mesenchymal Transition. Microrna, 2012. 1(1): p. 2-10.
18. Lee, Y., et al., MicroRNA-124 regulates osteoclast differentiation. Bone, 2013. 56(2): p. 383-9.
19. Lock, F.E., et al., Differential regulation of adhesion complex turnover by ROCK1 and ROCK2. PLoS One, 2012. 7(2): p. e31423.
20. Lynch, J., et al., MiRNA-335 suppresses neuroblastoma cell invasiveness by direct targeting of multiple genes from the non-canonical TGF-beta signaling pathway. Carcinogenesis, 2012. 33(5): p. 976-85.
21. Zheng, F., et al., The putative tumour suppressor microRNA-124 modulates hepatocellular carcinoma cell aggressiveness by repressing ROCK2 and EZH2. Gut, 2012. 61(2): p. 278-89.
22. Louafi, F., R.T. Martinez-Nunez, and T. Sanchez-Elsner, MicroRNA-155 targets SMAD2 and modulates the response of macrophages to transforming growth factor-{beta}. J Biol Chem, 2010. 285(53): p. 41328-36.
23. Selbach, M., et al., Widespread changes in protein synthesis induced by microRNAs. Nature, 2008. 455(7209): p. 58-63.

24. Gudey, S.K., et al., TRAF6 stimulates the tumor-promoting effects of TGFbeta type I receptor through polyubiquitination and activation of presenilin 1. Sci Signal, 2014. 7(307): p. ra2.
25. Brown, K.A., et al., Induction by transforming growth factor-beta1 of epithelial to mesenchymal transition is a rare event in vitro. Breast Cancer Res, 2004. 6(3): p. R215-31.
26. Eger, A., et al., beta-Catenin and TGFbeta signaling cooperate to maintain a mesenchymal phenotype after FosER-induced epithelial to mesenchymal transition. Oncogene, 2004. 23(15): p. 2672-2680.
27. Nelson, W.J. and R. Nusse, Convergence of Wnt, beta-catenin, and cadherin pathways. Science, 2004. 303(5663): p. 1483-7.
28. Masuda, S., et al., Notch1 oncoprotein antagonizes TGF-beta/Smad-mediated cell growth suppression via sequestration of coactivator p300. Cancer Sci, 2005. 96(5): p. 274-82.
29. Schonthal, A.H., Role of PP2A in intracellular signal transduction pathways. Front Biosci, 1998. 3: p. D1262-73.
30. Eichhorn, P.J., M.P. Creyghton, and R. Bernards, Protein phosphatase 2A regulatory subunits and cancer. Biochim Biophys Acta, 2009. 1795(1): p. 1-15.
31. Kroon, J., et al., Glycogen synthase kinase-3β inhibition depletes the population of prostate cancer stem/progenitor-like cells and attenuates metastatic growth. 2013. 2013.
32. Bhardwaj, A., et al., Restoration of PPP2CA expression reverses epithelial-to-mesenchymal transition and suppresses prostate tumour growth and metastasis in an orthotopic mouse model. Br J Cancer, 2014. 110(8): p. 2000-10.
33. Porkka, K.P., et al., The miR-15a-miR-16-1 locus is homozygously deleted in a subset of prostate cancers. Genes Chromosomes Cancer, 2011. 50(7): p. 499-509.
34. Musumeci, M., et al., Control of tumor and microenvironment cross-talk by miR-15a and miR-16 in prostate cancer. Oncogene, 2011. 30(41): p. 4231-42.
35. Wu, M.Y. and C.S. Hill, Tgf-beta superfamily signaling in embryonic development and homeostasis. Dev Cell, 2009. 16(3): p. 329-43.
36. Chen, F., et al., MiR-15a-16 represses Cripto and inhibits NSCLC cell progression. Mol Cell Biochem, 2014. 391(1-2): p. 11-9.
37. Gray, P.C. and W. Vale, Cripto/GRP78 modulation of the TGF-beta pathway in development and oncogenesis. FEBS Lett, 2012. 586(14): p. 1836-45.
38. Rangel, M.C., et al., Role of Cripto-1 during epithelial-to-mesenchymal transition in development and cancer. Am J Pathol, 2012. 180(6): p. 2188-200.
39. Lawrence, M.G., et al., Reactivation of embryonic nodal signaling is associated with tumor progression and promotes the growth of prostate cancer cells. Prostate, 2011. 71(11): p. 1198-209.
40. Gray, P.C., et al., Cripto binds transforming growth factor beta (TGF-beta) and inhibits TGF-beta signaling. Mol Cell Biol, 2006. 26(24): p. 9268-78.
41. Kang, S., et al., miR-124 exhibits antiproliferative and antiaggressive effects on prostate cancer cells through PACE4 pathway. Prostate, 2014. 74(11): p. 1095-106.
42. Lim, L.P., et al., Microarray analysis shows that some microRNAs downregulate large numbers of target mRNAs. Nature, 2005. 433(7027): p. 769-73.
43. Geng, Y., et al., Insulin receptor substrate 1/2 (IRS1/2) regulates Wnt/beta-catenin signaling through blocking autophagic degradation of dishevelled2. J Biol Chem, 2014. 289(16): p. 11230-41.
44. Carew, R.M., et al., Insulin receptor substrate 2 and FoxO3a signaling are involved in E-cadherin expression and transforming growth factor-beta1-induced repression in kidney epithelial cells. FEBS J, 2011. 278(18): p. 3370-80.
45. Sorokin, A.V. and J. Chen, MEMO1, a new IRS1-interacting protein, induces epithelial-mesenchymal transition in mammary epithelial cells. Oncogene, 2013. 32(26): p. 3130-8.
46. Heni, M., et al., Insulin receptor isoforms A and B as well as insulin receptor substrates-1 and -2 are differentially expressed in prostate cancer. PLoS One, 2012. 7(12): p. e50953.

47. Neuhausen, S.L., et al., Prostate cancer risk and IRS1, IRS2, IGF1, and INS polymorphisms: strong association of IRS1 G972R variant and cancer risk. Prostate, 2005. 64(2): p. 168-74.
48. Ragan, C., et al., Transcriptome-wide prediction of miRNA targets in human and mouse using FASTH. PLoS One, 2009. 4(5): p. e5745.
49. Chen, Y., et al., Dysregulation of the MiR-324-5p-CUEDC2 Axis Leads to Macrophage Dysfunction and Is Associated with Colon Cancer. Cell Rep, 2014. 7(6): p. 1982-93.
50. Yagi, K., et al., c-myc is a downstream target of the Smad pathway. J Biol Chem, 2002. 277(1): p. 854-61.
51. He, T.C., et al., Identification of c-MYC as a target of the APC pathway. Science, 1998. 281(5382): p. 1509-12.
52. Cowling, V.H. and M.D. Cole, E-cadherin repression contributes to c-Myc-induced epithelial cell transformation. Oncogene, 2007. 26(24): p. 3582-6.
53. Tavazoie, S.F., et al., Endogenous human microRNAs that suppress breast cancer metastasis. Nature, 2008. 451(7175): p. 147-52.
54. Sampson, V.B., et al., MicroRNA let-7a down-regulates MYC and reverts MYC-induced growth in Burkitt lymphoma cells. Cancer Res, 2007. 67(20): p. 9762-70.
55. Qu, X., et al., A signal transduction pathway from TGF-beta1 to SKP2 via Akt1 and c-Myc and its correlation with progression in human melanoma. J Invest Dermatol, 2014. 134(1): p. 159-67.
56. Sachdeva, M., et al., p53 represses c-Myc through induction of the tumor suppressor miR-145. Proc Natl Acad Sci U S A, 2009. 106(9): p. 3207-12.
57. Bommer, G.T., et al., p53-mediated activation of miRNA34 candidate tumor-suppressor genes. Curr Biol, 2007. 17(15): p. 1298-307.
58. Christoffersen, N.R., et al., p53-independent upregulation of miR-34a during oncogene-induced senescence represses MYC. Cell Death Differ, 2010. 17(2): p. 236-45.
59. Lal, A., et al., miR-24 Inhibits cell proliferation by targeting E2F2, MYC, and other cell-cycle genes via binding to "seedless" 3'UTR microRNA recognition elements. Mol Cell, 2009. 35(5): p. 610-25.
60. Papadimitriou, E., et al., Differential regulation of the two RhoA-specific GEF isoforms Net1/Net1A by TGF-beta and miR-24: role in epithelial-to-mesenchymal transition. Oncogene, 2012. 31(23): p. 2862-75.
61. Singh, S.K., et al., REST maintains self-renewal and pluripotency of embryonic stem cells. Nature, 2008. 453(7192): p. 223-7.
62. O'Donnell, K.A., et al., c-Myc-regulated microRNAs modulate E2F1 expression. Nature, 2005. 435(7043): p. 839-43.
63. Dews, M., et al., The myc-miR-17~92 axis blunts TGF{beta} signaling and production of multiple TGF{beta}-dependent antiangiogenic factors. Cancer Res, 2010. 70(20): p. 8233-46.
64. Sun, Y., et al., Regulation of beta -catenin transformation by the p300 transcriptional coactivator. Proc Natl Acad Sci U S A, 2000. 97(23): p. 12613-8.
65. Janknecht, R., N.J. Wells, and T. Hunter, TGF-beta-stimulated cooperation of smad proteins with the coactivators CBP/p300. Genes Dev, 1998. 12(14): p. 2114-9.
66. Pursglove, S.E. and J.P. Mackay, CSL: a notch above the rest. Int J Biochem Cell Biol, 2005. 37(12): p. 2472-7.
67. Vo, N. and R.H. Goodman, CREB-binding protein and p300 in transcriptional regulation. J Biol Chem, 2001. 276(17): p. 13505-8.
68. Chrivia, J.C., et al., Phosphorylated CREB binds specifically to the nuclear protein CBP. Nature, 1993. 365(6449): p. 855-9.
69. Stein, R.W., et al., Analysis of E1A-mediated growth regulation functions: binding of the 300-kilodalton cellular product correlates with E1A enhancer repression function and DNA synthesis-inducing activity. J Virol, 1990. 64(9): p. 4421-7.

70. Eckner, R., et al., Molecular cloning and functional analysis of the adenovirus E1A-associated 300-kD protein (p300) reveals a protein with properties of a transcriptional adaptor. Genes Dev, 1994. 8(8): p. 869-84.
71. Bedford, D.C., et al., Target gene context influences the transcriptional requirement for the KAT3 family of CBP and p300 histone acetyltransferases. Epigenetics, 2010. 5(1): p. 9-15.
72. Ishihama, K., et al., Expression of HDAC1 and CBP/p300 in human colorectal carcinomas. J Clin Pathol, 2007. 60(11): p. 1205-10.
73. Heemers, H.V., J.D. Debes, and D.J. Tindall, The role of the transcriptional coactivator p300 in prostate cancer progression. Adv Exp Med Biol, 2008. 617: p. 535-40.
74. Pena, C., et al., The expression levels of the transcriptional regulators p300 and CtBP modulate the correlations between SNAIL, ZEB1, E-cadherin and vitamin D receptor in human colon carcinomas. Int J Cancer, 2006. 119(9): p. 2098-104.
75. Yokomizo, C., et al., High expression of p300 in HCC predicts shortened overall survival in association with enhanced epithelial mesenchymal transition of HCC cells. Cancer Lett, 2011. 310(2): p. 140-7.
76. Ghosh, A.K. and J. Varga, The transcriptional coactivator and acetyltransferase p300 in fibroblast biology and fibrosis. J Cell Physiol, 2007. 213(3): p. 663-71.
77. Kaimori, A., et al., Histone deacetylase inhibition suppresses the transforming growth factor beta1-induced epithelial-to-mesenchymal transition in hepatocytes. Hepatology, 2010. 52(3): p. 1033-45.
78. Grimson, A., et al., MicroRNA targeting specificity in mammals: determinants beyond seed pairing. Mol Cell, 2007. 27(1): p. 91-105.
79. Ma, L., et al., miR-9, a MYC/MYCN-activated microRNA, regulates E-cadherin and cancer metastasis. Nat Cell Biol, 2010. 12(3): p. 247-56.
80. Bonev, B., P. Stanley, and N. Papalopulu, MicroRNA-9 Modulates Hes1 ultradian oscillations by forming a double-negative feedback loop. Cell Rep, 2012. 2(1): p. 10-8.
81. Mees, S.T., et al., EP300--a miRNA-regulated metastasis suppressor gene in ductal adenocarcinomas of the pancreas. Int J Cancer, 2010. 126(1): p. 114-24.
82. Cai, Z.G., et al., Aberrant expression of microRNAs involved in epithelial-mesenchymal transition of HT-29 cell line. Cell Biol Int, 2013. 37(7): p. 669-74.
83. Oswald, F., et al., RBP-Jkappa/SHARP recruits CtIP/CtBP corepressors to silence Notch target genes. Mol Cell Biol, 2005. 25(23): p. 10379-90.
84. Frank, S.A., in Dynamics of Cancer: Incidence, Inheritance, and Evolution. 2007: Princeton (NJ).
85. Zhou, B., et al., Interactions between beta-catenin and transforming growth factor-beta signaling pathways mediate epithelial-mesenchymal transition and are dependent on the transcriptional co-activator cAMP-response element-binding protein (CREB)-binding protein (CBP). J Biol Chem, 2012. 287(10): p. 7026-38.
86. van der Pluijm, G., Epithelial plasticity, cancer stem cells and bone metastasis formation. Bone, 2011. 48(1): p. 37-43.
87. Korpal, M., et al., The miR-200 family inhibits epithelial-mesenchymal transition and cancer cell migration by direct targeting of E-cadherin transcriptional repressors ZEB1 and ZEB2. J Biol Chem, 2008. 283(22): p. 14910-4.
88. Puhr, M., et al., Epithelial-to-mesenchymal transition leads to docetaxel resistance in prostate cancer and is mediated by reduced expression of miR-200c and miR-205. Am J Pathol, 2012. 181(6): p. 2188-201.
89. Mizuguchi, Y., et al., Cooperation of p300 and PCAF in the control of microRNA 200c/141 transcription and epithelial characteristics. PLoS One, 2012. 7(2): p. e32449.

SUPPLEMENTARY DATA

Supplementary table 1

miRNA	Gene (Notch pathway)	Gene (TGF-β pathway)
hsa-miR-106b-5p	KAT2B	SMAD9
hsa-miR-129-5p	NOTCH1	BMPR2

Supplementary Table I. List of experimentally validated miRNA – gene interactions for Notch signaling and TGF-β signaling pathway.

Supplementary Table 2

miRNA	Gene (Notch pathway)	Gene (Wnt pathway)
hsa-miR-181a-5p	NOTCH2,LFNG,KAT2B	WNT16,NLK,WNT3A, WNT2
hsa-miR-183-5p	NOTCH2,**PSEN1**	BTRC,CCND1,PPP3R1, **PSEN1**
hsa-miR-562	**PSEN1**	**PSEN1**
hsa-miR-25-3p	KAT2B	TP53
hsa-miR-221-3p	**DVL2**	DKK2,CTNNB1,**DVL2**
hsa-miR-449a	HDAC1	CCND1
hsa-miR-181b-5p	KAT2B	NLK
hsa-miR-137	**CTBP1**	**CTBP1**
hsa-miR-181c-5p	NOTCH2	NLK
hsa-miR-29c-3p	NUMB	JUN

Supplementary Table II. List of experimentally validated miRNA – gene interactions for Notch signaling and Wnt signaling pathway.

Supplementary Table 3

miRNA	Gene (Wnt pathway)	Gene (TGF-β pathway)
hsa-miR-192-5p	FZD7,CTNNBIP1,TBL1X,APC,VANGL1,WNT3,PRICKLE1,NLK,FZD4, MAPK9, GPC4,FZD1,TCF7	ID2,ID4,ACVRD2B,E2F5,ID1,ACVR2A,BM PR2,RPSKB1
hsa-miR-7-5p	CAMK2D,LRP6,MAPK9,WNT8B, **PPP2R1B**	**PPP2R1B**,BMPR2
hsa-let-7b-5p	CCND2,CUL1,PLCB3,CCND1	THBS1,CUL1,E2F5
hsa-miR-26a-5p	GSK3B,CCND2,**SMAD4**,**MYC**	**SMAD4**,**MYC**,SMAD1
hsa-miR-17-5p	MAPK9,CCND1,**SMAD4**,**MYC**	THBS1,**SMAD4**,**MYC**,TGFBR2,BMPR2
hsa-miR-101-3p	FZD6,JUN,RAC1	TGFBR1,ACVR2B
hsa-miR-186-5p	WNT5A,**SMAD4**,CNSK1A1	AVCR1,**SMAD4**,SMAD5,ACVR2A
hsa-miR-20a-5p	CCND1,**MYC**,**SMAD4**	THBS1,**SMAD4**,**MYC**,TGFBR2,BMPR2
hsa-miR-18a-5p	DAAM2,**SMAD4**	**SMAD4**,TGFBR2
hsa-miR-199a-3p	MAPK9,MAPK8	MAPK1
hsa-miR-148b-3p	FBXW11,TBL1XR1	INHBA
hsa-let-7f-5p	CCND1,**MYC**	**MYC**
hsa-miR-425-5p	CCND1,**PPP2CB**	**PPP2CB**
hsa-let-7a-5p	CCND2,**MYC**	THBS1,**MYC**
hsa-miR-130b-3p	TCF4,**SMAD4**	ACVR1,**SMAD4**,TGFBR2
hsa-miR-374b-5p	FZD8,CCND1	CDKN2B
hsa-miR-22-3p	FRAT2,PRKACA	SP1,BMP7
hsa-let-7c	**MYC**	TGFBR1,**MYC**
hsa-miR-141-3p	TCF7L1	TGFB2
hsa-miR-125b-5p	TP53	BMPR1B
hsa-miR-584-5p	**ROCK1**	**ROCK1**
hsa-miR-29b-3p	CTNNBIP1	ACVR2A,SP1
hsa-miR-128	WNT3A	TGFBR1,BMPR2
hsa-miR-302a-3p	CCND2	LEFTY2
hsa-let-7g-5p	**MYC**	**MYC**
hsa-miR-483-3p	**SMAD4**	**SMAD4**
hsa-miR-302d-3p	CCND2	LEFTY2
hsa-miR-133a	**RHOA**	**RHOA**
hsa-miR-140-3p	MAPK8	ACVR2B
hsa-miR-34b-5p	**MYC**	**MYC**
hsa-miR-142-3p	GPC4	TGFBR1,BMP8A
hsa-miR-146a-5p	**ROCK1**	**ROCK1**
hsa-miR-590-3p	PPP2R5A	ID4
hsa-miR-34c-5p	**MYC**	**MYC**
hsa-miR-34b-3p	**MYC**	**MYC**
hsa-miR-196a-5p	CCND2	BMP4
hsa-miR-185-5p	**RHOA**	**RHOA**
hsa-miR-378a-3p	**MYC**	**MYC**
hsa-miR-138-5p	**ROCK2**	**ROCK2**

Supplementary Table III. List of experimentally validated miRNA – gene interactions for Wnt signaling and TGF-β signaling pathway.

3

miR-25 modulates invasiveness and dissemination of human prostate cancer cells via regulation of α_v- and α_6 integrin expression

Eugenio Zoni
Geertje van der Horst
Marjan van de Merbel
Lanpeng Chen
Jayant K. Rane
Rob C.M. Pelger
Anne T. Collins
Tapio Visakorpi
Ewa B. Snaar-Jagalska
Norman J. Maitland
Gabri van der Pluijm

Cancer Research 2015 Jun 1;75(11):2326-36.

Abstract

Altered microRNA (miR) expression is associated with tumor formation and progression of various solid cancers. A major challenge in miR expression profiling of bulk tumors is represented by the heterogeneity of the subpopulations of cells that constitute the organ, as well as the tumor tissue. Here we analyzed the expression of miRs in a subpopulation of epithelial stem/progenitor-like cells in human prostate cancer (PCSC) and compared their expression profile to more differentiated cancer cells. In both cell lines and clinical prostate cancer specimens we identified that miR-25 expression in PCSCs was low/absent and steadily increased during their differentiation into cells with a luminal epithelial phenotype. Functional studies revealed that overexpression of miR-25 in prostate cancer cell lines and selected subpopulation of highly metastatic and tumorigenic cells ($ALDH^{high}$) strongly affected the invasive cytoskeleton causing reduced migration *in vitro* and metastasis via attenuation of extravasation *in vivo*. Here we show, for the first time, that miR-25 can act as a tumor suppressor in highly metastatic PCSCs by direct functional interaction with the 3'UTR of pro-invasive α_v- and α_6 integrins. Taken together, our observations suggest that miR-25 is a key regulator of invasiveness in human prostate cancer through its direct interactions with α_v- and α_6 integrin expression.

Introduction

Prostate cancer is the second most frequently diagnosed cancer and the sixth leading cause of death from cancer in males worldwide (1). Despite the progress in the pathogenesis, detection, and treatment of primary tumor, the main problem for prostate cancer patients remains the risk of metastasis formation and tumor recurrence after surgical removal and/or treatment of the primary tumor.

From a hierarchical point of view, normal and transformed epithelial tissues are indeed characterized by a cellular heterogeneity, in which different cell types contribute to the maintenance of the complexity of tissues (2). One of the major challenges in the field of new therapy development for advanced cancer is to specifically target “driver” cancer cell subpopulations, that seem to be involved in tumor maintenance, metastasis and therapy resistance (3). Accumulating evidence shows that prostate cancer stem/progenitor-like cells play key roles in tumor initiation, local and distant relapse, metastasis, and castration- & chemotherapy resistance (4,5). One of the driving forces of oncological transformation of normal epithelial stem cells (SC) into cancer stem cells (CSCs), is the deregulated gene expression of tumor suppressors and oncogenes (6). Furthermore, oncological research has highlighted an emerging role for microRNAs (miRs) as crucial regulators of such oncogenes and tumor suppressors in cancer (7). miRs are a class of small non-coding RNA molecules (18-25 nucleotides long), which modulate gene expression by binding to the 3’-untranslated regions (3’-UTR) of target mRNAs and promoting mRNA degradation or translational repression (8). Several studies have delineated and compared the expression of miRs in bulk tissues from human prostate cancer and normal prostate and have shown significant correlations between miRs levels, prostate cancer progression and response to chemotherapy (9,10). In addition, these studies have highlighted the diagnostic and prognostic value of miRs detection in blood and urine, suggesting the possible relevance of the use of miRs as prostate cancer biomarkers.

Most attempts to decipher the miRs signatures have been performed in clinical samples of bulk tumor tissues or heterogeneous prostate cancer cell lines. In these heterotypic and heterogeneous cell populations, this strategy cannot clearly discriminate between the “driver” subpopulation and other, non-tumorigenic and more differentiated cancer cell subpopulations. In bulk tumor tissues, it is even more difficult to discriminate between tumor-derived and stroma-derived miR expression profiles.

Here we examined the expression of miRs in the “driver” subpopulation of human stem/progenitor-like prostate cancer cells (cell lines, patient samples) that was previously shown to drive tumorigenesis and metastasis in preclinical prostate cancer models of bone metastasis *in vivo* (11). Based on the list of differentially expressed miRs,

miR-25 was selected because a number of its putative target genes are predicted to be involved in the stimulation of cancer invasiveness. In both clinical prostate cancer specimens and prostate cancer cell lines we found that miR-25 is low/absent in the $\alpha 2\beta 1^{hi}$ /$CD133^{+}$ compartment, also referred to as stem-like cells (SC) in recent publication (12). and steadily increases during differentiation into luminal epithelial cells in clinical samples. Here we validate, for the first time, the direct functional interaction between miR-25 and α_v- and α_6 integrins linked to the cytoskeletal organization and invasive behavior *in vitro*. In line with these observations, we further demonstrate that miR-25 targeted α_v- and α_6 integrins in selected $ALDH^{high}$ subpopulation of cancer stem/progenitor cells and reduced invasion by blocking the extravasation of human prostate cancer cells in the intact organism.

Materials and Methods

ALDEFLUOR® assay and real time PCR-based microRNA expression profiling

Aldehyde Dehydrogenase (ALDH) activity of the cells was measured using the ALDEFLUOR® assay kit (StemCell Technologies, Durham, USA) according to the manufacturer's protocol (11). ALDH substrate was added to the cells and converted by intracellular ALDH into a fluorescent product. For FACS sorting cells were labelled with ALDEFLUOR® kit and sorted using FACS ARIA cell sorter (BD Bioscience, Breda, The Netherlands) ($ALDH^{high}$ = highest 10% $ALDH^{+}$; $ALDH^{low}$ = lowest 10% $ALDH^{-}$ cells). microRNA expression profiling was performed using RT^2 miRNA PCR array (SA-biosciences, Frederick, USA) according to the manufacturer's protocol. Data were normalized using SNORD48 and U6 RNA housekeeping genes. Inclusion criteria were Ct value <35, fold induction >2 and <-2 and similar data in 2 independent experiments.

Prostate cancer cell lines and transfection with miR-25 precursor molecule

Human osteotropic prostate cancer cell lines PC-3M-Pro4Luc2 and C4-2B cells were maintained in DMEM with 10% FCII, 1% Penicillin-Streptomycin (Life Technologies, USA) and 0.8 mg/ml Neomycin (Santacruz, USA) and T-medium DMEM (Sigma-Aldrich, The Netherlands) with 20% F-12K nutrient mixture Kaighn's modification (GibcoBRL), 10% FCS, 1% Insulin-Transferin-Selenium, 0.125 mg/ml biotin, 12.5 mg/ml adenine, 6.825 ng/ml T3 and 1% penicillin/streptomycin respectively. Cells were maintained at 37°C with 5% CO_2.

For transient transfection, Lipofectamine® 2000 (Invitrogen, USA) was used according to manufacturer's protocol with Pre-miR-25 (ID: PM10584; Life Technologies) and pre-miRNA negative control (scramble) (ID: AM17110; Life Technologies). Total RNA was collected after 72 hours.

Collection of samples from patient, isolation of subpopulation from primary prostate epithelial cells and expression array

Prostate epithelial tissue was collected with ethical permission from York District Hospital (York) and Castle Hill Hospital (Cottingham, Hull). Primary epithelial prostate cells were expended in culture and selected for $\alpha_2\beta_1$ integrin expression using rapid adhesion to type collagen-I coated plates (13). $\alpha_2\beta_1^{hi}$ cells were subsequently enriched for $CD133^{-}$ and $CD133^{+}$ fraction using MACS cell sorting according to the manufacturer's protocol (Milteny Biotec) (5,12,14). Cultured cells were harvested at passage 2 and total RNA was extracted using miRVana kit (Life Technology, Paisley, UK). Agilent V3 arrays

were used to perform miR microarray analysis and the data was processed using Agilent Feature extraction software. The data were quantile normalized, and RMA summarized.

miRNA target prediction and bioinformatic analysis of cluster of genes

Targetscan v6.2, miRDB (15) and microT-CDS (16) were used to identify novel miR-25 predicted targets. Functional annotation was performed using DAVID Bioinformatics Resources 6.7 (17,18) and KEGG database (19).

RNA isolation and real-time qPCR

Total RNA was isolated using Trizol (Invitrogen, USA), cDNA was synthesized by reverse transcription (Promega, USA) according to manufacturer's protocol and qRT-PCR performed with Biorad CFX96 system (Biorad, The Netherlands). Expression was normalized to GAPDH. (Primer sequences in **supplementary table I**).

Migration assay

Cells were starved overnight in medium containing 0.3% serum and then seeded in medium containing 0.3% serum in Transwell chamber (Corning 8-µm pore size). The lower chamber was filled with medium containing 10% serum. After 18 hours of incubation, cells on the upper side of the filters were removed and cells migrated to the lower side were fixed with 4% paraformaldehyde, stained with 0.1% crystal violet (Sigma-Aldrich, USA) and counted.

Proliferation assay

Cells were seeded at density of 2,000 cells/well 24 hours and allowed to grow for 24, 48, 72. After incubation, 20 µl of 3-(4,5 dimethylthiazol-2-yl)-5-(3-carboxymethoxyphenyl)-2-(4-sulfophenyl)-2H-tetrazolium was added and mitochondrial activity was measured after 2 hours incubation at 37°C. (CellTiter96 Aqueous Non-radioactive Cell proliferation assay, Promega, USA).

FACS analysis

Protein expression was measured with flow-cytometry. 1 x 10^5 cells were incubated for 45 min at 4°C in FACS wash buffer containing PBS + 1% FCS + 0.1% Natriumazide NaN_3 and 10 µl antibody (αV-PE, α2-FITC, α6-APC, Milteny). Cells were washed with PBS, protein measured with FACS Calibur (BD Biosciences, USA) and data analysed with FCS express software™ (De Novo software, USA).

Phalloidin staining

PC-3M-Pro4luc2 transfected with Pre-miR-25 and scramble negative control were seeded onto glass slides, fixed with 4% paraformaldehyde and stained with 0.25 μM Phalloidin (Life technologies, USA). TOPRO (Life technologies) was used for nuclei visualization. Images were acquired with confocal microscope leica SP5 (Leica, Germany) and analysed with ImageJ (NIH).

Reporter constructs and luciferase assay

497 bp and 485 bp nucleotide sequences corresponding to portion of the 3' UTR of ITGA6 and ITGAV respectively, including the conserved predicted binding site (seed sequence) for miR-25 were cloned downstream of the *firefly* Luciferase2 sequence in a PGL4.10 vector (Promega, USA) using XbaI (Promega) and FseI (New England Biolabs, USA) restriction enzymes. 1184 bp sequence of human elongation factor 1α (hEF1α) promoter was inserted into the multiple cloning site (MCS) of the PGL4.10 upstream the luciferase2 sequence using KpnI and HindIII (Promega). Mutagenesis was performed using QuikChange® (Stratagene, USA) site-directed mutagenesis approach. (Primer sequences in **supplementary table II**).

Zebrafish maintenance

Tg(mpo:GFP)i114 zebrafish line (20,21) was handled compliant to local animal welfare regulations and maintained according to standard protocols (www.ZFIN.org).

Zebrafish embryo preparation and tumor cell implantation

2 days-post fertilisation (dpf) dechorionized zebrafish embryos were anaesthetized with 0.003% tricaine (Sigma) and placed on a 10-cm Petridish coated with 3% agarose. PC-3M-Pro4mCherry cells were transfected 48h before implantation. Single cell suspensions were re-suspended in PBS, kept at room temperature before implantation and implanted within 3 h. The cell suspension was loaded into borosilicate glass capillary needles (1 mm O.D. × 0.78 mm I.D.; Harvard Apparatus) and the injections were performed using a Pneumatic Picopump and a manipulator (WPI, UK). Approximately 400 cells were injected at around 60 μm above the ventral end of the duct of Cuvier (DoC), where the DoC opens into the heart. After implantation with mammalian cells, zebrafish embryos (including non-implanted controls) were maintained at 33°C, to compromise between the optimal temperature requirements for fish and mammalian cells (22). Data are representative of at least two independent experiments with at least fifty embryos per group. Experiments were discarded when the survival rate of the control group was less than 80%.

Statistical analysis

Statistical analysis was performed with GraphPad Prism 6.0 (GraphPad software) using t-test for comparison between two groups. Data is presented as mean ± SEM. P-values ≤ 0.05 were considered to be statistically significant (* $P < 0.05$, ** $P < 0.01$, *** $P < 0.001$).

Results

miR-25 expression is down-regulated in normal and transformed prostate stem cells (PCSC) and steadily increases upon luminal differentiation.

To investigate the expression of miRs in prostate cancer stem cells (PCSCs), we used the ALDEFLUOR assay, which involves viable cell sorting based on ALDH enzyme activity (23,24). After viable sorting ALDH^{high} and ALDH^{low} subpopulations of PC-3M-Pro4Luc2 were used to identify the differential miR expression profiles of cancer stem cells (ALDH^{high}) and committed non-tumorigenic & non-metastatic (ALDH^{low}) cells (11). Real Time PCR-based miR expression profiling revealed that miR-25 was the most down-regulated microRNA in cancer stem cells (ALDH^{high}) compared to ALDH^{low} subpopulation of cells (LOG10-Fold change -2,76 p-value=0,05). (**Fig. 1A**).

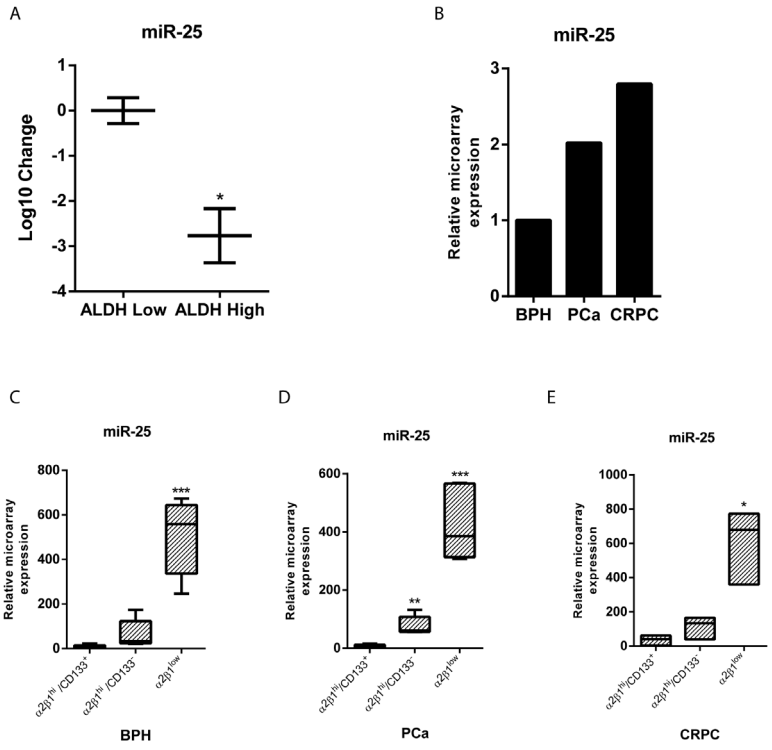

Figure 1. Differential expression of miR-25 in prostate cancer, prostate cancer stem-like cells, and benign prostate epithelial stem cells. A) miR-25 expression in ALDH^{high} versus ALDH^{low} subpopulation isolated from PC-3M-Pro4Luc2 cells measured with real time PCR-based miRNA expression profiling; error bars, ±SEM (n = 2). **B**) relative array expression of miR-25 in BPH, PCa (prostate cancer), and CRPC samples isolated from patients. **C**) relative array expression of miR-25 in α2β1hi/CD133+,

α2β1hi/CD133−, and α2β1low compartment, also referred to as stem-like cells, TA cells, and CB cells, respectively (12), isolated from BPH (n = 5 patients), PCa (prostate cancer; n = 5 patients; **D**), and CRPC (n = 3 patients; **E**); error bars, ±SEM. *, P < 0.05; **, P < 0.01; ***, P < 0.001.

We next investigated miR expression in subpopulations isolated from prostate tissue and primary epithelial cultures derived from patients with Benign Prostatic Hyperplasia (BPH), hormone-naïve prostate cancer (PCa, > Gleason 7) and castration-resistant prostate cancer (CRPC) (12). First we quantified the expression of miR-25 in unfractionated soft tissue collected from BPH, PCa and CRPC and found increased miR-25 expression upon tumor progression. (**Fig. 1B**). Then, after expansion of primary prostate cells in culture, we compared miR-25 expression in three cell populations: $\alpha2\beta1^{hi}$ /$CD133^{+}$, $\alpha2\beta1^{hi}$ /$CD133^{-}$, and $\alpha2\beta1^{low}$, also referred to as stem-like cells (SC), transit amplifying cells (TA) and committed basal cells (CB), respectively (5,12,14,25). Interestingly, miR-25 is significantly and strongly down-regulated in the $\alpha2\beta1^{hi}$ /$CD133^{+}$ population compared to the $\alpha2\beta1^{hi}$ /$CD133^{-}$ and $\alpha2\beta1^{low}$ compartments, irrespective of their pathological status (i.e. BPH, PCa and CRPC) (**Fig. 1C, D, E**).
Taken together, our data show consistent relative low expression levels of miR-25 in the cancer stem/progenitor subpopulation of cells in both human prostate cancer cell lines and the compartment defined as $\alpha2\beta1^{hi}$ /$CD133^{+}$ cells isolated from prostate cancer patients (12,25). The expression of miR-25 steadily and consistently increases during epithelial differentiation in patient-derived benign prostates (BPH) and malignant prostate samples.

Identification and transcriptional analysis of miR-25 predicted target genes.

Next Targetscan (Release 6.2) was used to identify novel miR-25 predicted target genes (26). Using this approach we identified 893 conserved putative target genes, with a total of 992 conserved sites and 211 poorly conserved sites. Among the list of predicted targets, 63 genes were mapped, using the database for annotation, visualization and integrated discovery DAVID (17,18), in processes linked to invasion and pathways related to prostate cancer and bone metastasis (Regulation of f-actin cystoskeleton, ECM-receptor interaction, TGF-β signalling pathway, MAPK signalling pathway and cell cycle). Interestingly, our *in silico* analysis showed that the regulation of F-actin cytoskeleton was one of the predicted pathways that is potentially affected by miR-25 (p-value = 2.1E-2). Mapping of the predicted miR targets to the regulation of F-actin cytoskeleton, KEGG pathway identified multiple genes involved in important processes for cell motility, migration, invasion and cytoskeleton dynamic. (**Fig. 2A**).

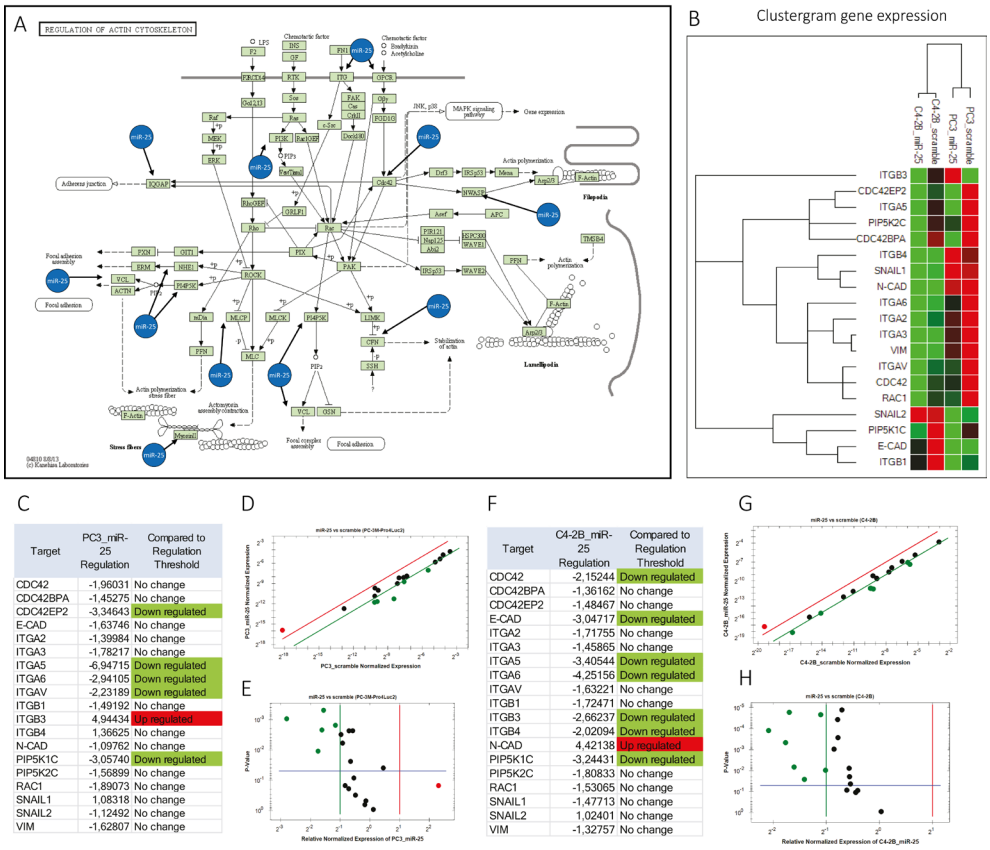

Target	PC3_miR-25 Regulation	Compared to Regulation Threshold
CDC42	-1,96031	No change
CDC42BPA	-1,45275	No change
CDC42EP2	-3,34643	Down regulated
E-CAD	-1,63746	No change
ITGA2	-1,39984	No change
ITGA3	-1,78217	No change
ITGA5	-6,94715	Down regulated
ITGA6	-2,94105	Down regulated
ITGAV	-2,23189	Down regulated
ITGB1	-1,49192	No change
ITGB3	4,94434	Up regulated
ITGB4	1,36625	No change
N-CAD	-1,09762	No change
PIP5K1C	-3,05740	Down regulated
PIP5K2C	-1,56899	No change
RAC1	-1,89073	No change
SNAIL1	1,08318	No change
SNAIL2	-1,12492	No change
VIM	-1,62807	No change

Target	C4-2B_miR-25 Regulation	Compared to Regulation Threshold
CDC42	-2,15244	Down regulated
CDC42BPA	-1,36162	No change
CDC42EP2	-1,48467	No change
E-CAD	-3,04717	Down regulated
ITGA2	-1,71755	No change
ITGA3	-1,45865	No change
ITGA5	-3,40544	Down regulated
ITGA6	-4,25156	Down regulated
ITGAV	-1,63221	No change
ITGB1	-1,72471	No change
ITGB3	-2,66237	Down regulated
ITGB4	-2,02094	Down regulated
N-CAD	4,42138	Up regulated
PIP5K1C	-3,24431	Down regulated
PIP5K2C	-1,80833	No change
RAC1	-1,53065	No change
SNAIL1	-1,47713	No change
SNAIL2	1,02401	No change
VIM	-1,32757	No change

Figure 2. In silico analysis for predicted pathway identification and validation by RT-qPCR. A) interaction between miR-25 and predicted target genes overlaid on KEGG regulation of the actin cytoskeleton pathway. **B**) clustergram of mRNA expression assessed by RT-qPCR for selected target among those represented in A. Analysis performed in PC-3M-Pro4Luc2 and C4-2B cells (N = 3). Colors match with those represented in B, D, E, F, G, H (green, downregulation; red, upregulation). **C**) mRNA regulation of selected target genes on PC-3M-Pro4Luc2–overexpressing miR-25; regulation is highlighted in green (down) and red (up). Colors are matched with scatter plot (**D**) with threshold selected (threshold value = 2) and significant values are represented in volcano plot (**E**). **F**) mRNA regulation of selected target genes on C4-2B–overexpressing miR-25; regulation is highlighted in green (down) and red (up). Colors are matched with scatter plot (**G**) with threshold selected (threshold value = 2) and significant values are represented in volcano plot (**H**).

Strikingly, miR-25 was predicted to target IQGAP2 (a GTP-dependent protein involved in the cytoskeletal reorganization), WASL and CFL2 (involved in the actin polymerization and depolymerization), CDC42 (required for rounded/ameboid movements of single tumor cells), MYH9 (cellular myosin with a role in cytokinesis and cell shape), PIP4K2C and PIP5K1C (kinase which mediates RAC1-dependent reorganization of actin filaments

(27)). RAC1 is involved in focal adhesion and is required for mesenchymal movements of single tumor cells (28)), PIKFYVE (which plays a role in endosome-related membrane trafficking), PPP1R12A (regulates myosin phosphatase activity), SLC9A1 (sodium/hydrogen exchanger involved in focal adhesion), ITGA5 (a.k.a. fibronectin receptor, significantly down-regulated by miR-25 in both cell lines as shown by qRT-PCR analysis **(Fig. 2 B,C,D,E and Fig. 2 F,G,H)**) and ITGAV (a.k.a. vitronectin receptor), ITGA6 (laminin-10/11 receptor) and Vinculin (VCL, however not affected by miR-25 as shown by western blot **(Suppl. Fig. 1A)** that are all involved in cell-matrix interactions and adhesion. Among the target genes involved in the regulation of the F-actin cytoskeleton, ITGAV and ITGA6 are members of the integrin family of transmembrane receptors that regulate cell adhesion, migration and remodelling of the ECM (29-31). Additionally, ITGAV and ITGA6 were also identified as miR-25 predicted targets using miRDB (15) and microTCDS (16). Moreover integrin-transmembrane receptors regulate the activation of Rho-GTPases, RAC1 and CDC42 (32). Interestingly, our mRNA analysis **(Fig. 2B)** revealed that miR-25 significantly down-regulated CDC42 and its effector proteins CDC42BPA and CDC42EP2 and decreased mRNA of RAC1 **(Fig. 2 C,D,E and Fig. 2 F,G,H).** Additionally, our RT-qPCR analysis revealed that miR-25 could significantly decreased PIP5K1C, kinase involved in RAC1 signaling and predicted target of miR-25 in both cell lines **(Fig. 2 C,D,E and Fig. 2 F,G,H).**

Previously we have shown that ITGAV is required for the acquisition of a stem/progenitor phenotype (31). Additionally, ITGAV and ITGA6 are highly expressed in prostate progenitor cells and ITGA6 has been established as maker for progenitor cells in prostate and breast cancer. These results suggested a functional link between miR-25 and ITGAV and ITGA6 expression regulation in prostate cancer, for which no information is currently available.

miR-25 overexpression down-regulates α_v and α_6 integrins in human prostate cancer cell lines and selected ALDH^{high} subpopulation

To investigate the functional interaction between miR-25 and the predicted target genes we isolated ALDH^{high} and ALDH^{low} from PC-3M-Pro4Luc2 prostate cancer cell line by flow cytometry. As expected, the clonogenic and migratory potential of ALDH^{high} vs ALDH^{low} cells was higher (11) (**Suppl. Fig. 1B, C**). Furthermore, ITGAV and ITGA6 expression was also higher in ALDH^{high} vs ALDH^{low} cells as expected, thus confirming the inverse correlation with miR-25 expression (11) (**Suppl. Fig. 1D**). We used ITGA2, an established prostate cancer stem cell marker, as positive control and confirmed its increased expression in ALDH^{high} cells (5,11) (**Suppl. Fig. 1D**).

The functional interaction between miR-25 and ITGAV and ITGA6 expression in human prostate cancer cell lines and selected subpopulation of cells (ALDH^{high} stem/progenitors

and ALDH^{low} committed cells) was evaluated by transfection with 60nM of pre-miR-25 or pre-negative control sequence.

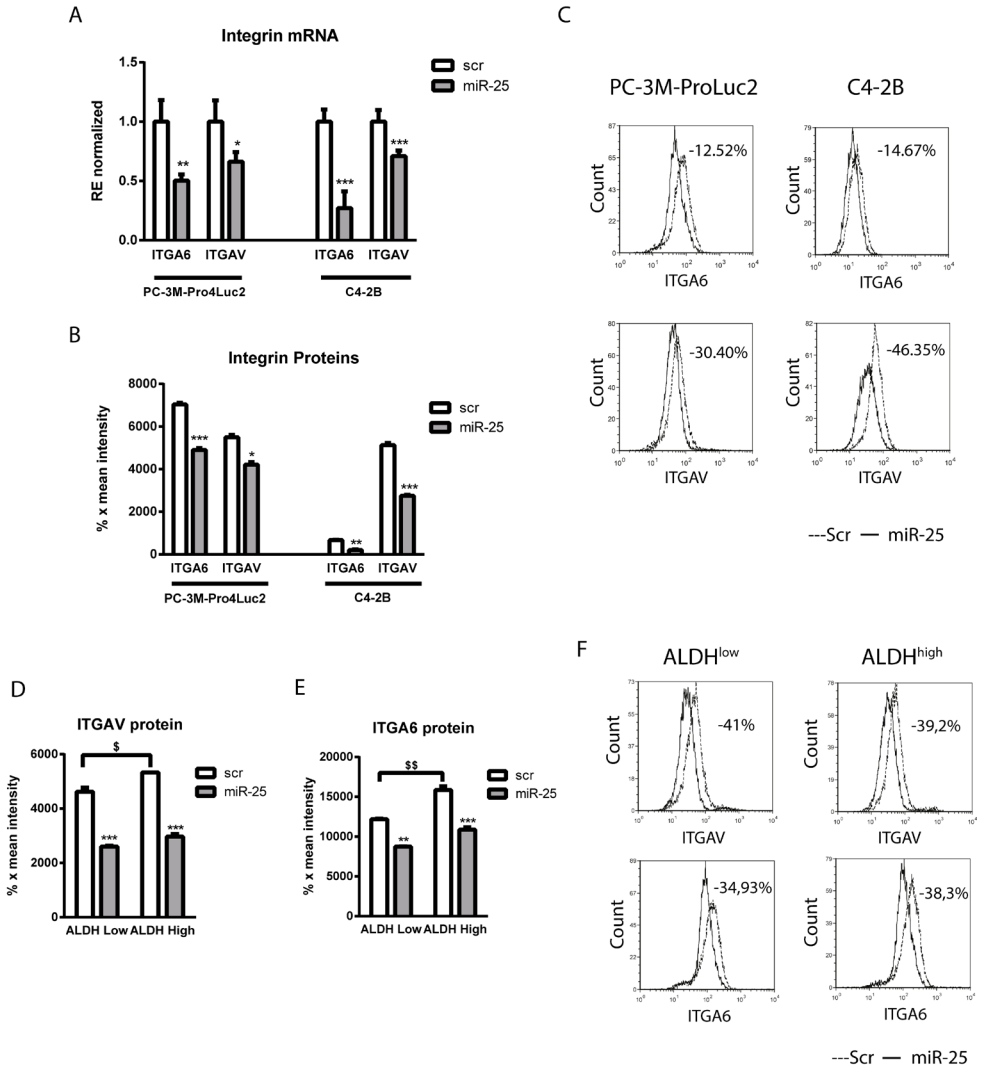

Figure 3. miR-25 overexpression decreases ITGAV and ITGA6 expression at mRNA and protein level in prostate cancer cells and selected ALDH^{high} subpopulation of cells. A) PC-3M-Pro4Luc2– and C4-2B–overexpressing miR-25; relative expression is compared with scramble negative control and all values were normalized to GAPDH; error bars, ±SEM (n = 3). **B**) mean intensity of ITGAV and ITGA6 fluorescence in PC-3M-Pro4Luc2– and C4-2B–overexpressing miR-25 compared with scramble-negative control determined by FACS analysis; error bars, ±SEM (n = 3). **C**) histogram of flow cytometric analysis of ITGAV and ITGA6 protein expression. Expression levels in cells overexpressing miR-25 (continued line)

are compared with scramble-negative control (dashed line). **D**) and **E**) mean intensity of ITGAV and ITGA6 fluorescence in $ALDH^{high}$- versus $ALDH^{low}$-overexpressing miR-25 compared with scramble-negative control determined by FACS analysis; error bars, ±SEM (n = 2). **F**) histogram of flow cytometric analysis of ITGAV and ITGA6 protein expression. Expression levels in $ALDH^{high}$ versus $ALDH^{low}$ subpopulation–overexpressing miR-25 (continued line) are compared with scramble-negative control (dashed line). * and $, P < 0.05; ** and $$, P < 0.01; ***, P < 0.001.

Overexpression of miR-25 significantly attenuated ITGAV and ITGA6 mRNA expression in PC-3M-Pro4Luc2 and C4-2B (ITGAV p-value = 0.05 and 0.001 respectively; ITGA6 p-value = 0.01 and 0.001 respectively) (**Fig. 3A**). Interestingly, forced overexpression of miR-25 also led to a significant reduction in ITGA5 expression in both cell lines (p-value= 0.01 and 0.001 respectively) and reduced levels of ITGA3, ITGB1 and ITGB4 in C4-2B (p-value= 0.01, 0.001 and 0.05 respectively). (**Suppl. Fig. 1E,F and Fig. 2B,C,D,E,F,G,H**). As expected, no consistent inhibitory effect was observed on ITGA2 expression.
Strikingly, upon transfection of PC-3M-Pro4Luc2 and C4-2B cells with pre-miR-25 (or pre-negative control) for 72 hours ITGAV and ITGA6 protein expression were also significantly down-regulated not only in the bulk cell lines (**Fig. 3B, C**) but also in selected $ALDH^{low}$ and highly aggressive $ALDH^{high}$ subpopulation of stem/progenitor cells transfected with pre-miR-25 (or pre-negative control) after viable cell sorting (**Fig. 3D, E**, **F)**.

miR-25 overexpression decreases migration of metastasis-initiating human prostate cancer cells and affects cytoskeleton dynamics

Prostate cancer cell migration in both PC-3M-Pro4Luc2 and C4-2B cells was significantly attenuated upon miR-25 overexpression (PC-3M-Pro4Luc2, 88% decrease, p-value= 0.001; C4-2B, 49% decrease, p-value=0.01 after 72 hrs) (**Fig. 4 A, B**).
Strikingly, miR-25 was able to strongly and significantly reduce migration also in selected highly migratory $ALDH^{high}$ subpopulation of stem/progenitor-like cells transfected after viable cell sorting (P<0.001) **(Fig. 4 C,D)**.
In contrast to migration, cell proliferation was not affected by forced miR-25 overexpression compared to the scrambled negative control sequence (**Suppl. Fig. 2A, B**). miR-25 also induced a switch to a less invasive phenotype characterized by a dramatic change in cell morphology (**Suppl. Fig. 2C**). Phalloidin staining revealed an almost complete loss of actin filopodia and cytoskeletal reorganization associated with a strong decrease in the average F-actin fluorescence (p-value= 0.01) (**Fig. 4E, F**). Additionally, migration was monitored in $ALDH^{high}$ and $ALDH^{low}$ subpopulation 4 days after sorting (i.e. 72 hours after transfection of selected subpopulation) and confirmed significantly higher conserved migratory potential in $ALDH^{high}$ cells compared to $ALDH^{low}$ (**Fig. 4 G, H**). Taken together these results suggest a critical role of miR-25 in the

regulation of an invasive phenotype by modulating cytoskeletal integrity, organization and motility in humane prostate cancer cell lines and selected aggressive tumor- and metastasis-initiating ALDH^{high} subpopulation (11).

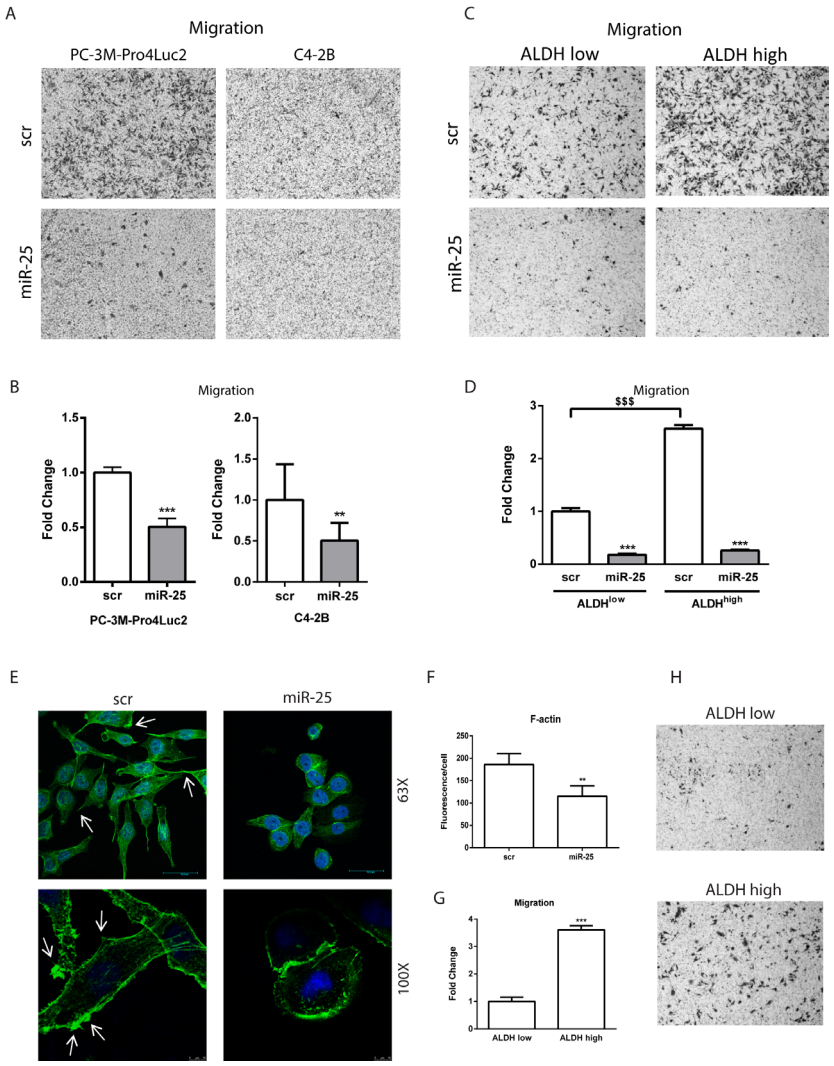

Figure 4. miR-25 overexpression affect cell morphology and decreases migration in prostate cancer cells and selected ALDH^{high} subpopulation of cells. A) representative images of PC-3M-Pro4Luc2 and C4-2B migrating in Transwell chambers after transfection with pre–miR-25 and prenegative control. **B**) mean number of migrated PC-3M-Pro4Luc2 and C4-2B cells per field transfected with scramble-negative control and pre–miR-25; error bars, ±SEM (n = 2). **C**) representative images of ALDH^{high} and ALDH^{low} subpopulation of cells migrating in Transwell chambers after transfection with pre–miR-25 and prenegative control; error bars, ±SEM (n = 2). **D**) mean number of migrated ALDH^{high} and

$ALDH^{low}$ subpopulation of cells per field transfected with scramble-negative control and pre–miR-25; error bars, ±SEM (n = 2). **E**) representative confocal images of PC-3M-Pro4Luc2 transfected with pre–miR-25 and prenegative control stained for F-actin with phalloidin (green) and nuclei with TO-PRO (blue). **F**) corrected total cell fluorescent of PC-3M-Pro4Luc2 transfected with scramble and pre–miR-25 measured with ImageJ and calculated as (integrated density − (area of selected cells × mean fluorescence of background readings)); error bars, ±SEM (n = 3 measurements). **G**) and **H**) mean number of migrated $ALDH^{high}$ and $ALDH^{low}$ subpopulation of cells per field and representative images of the $ALDH^{high}$ and $ALDH^{low}$ subpopulation of cells migrating in Transwell chambers; error bars, ±SEM (n = 2). **, P < 0.01; *** and $$$, P < 0.001.

The miR-25 induced change to a less invasive phenotype does not coincide with major changes in the expression of epithelial markers, suggesting that the observed morphological changes are most likely due to altered integrin expression as we demonstrated previously for α_v-integrins (31) (**Suppl. Fig. 2D, E**).

miR-25 directly targets pro-invasive α_6- and α_v-integrins

Next we investigated the putative direct functional interaction between miR-25 and its predicted ITGA6 and ITGAV target genes. For this we cloned 497 bp and 485 bp nucleotide sequences corresponding to a portion of the 3' UTR of ITGA6 and ITGAV respectively, including the conserved predicted binding site (seed sequence) for miR-25, downstream of the *firefly* luciferase2 sequence in a pGL4.10 vector background (see Materials & Methods) **(Fig. 5A)**.

To achieve high expression of the reporter system a 1184bp sequence corresponding to human elongation factor 1α (hEF1α) promoter was inserted into the multiple cloning site (MCS) of the pGL4.10 upstream to the luciferase2 sequence. The reporter constructs, containing mutant miR-25 binding site in the 3' UTR of the descripted genes, were also generated and used as a control. Transfection of pre-miR-25 resulted in a significant reduction of luciferase activity in the wild-type but not in the mutant 3' UTR of the ITGA6 and ITGAV genes (p-value= 0.05 for both genes) (**Fig. 5B, C**). These results, combined with the transcriptional and translational analysis described above, show for the first time that miR-25 directly targets ITGA6 and ITGAV expression.

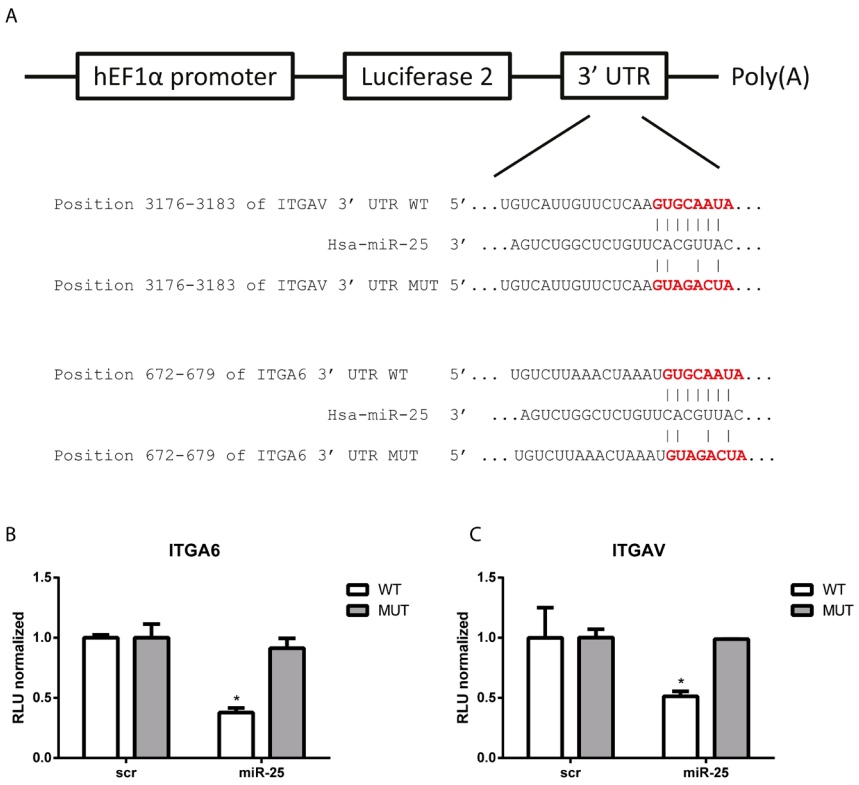

Figure 5. miR-25 directly regulates ITGAV and ITGA6. A) portion of 3′-UTR of ITGAV or ITGA6 containing the miR-25 predicted–binding site was cloned in PGL4-basic vector modified with hEF1α promoter. Scramble-negative control or pre–miR-25 was cotransfected with WT or MUT construct for ITGA6 (**B**) or ITGAV (**C**) together with CAGGS-renilla plasmid. RLU is calculated as ratio luciferase/renilla and normalized for scramble-negative control; error bars, ±SEM (n = 3). *, P < 0.05.

miR-25 inhibits distant metastasis of human prostate cancer cells in zebrafish

To investigate the ability of miR-25 to interfere with migration and invasion in the intact organism PC-3M-Pro4 prostate cancer cells, that stably express the NIRF protein mCherry, were injected into the circulatory system of zebrafish embryos and their tumor extravasation and distant metastasis formation was examined (33). The embryonic vascular system of zebrafish is fully functional and allows efficient detection of extravasating tumor cells (34). In addition, in the Tg(mpo:GFP)i114, the embryos are transparent and the immune system is not fully developed permitting successful xenotransplantation of human tumor cells (22). This makes the zebrafish model system highly appropriate for observing interaction between tumor cells and vasculature at the single cell level (35). We transfected PC-3M-Pro4mCherry cells to overexpress pre-miR-25

(or pre-negative control) and inoculated the cancer cells into the duct of Cuvier (DoC) of 2-day-old zebrafish embryos (100 embryos injected per group) (33). Disseminated cells were arrested in the host vasculature in the first hours, and extravasation was detected from 12hpi (hours post implantation). Perivascular tumor cells were observed in multiple foci, including the optic veins, the inter-segmental vessels, the dorsal aorta and the caudal vein. However, exclusively at the posterior ventral end of the tissue caudal hematopoietic (CHT, as indicated in **Fig. 6**) in the tail, perivascular tumor cells were able to invade into the neighboring tail fin. At day 1 post-implantation (1 dpi) miR-25 overexpression caused a robust and significant reduction in the distal colonization and invasion from CHT into the tail fin compared to the scramble control cells (**Fig. 6A**). miR-25 was able to completely abolish invasion which was detected in 20% of the embryos injected with cells transfected with pre-negative control. At day 2 post-implantation (2 dpi), 40% of embryos injected with cells overexpressing the negative control showed invasion from CHT, compared to 20% of embryos injected with cells overexpressing miR-25 (**Fig. 6 B, C**). In addition, miR-25 was able to significantly reduce the number of tumorigenic foci/embryo at 1 dpi while no significant difference was measured at 2 dpi (**Fig. 7 A, B, C**).

Taken together, our experimental metastasis data support the findings *in vitro* and indicate that miR-25 negatively regulates the acquisition of an invasive, metastatic phenotype in human prostate cancer cells.

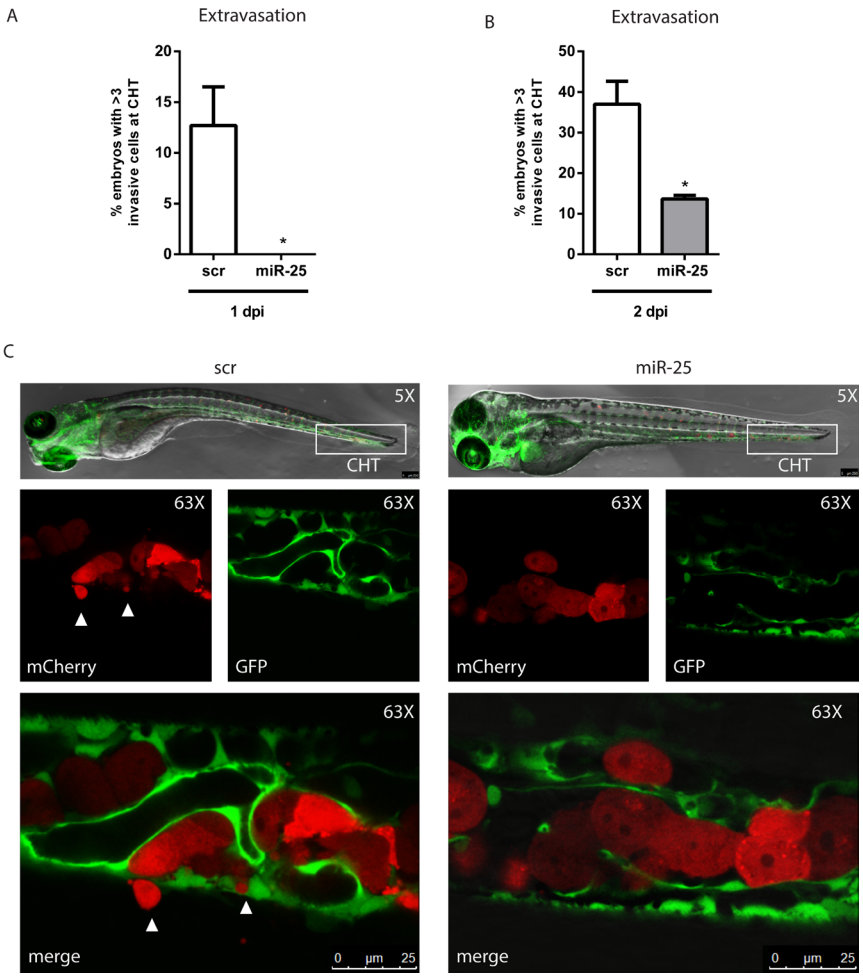

Figure 6. miR-25–overexpressing cells injected in zebrafish circulation show reduced extravasation. Of note, 100 embryos per group were injected and the percentage of embryos with invasion at CHT (invasion defined as >3 cells extravasating/embryo) was counted at day 1 post-injection (1 dpi; **A**) and day 2 postinjection (2 dpi; **B**); error bars, ±SEM (n = 2 experiments). **C**) representative confocal images of zebrafish embryos injected with PC-3M-Pro4mCherry cells overexpressing miR-25 or negative control. Cells overexpressing miR-25 were lodged into circulation, whereas cells overexpressing negative control started to show extravasation, full out of CHT and from CHT into the neighboring tail fin at 1 dpi. *, $P < 0.05$.

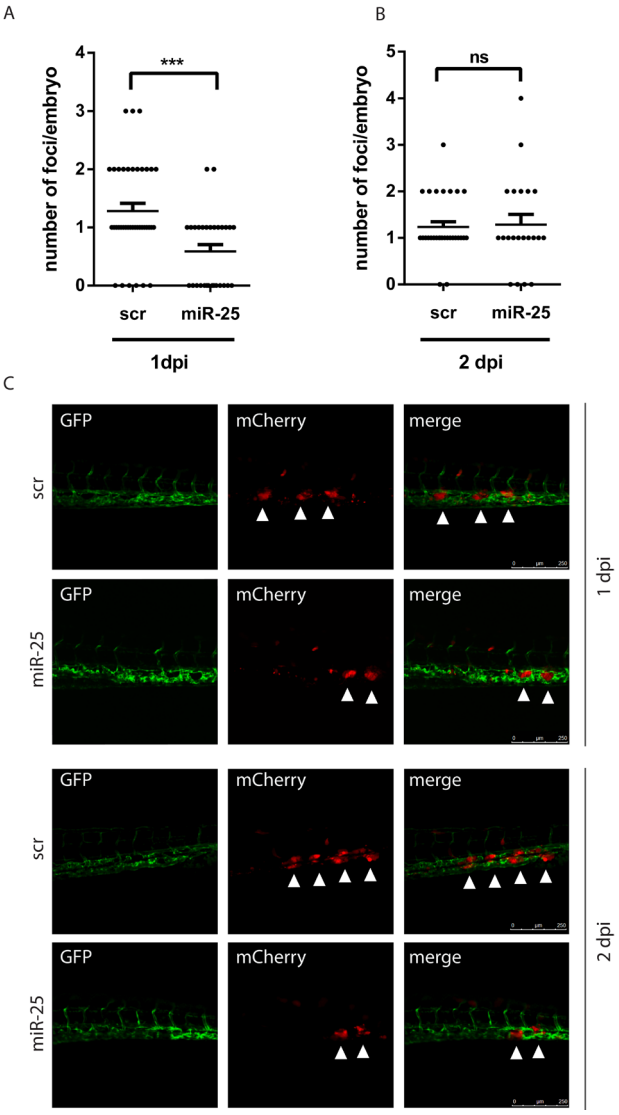

Figure 7. miR-25–overexpressing cells injected in zebrafish circulation show reduced tumor foci (colonization). A) number of tumor foci is reduced in embryos injected with cells overexpressing miR-25 compared with negative control at 1 day post-injection (1 dpi). **B**) no difference in the number of foci from embryos injected with cells overexpressing miR-25 and scr was measured at day 2 post-injection (2 dpi). 100 embryos per group were injected; error bars indicate ±SEM (n = 2 experiments). **C**) representative confocal images of zebrafish embryos injected with PC-3M-Pro4mCherry cells overexpressing miR-25 or negative control at 1 dpi and 2 dpi. ***, $P < 0.001$.

Discussion

In this study, miR-25 was identified as an important regulator of the invasive program in non-transformed and malignant human prostate epithelial tissues. In human prostate cancer cell lines and patient-derived primary prostate tumors, miR-25 expression was low/absent in the $\alpha2\beta1^{hi}$ /$CD133^{+}$ (SC) cell subpopulation but its expression steadily increased during differentiation to $\alpha2\beta1^{hi}$ /$CD133^{-}$ (TA) cells and $\alpha2\beta1^{low}$ (CB) cells committed for terminal differentiation (12). Here we identified, for the first time, the pro-invasive α_v- and α_6-integrins as functional target genes of miR-25. Forced overexpression of miR-25 in human prostate cancer cells and in highly metastatic and aggressive subpopulation of cells ($ALDH^{high}$) leads to a strong and significant decline in α_v- and α_6-integrin driven invasive behavior *in vitro* and blockage of metastatic colonization in the intact organism.

Consistent with these observations, overexpression of miR-25 decreased migration and strongly affected cell morphology of prostate cancer cells through its direct effect on the cytoskeletal arrangement and dynamics. miR-25 may, therefore, represent one of the key regulators of the invasive program in the human prostate epithelium, in particular in the maintenance of an aggressive phenotype in human prostate cancer “driver” subpopulation of stem/progenitor-like cells.
The results from this study support the notion that the stem/progenitor subpopulation in human prostate cancer displays increased clonogenic, migratory properties *in vitro* and stronger tumor- and metastasis-initiating properties in preclinical *in vivo* models (11).
miR-25 is part of the miR-106b-25 cluster which was previously reported to be up-regulated in primary tumors and distant metastasis in prostate cancer (36-40). A likely explanation for these apparent contradictory observations is that cancer cell lines and bulk tumor tissues are not homogeneous and consist of a mixture of heterogeneous subpopulations of cells (2). The findings reported here suggest that cellular heterogeneity may limit the appropriate interpretation of RNA expression-based analysis data obtained from *bulk* tissues. The cellular composition and proportion of $\alpha2\beta1^{hi}$/$CD133^{+}$, $\alpha2\beta1^{hi}$/$CD133^{-}$ and $\alpha2\beta1^{low}$, also referred to as stem-like cells (SC), transit amplifying cells (TA) and committed basal cells (CB) (12) in the normal prostate epithelium vs prostate cancer epithelium is indeed generally very different (5). For instance, the “driver” stem/progenitor subpopulation in the human prostate often represents only 0.02% of all prostate epithelial cells (5,41). The increase in absolute expression levels of miR-25 in bulk tissues during prostate cancer progression may,

therefore, be indicative of an increase in the proportion of more differentiated, less invasive, miR-25^{high} luminal epithelial cells.

Here we focused primarily on the differential miR expression in α2β1^{hi} /CD133^{+} cells as a cellular subpopulation that "drives" tumorigenesis and metastasis (14). Our findings, indeed, confirmed that miR-25 is overexpressed in hormone-naive and castration-resistant prostate cancer as previously reported by others (38,42). Intriguingly, we found that -despite the previously observed upregulation of miR-25 in bulk prostate cancer tissues (38) the expression of miR-25 in the α2β1^{hi} /CD133^{+} cells isolated from prostate cancer patients matched its expression in the tumor- and metastasis-initiating ALDH^{high} prostate cancer stem/progenitor subpopulation (11). Our analysis on the α2β1^{hi} /CD133^{+}, α2β1^{hi} /CD133^{-} and α2β1^{low} cell compartment enriched from primary prostate cancer samples supports the notion that miR-25 is down-regulated in the stem/progenitor cell compartment and that its expression steadily increases during differentiation. Consistent with our findings, the expression of the miR-106b-25 cluster appears to mediate neuronal differentiation of adult neural stem/progenitor cells and, interestingly, induction of miR-106b-25 in hypoxic conditions was recently linked to increased expression of neuronal markers in prostate cancer cell lines (43,44).

Thus, our work and these results suggest that lower miR-25 expression is needed to maintain stem/progenitor phenotype and its increase is associated with cellular differentiation.

In line with the miR-25 data presented in this study, we previously found that α_v-integrins play a pivotal role in the acquisition of a migratory stem/progenitor phenotype, tumorigenicity and the formation of distant bone metastasis *in vivo* (31,45). Moreover, $\alpha_6\beta_4$ integrin expression has already been associated with prostate cancer invasion, metastasis and disease progression (46-48). In addition, integrins provide a structural link between F-actin and the extracellular matrix and contribute to formation of focal adhesion points (49). Our confocal analysis showed that overexpression of miR-25 dramatically affected cell morphology and impaired F-actin polymerization, reducing focal adhesion sites. It seems, therefore that miR-25 is a key player in the organization of the F-actin and exerts a crucial role in the regulation of an aggressive and migratory phenotype with its direct effect on integrin expression. In addition, organization of F-actin is linked to activation of integrin-transmembrane receptor which regulates the activation of Rho-GTPases, RAC1 and CDC42 (32). Aberrant migration and invasion of cancer cells are key components of their invasive-metastatic phenotype. Individual tumor cells with an elongated, morphology like PC-3M-Pro4Luc2, often migrate in a "mesenchymal manner", which requires activation of RAC1, decreased by miR-25 (28). In contrast, single tumor cells with a less mesenchymal phenotype, like C4-2B, migrate with an "amoeboid mode" which requires signalling of CDC42, significantly down-

regulated after miR-25 overexpression (28). Our *in silico* analysis, revealed that PIP5K1C and PIP4K2C, kinases involved RAC1 signalling, are also predicted target of miR-25. In addition, our transcriptional analysis indicated that miR-25 down-regulates CDC42 mRNA together with CDC42BPA and CDC42EP2 mRNA (CDC42 effector proteins). This information combined with the evidence provided by our mRNA and protein analysis on integrin expression in bulk cell lines and selected subpopulation of highly metastatic cells ($ALDH^{high}$), suggest that miR-25 could be a central player in F-actin organization and cytoskeletal dynamics. However, the observed miR-25- induced loss of a migratory phenotype, confirmed in selected $ALDH^{high}$ subpopulation of stem/progenitor-like cells, could not be fully explained by the acquisition of more epithelial characteristics (or blockage of EMT-like processes), despite the fact that E-Cadherin is a validated target gene of miR-25 (50).

Consistent with our *in vitro* observations, complete blocking of metastasis by prostate cancer cells overexpressing miR-25 at 1 dpi and a strong reduction at 2 dpi was found in embryonic zebrafish model (33). These observations indicate that the morphological alterations produced by miR-25 disrupt extravasation and colonisation at distant sites *in vivo.*

In conclusion, we identified -for the first time- a direct functional interaction between miR-25 and integrins as key regulators of prostate cancer invasiveness and metastasis. Our *in vitro* and *in vivo* data indicate that miR-25 can have a suppressor role in aggressive human prostate cancer cells (cell lines and selected subpopulation of $ALDH^{high}$ cells) by blocking invasion, and metastasis by promoting prostate epithelial differentiation and by disrupting. From a therapeutic perspective, miR-25 seems an interesting small molecule for specific targeting of stem/progenitor-like cells in aggressive human prostate cancer.

Acknowledgements

We would like to thank Guido de Roo from the Flow cytometry facility (Dept. of Hematology, LUMC, The Netherlands) and Dr. Twan de Vries (Dept. of Cardiology, LUMC, The Netherlands) for kindly providing construct with hEF1α promoter. We also would like to thank Chris van der Bent and Hetty Sips (Dept. of Endocrinology, LUMC, The Netherlands) for help and technical support. The research leading to these results has received funding from the FP7 Marie Curie ITN under grant agreement n°264817 - BONE-NET (EZ) and n°238278 - PRONEST (JR). This project receives also additional support from Prostate Action UK (EZ, JR) and from the Dutch Cancer Society (UL-2011-4930) (GvdH).

REFERENCES

1. Jemal A, Center MM, DeSantis C, Ward EM. Global patterns of cancer incidence and mortality rates and trends. Cancer Epidemiol Biomarkers Prev 2010;19(8):1893-907.
2. Shackleton M, Quintana E, Fearon ER, Morrison SJ. Heterogeneity in cancer: cancer stem cells versus clonal evolution. Cell 2009;138(5):822-9.
3. Dean M, Fojo T, Bates S. Tumour stem cells and drug resistance. Nat Rev Cancer 2005;5(4):275-84.
4. Maitland NJ, Collins AT. Prostate cancer stem cells: a new target for therapy. J Clin Oncol 2008;26(17):2862-70.
5. Collins AT, Berry PA, Hyde C, Stower MJ, Maitland NJ. Prospective identification of tumorigenic prostate cancer stem cells. Cancer research 2005;65(23):10946-51.
6. Reya T, Morrison SJ, Clarke MF, Weissman IL. Stem cells, cancer, and cancer stem cells. Nature 2001;414(6859):105-11.
7. Calin GA, Croce CM. MicroRNA signatures in human cancers. Nat Rev Cancer 2006;6(11):857-66.
8. Bartel DP. MicroRNAs: target recognition and regulatory functions. Cell 2009;136(2):215-33.
9. Mitchell PS, Parkin RK, Kroh EM, Fritz BR, Wyman SK, Pogosova-Agadjanyan EL, et al. Circulating microRNAs as stable blood-based markers for cancer detection. Proc Natl Acad Sci U S A 2008;105(30):10513-8.
10. Bryant RJ, Pawlowski T, Catto JW, Marsden G, Vessella RL, Rhees B, et al. Changes in circulating microRNA levels associated with prostate cancer. Br J Cancer 2012;106(4):768-74.
11. van den Hoogen C, van der Horst G, Cheung H, Buijs JT, Lippitt JM, Guzman-Ramirez N, et al. High aldehyde dehydrogenase activity identifies tumor-initiating and metastasis-initiating cells in human prostate cancer. Cancer research 2010;70(12):5163-73.
12. Rane JK, Scaravilli M, Ylipaa A, Pellacani D, Mann VM, Simms MS, et al. MicroRNA expression profile of primary prostate cancer stem cells as a source of biomarkers and therapeutic targets. Eur Urol 2015;67(1):7-10.
13. Collins AT, Habib FK, Maitland NJ, Neal DE. Identification and isolation of human prostate epithelial stem cells based on alpha(2)beta(1)-integrin expression. J Cell Sci 2001;114(Pt 21):3865-72.
14. Richardson GD, Robson CN, Lang SH, Neal DE, Maitland NJ, Collins AT. CD133, a novel marker for human prostatic epithelial stem cells. J Cell Sci 2004;117(Pt 16):3539-45.
15. Wang X. miRDB: a microRNA target prediction and functional annotation database with a wiki interface. Rna 2008;14(6):1012-7.
16. Paraskevopoulou MD, Georgakilas G, Kostoulas N, Vlachos IS, Vergoulis T, Reczko M, et al. DIANA-microT web server v5.0: service integration into miRNA functional analysis workflows. Nucleic acids research 2013;41(Web Server issue):W169-73.
17. Huang da W, Sherman BT, Lempicki RA. Systematic and integrative analysis of large gene lists using DAVID bioinformatics resources. Nat Protoc 2009;4(1):44-57.
18. Huang da W, Sherman BT, Lempicki RA. Bioinformatics enrichment tools: paths toward the comprehensive functional analysis of large gene lists. Nucleic Acids Res 2009;37(1):1-13.
19. Kanehisa M, Goto S. KEGG: kyoto encyclopedia of genes and genomes. Nucleic Acids Res 2000;28(1):27-30.
20. Stoletov K, Montel V, Lester RD, Gonias SL, Klemke R. High-resolution imaging of the dynamic tumor cell vascular interface in transparent zebrafish. Proc Natl Acad Sci U S A 2007;104(44):17406-11.
21. Lawson ND, Weinstein BM. In vivo imaging of embryonic vascular development using transgenic zebrafish. Dev Biol 2002;248(2):307-18.

22. Haldi M, Ton C, Seng WL, McGrath P. Human melanoma cells transplanted into zebrafish proliferate, migrate, produce melanin, form masses and stimulate angiogenesis in zebrafish. Angiogenesis 2006;9(3):139-51.
23. Ginestier C, Hur MH, Charafe-Jauffret E, Monville F, Dutcher J, Brown M, et al. ALDH1 is a marker of normal and malignant human mammary stem cells and a predictor of poor clinical outcome. Cell Stem Cell 2007;1(5):555-67.
24. Douville J, Beaulieu R, Balicki D. ALDH1 as a Functional Marker of Cancer Stem and Progenitor Cells. Stem Cells and Development 2009;18(1):17-25.
25. Kroon P, Berry PA, Stower MJ, Rodrigues G, Mann VM, Simms M, et al. JAK-STAT blockade inhibits tumor initiation and clonogenic recovery of prostate cancer stem-like cells. Cancer research 2013;73(16):5288-98.
26. Lewis BP, Burge CB, Bartel DP. Conserved seed pairing, often flanked by adenosines, indicates that thousands of human genes are microRNA targets. Cell 2005;120(1):15-20.
27. Kuhn AR, Schlauch K, Lao R, Halayko AJ, Gerthoffer WT, Singer CA. MicroRNA expression in human airway smooth muscle cells: role of miR-25 in regulation of airway smooth muscle phenotype. Am J Respir Cell Mol Biol 2010;42(4):506-13.
28. Gadea G, Sanz-Moreno V, Self A, Godi A, Marshall CJ. DOCK10-mediated Cdc42 activation is necessary for amoeboid invasion of melanoma cells. Curr Biol 2008;18(19):1456-65.
29. Hynes RO. Integrins: bidirectional, allosteric signaling machines. Cell 2002;110(6):673-87.
30. Legate KR, Wickstrom SA, Fassler R. Genetic and cell biological analysis of integrin outside-in signaling. Genes Dev 2009;23(4):397-418.
31. van den Hoogen C, van der Horst G, Cheung H, Buijs JT, Pelger RC, van der Pluijm G. Integrin alphav expression is required for the acquisition of a metastatic stem/progenitor cell phenotype in human prostate cancer. Am J Pathol 2011;179(5):2559-68.
32. Huveneers S, Danen EH. Adhesion signaling - crosstalk between integrins, Src and Rho. J Cell Sci 2009;122(Pt 8):1059-69.
33. Drabsch Y, He S, Zhang L, Snaar-Jagalska BE, Ten Dijke P. Transforming growth factor-beta signalling controls human breast cancer metastasis in a zebrafish xenograft model. Breast Cancer Res 2013;15(6):R106.
34. Isogai S, Lawson ND, Torrealday S, Horiguchi M, Weinstein BM. Angiogenic network formation in the developing vertebrate trunk. Development 2003;130(21):5281-90.
35. Stoletov K, Kato H, Zardouzian E, Kelber J, Yang J, Shattil S, et al. Visualizing extravasation dynamics of metastatic tumor cells. J Cell Sci 2010;123(Pt 13):2332-41.
36. Hudson RS, Yi M, Esposito D, Glynn SA, Starks AM, Yang Y, et al. MicroRNA-106b-25 cluster expression is associated with early disease recurrence and targets caspase-7 and focal adhesion in human prostate cancer. Oncogene 2013;32(35):4139-47.
37. Poliseno L, Salmena L, Riccardi L, Fornari A, Song MS, Hobbs RM, et al. Identification of the miR-106b~25 microRNA cluster as a proto-oncogenic PTEN-targeting intron that cooperates with its host gene MCM7 in transformation. Sci Signal 2010;3(117):ra29.
38. Ambs S, Prueitt RL, Yi M, Hudson RS, Howe TM, Petrocca F, et al. Genomic profiling of microRNA and messenger RNA reveals deregulated microRNA expression in prostate cancer. Cancer research 2008;68(15):6162-70.
39. Szczyrba J, Loprich E, Wach S, Jung V, Unteregger G, Barth S, et al. The microRNA profile of prostate carcinoma obtained by deep sequencing. Mol Cancer Res 2010;8(4):529-38.
40. Martens-Uzunova ES, Jalava SE, Dits NF, van Leenders GJ, Moller S, Trapman J, et al. Diagnostic and prognostic signatures from the small non-coding RNA transcriptome in prostate cancer. Oncogene 2012;31(8):978-91.
41. Polson ES, Lewis JL, Celik H, Mann VM, Stower MJ, Simms MS, et al. Monoallelic expression of TMPRSS2/ERG in prostate cancer stem cells. Nature communications 2013;4:1623.

42. Volinia S, Calin GA, Liu CG, Ambs S, Cimmino A, Petrocca F, et al. A microRNA expression signature of human solid tumors defines cancer gene targets. Proc Natl Acad Sci U S A 2006;103(7):2257-61.
43. Liang H, Studach L, Hullinger RL, Xie J, Andrisani OM. Down-regulation of RE-1 silencing transcription factor (REST) in advanced prostate cancer by hypoxia-induced miR-106b~25. Exp Cell Res 2014;320(2):188-99.
44. Brett JO, Renault VM, Rafalski VA, Webb AE, Brunet A. The microRNA cluster miR-106b~25 regulates adult neural stem/progenitor cell proliferation and neuronal differentiation. Aging (Albany NY) 2011;3(2):108-24.
45. Birnie R, Bryce SD, Roome C, Dussupt V, Droop A, Lang SH, et al. Gene expression profiling of human prostate cancer stem cells reveals a pro-inflammatory phenotype and the importance of extracellular matrix interactions. Genome Biol 2008;9(5):R83.
46. Eaton CL, Colombel M, van der Pluijm G, Cecchini M, Wetterwald A, Lippitt J, et al. Evaluation of the Frequency of Putative Prostate Cancer Stem Cells in Primary and Metastatic Prostate Cancer. Prostate 2010;70(8):875-82.
47. Tantivejkul K, Kalikin LM, Pienta KJ. Dynamic process of prostate cancer metastasis to bone. Journal of Cellular Biochemistry 2004;91(4):706-17.
48. Ricci E, Mattei E, Dumontet C, Eaton CL, Hamdy F, van der Pluije G, et al. Increased Expression of Putative Cancer Stem Cell Markers in the Bone Marrow of Prostate Cancer Patients Is Associated With Bone Metastasis Progression. Prostate 2013;73(16):1738-46.
49. Cluzel C, Saltel F, Lussi J, Paulhe F, Imhof BA, Wehrle-Haller B. The mechanisms and dynamics of (alpha)v(beta)3 integrin clustering in living cells. J Cell Biol 2005;171(2):383-92.
50. Xu X, Chen Z, Zhao X, Wang J, Ding D, Wang Z, et al. MicroRNA-25 promotes cell migration and invasion in esophageal squamous cell carcinoma. Biochem Biophys Res Commun 2012;421(4):640-5.

SUPPLEMENTARY DATA

Table I. Real time-qPCR primers		
GENE	**Forward Primer**	**Reverse Primer**
ITGA2	TTTGGTAGTGTGCTGTGTTC	GACTCTTCCTTCCTCTTTCTTTAG
ITGA3	GCATCAACGTGACGAACACC	TCTGGTTCCGTTTGAAGGGG
ITGA5	AGTCCTCACTGTCCAGCTCA	GCTCAGTGGCTCCTTCTCTG
ITGA6	GCTGGTTATAATCCTTCAATATCAATTGT	TTGGGCTCAGAACCTTGGTTT
ITGAV	GCTGGACTGTGGAGAAGAC	AAGTGAGGTTCAGGGCATTC
ITGB1	AGCAACGGACAGATCTGCAA	GCTGGGGTAATTTGTCCCGA
ITGB3	GTCTGCCACAGCAGTGACTT	CTTGTAGCGGACACAGGAGA
ITGB4	CTGTGTGCACGAGGGACATT	AAGGCTGACTCGGTGGAGAA
CDH1	TTGACGCCGAGAGCTACAC	GACCGGTGCAATCTTCAAA
CDH2	CAGACCGACCCAAACAGCAAC	GCAGCAACAGTAAGGACAAACATC
VIM	CCAAACTTTTCCTCCCTGAACC	CGTGATGCTGAGAAGTTTCGTTGA
ZEB1	CCATATTGAGCTGTTGCCGC	GCCCTTCCTTTCCTGTGTCA
ZEB2	GACCTGGCAGTGAAGGAAAA	GGCACTTGCAGAAACACAGA
SNAIL1	ACCACTATGCCGCGCTCTT	GGTCGTAGGGCTGCTGGAA
SNAIL2	TGTGTGGACTACCGCTGC	TCCGGAAAGAGGAGAGAGG
PIP5K2C	CATGCATAGCAACCTCTCCA	ACTGACTCGGTACATCCCCA
PIP5K1C	CTGGAGGTACCGGACGAG	ACAGAACCTCTGTTGGGGC
RAC1	TCTCCAGGAAATGCATTGGT	CTGATGCAGGCCATCAAGT
CDC42EP2	GTCCAGCTCCTGAGACCTTG	TCACCGAGGGTTACTTGTCC
CDC42BPA	CATTCTCGAATACCTAGAATGGG	CAAAAGCTCCTCGACCAATC
CDC42	CCCGGTGGAGAAGCTGAG	CGCCCACAACAACACACTTA
TWIST	GCCGGAGACCTAGATGTCATT	TTTTAAAAGTGCGCCCCACG
GAPDH	GACAGTCAGCCGCATCTTC	GCAACAATATCCACTTTACCAGAG

Table II. Primers used for cloning and mutagenesis		
GENE	**Forward Primer**	**Reverse Primer**
3'UTR ITGAV WT	GCATATTCTAGACCTATGTGCAGCCACTACCC	GCATATGGCCGGCCTTCCAGCCTGAAATA CAATGC
3'UTR ITGA6 WT	GCATATTCTAGAACATCATGTGTTGGGGAAGG	GCATATGGCCGGCCAAAGTGATGACCTCCC ATGC
3'UTR ITGAV MUT	GAATCTTTGATGTTTTTTGTCATTGTTCTCAAGTAGA CTATAACAATGTAACCAAATCTAGATAATTTCAAA	TTTGAAATTATCTAGATTTGGTTACATTGTT ATAGTCTACTTGAGAACAATGACAAAAAAC ATCAAAGATTC
3'UTR ITGA6 MUT	CGGAAAGTGCTGTCTTAAACTAAATGTAGACTAGAAG GTGATGTTGCCATCC	GGATGGCAACATCACCTTCTAGTCTACATT TAGTTTAAGACAGCACTTTCCG

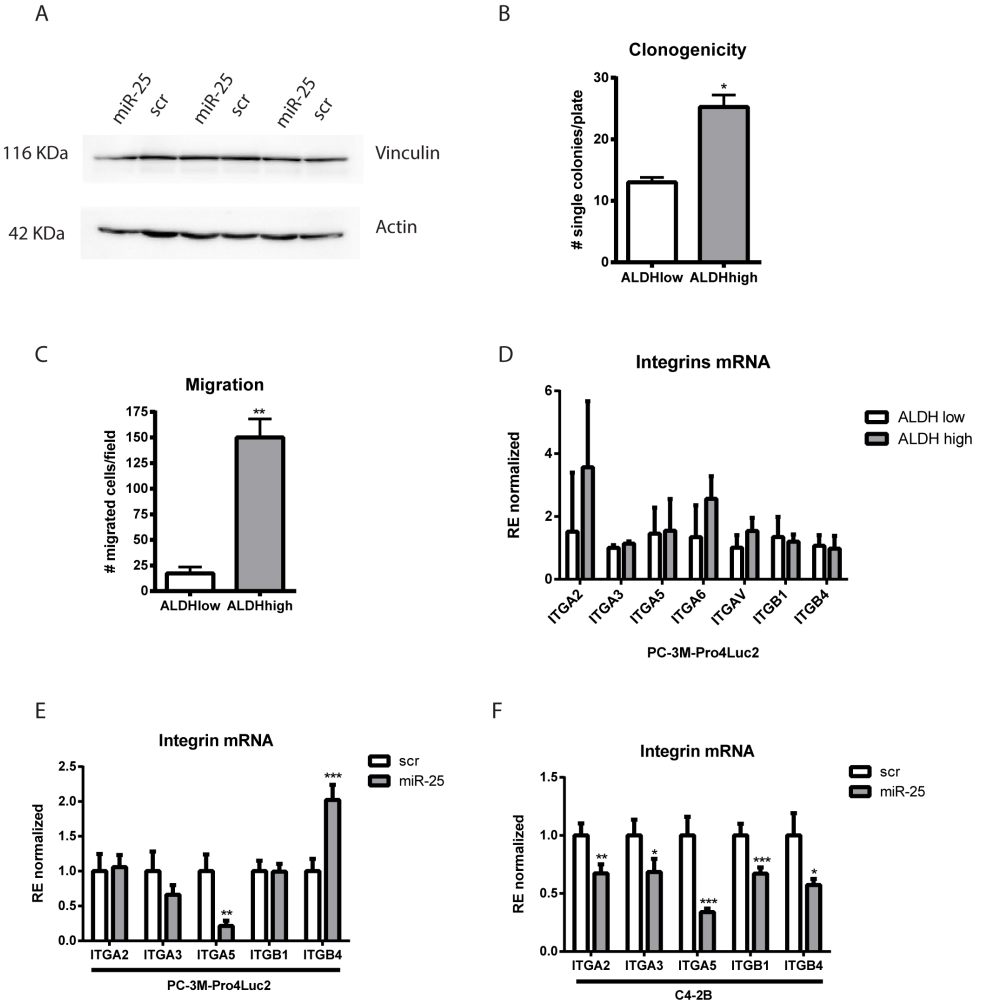

Supplementary Figure S1. ALDHhigh prostate cancer cells display enhanced colony formation and migration compared to ALDHlow cells. A) Western Blot analysis for Vinculin (VCL) expression after miR-25 transfection. No effect on protein is detected. **B**) Number of colonies per 96-well plate in single cell diluted culture after 2 weeks. **C**) Mean number of migrated ALDHhigh and ALDHlow PC-3M-Pro4Luc2 cells. Error bars indicate ±SEM **D**) qRT-PCR analysis on ITGA2, ITGA3, ITGA5, ITGA6, ITGAV, ITGAB1, ITGB4 on ALDHhigh VS ALDHlow PC-3M-Pro4Luc2 cells. ITGB3 displayed very low expression (ct > 35, data not shown). **E-F**) qRT-PCR analysis on ITGA2, ITGA3, ITGA5, ITGAB1, ITGB4 in PC-3M-Pro4Luc2 and C4-2B transfected with pre-miR-25 and negative control. ITGB3 displayed very low expression (ct > 35, data not shown). Error bars indicate ±SEM (n=3).

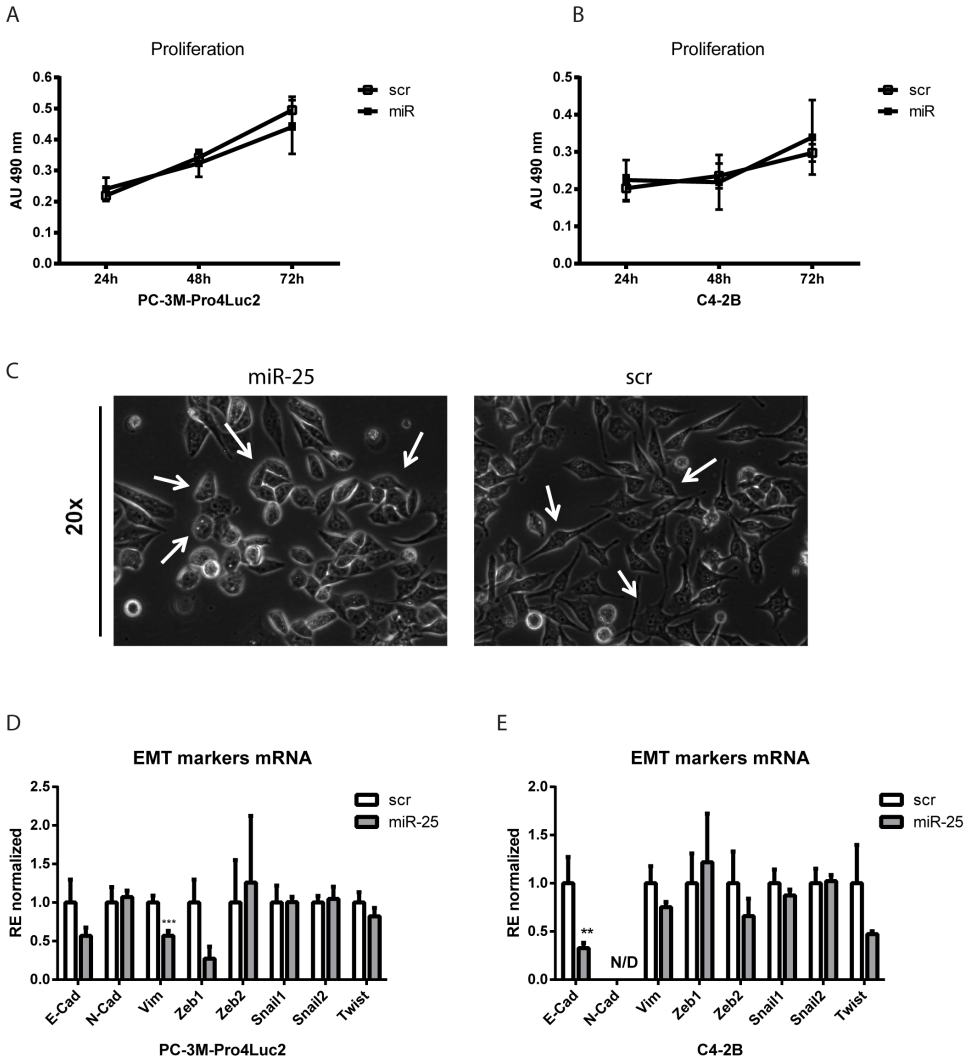

Supplementary Figure S2. miR-25 strongly changes cell morphology without affecting proliferation. A) MTS proliferation assay measured at 490nm 24-48-72 hours after miR-25 and control overexpression in PC-3M-Pro4Luc2 and **B**) C4-2B cells. **C**) Representative bright field picture of PC-3M-Pro4Luc2 cells overexpressing miR-25 and negative control 72 hours after transfection. miR-25 induces dramatic change in cell morphology. **D-E**) qRT-PCR on EMT markers (E-Cad, N-cad, Vim, Zeb1, Zeb2, Snail1, Snail2, Twist) in PC-3M-Pro4Luc2 and C4-2B respectively. Relative expression is compared to scramble negative control and all values were normalized to GAPDH. Error bars indicate ±SEM (n=3).

4

miR-25 modulates the cross-talk between canonical and non-canonical Wnt signaling

Eugenio Zoni
Janine Melsen
Marjan van de Merbel
Rob C. M. Pelger
Gabri van der Pluijm

Manuscript in Preparation

Abstract

Prostate cancer is considered the most common cancer and represents the second leading cause of death from cancer in men in the Western world. Once that the tumor has metastasized to the bone, no cure is available. To date, the molecular mechanisms responsible for cancer relapse and metastasis formation have not yet been elucidated. However, epithelial-to-mesenchymal transition (EMT) has been established as one of the key events that lead to cancer invasion, the occurrence of distant metastasis and therapy resistance. Cells that undergo EMT acquire a more motile phenotype and become highly migratory. The functional role of the so-called non-canonical WNT/planar cell polarity (WNT/PCP) pathway in the acquisition and maintenance of a motile phenotype has been firmly established.

In this paper we have studied a class of non-coding RNAs, the so-called microRNAs, that regulate gene expression and may play pivotal roles in carcinogenesis and tumor progression. We found that miR-25 that was shown previously to impair migration in a subpopulation of highly metastatic, cancer stem-like cells-, modulates the cross-talk between canonical and non-canonical WNT/PCP pathway. Our data show, for the first time, that miR-25 can modulate the expression of Dapper Homolog 1 (DACT1), an antagonist of β-catenin, thereby increasing canonical WNT signaling. TGF-β is considered to be one of the major drivers of EMT in various carcinomas, including those of the human prostate cancer. Our study, suggest that miR-25 might interfere with the cross-talk between WNT and TGF-β signaling and is capable to block the induction of migration produced by TGF-β in PC-3M-Pro4Luc2 human prostate cancer cells. Taken together, our observations suggest that targeting of non-canonical WNT/PCP pathway represents an interesting therapeutic strategy to block (or reverse) the acquisition of an invasive, stem/progenitor-like phenotype in human prostate cancer.

Introduction

Prostate cancer is the most common cancer in males and the second leading cause of death from cancer in the western male population (1). Occurrence of bone metastasis during the castration resistant phase represents one of the major problem for the patients, for which no therapeutic treatment is available at the moment. Despite the progresses in cancer biology, the mechanisms responsible for cancer relapse and metastasis formation have remained largely elusive. It is established that one of the critical event which precedes the formation of distant metastasis is the transition from an epithelial-like to mesenchymal-like state at the primary tumor (epithelial-to-mesenchymal transition, EMT) (2). Cells undergoing EMT become more motile and invasive and also display therapy resistance (3,4). One of the signaling pathways that are involved in the modulation of motility is represented by the so-called non-canonical WNT/planar cell polarity (WNT/PCP) pathway (5,6). The role for canonical WNT signaling during the initial phases of cancer initiation is indeed established. However, accumulating evidence suggests a critical role of the non-canonical WNT/PCP pathway during the second phase of the disease, when cancer progress, invades and metastasizes (5). microRNAs are a small class of non-coding RNA molecules that regulates gene expression and for which the role in pathogenesis and progression of prostate cancer is established (7). Several studies have also highlighted the predictive value of measuring the levels of microRNA in urine and blood to monitor the progression of the disease (8). However, there is a remarkable lack of information about the role of microRNA in aggressive subpopulation of cancer stem/progenitor like cells, characterized by high invasiveness and capable of forming metastasis. According to this scenario, the non-canonical WNT/PCP pathway represents one of the important player in the maintenance of high migration and invasion in these cells. Recently we have shown that miR-25 is strongly downregulated in a subpopulation of highly migratory and metastatic $ALDH^{high}$ cells in human prostate cancer (9).

In this study, we investigated whether miR-25 can interfere with the non-canonical WNT/PCP pathway in human prostate cancer cells. Our results indicate that miR-25 represents an interesting player in the maintenance of the balance between canonical and non-canonical WNT/PCP pathway. We show here -for the first time- that miR-25 modulates the expression of Dapper Homolog 1 (DACT1), an antagonist of β-catenin (10), thereby interfering with WNT signaling. Moreover we provide evidence that miR-25 interferes with the cross-talk between WNT and TGF-β signaling leading to attenuated TGF-β-induced migration of human prostate cancer cells. Together, our data highlight the role of miR-25 in prostate cancer progression, in particular the targeting of non-canonical WNT/PCP pathways as critical mediators of tumor invasiveness.

Materials and Methods

Cell lines and culture conditions

Human osteotropic prostate cancer cell lines PC-3M-Pro4 and PC-3M-Pro4Luc2 cells were maintained in DMEM with 10% FCII, 1% Penicillin-Streptomycin (Life Technologies) and 0.8 mg/ml Neomycin (Santacruz, USA) for cells expressing Luciferase 2. Human embryonic kidney HEK293T cells were maintained in DMEM with 10% FCS and 1% Penicillin-Streptomycin (Life Technologies, USA). Cells were maintained at 37°C with 5% CO_2.

Transient transfection with pre-miR-25 or pre-negative control and luciferase reporter assay

For microRNA overexpression, transfection was performed with Lipofectamine® 2000 (Invitrogen, USA) according to manufacturer's protocol with Pre-miR-25 (ID: PM10584; Life Technologies) and pre-miRNA negative control (scramble) (ID: AM17110; Life Technologies). Total RNA was collected after 72 hours to assess positive overexpression and target gene down-regulation.

For luciferase reporter assay, PC-3M-Pro4, HEK293T or HEK293T knock-down cells were seeded 10,000 cells in 500 µL medium in a 24-wells plate and Lipofectamine® 2000 used according to manufacturer's protocol. For experiments in combination with miR-25 overexpression, for each condition, 100 ng of BAT-luciferase (reporter for canonical WNT signaling (11)) or ATF2-luciferase (reporter for non-canonical WNT signaling (12-14)) or CAGA-Luc (TGF-β reporter) and 10 ng CAGGS-renilla were used. After 24 hours, medium was replaced and cells were treated with 0.6, 1.8, 3.0 µM SB216763 (Sigma-Aldrich, The Netherlands); 5, 12.5, 20 mM LiCl; 50, 75, 100 mM GIN (11) or 100 µM PNU-74654 (Sigma-Aldrich) or 0.1, 0.5, 1, 5, 10 ng/mL TGF-β for 24 hours before assessment of Luciferase activity. The *Photonis pyralis* (firefly) luciferase (Fluc) and *Renilla reniformis* luciferase (Rluc) activities in the lysates were measured with Dual Luciferase Assay (Promega, USA). Data are shown as Relative Light Units (RLU, Fluc normalized for Rluc levels).

RNA extraction and qRT-PCR

RNA was extracted using Trizol (Invitrogen) and cDNA synthesized by reverse transcription (Promega, USA) according to manufacturer's protocol. qRT-PCR was performed with Biorad CFX96 system (Biorad, The Netharlands). DACT1 (FW: GGCGACCTTGAGTCTCTCAG; RV: CTGAGGCCTGGTCTTCACAG) expression was normalized to GAPDH (FW: GACAGTCAGCCGCATCTTC; RV: GCAACAATATCCACTTTACCAGAG) and/or HPRT (FW: AGACTTTGCTTTCCTTGGTCAGG; RV: GTCTGGCTTATATCCAACACTTCG).

miRNA target prediction and bioinformatic analysis of cluster of genes

Targetscan v6.2 and microT-CDS (15) were used to identify miR-25 predicted targets. Functional annotation was performed using DAVID Bioinformatics Resources 6.7 (16,17) and KEGG database (18).

ALDEFLUOR® assay

Aldehyde Dehydrogenase (ALDH) activity was measured using the ALDEFLUOR® assay kit (StemCell Technologies, USA) according to the manufacturer's protocol (19). ALDH substrate was added to the cells and fluorescent product measured by flowcytometry. For sorting, FACS ARIA cell sorter (BD Bioscience) was used. After sorting, RNA was collected from $ALDH^{high}$= highest 10% and gene expression compared to $ALDH^{low}$ = lowest 10%).

Migration assay

To assess migration, cells were starved overnight in medium containing 0.3% serum and 60,000 cells seeded the day after in medium containing 0.3% serum in Transwell (8-µm) upper-chamber (Corning, The Netherlands). The lower chamber was filled with medium containing 10% serum. After 16-18 hours of incubation, cells on the upper side of the filters were removed and cells on the lower side were fixed with 4% paraformaldehyde and stained with 0.1% crystal violet for 30 min at RT (Sigma-Aldrich, USA). Cell migrated were subsequently counted.

Statistical analysis

Statistical analysis was performed with GraphPad Prism 6.0 (GraphPad software, USA). T-test was used for comparison between two groups. Data is presented as mean ± SEM. P-values ≤ 0.05 are considered to be statistically significant (* $P < 0.05$, ** $P < 0.01$, *** $P < 0.001$).

Results

miR-25 induces canonical-WNT signaling via a WNT-dependent mechanism

To investigate the effect of miR-25 on WNT signaling pathway, we employed a canonical WNT signaling bioluminescent reporter, BAT-Firefly Luciferase (Fluc) (20,21) and CAGGS-Renilla luciferase (Rluc) as control for transfection efficiency. miR-25 overexpression in PC-3M-Pro4 human prostate cancer cell line resulted in significant increase in BAT-Fluc signaling indicating up-regulation of canonical WNT signaling (**Fig. 1 A, B and C,** Control=vehicle condition). Our group has previously shown that inhibition of GSK3-β produced increase in canonical WNT signaling in human prostate cancer (11). Interestingly, we found that treatment with different GSK3-β inhibitors (SB216763 (22), LiCl (11) and GIN (23)) combined with miR-25 overexpression resulted in significant enhancement of canonical WNT signaling, suggesting an additive effect of miR-25 on GSK3-β inhibition (**Fig. 1 A, B and C** respectively). To assess whether the observed effect of miR-25 was WNT-dependent, we used a downstream inhibitor of canonical WNT signaling, PNU-74654, and measured the activity of canonical WNT reporter upon miR-25 overexpression alone or in combination with PNU-74654. We confirmed that miR-25 was capable of inducing canonical-WNT signaling and found that simultaneous incubation with 100 μM of PNU-74654 led to complete reversal of the induction of WNT signaling in PC-3M-Pro4 cells (**Fig. 1 D**). Together, these suggest that the effect of miR-25 on canonical WNT signaling is direct and can be reversed upon treatment with downstream WNT inhibitors.

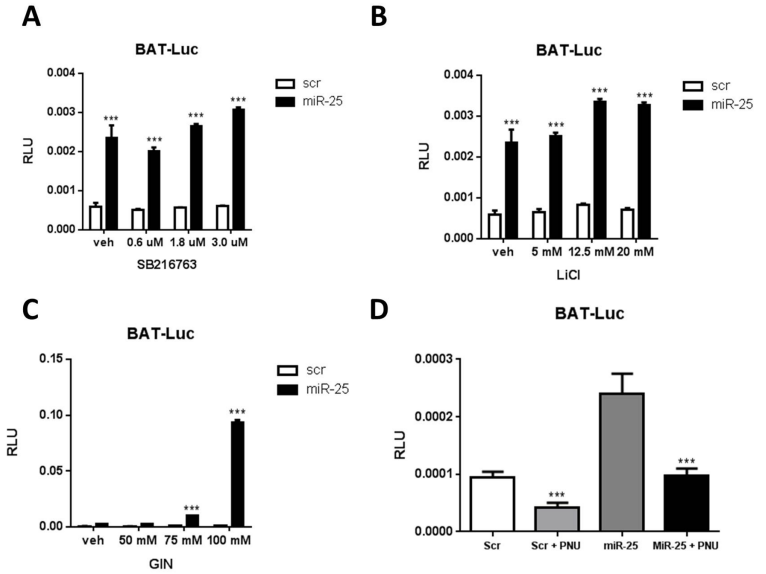

Figure 1. miR-25 overexpression directly induces canonical WNT signaling. **A-C**) Treatment with different concentration of GSK3-β inhibitor SB216763 (**A**), LiCl (**B**) and GIN (**C**) in combination with miR-25 overexpression produced additive effect on canonical WNT signaling induction. **D**) Administration of downstream inhibitor of WNT signaling PNU-74654 (PNU) can reverse the induction of WNT signaling produced by overexpression of miR-25. Error Bars ± SEM. $p < 0.05$ (*), $p < 0.001$ (***).

miR-25 downregulates Dapper, an antagonist of β-catenin, Homolog 1 (DACT1)

To study whether novel miR-25 predicted target gene(s) involved in WNT signaling could be identified, we predicted gene targets of miR-25 by publically-available tools *in silico*. Our analysis found that Dapper, an antagonist of β-catenin, homolog 1 (DACT1) was shown as miR-25 predicted target gene in two independent online bioinformatic tools, TargetScan (24) and microTCDS (15).

Previously we have shown that miR-25 is strongly downregulated in a subpopulation of highly tumorigenic and metastatic, stem-like $ALDH^{high}$ cells compared to non-tumorigenic and non-metastatic $ALDH^{low}$ subpopulation isolated from PC-3M-Pro4Luc2 human prostate cancer cell line (9). Therefore, we hypothesized that miR-25 and DACT1 expression in $ALDH^{high}$ vs. $ALDH^{low}$ subpopulation could be inversely correlated. To test this hypothesis, we measured the expression of DACT1 mRNA in subpopulation of $ALDH^{high}$ compared to $ALDH^{low}$, isolated after viable cell sorting from PC-3M-Pro4Luc2 human prostate cancer cells with ALDEFLUOR kit (19). Our mRNA analysis showed that DACT1 mRNA is, indeed, significantly higher in $ALDH^{high}$ vs. $ALDH^{low}$ subpopulation (**Fig. 2A**). Next we evaluated whether transient overexpression of miR-25 could reduce the

mRNA level of its predicted target gene DACT1 in two independent cell lines. Interestingly, we found that overexpression of miR-25 could significantly decrease mRNA expression of DACT1 in PC-3M-Pro4Luc2 cells ($p<0.01$) and similar trend was observed in HEK293T cells (**Fig. 2B and C** respectively).

Taken together, miR-25 and DACT1 expression are inversely correlated in $ALDH^{high}$ compared to $ALDH^{low}$ subpopulation as we hypothesized. Moreover, miR-25 overexpression may directly inhibit the predicted target gene DACT1 as was found from the *in silico* analysis described above.

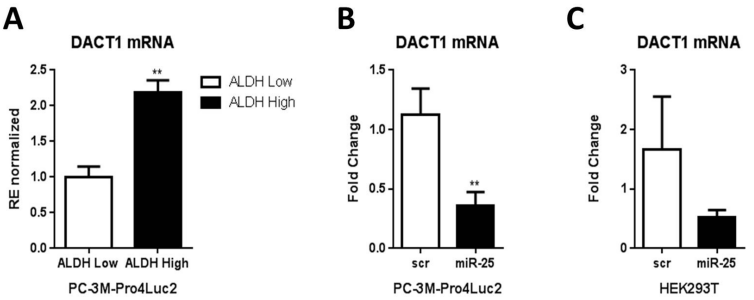

Figure 2. DACT1 is elevated in $ALDH^{high}$ vs $ALDH^{low}$ subpopulation and miR-25 overexpression downregulate its mRNA expression. A) qRT-PCR in $ALDH^{high}$ vs. $ALDH^{low}$ subpopulation isolated from PC-3M-Pro4Luc2 human prostate cancer cell line show increased expression of DACT1 in $ALDH^{high}$ cells. **B**) mRNA analysis after 72 hours following miR-25 overexpression shows significant reduction in the level of DACT1 mRNA in PC-3M-Pro4Luc2 cells. **C**) mRNA analysis after 72 hours following miR-25 overexpression shows reduction in the level of DACT1 mRNA in HEK293T cells. Error Bars ± SEM. $p < 0.01$ (**).

DACT1 knock-down partially recapitulates miR-25 overexpression phenotype

To functionally evaluate the biological role of DACT1 we used two shRNAs direct against DACT1 and one shRNA control to perform stable knock-down of this gene in the two independent cell lines PC-3M-Pro4Luc2 and HEK293T cells.

We found that DACT1 knock-down affected cell morphology and cellular density in both cell lines employed with both shRNA constructs (**Fig. 3A**). ShRNA#63 drastically reduced cellular density and ShRNA#64 induced a spindle-shape phenotype (**Fig. 3A**). Specificity of knock-down was confirmed by qRT-PCR for both shRNA and showed significant decreased DACT1 expression with shRNA#63 (ShDACT1_#63) and partial knock-down was achieved with shRNA#64 (ShDACT1_#64) (**Fig. 3B**). As expected, we measured a

significant increase in BAT luciferase activity with both shRNAs construct against DACT1 used to perform the knock-down ($p<0.001$ for both shRNAs) (**Fig. 3C**).

Given the stimulatory effect on canonical WNT signaling upon miR-25 overexpression, these findings all together reinforce the hypothesis that miR-25 interferes with WNT signaling via DACT1.

Previously we have demonstrated that miR-25 overexpression strongly inhibits cell migration in human prostate cancer (9). This led us to hypothesize that DACT1 knock-down could result in a similar functional phenotype. We used transwell boyden chambers to measure migration in PC-3M-Pro4Luc2 and HEK293T cells with DACT1 knock-down (**Fig. 3D**). Interestingly, we found a strong and significant inhibition of migration in HEK293T cells ($p<0.001$ for both shRNAs) (**Fig. 3E**). However, no decrease in migration was detected in PC-3M-Pro4Luc2 cells which showed a surprising increase in motility with shRNA#63 ($p<0.001$) and no effect with shRNA#64 (**Fig. 3F**). These data suggest that miR-25 overexpression and DACT1 knock-down result in a similar effect on WNT signaling activity. However DACT1 knock-down can only partially recapitulate, in the human prostate cancer cell line, the phenotype produced by miR-25 overexpression.

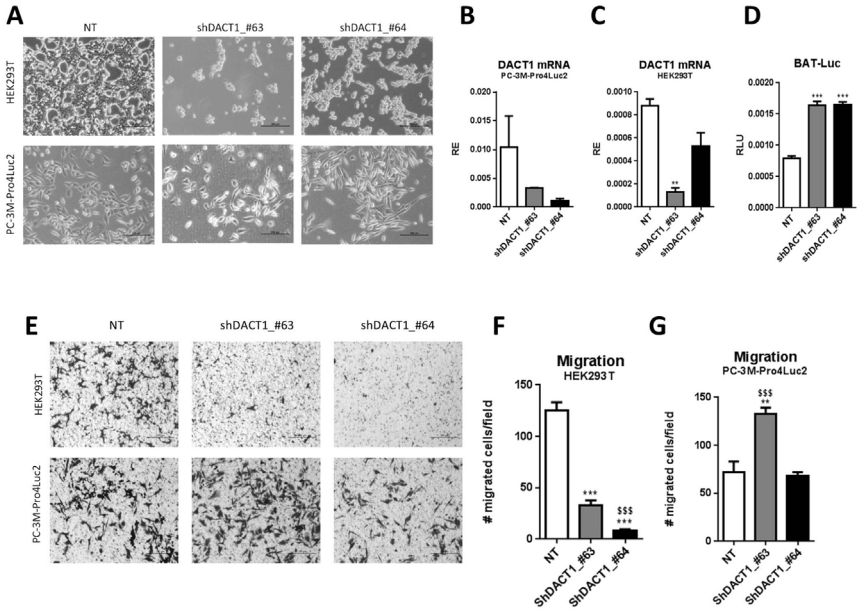

Figure 3. DACT1 knock-down affects cell morphology and partially recapitulates the miR-25 overexpression phenotype in human prostate cancer cells. **A**) DACT1 knock-down induces changes in cell morphology compared to shRNA control (NT, left panels, top = HEK293T and bottom = PC-3M-Pro4Luc2 cells); effect on cellular density is observed for both shRNAs in both cell lines (central and right

panels, top for HEK293T and bottom for PC-3M-Pro4Luc2); in PC-3M-Pro4Luc2 shDACT1_64 induces a spindle cell shape phenotype (left bottom panel) compared to a more epithelial-like morphology induced by shDACT1_63 (central bottom panel). **B-C**) qRT-PCR confirms DACT1 knock-down with both shRNAs in both the cell lines used **D**) Bioluminescent reporter for canonical WNT signaling (BAT-Luc) in HEK293T cells support knock-down of antagonist of β-catenin (DACT1) and shows increased bioluminescent activity for both shRNAs used. **E**) Representative pictures of HEK293T and PC-3M-Pro4Luc2 cells with knock-down for DACT1 with two shRNAs. **F**) Both shRNAs for DACT1 significantly reduce migration in HEK293T cells. *** vs NT (ShRNA control) and $$$ vs shDACT1_#64. **G**) shDACT1_#63 induce migration in PC-3M-Pro4Luc2 cells (*** vs NT, ShRNA control and $$$ vs shDACT1_#64). Error Bars ± SEM. p< 0.01 (**), p<0.001 (***, $$$).

TGF-β modulates the cross-talk between canonical- and non-canonical WNT signaling and miR-25 interferes with TGF-β signaling

One of the critical events during prostate cancer progression is represented by epithelial-to-mesenchymal transition (EMT) (25). In this process, TGF-β represents one of the major drivers of EMT and promotes migration (26). The notion that Wnt/PCP and canonical-Wnt signaling are both part of a negative feedback-loop where Wnt/PCP negatively regulates canonical-Wnt signaling and *vice versa* (27) led us to test whether TGF-β could modulate canonical and non-canonical WNT signaling in our model. To this aim, we transfected PC-3M-Pro4 human prostate cancer cells with canonical (BAT-Luc (11)) and non-canonical (ATF2 Luc (12)) WNT bioluminescent reporter. Treatment with different concentrations of TGF-β (1, 5, 10 ng/mL) induced a significant, dose-dependent decrease in both canonical WNT signaling (**Fig. 4A**) and non-canonical WNT signaling (**Fig. 4B**).

Given the stimulatory role of miR-25 on canonical WNT signaling, and its inhibitory effect on cell migration, we hypothesized that the modulation of canonical and non-canonical WNT signaling produced by TGF-β could be modulated by miR-25. To test this, we transfected PC-3M-Pro cells with a bioluminescent Smad-dependent TGF-β reporter (CAGA-Luc) and simultaneously overexpressed miR-25 and a scramble negative control. 24h after transfection, cells were treated with TGF-β (0.1, 0.5, 1 ng/mL) and assessment of bioluminescent activity revealed that miR-25 was capable of blocking TGF-β signaling (**Fig. 4C**). Interestingly, we found that overexpression of miR-25 abolished the pro-migratory effect of TGF-β compared so scramble negative control (**Fig. 4D**). Taken together our results suggest that miR-25 might represent an interesting player in the modulation that TGF-β exerts on canonical and non-canonical WNT signaling.

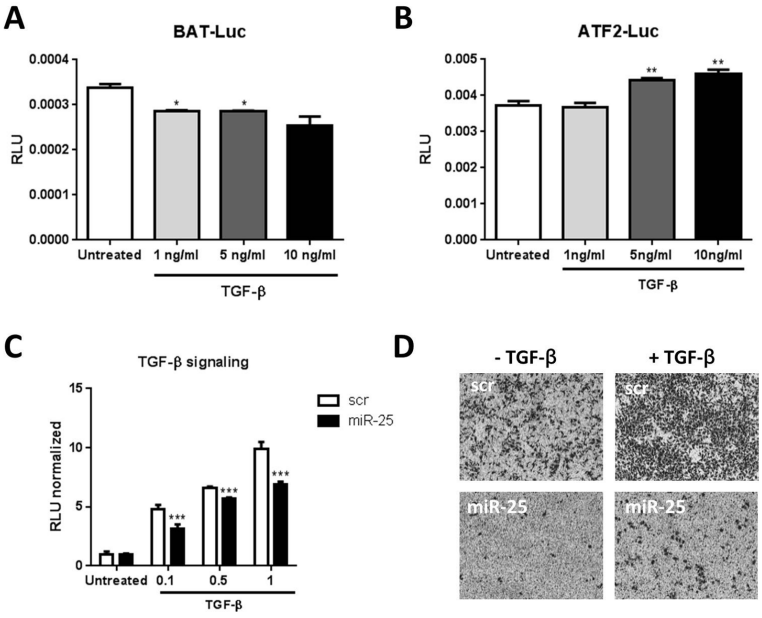

Figure 4. TGF-β modulates canonical and non-canonical WNT signaling in a different manner (A,B) and miR-25 interferes with TGF-β signaling and cell migration under basal- and TGF-β stimulated conditions (C,D). **A**) Canonical WNT signaling activity measured by bioluminescent reporter (BAT-Luc) in presence of an increasing dose range of TGF-β (1, 5, 10 ng/mL) (* p<0.05 vs. Untreated). **B**) Non-canonical WNT signaling activity measured by bioluminescent reporter (ATF2-Luc) in presence of an increasing dose range of TGF-β (1, 5, 10 ng/mL) (** p<0.01 vs. Untreated). **C**) miR-25 reduces the activity of TGF-β signaling and is capable of blocking the stimulation with an increasing dose range of TGF-β (0.1, 0.5, 1 ng/mL). (***, p<0.001 with two way ANOVA). **D**) miR-25 overexpression can block the induction of migration produced by 1ng/mL of TGF-β compared to scramble negative control.

Discussion

The role of the canonical WNT developmental pathway in tumorigenesis has been firmly established in several types of cancers (28). However, more recent oncological research has highlighted the critical contribution of the so-called non-canonical WNT/planar cell polarity (PCP) pathway in the progression phase of the disease, typically characterized by cell migration, invasion and formation of metastasis (5).
Previously we have shown that miR-25 is downregulated in a subpopulation of highly migratory and metastatic cells ($ALDH^{high}$) and this miR appears to be a critical player in the modulation of cell motility, migration and differentiation of human prostate cancer cells (9). Here we investigated the role of miR-25 in the modulation of canonical and non-canonical WNT signaling and identified Dapper, Antagonist of β-catenin, homolog 1 (DACT1) as a miR-25 predicted target gene. Wnt/PCP and canonical-Wnt signaling are part of a negative feedback-loop where Wnt/PCP negatively regulates canonical-Wnt signaling and *vice versa* (27). One of the important mediator of this feedback mechanism is represented by Dishevelled (Dvl) which is considered to be the "Hub of Wnt signaling" (29). In this context, when canonical WNT signaling is active, the recruitment of Dvl by Frizzled prevents the constitutive destruction of β-catenin and results in its accumulation and subsequent nuclear translocation (29). DACT1 has been shown to negatively regulate canonical WNT signaling by promoting lysosomal degradation of Dvl, leading to degradation of β-catenin (30). Real-time measure of canonical WNT signaling by bioluminescent reporter in prostate cancer cells in which DACT1 was knocked down supported this notion. The WNT/PCP pathway is critically involved in cytoskeletal remodeling and cell motility (30). Interestingly, loss of DACT1 has been shown to disrupt WNT/PCP pathway, altering Dvl activity and leading to malformation in mice (30). Here we found that miR-25 might target directly DACT1 mRNA, suggesting that a regulatory role for this miR in the WNT/PCP pathway. Previously, we demonstrated that miR-25 can disrupt cell migration and identified several predicted target genes involved in the modulation of F-actin assembly and in the remodeling of the cytoskeleton (9). Our data show that miR-25 expression is capable of stimulating the canonical WNT signaling pathway. Given the negative feedback-loop between canonical and non-canonical WNT/PCP signaling, we speculated that miR-25-induced activation of canonical WNT signaling will result in the attenuation of the non-canonical WNT/PCP pathway leading to a reduction in cell migration. In support of this observation, transcriptional analysis revealed that DACT1 is significantly up-regulated in invasive, metastatic $ALDH^{high}$ vs sessile, non-metastatic $ALDH^{low}$ subpopulation of prostate cancer cells. Moreover, we have previously demonstrated that miR-25 is strongly downregulated in $ALDH^{high}$ compared to $ALDH^{low}$ subpopulation of PC-3M-Pro4Luc2

human prostate cancer cells (9). Taken together, our data show an inverse correlation between miR-25 and DACT1 expression in $ALDH^{high}$ cells, suggesting that WNT/PCP pathway might be directly involved in the maintenance of an invasive phenotype in this subpopulation of cells. DACT1 knock-down in HEK293T cells resulted in a complete loss of migratory properties and recapitulated the miR-25 overexpression phenotype. However, the fact that the knock-down of DACT1, in PC-3M-Pro4Luc2 cells, failed to interfere with migration, suggests the presence of additional mechanisms that might determine their malignant phenotype. For example, PC-3M-Pro4Luc2 cells express high levels of α_6 and α_v integrins, that are directly targeted by miR-25 and that are functionally involved in the activation of latent TGF-β, motility, invasion and metastasis (9). Moreover, one single microRNA can downregulate multiple genes at the same time, leading to a global functional effect that logically cannot be entirely reproduced by the downregulation of a single gene.
Our group described previously that TGF-β increases the size of $ALDH^{high}$ stem-like subpopulation of human prostate cancer cells (31). Here we show that TGF-β negatively regulates canonical WNT signaling and positively regulates non-canonical WNT/PCP pathway. This reinforces the tumor supportive role of TGF-β and its involvement in EMT and cell migration. In the perspective of a reciprocal feedback-loop between canonical and non-canonical WNT/PCP signaling, DACT family proteins have been identified in mammals as multi-adapter molecules with the ability to modulate and integrate WNT and TGF-β signaling (10). Here we showed that miR-25 inhibits TGF-β signaling and strongly reduced the migratory effect induced by TGF-β. These data, combined with the notion in literature, suggest that DACT1 might represent an important player in the modulation between the cross-talk between TGF-β and WNT signaling and that miR-25 might interfere with this balance.

Finally, although additional experiments are required to elucidate the exact role of miR-25 in this process, we hypothesized a model in which non-canonical WNT/PCP pathway and TGF-β signaling maintain the highly migratory phenotype in PC-3M-Pro4Luc2 human prostate cancer cells. It is remarkable indeed that our bioluminescent measurement of WNT reporters revealed that the order of magnitude difference between non-canonical WNT/PCP compared to canonical WNT signaling is approximately a factor of 10. This suggests that there is a basal disbalance between canonical and non-canonical WNT/PCP signaling that result in a shift toward WNT/PCP pathway and that functionally sustain motility and migration. PC-3M-Pro4Luc2 cells are indeed highly migratory and metastatic upon inoculation in mice. Furthermore, the fact that overexpression of miR-25 leads to downregulation of DACT1, coinciding with loss of migration and strong induction of canonical WNT signaling, indicates that DACT1 might

regulate this process. Moreover, administration of TGF-β reduces canonical WNT signaling and augments non-canonical WNT/PCP signaling, which support the notion that TGF-β strongly induces the acquisition of an invasive phenotype.

REFERENCES

1. Jemal A, Center MM, DeSantis C, Ward EM. Global patterns of cancer incidence and mortality rates and trends. Cancer Epidemiol Biomarkers Prev 2010;19(8):1893-907.
2. Ombrato L, Malanchi I. The EMT universe: space between cancer cell dissemination and metastasis initiation. Crit Rev Oncog 2014;19(5):349-61.
3. Mitra A, Mishra L, Li S. EMT, CTCs and CSCs in tumor relapse and drug-resistance. Oncotarget 2015;6(13):10697-711.
4. Zoni E, van der Pluijm G, Gray PC, Kruithof-de Julio M. Epithelial Plasticity in Cancer: Unmasking a MicroRNA Network for TGF-beta-, Notch-, and Wnt-Mediated EMT. J Oncol 2015;2015:198967.
5. Wang Y. Wnt/Planar cell polarity signaling: a new paradigm for cancer therapy. Mol Cancer Ther 2009;8(8):2103-9.
6. Luga V, Zhang L, Viloria-Petit AM, Ogunjimi AA, Inanlou MR, Chiu E, et al. Exosomes mediate stromal mobilization of autocrine Wnt-PCP signaling in breast cancer cell migration. Cell 2012;151(7):1542-56.
7. Bartel DP. MicroRNAs: target recognition and regulatory functions. Cell 2009;136(2):215-33.
8. Mitchell PS, Parkin RK, Kroh EM, Fritz BR, Wyman SK, Pogosova-Agadjanyan EL, et al. Circulating microRNAs as stable blood-based markers for cancer detection. Proc Natl Acad Sci U S A 2008;105(30):10513-8.
9. Zoni E, van der Horst G, van de Merbel AF, Chen L, Rane JK, Pelger RC, et al. miR-25 Modulates Invasiveness and Dissemination of Human Prostate Cancer Cells via Regulation of alphav- and alpha6-Integrin Expression. Cancer Res 2015;75(11):2326-36.
10. Schubert FR, Sobreira DR, Janousek RG, Alvares LE, Dietrich S. Dact genes are chordate specific regulators at the intersection of Wnt and Tgf-beta signaling pathways. BMC Evol Biol 2014;14:157.
11. Kroon J, in 't Veld LS, Buijs JT, Cheung H, van der Horst G, van der Pluijm G. Glycogen synthase kinase-3beta inhibition depletes the population of prostate cancer stem/progenitor-like cells and attenuates metastatic growth. Oncotarget 2014;5(19):8986-94.
12. Ohkawara B, Niehrs C. An ATF2-based luciferase reporter to monitor non-canonical Wnt signaling in Xenopus embryos. Dev Dyn 2011;240(1):188-94.
13. van der Sanden MH, Meems H, Houweling M, Helms JB, Vaandrager AB. Induction of CCAAT/enhancer-binding protein (C/EBP)-homologous protein/growth arrest and DNA damage-inducible protein 153 expression during inhibition of phosphatidylcholine synthesis is mediated via activation of a C/EBP-activating transcription factor-responsive element. J Biol Chem 2004;279(50):52007-15.
14. Bruhat A, Jousse C, Carraro V, Reimold AM, Ferrara M, Fafournoux P. Amino acids control mammalian gene transcription: activating transcription factor 2 is essential for the amino acid responsiveness of the CHOP promoter. Mol Cell Biol 2000;20(19):7192-204.
15. Paraskevopoulou MD, Georgakilas G, Kostoulas N, Vlachos IS, Vergoulis T, Reczko M, et al. DIANA-microT web server v5.0: service integration into miRNA functional analysis workflows. Nucleic Acids Res 2013;41(Web Server issue):W169-73.
16. Huang da W, Sherman BT, Lempicki RA. Systematic and integrative analysis of large gene lists using DAVID bioinformatics resources. Nat Protoc 2009;4(1):44-57.
17. Huang da W, Sherman BT, Lempicki RA. Bioinformatics enrichment tools: paths toward the comprehensive functional analysis of large gene lists. Nucleic Acids Res 2009;37(1):1-13.
18. Kanehisa M, Goto S. KEGG: kyoto encyclopedia of genes and genomes. Nucleic Acids Res 2000;28(1):27-30.
19. van den Hoogen C, van der Horst G, Cheung H, Buijs JT, Lippitt JM, Guzman-Ramirez N, et al. High aldehyde dehydrogenase activity identifies tumor-initiating and metastasis-initiating cells in human prostate cancer. Cancer Res 2010;70(12):5163-73.

20. van Bezooijen RL, Svensson JP, Eefting D, Visser A, van der Horst G, Karperien M, et al. Wnt but not BMP signaling is involved in the inhibitory action of sclerostin on BMP-stimulated bone formation. J Bone Miner Res 2007;22(1):19-28.
21. Maretto S, Cordenonsi M, Dupont S, Braghetta P, Broccoli V, Hassan AB, et al. Mapping Wnt/beta-catenin signaling during mouse development and in colorectal tumors. Proc Natl Acad Sci U S A 2003;100(6):3299-304.
22. Lochhead PA, Kinstrie R, Sibbet G, Rawjee T, Morrice N, Cleghon V. A chaperone-dependent GSK3beta transitional intermediate mediates activation-loop autophosphorylation. Mol Cell 2006;24(4):627-33.
23. Engler TA, Henry JR, Malhotra S, Cunningham B, Furness K, Brozinick J, et al. Substituted 3-imidazo(1,2-a)pyridin-3-yl- 4-(1,2,3,4-tetrahydro-(1,4)diazepino-(6,7,1-hi)indol-7-yl)pyrrole-2,5-diones as highly selective and potent inhibitors of glycogen synthase kinase-3. J Med Chem 2004;47(16):3934-7.
24. Agarwal V, Bell GW, Nam JW, Bartel DP. Predicting effective microRNA target sites in mammalian mRNAs. Elife 2015;4.
25. Mani SA, Guo W, Liao MJ, Eaton EN, Ayyanan A, Zhou AY, et al. The epithelial-mesenchymal transition generates cells with properties of stem cells. Cell 2008;133(4):704-15.
26. Buijs JT, Henriquez NV, van Overveld PG, van der Horst G, ten Dijke P, van der Pluijm G. TGF-beta and BMP7 interactions in tumour progression and bone metastasis. Clin Exp Metastasis 2007;24(8):609-17.
27. Veeman MT, Axelrod JD, Moon RT. A second canon. Functions and mechanisms of beta-catenin-independent Wnt signaling. Dev Cell 2003;5(3):367-77.
28. Logan CY, Nusse R. The Wnt signaling pathway in development and disease. Annu Rev Cell Dev Biol 2004;20:781-810.
29. Gao C, Chen YG. Dishevelled: The hub of Wnt signaling. Cell Signal 2010;22(5):717-27.
30. Wen J, Chiang YJ, Gao C, Xue H, Xu J, Ning Y, et al. Loss of Dact1 disrupts planar cell polarity signaling by altering dishevelled activity and leads to posterior malformation in mice. J Biol Chem 2010;285(14):11023-30.
31. van den Hoogen C, van der Horst G, Cheung H, Buijs JT, Pelger RC, van der Pluijm G. The aldehyde dehydrogenase enzyme 7A1 is functionally involved in prostate cancer bone metastasis. Clin Exp Metastasis 2011;28(7):615-25.

5

ALK1Fc suppresses tumor growth by impairing angiogenesis and proliferation of human prostate cancer cells *in vivo*

Eugenio Zoni*
Sofia Karkampouna*
Peter C. Gray
Marie-José Goumans
Lukas J.A.C. Hawinkels
Gabri van der Pluijm
Peter ten Dijke
Marianna Kruithof-de Julio

*Authors Contributed Equally

Adapted from Manuscript Submitted

Abstract

Prostate cancer is the second most common cancer in men worldwide. Despite current therapies, when cancer progress, patient develop metastasis, mainly in the bones. Therefore, targeting the molecular pathways that underlie primary tumor growth and spread of metastases is of great clinical value. Bone morphogenetic proteins (BMPs) play a critical role in prostate cancer. BMP9 and the closely related BMP10 signal via the transmembrane serine kinase receptors *A*ctivin receptor-*L*ike *K*inase 1 (ALK1) and ALK2 and the cytoplasmic proteins SMAD1 and SMAD5. The human ALK1 extracellular domain (ECD) binds BMP9 and BMP10 with high affinity and we show that a soluble chimeric protein consisting of the ALK1 ECD fused to human Fc (ALK1Fc) prevents activation of endogenous signaling via ALK1 and ALK2. We also show for the first time in prostate cancer that ALK1Fc reduces BMP9-mediated signaling and decreases tumor cell proliferation *in vitro.* In line with these observations, we demonstrate that ALK1Fc impairs angiogenesis and reduces tumor growth *in vivo.* Our data show that BMP9 correlates with poor survival and is upregulated in high risk prostate cancer patients. We identify BMP9 as a putative therapeutic target and ALK1Fc as a potential therapy capable of targeting tumor cells and the supportive tumor angiogenesis. Together these findings justify the continued clinical development of drugs blocking ALK1 and ALK2 receptor activity.

Introduction

Prostate cancer is the second most common cancer in men worldwide (1). Currently prostate cancer, when still in its first phase of androgen dependency, can be successfully treated surgically. However, once the cancer develops in an androgen-independent state, therapy is no longer useful or successful and lethality is almost invariably due to the consequences of metastasis. Therefore, understanding the molecular pathways that underlie the emergence and spread of metastases from primary tumors are of great biological and clinical value.

Expression of several BMPs has been examined in prostatic tissue with benign prostatic hyperplasia (BPH), non-metastatic and metastatic prostatic adenocarcinoma and has been associated with cancer aggressiveness (2). However, little is known about the roles of BMP9 and BMP10 and their signaling receptors, ALK1 and ALK2, in prostate cancer and particularly in androgen independent and metastatic prostate cancer. Previous studies have highlighted the role of ALK1 as key regulator of normal as well as tumor angiogenesis (3, 4). BMP9 and BMP10 are high affinity ligands for ALK1, which is predominantly expressed in endothelial cells (5). Alternatively, BMP9 signals through the BMP type I receptor ALK2 (6-8). Binding of BMP9/BMP10 to ALK1/ALK2 results in phosphorylation and activation of downstream effectors SMAD1/SMAD4 and/or SMAD5 (7-9). In ovarian cancer, BMP9 acts as proliferative factor, promoting human epithelial ovarian cancer and human immortalized ovarian surface epithelial cell proliferation through ALK2/SMAD1/SMAD4 pathway (8). Similarly, BMP9 stimulates proliferation of liver cancer cells (10) and osteosarcoma growth (11). Among the BMPs, BMP9 is the most recently identified (12) and least studied ligand. Current research has not only attributed a tumor-promoting role to BMP9 (8, 10, 11) but also tumor suppressing properties (13-15) in different types of cancer, including prostate cancer.

Several studies have highlighted the role of BMP9/ALK1 in the genetics and development of blood vessel formation, outlining its critical involvement in pathological and tumor angiogenesis (16, 17). Interestingly, alterations of signal transduction pathways that are important for blood vessel formation, such as the NOTCH pathway, have also been associated with arterio-venous malformations (18, 19). Recently, BMP9 and BMP10 signaling were linked to NOTCH signaling, one of the major pathways involved in prostate cancer development, progression and bone metastasis (20). Expression profiling studies have shown that members of the NOTCH pathway are characteristic of high grade (Gleason 4+4=8) micro-dissected prostate cancer cells compared to low grade (Gleason 3+3=6) (21). Moreover, inhibition of NOTCH1 reduces prostate cancer cell growth, migration and invasion (22). Interestingly, NOTCH signaling pathway activates ALDH1A1, a well-known marker of prostate cancer stem cells (23-26).

In order to understand the role of BMP9 in prostate cancer tumor progression, we employed the soluble chimeric protein ALK1Fc (ACE-041) (27) which binds BMP9 and BMP10 with high affinity and blocks their signaling via ALK1 and ALK2 receptors by acting as a ligand trap (28, 29). BMP9 induces endothelial cell proliferation and vessel formation (30) while ALK1Fc has previously been shown to inhibit vascularization and tumor growth of breast cancer *in vivo* in an orthotopic transplantation model (28). ALK1Fc binds and neutralizes only BMP9 and BMP10 ligands and not TGFβ (28, 29), which also plays important roles in angiogenic processes. Phase I clinical trials have been completed using ALK1Fc as anti-angiogenesis therapy in myeloma (clinicaltrials.gov identifier NCT00996957).

Here we show, for the first time in prostate cancer, that ALK1Fc reduces BMP9 signaling and decreases proliferation of highly metastatic and tumor initiating human prostate cancer cells *in vitro.* We further demonstrate that ALK1Fc impairs angiogenesis, affects tumor cell proliferation and reduces tumor growth *in vivo.* Taken together these data suggest BMP9 as a possible therapeutic target in prostate cancer and justify the continued clinical development of additional drugs that block signaling via ALK1 and ALK2.

Materials and Methods

Cell line and culture conditions

The human osteotropic prostate cancer cell line PC-3M-Pro4luc2 (31) was maintained in DMEM supplemented with 10% FCII, 0.8 mg/ml Neomycin (Santacruz, Dallas, USA) and 1% Penicillin-Streptomycin (Life Technologies, Carlsbad, USA). C4-2B cells were maintained in T-medium DMEM (Sigma-Aldrich, The Netherlands) supplemented with 20% F-12K nutrient mixture Kaighn's modification (GibcoBRL), 10% FCS, 0.125 mg/ml biotin, 1% Insulin-Transferin-Selenium, 6.825 ng/ml T3, 12.5 mg/ml adenine and 1% penicillin/streptomycin. Cells were maintained at 37°C with 5% CO_2.

Luciferase reporter gene constructs

PC-3M-Pro4Luc2 cells were seeded at a density of 50,000 cells in 500 µL medium in a 24-well plate. Transient transfection of reporter constructs was performed with Lipofectamine2000 (Life Technologies) according manufacturer's protocol. For each well, 100 ng of NICD-*ff-luciferase*,10 ng CAGGS-*Renilla luciferase,* 100 ng BRE renilla and 100 ng BREluc/well were transfected. After 24 hours, medium was replaced and cells were treated with BMP9 for 24h. The *Firefly* luciferase and *Renilla* luciferase levels in the lysates were measured using Dual Luciferase Assay (Promega, Madison, USA).

RNA isolation and real-time qPCR

Total RNA was isolated with Trizol Reagent (Invitrogen, Waltham, USA) and cDNA was synthesized by reverse transcription (Promega, Madison, USA) according to the manufacturer's protocol. qRT-PCR was performed with Biorad CFX96 system (Biorad, Veenendaal, The Netherlands). Gene expression was normalized to GAPDH or β-actin. (For primer sequences see Supplementary Table I). Total RNA from frozen section (5µm) was isolated with Qiagen Mini Isolation kit (Venlo, The Netherlands) according to the manufacturer's protocol. Primer sequences are listed in Suppl. Table 1.

MTS assay

Cells were seeded at density of 2,000 cells/well and treated with ALK1Fc or CFc (10ug/ml, Acceleron, USA) allowed to grow for 24, 48, 72 and 96 hours. After incubation, 20 µl of 3-(4,5 dimethylthiazol- 2- yl)- 5 -(3 -carboxymethoxyphenyl)- 2 -(4 -sulfophenyl)- 2 H-tetrazolium was added and mitochondrial activity was measured after 2 hours incubation at 37°C. MTS absorbance values are positively proportional to total number of metabolically active cells providing an indirect correlation with cell proliferation rate (50) (CellTiter96 Aqueous Non-radioactive Cell proliferation assay, Promega).

Animals

Male 6-8 week-old athymic nude mice (Balb/c *nu/nu*), purchased from Charles River (L'Arbresle, France), were used in all *in vivo* experiments (n=15 per group). Mice were housed in individual ventilated cages under sterile condition, and sterile food and water were provided *ad libitum*. Animal experiments were approved by the local committee for animal health ethics and research of Leiden University (DEC #11246), and carried out in accordance with European Communities Council Directive 86/609/EEC. After the experimental periods, mice were injected with hypoxia probe (6mg/kg, Burlington, Massachusetts, USA) and lectin-Tomato (1 mg/kg, Vector Laboratories, USA) intravenously prior to perfusion and sacrified according to our mouse protocol. Tumors were dissected and processed for further histomorphological analysis as described below.

Orthotopic prostate transplantation and ALK1Fc treatment

25000 PC-3M-Pro4luc2 cells (10 ul final volume) were injected in the dorsal lobe of nude mice. In brief: After anesthetizing the mice with isoflurane, each mouse was placed on its back and a small incision was made along the lower midline of the peritoneum for about 1 cm. The prostate dorsal lobes were exteriorized and stabilized gently. A 30-gauge needle attached to a 1-cc syringe was inserted into the right dorsal lobe of the prostate. 10 µl of the material was slowly injected. A well-localized bleb indicates a successful injection. After retracting the needle a Q-tip was placed over the injection site for about 1 min to prevent bleeding and spillage of material. The prostate was then returned to the peritoneum and the abdominal wall and skin layer was sutured. After establishment of the primary tumor, at 10 days after the orthotopic transplantation, mice were intraperitoneally injected with Control-Fc (CFc) or ALK1Fc compounds (1 mg/kg) twice per week. Administration of compounds was performed for four weeks. ALK1-Fc is a fusion protein comprised of the extracellular domain of human ALK1 fused to the Fc region of IgG and was obtained from Acceleron Pharma, Cambridge, USA. The Fc domain of IgG_1 was used as a control (MOPC-21; Bio Express, West Lebanon NH).

Whole body bioluminescent imaging (BLI)

Tumor growth was monitored weekly by whole body bioluminescent imaging (BLI) using an intensified-charge-coupled device (I-CCD) video camera of the *in vivo* Imaging System (IVIS100, Xenogen/Perkin Elmer, Alameda, CA, USA) as described previously (51). In the SD-208 in vivo treatment experiment the newer IVIS Lumina II (Xenogen/Perkin Elmer, Alameda, CA, USA) was used for BLI measurements. Mice were anesthetized using isoflurane and injected intraperitoneally with 2 mg D-luciferin (Per bio Science Nederland B.V., Etten-Leur, the Netherlands). Analyses for each tumors were

performed after definition of the region of interest and quantified with Living Image 4.2 (Caliper Life Sciences, Teralfene, Belgium). Values are expressed as relative light units (RLU) in photons/sec.

Immunofluorescence

Immunofluorescence staining was performed as described previously (52). In brief, Immunofluorescence staining was performed on 5-µm paraffin embedded sections. For antigen retrieval, sections were boiled in antigen unmasking solution (Vector Labs, Peterborough, UK) and stained with CD31 (Sigma) or ALDH1A1 (Abcam) antibodies. Sections were blocked with 1% bovine serum albumin (BSA)-PBS-0.1% v/v Tween-20 and incubated with primary antibodies diluted in the blocking solution, overnight at 4°C or room temperature. Sections then were incubated with secondary antibodies labelled with Alexa Fluor 488, 555, or 647 (Invitrogen/Molecular Probes, Waltham, USA) at 1:250 in PBS-0.1% Tween-20. Nuclei were visualized by TO-PRO3 (Invitrogen/Molecular Probes, 1:1000 diluted in PBS-0.1% Tween-20) or DAPI, which was included in the mounting medium (Prolong G, Invitrogen/Molecular Probes).

Western immunoblotting

Proteins were extracted by using RIPA buffer (Thermo Scientific) and protein concentrations were quantified according to manufacturer's protocol (Thermo Scientific). Proteins samples (20 µg per sample) were separated by 15% SDS-PAGE followed by transfer to a blotting membrane. The membrane was blocked with 5% Milk, dissolved in PBS-Tween for 1 hour at room temperature. The membrane was incubated with 1:1000 primary antibody (anti-NOTCH1, Cell Signaling, catalogue number 3608) at 4ºC overnight. Subsequently, the membrane was incubated with 1:10000 secondary horseradish peroxidase (HRP) antibody. All antibodies were dissolved in PBS-Tween. Chemi-luminescence was used to visualize the bands.

Clonogenic assay

Clonogenic assay was performed in 6 well plate. 100 cells were seeded in 2mL of medium and incubated at 37°C in presence of 5% CO_2 for two weeks. Plates were washed with PBS and cells fixed for 5 min with a solution of 4% PFA. Colonies were stained with 0.1% crystal violet (Sigma-Aldrich, The Netherlands) and plates were imaged before processing the data (53).

Statistical analysis

Statistical analysis was performed with GraphPad Prism 6.0 (GraphPad software) using t-test or ANOVA for comparison between more groups. Data is presented as mean ± SEM. P-values ≤ 0.05 were considered to be statistically significant (* $P < 0.05$, ** $P < 0.01$, *** $P < 0.001$).

Results

High expression of BMP9 and ALK1 correlates with poor survival

We investigated the correlation of survival with BMP9 and ALK1 expression in an independent publically available PCa dataset (GSE21032). BMP9 and ALK1 expression were associated with poor prognosis (**Fig. 1 A and B top**; Hazard Ratio (HR)=2.38 and p=0.007 for BMP9 and HR=2.62 and p=0.007 for ALK1). Additionally, the expression of BMP9 and ALK1 in stratified risk groups was significantly higher in the high vs. low risk group (**Fig. 1 A and B Bottom**; p=1.3e-34 for BMP9 and p=3.46e-19 for ALK1). Taken together, these data demonstrate that BMP9 and ALK1 are selectively highly expressed in aggressive PCa and that their expression correlates with poor prognosis.

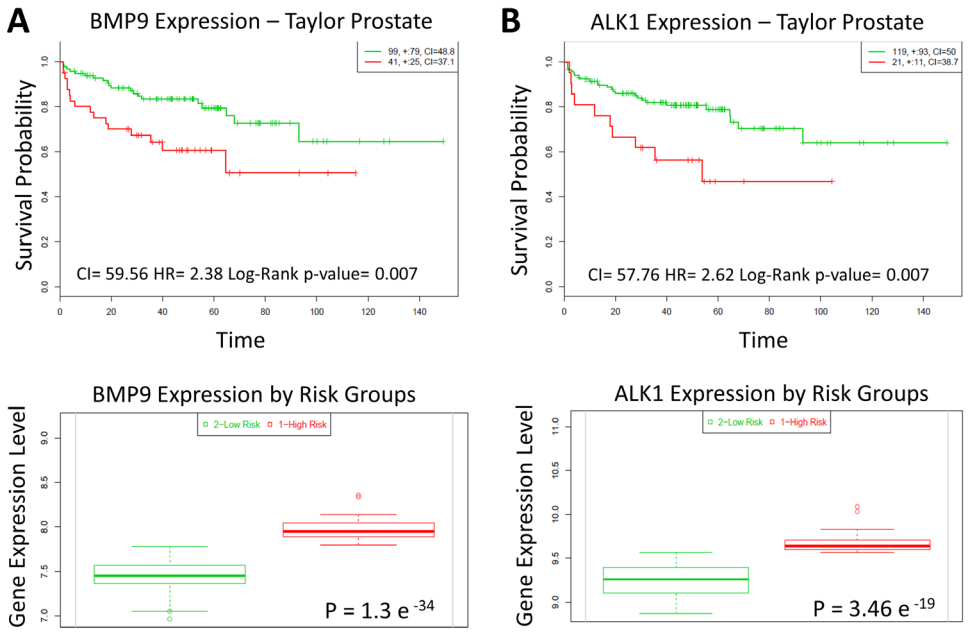

Figure 1. BMP9 and ALK1 correlate with poor patient prognosis. A-B) Top panels: Kaplan-Meier survival curves of censored Cox analysis in Taylor-MSKCC prostate database stratified by maximized BMP9 and ALK1 expression risk groups. Red = high expression; Green = low expression. Bottom panels: BMP9 and ALK1 expression levels stratified by risk groups. Red = high Risk and high BMP9 and ALK1 expression; Green = low risk and low BMP9 and ALK1 expression.

ALK1Fc reduces primary prostate tumor burden *in vivo*

To investigate the role of BMP9 in prostate cancer progression, ALK1Fc was administered in a mouse model of prostate cancer. Orthotopic prostate tumor growth was induced by intra-prostatic inoculation of human prostate cancer PC-3M-Pro4luc2 cells in Balb/c nude mice and tumor progression was followed by bioluminescence imaging (BLI) (31) (**Fig.2A**). Based on the BLI signal the mice were distributed between two treatment groups: ALK1Fc or CFc (n=15 per group). The compounds were injected twice weekly and tumor imaging and body weights were monitored weekly for 5 weeks (**Suppl. Fig.1**). Tumor burden was quantitatively assessed for each animal during the course of treatment. The group of animals that received ALK1Fc exhibit smaller tumor size compared to the animals that received CFc based on the size after resection (**Fig. 2B**) and bioluminescence quantification (**Fig. 2C**, p<0.001).

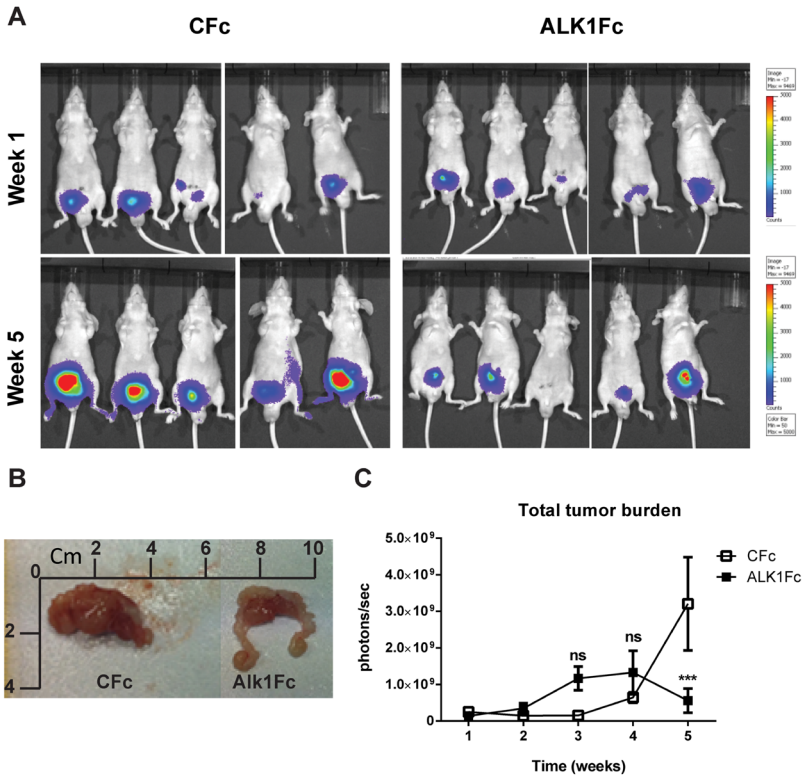

Figure 2. Effect of ALK1Fc *in vivo*. A) PC-3M-Pro4Luc2 cells were orthotopically injected in the anterior lobe of prostate glands of nude mice (n=15 per group). Detection of primary tumor burden was observed at 2 weeks after injection, with the time point designated as "week 1" at the start of treatment with ALK1Fc or CFc. Representative examples of bioluminescent images of tumor burden at the start of treatment with ALK1Fc/ CFc (week 1) and at the end point (week 5). **B**) Representative images of primary

tumor size (in centimeters) from a recipient of CFc versus ALK1Fc treatment after 5 weeks. **C**) Quantification of bioluminescent signal (photons/sec) in mice treated with either CFc (n=14) or ALK1Fc (n=15) for 5 weeks. Error bars indicate ± SEM. P value <0.001 (***).

Alk1Fc reduces vascular density of the primary prostate tumor

The degree of tumor angiogenesis is critical for progressive tumor growth beyond a few mm^3 in size. Intravenous lectin perfusion was used to map the perfused elements of the tumor vasculature in mice. Fluorescent-conjugated lectin (lectin-Tomato) was visualized in tumor tissue sections and quantified. Vascular density, indicated by the overall lectin presence, was decreased in the tumors treated with ALK1Fc compared to the CFc group (**Fig. 3A, B**). We evaluated the presence of endothelial cells in tumor sections by CD31 immunofluorescence. CD31 expression was decreased after treatment with ALK1Fc indicating fewer endothelial cells and vessels (**Fig. 3C, D**). Hypoxia is an important component of angiogenesis and critical for tumor formation. A hypoxia-induced probe was injected in tumor bearing mice just prior to sacrifice and the hypoxic areas within the tumors were visualized after tumor resection (**Fig. 3E, F**). Hypoxic areas are found in both treatment groups; however, the overall amount of hypoxia is significantly higher ($p< 0.05$) in ALK1Fc-treated, tumor-bearing mice over the CFc-treated groups. We assessed the presence of cell proliferation and cell death in these tumors by immunofluorescence for the mitosis marker phosphorylated histone 3 (PH3) and the apoptosis marker cleaved caspase 3 (CASP3). Dividing PH3 positive cells are predominantly located in normoxic areas (**Fig.3E, left panel**). Quantification of immunofluorescence signal shows that the number of dividing cells is lower in the ALK1Fc-treated animals (**Fig. 3G**; $p<0.05$). Detection of apoptotic cells (Caspase-3 positive) is higher in the ALK1Fc-treated tumors (**Fig. 3H**; $p<0.05$) and occurs mostly, however not exclusively, in hypoxic areas (**Fig.3E**), suggesting a correlation between the hypoxia and tumor cell death.

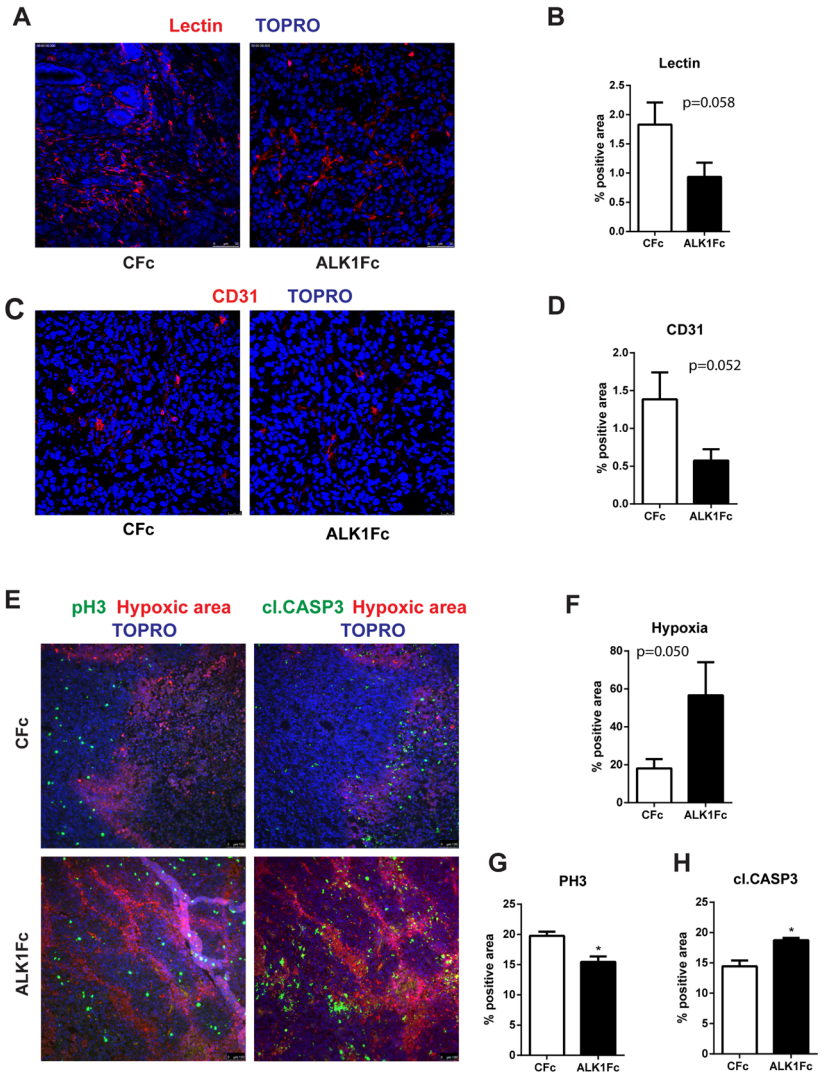

Figure 3. Effect of ALK1Fc on vascular density, cell proliferation and apoptosis *in vivo*. **A**) Representative images of lectin detection in primary prostate tumor samples after perfusion with fluorescent-labelled lectin-Tomato (red). TOPRO (blue) marks the nuclei. Treatment groups: ALK1Fc or CFc. **B**) Quantification of lectin positive surface area in all tumor samples of each group (n=6 for CFc, n=7 for ALK1Fc). (**C**) Representative images of CD31 (red) immunofluorescence staining in primary prostate tumor samples after 5 weeks of treatment with either ALK1Fc or CFc. **D**) Quantification of CD31 positive surface area in all tumor samples of each group (n=6 for CFc, n=7 for ALK1Fc). **E**) Representative images of hypoxia immunofluorescence staining (red) in primary prostate tumor samples after 5 weeks of treatment with either ALK1Fc or CFc. Hypoxia probe was injected prior to sacrifice and was detected by a specific fluorescent antibody. Immunofluorescence images for colocalization of apoptotic or proliferating cells in hypoxic/ normoxic area within the prostate tumor area in ALK1Fc and CFc treated

animals. pH3: PhosphoHistone 3 proliferation marker (green); cleaved caspase 3 apoptosis marker (green); Hypoxic probe-antibody; hypoxic area (red). **F**) Quantification of hypoxia positive area in all tumor samples of each group (n=6 for CFc, n=7 for ALK1Fc). **G**) Quantification of pH3 positive area in all tumor samples of each group (n=6 for CFc, n=7 for ALK1Fc). **H**) Quantification of cleaved caspase 3 positive (apoptotic cells) in all tumor samples of each group (n=6 for CFc, n=7 for ALK1Fc).

ALK1Fc decreases proliferation of human prostate cancer cells

To investigate how ALK1Fc can decrease tumor growth, we investigated the effect of ALK1Fc on prostate cancer cells. We measured the mRNA levels of BMP9 type I receptors ALK1 and ALK2 in the PC-3M-Pro4Luc2 (31) human prostate cancer cell line and tested the response of these cells to BMP9. Consistent with what was previously reported in highly metastatic PC-3 and PC-3M prostate cancer cells (32), qRT-PCR analysis in osteotropic PC-3M-Pro4Luc2 cells revealed undetectable levels of ALK1 mRNA but clearly measurable levels of ALK2 mRNA (**Suppl. Fig. 2A**). Treatment with BMP9 showed a dose-dependent induction of BRE-*Renilla* luciferase activity in PC-3M-Pro4Luc2 cells (p-value=0.005 and 0.05 with 0.5 nM and 1 nM BMP9, respectively) indicative of conserved and active signaling machinery (**Suppl. Fig. 2B**). Using the 1nM BMP9 dose for subsequent experiments, we tested the combined effect of BMP9 with either ALK1Fc or CFc on BRE reporter assay. Treatment with ALK1Fc (10 ug/mL) completely abolished the BMP9-mediated BRE luciferase (luc) activity (**Suppl. Fig. 2C**; BMP9+ALK1Fc) to levels similar to the non-stimulated control (Untreated). Treatment with BMP9+CFc (10 ug/mL) led to induction of BRE-luc activity of similar level as the BMP9 treatment (**Suppl. Fig. 2C**; p-value <0.05). Taken together, these results indicate that ALK1Fc blocks ALK2-mediated BMP9 signaling in PC-3M-Pro4Luc2 cells.

We further show that treatment of with 10 ug/mL ALK1Fc, but not control Fc (CFc), strongly reduced BMP9-induced PC-3M-Pro4Luc2 cell proliferation (p<0.001 at day 4 comparing vehicle vs BMP9 or ALK1Fc treatment, respectively) (**Fig. 4A**). The effect of ALK1Fc on cell proliferation appeared to be specific since it had no effect on cell proliferation in the absence of BMP9 treatment (**Suppl. Fig.2D**). The proliferative effect of BMP9 was also tested in the C4-2B prostate cancer cell line; however no significant difference was observed (**Suppl. Fig. 2E**). When we treated PC-3M-Pro4Luc2 cells with BMP9 in combination with an ALK2 kinase inhibitor (LDN193189, LDN) (33, 34) we observed a complete loss of BMP9-induced proliferation (**Fig. 4B**). LDN treatment also blocked BMP9 stimulation of the BRE-luc reporter in PC-3M-Pro4 cells (**Suppl. Fig. 2F**) but had minimal impact on basal proliferation levels in the absence of exogenously added BMP9 (**Suppl. Fig. 2G**). Finally, we evaluated the clonogenic ability of PC-3M-Pro4Luc2 cells after BMP9 treatment alone (**Suppl. Fig.3A**) and confirmed that BMP9 affects cell proliferation, strongly increasing the size of the colonies (**Suppl. Fig.3B**,

p<0.05). However, BMP9 showed no effect on colony formation/self-renewal ability of PC-3M-Pro4Luc2 since the total number of colonies formed is similar (**Suppl. Fig. 3C**). Together, these data indicate that ALK1Fc strongly reduces BMP9- induced proliferation of human prostate cancer cells.

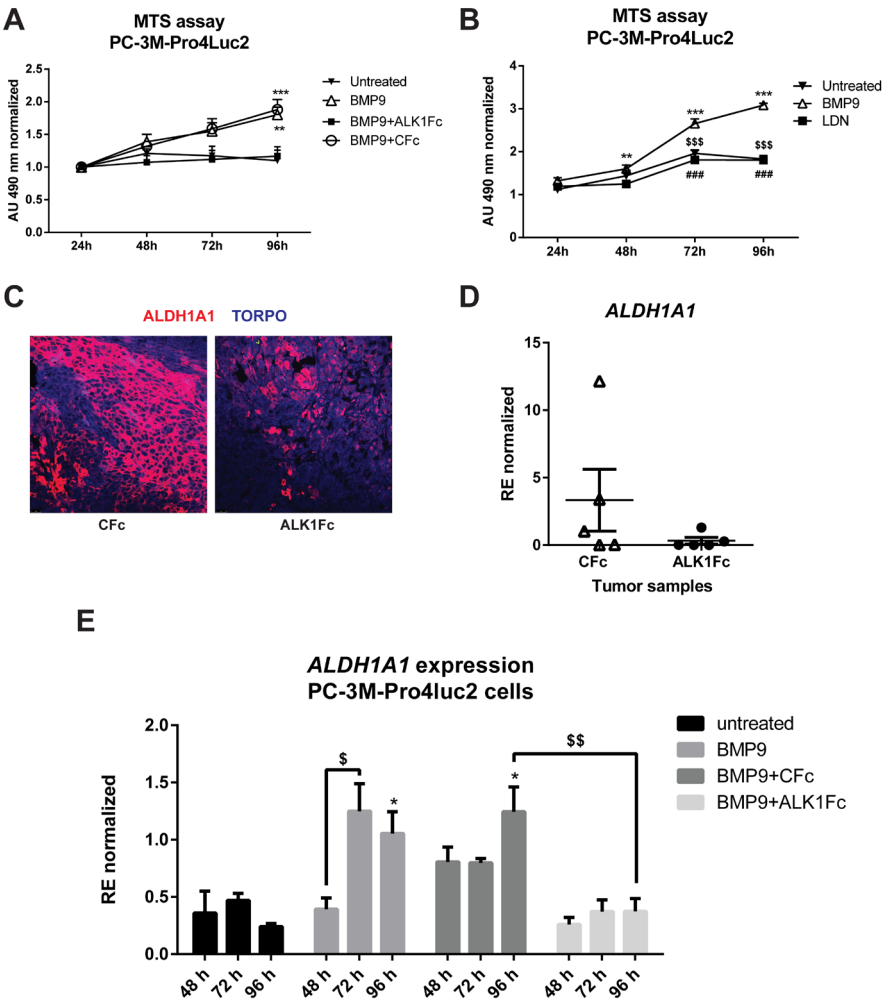

Figure 4. Effect of BMP9 and ALK1Fc on proliferation and ALDH1A1 expression. **A**) MTS assay (24, 48, 72, 96 hours) was performed in PC-3M-Pro4Luc2 cells stimulated with recombinant BMP9 (1 nM), BMP9 (1 nM)+ALK1Fc (10 ug/ml) or BMP9 (1 nM)+CFc (10 ug/ml). Accumulation of MTS was measured based on absorbance at 490 nm. Values are normalized to the basal measurements at 24 hours after cell seeding and treatments. Graph represents values for three independent experiments (n=3). Error bars indicate ± SEM. P value < 0.01 (**) BMP9 vs Untreated and P-value < 0.001 (***) BMP9+CFc vs Untreated. **B**) MTS assay (24, 48, 72 and 96 hours). PC-3M-Pro4Luc2 cells were seeded at low density in 96-well plates and

treated with BMP9 (1 nM), LDN (BMP type I receptor inhibitor LDN193189, 120nM) or LDN+BMP9. (n=2). Error bars indicate SEM. **C**) Representative images of ALDH1A1 immunofluorescence in prostate tumor samples from ALK1Fc and CFc treated animals. ALDH1A1: red; TOPRO: blue nuclear dye. **D**) Quantification of ALDH1A1 mRNA by Q-PCR in tumor samples of each group (n=5 for CFc, n=5 for ALK1Fc). **E**) Expression of ALDH1A1 in PC-3M-Pro4Luc2 cells. Relative mRNA expression was measured by Q-PCR from cDNA obtained from PC-3M-Pro4Luc2 cells treated with BMP9, BMP9+ALK1Fc, BMP9+CFc, for 48, 72 and 96 hours. Values are normalized to β-actin expression. Error bars are ±SEM (n=3).

Expression of BMP9, ALK1 and ALK2 in human and murine prostate tumor tissues

We investigated the mRNA expression of BMP9, ALK1 and ALK2 in 48 benign prostate tumors and 47 malignant prostate tumors (35) using bioinformatics analysis and data mining platforms (R2: microarray analysis and visualization platform http://r2.amc.nl, source: GEO ID: GSE29079) (**Suppl. Fig.3D, E and F**). While levels of *ALK1* transcripts are decreased in the malignant tumor group compared to the benign group ($p<0.001$), levels of *ALK2* transcripts are significantly increased ($p<0.01$) in the malignant tumor group compared to the benign group. BMP9 mRNA expression is similar in both groups ($p=0.28$). Previously, Bacac *et al.* (36) performed cDNA microarray analysis using laser-micro dissected stromal cells from murine prostate intraepithelial neoplasia (PIN) and invasive prostate tumors. Analysis of *ALK1, ALK2* and *BMP9* (**Suppl. Fig.3G, H and I**) expression in this dataset indicated elevated mRNA expression of *ALK1*, *ALK2* and *BMP9* during the invasive stage of murine prostate cancer.

ALK1Fc inhibits ALDH1A1 expression *in vivo* and interferes with NOTCH signaling

Given its ability to reduce primary tumor burden and block BMP9-induced tumor cell proliferation *in vitro* we assessed the effects of ALK1Fc on the relative expression of the *ALDH1A1* marker that is associated with cancer stem cell-like cells and poor patient prognosis (25, 26). Treatment of prostate tumor bearing mice with ALK1Fc affected the number of proliferative ALDH1A1 positive cells in the prostate tumor tissues both at protein (**Fig. 4C**) and mRNA level (**Fig. 4D**). *In vitro* stimulation with BMP9 of the same cell line used to induce tumors in the xenograft mouse model, confirmed that treatment with BMP9 or BMP9+CFc upregulates ALDH1A1 expression while BMP9+ALK1Fc treatments does not have any effect (**Fig. 4E**).

ALDH1A1 is known to be regulated by NOTCH signaling (23-25) and NOTCH1 plays a prominent role in prostate cancer cell proliferation and migration (22, 37-40). Larrivée et al. have shown that ALK1 and NOTCH converge on common downstream pathways and that BMP9 treatment alone upregulates JAG1 expression in HUVEC non-transformed

cells (41). To verify the effect of BMP9 on NOTCH signaling activation in our cancer model, we used qRT-PCR to quantify the expression of *JAG1* after BMP9 stimulation in presence of ALK1Fc or CFc. Our transcriptional analysis showed that BMP9 and BMP9+CFc induce mRNA expression of *JAG1* and that ALK1Fc reduces the BMP9-mediated induction of *JAG1* (**Fig. 5A**). To assess the clinical relevance of BMP9/ALK2-mediated NOTCH pathway activation in human prostate cancer, we performed bioinformatics analysis using data mining platforms (R2: microarray analysis and visualization platform http://r2.amc.nl, source: GEO ID: GSE29079). Transcript levels of the NOTCH ligand *JAG1* were significantly higher in the malignant tumor group compared to the benign group (**Fig. 5B**) and positively correlate with *ALK2* expression and disease progression (**Fig.5D**). In addition, the prostate tumor microarray data indicate a positive correlation between the level of *NOTCH1* receptor expression and human progression to malignancy (**Fig. 5C**) as well as *ALK2* expression (**Fig. 5E**). In addition, overexpression of JAG1 in PC-3M-Pro4Luc2 human prostate cancer cells increases metabolic activity measured by MTS assay (**Fig. 5F**).

We targeted expression of NOTCH1 in PC-3M-Pro4Luc2 using a specific shRNA (shNOTCH1) and assessed resulting NOTCH1 levels by western blot and by reporter assay (**Suppl. Fig. 4A and B**). NOTCH1 knockdown cells had decreased proliferation compared to cells transduced with non-targeting shRNA lentivirus ($p<0.05$ at 48h and at 72h) (**Fig. 5G**). We observe that stimulation of shNOTCH1-cells with BMP9 increases their proliferation rate (**Fig. 5H**) and that shNOTCH1-cells display decreased levels of JAG1 mRNA (**Suppl. Fig . 4C**). These data suggest that BMP9/ALK2 induces activation of NOTCH signaling (JAG1 and NOTCH1) and enhanced cell proliferation both of which are associated with tumor progression in PCa.

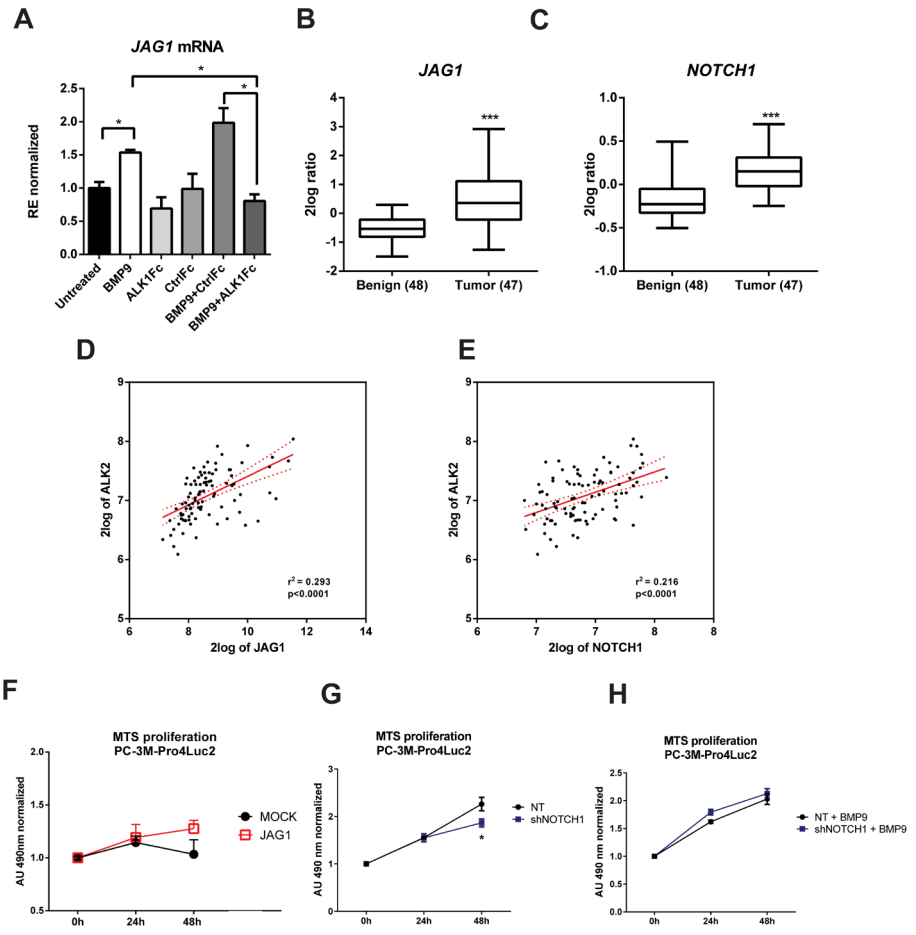

Figure 5. Effect of BMP9 and ALK1Fc on NOTCH signaling pathway and correlation study. A) Expression of *JAG1* in PC-3M-Pro4Luc2 cells. Relative mRNA expression was measured by qPCR from cDNA obtained from PC-3M-Pro4Luc2 cells treated with BMP9, ALK1Fc, CFc, BMP9+ALK1Fc or BMP9+CFc for 96 hours. Values are normalized to β-actin expression. Error bars are ±SEM (n=3). **B-C**) Bioinformatics analysis of AMC OncoGenomics database (Sueltman transcript comparison) showing mRNA expression of *JAG1* **B**) and *NOTCH1* **C**) in prostate tissues among benign prostate tissues (n=48) versus tumor tissues (n=47). Values are expressed as 2log ratio tumor/ benign. ns: not significant. P value < 0.001 (***). **D**) Correlation analysis of *JAG1* and *ALK2* expression (p<0.0001) and **E**) correlation analysis of NOTCH1 and ALK2 expression (p<0.0001) in prostate tissues among benign prostate tissues (n=48) versus tumor tissues (n=47). Bioinformatic analysis was performed using the AMC OncoGenomics database (Sueltman transcript comparison), values are expressed as 2log ratio tumor/ benign. ns: not significant. **F**) MTS assay (24, 48 hours) in PC-3M-Pro4Luc2 cells transfected with 1ug JAG1 or Mock expression vector (n=2). **G-H**) MTS assay (24, 48, 72 and 96 hours) in PC-3M-Pro4Luc2 cells were transduced with short hairpin RNA against NOTCH1 (shNOTCH1) lentiviral vector or non-targeting (NT) shRNA vector (mock) and

plated at low density. Treatment with BMP9 (1 nM) was done once at cell seeding (t=0) MTS absorbance was measured. Values are normalized to the basal measurements t=0 after cell seeding and treatments. Graph represents values for three independent experiments (n=3). Error bars indicate SEM. P value <0.05 (*).

Discussion

In this study, we find that BMP9 and ALK1 correlate with poor survival in prostate cancer patients and that BMP9 has a tumor-promoting effect on human prostate cancer cells both *in vitro* and *in vivo*. We demonstrate that blocking BMP9 signaling with ALK1Fc efficiently diminishes prostate cancer cell proliferation and substantially attenuates tumor growth in an orthotopic model of human prostate cancer.

BMP9 was first identified in the liver (12) and active forms are present in serum (8). BMP9 is a ligand for the ALK1 receptor in endothelial cells (5) and exerts stimulatory or inhibitory effects on endothelial cell growth and migration depending on the cellular context (30, 42). Aberrant regulation of TGF-β and BMP signaling often results in cancer progression (43, 44). In particular, BMP ligands, such as BMP9 as well as BMP type I receptors (e.g. ALK1 and ALK2) have been associated with tumor angiogenesis and cancer progression. BMP9 signals through ALK2 in non-endothelial cells such as in ovarian epithelium, where it has been shown to promote ovarian cancer cell proliferation (8). Similarly, in hepatocellular carcinoma BMP9 has been reported to act as proliferative and survival factor (10). Studies have also highlighted the role of BMP9 in reducing breast cancer cell growth and metastasis (45-47). However, the role of BMP9 and ALKs in promoting or suppressing different cancer types remains controversial. Collectively, this indicates that the effect of BMP9 on tumor promotion vs tumor suppression could be context and cancer-type specific, thus providing the rationale for to elucidate the role of BMP9 in prostate cancer, for which no information is available to our knowledge.

We searched publicly available databases of human prostate cancer specimens and found that ALK2 is significantly upregulated in malignant vs. benign tumor tissue samples whereas ALK1 has the opposite expression pattern, although shown to correlate with poor survival in other dataset (35). However, these data are consistent with our model in which the tumor-promoting effects of BMP9 are mediated by ALK2. Additionally, microarray analysis of data from mouse prostate intraepithelial neoplasia (PIN) versus invasive cancer in a multistage model of prostate carcinogenesis showed up-regulation of ALK2 and BMP9 at the invasive stage in the stromal compartment (48). Taken together, these data suggest a tumor-promoting role of BMP9 produced by the supportive stroma during prostate cancer progression. The fact that the BMP9 transcript levels registered in the selected dataset are similar in benign vs tumor stage in human prostate tumor samples, suggests a paracrine effect of BMP9 in human prostate cancer (35). Moreover, the significant increased expression of ALK2 in human prostate tumor tissue samples suggests that the BMP9 produced by the stromal compartment might be pro-tumorigenic as suggested by the anti-tumor effect of ALK1Fc that we have

documented here. This hypothesis is reinforced by our survival analysis which shows that BMP9 correlates with poor survival in human prostate cancer patients.

Our *in vitro* findings strengthen the afore-mentioned expression data and suggest that BMP9 increases proliferation of human prostate cancer cells. Moreover, our studies incorporating blockade of ALK2 activity by LDN193189 support the notion that ALK2 is critically involved in mediating BMP9-induced proliferation. As depicted in the supplementary data, treatment with ALK1Fc or LDN193189 alone did not affect proliferation of human prostate cancer cells suggesting a paracrine effect of stroma-derived BMP9 on tumor cells. While BMP9 did not influence clonogenic ability of human prostate cancer cells, it elicited a significant stimulatory effect on colony size suggesting it influences colony expansion rather than colony formation.

In our orthotopic model of human prostate cancer, ALK1Fc significantly reduced the prostate tumor burden compared to the control group and vascular density was also reduced in animals treated with ALK1Fc versus those treated with CFc. Interestingly, lectin distribution appeared to be less diffuse in ALK1Fc treated animals, suggesting an effect on vessel maintenance rather than angiogenesis. Strikingly, ALK1Fc treatment of tumor-bearing animals resulted in highly hypoxic tumors with a decreased number of CD31+ tumor capillaries suggesting that ALK1Fc may block BMP9-induced neovascularization.

As expected, areas of tumor proliferation and apoptosis were found to be mutually exclusive in their distribution. Apoptotic regions overlapped with hypoxic areas, suggesting that blockade of BMP9 by ALK1Fc might have an effect on proliferation and apoptosis of human prostate cancer cells in addition to targeting vessel maintenance (28).

SMAD1 and SMAD5 are intracellular effectors of BMP9 signaling that can directly interact with the JAG1 promoter following BMP9 treatment (49) and induce transcription of the NOTCH ligand JAG1 (41). Transcriptional analysis revealed that ALK1Fc systemically blocks the induction of JAG1 mRNA in the presence of BMP9 (49) supporting our hypothesis that the crosstalk between BMP9 and NOTCH signaling may have clinical implications in prostate cancer. Indeed, *in silico* analysis of a previously published dataset of human prostate cancer specimens confirms that both *NOTCH1* and *JAG1* are upregulated at the tumor stage (35). Our database analysis in a multistage model of prostate carcinogenesis on mouse prostate intraepithelial neoplasia (PIN) vs. invasive cancer further indicates that *Jag1* is significantly upregulated in the stroma during the invasive cancer stage (48).

Interestingly, NOTCH activates aldehyde dehydrogenase 1A1 (ALDH1A1) a well-known marker of highly tumorigenic prostate cancer stem-like cells (23-25). The $ALDH^{high}$ subpopulation contributes to both tumor initiation and progression and when highly

expressed in advanced-stage cancers correlates with poor survival in hormone-naïve patients (25). ALK1Fc-treated tumors showed significant reduction of ALDH1A1, which in combination with the data described above, suggests that ALK1Fc might potentially interfere with NOTCH signaling in the regulation of ALDH1A1.
In conclusion, our findings provide novel information on the role of BMP9 in human prostate cancer and suggest the promising use of BMP9 targeting molecules for the treatment of tumor and supportive microenvironment in prostate cancer patients.

Acknowledgements

We thank Acceleron Pharma for providing the ALK1Fc (RAP-041), Laurens van Meeteren and Marjan van de Merbel. The research leading to these results has received funding from the FP7 Marie Curie ITN under grant agreement No. 264817 - BONE-NET (EZ) and from the Netherlands Initiative of Regenerative Medicine (NIRM, grant No. FES0908).

REFERENCES

1. Jemal A, Center MM, DeSantis C and Ward EM. Global patterns of cancer incidence and mortality rates and trends. Cancer Epidemiol Biomarkers Prev. 2010; 19(8):1893-1907.
2. Ye L, Lewis-Russell JM, Kyanaston HG and Jiang WG. Bone morphogenetic proteins and their receptor signaling in prostate cancer. Histol Histopathol. 2007; 22(10):1129-1147.
3. Bendell JC, Gordon MS, Hurwitz HI, Jones SF, Mendelson DS, Blobe GC, Agarwal N, Condon CH, Wilson D, Pearsall AE, Yang Y, McClure T, Attie KM, Sherman ML and Sharma S. Safety, pharmacokinetics, pharmacodynamics, and antitumor activity of dalantercept, an activin receptor-like kinase-1 ligand trap, in patients with advanced cancer. Clinical cancer research : an official journal of the American Association for Cancer Research. 2014; 20(2):480-489.
4. Hawinkels LJ, Garcia de Vinuesa A and Ten Dijke P. Activin receptor-like kinase 1 as a target for anti-angiogenesis therapy. Expert Opin Investig Drugs. 2013; 22(11):1371-1383.
5. van Meeteren LA, Thorikay M, Bergqvist S, Pardali E, Gallo Stampino C, Hu-Lowe D, Goumans M-J and ten Dijke P. Anti-human Activin receptor-like kinase 1 (ALK1) antibody attenuates Bone morphogenetic protein 9 (BMP9)-induced ALK1 signaling and interferes with endothelial cell sprouting. Journal of Biological Chemistry. 2012; 287(22):18551-18561.
6. Bragdon B, Moseychuk O, Saldanha S, King D, Julian J and Nohe A. Bone morphogenetic proteins: a critical review. Cellular Signaling. 2011; 23(4):609-620.
7. David L, Mallet C, Mazerbourg S, Feige JJ and Bailly S. Identification of BMP9 and BMP10 as functional activators of the orphan activin receptor-like kinase 1 (ALK1) in endothelial cells. Blood. 2007; 109(5):1953-1961.
8. Herrera B, van Dinther M, Ten Dijke P and Inman GJ. Autocrine bone morphogenetic protein-9 signals through activin receptor-like kinase-2/Smad1/Smad4 to promote ovarian cancer cell proliferation. Cancer research. 2009; 69(24):9254-9262.
9. Scharpfenecker M, van Dinther M, Liu Z, van Bezooijen RL, Zhao Q, Pukac L, Lowik CW and ten Dijke P. BMP-9 signals via ALK1 and inhibits bFGF-induced endothelial cell proliferation and VEGF-stimulated angiogenesis. J Cell Sci. 2007; 120(Pt 6):964-972.
10. Herrera B, Garcia-Alvaro M, Cruz S, Walsh P, Fernandez M, Roncero C, Fabregat I, Sanchez A and Inman GJ. BMP9 is a proliferative and survival factor for human hepatocellular carcinoma cells. PloS one. 2013; 8(7):e69535.
11. Li R, Zhang W, Cui J, Shui W, Yin L, Wang Y, Zhang H, Wang N, Wu N, Nan G, Chen X, Wen S, Deng F, Zhang H, Zhou G, Liao Z, et al. Targeting BMP9-promoted human osteosarcoma growth by inactivation of notch signaling. Current cancer drug targets. 2014; 14(3):274-285.
12. Celeste AJ SJ, Cox K, Rosen V, Wozney JM. Bone morphogenetic protein-9, a new member of the TGF-beta superfamily. J Bone Min Res. 1994; Supp 1(136).
13. Wang K, Feng H, Ren W, Sun X, Luo J, Tang M, Zhou L, Weng Y, He T-C and Zhang Y. BMP9 inhibits the proliferation and invasiveness of breast cancer cells MDA-MB-231. Journal of cancer research and clinical oncology. 2011; 137(11):1687-1696.
14. Ye L, Kynaston H and Jiang WG. Bone morphogenetic protein-9 induces apoptosis in prostate cancer cells, the role of prostate apoptosis response-4. Molecular Cancer Research. 2008; 6(10):1594-1606.
15. Olsen OE, Wader KF, Misund K, Vatsveen TK, Ro TB, Mylin AK, Turesson I, Stordal BF, Moen SH, Standal T, Waage A, Sundan A and Holien T. Bone morphogenetic protein-9 suppresses

growth of myeloma cells by signaling through ALK2 but is inhibited by endoglin. Blood Cancer Journal. 2014; 4:e196.

16. Cunha SI and Pietras K. ALK1 as an emerging target for antiangiogenic therapy of cancer. Blood. 2011; 117(26):6999-7006.
17. Urness LD, Sorensen LK and Li DY. Arteriovenous malformations in mice lacking activin receptor-like kinase-1. Nature genetics. 2000; 26(3):328-331.
18. Gale NW, Dominguez MG, Noguera I, Pan L, Hughes V, Valenzuela DM, Murphy AJ, Adams NC, Lin HC, Holash J, Thurston G and Yancopoulos GD. Haploinsufficiency of delta-like 4 ligand results in embryonic lethality due to major defects in arterial and vascular development. Proceedings of the National Academy of Sciences of the United States of America. 2004; 101(45):15949-15954.
19. Krebs LT, Shutter JR, Tanigaki K, Honjo T, Stark KL and Gridley T. Haploinsufficient lethality and formation of arteriovenous malformations in Notch pathway mutants. Genes & development. 2004; 18(20):2469-2473.
20. Carvalho FL, Simons BW, Eberhart CG and Berman DM. Notch signaling in prostate cancer: a moving target. The Prostate. 2014; 74(9):933-945.
21. Ross AE, Marchionni L, Vuica-Ross M, Cheadle C, Fan J, Berman DM and Schaeffer EM. Gene expression pathways of high grade localized prostate cancer. The Prostate. 2011.
22. Wang Z, Li Y, Banerjee S, Kong D, Ahmad A, Nogueira V, Hay N and Sarkar FH. Down-regulation of Notch-1 and Jagged-1 inhibits prostate cancer cell growth, migration and invasion, and induces apoptosis via inactivation of Akt, mTOR, and NF-kappaB signaling pathways. J Cell Biochem. 2010; 109(4):726-736.
23. Zhao D, Mo Y, Li M-T, Zou S-W, Cheng Z-L, Sun Y-P, Xiong Y, Guan K-L and Lei Q-Y. NOTCH-induced aldehyde dehydrogenase 1A1 deacetylation promotes breast cancer stem cells. The Journal of Clinical Investigation. 2014; 124(12):0-0.
24. Ginestier C, Hur MH, Charafe-Jauffret E, Monville F, Dutcher J, Brown M, Jacquemier J, Viens P, Kleer CG, Liu S, Schott A, Hayes D, Birnbaum D, Wicha MS and Dontu G. ALDH1 is a marker of normal and malignant human mammary stem cells and a predictor of poor clinical outcome. Cell stem cell. 2007; 1(5):555-567.
25. Le Magnen C, Bubendorf L, Rentsch CA, Mengus C, Gsponer J, Zellweger T, Rieken M, Thalmann GN, Cecchini MG, Germann M, Bachmann A, Wyler S, Heberer M and Spagnoli GC. Characterization and clinical relevance of ALDHbright populations in prostate cancer. Clinical cancer research : an official journal of the American Association for Cancer Research. 2013; 19(19):5361-5371.
26. Li T, Su Y, Mei Y, Leng Q, Leng B, Liu Z, Stass SA and Jiang F. ALDH1A1 is a marker for malignant prostate stem cells and predictor of prostate cancer patients' outcome. Laboratory investigation; a journal of technical methods and pathology. 2010; 90(2):234-244.
27. Seehra J, Knopf J, Pearsall RS, Grinberg A and Kumar R. (2009). Antagonists of bmp9, bmp10, alk1 and other alk1 ligands, and uses thereof. Google Patents).
28. Mitchell D, Pobre EG, Mulivor AW, Grinberg AV, Castonguay R, Monnell TE, Solban N, Ucran JA, Pearsall RS, Underwood KW, Seehra J and Kumar R. ALK1-Fc inhibits multiple mediators of angiogenesis and suppresses tumor growth. Mol Cancer Ther. 2010; 9(2):379-388.
29. Cunha SI, Pardali E, Thorikay M, Anderberg C, Hawinkels L, Goumans M-J, Seehra J, Heldin C-H, ten Dijke P and Pietras K. Genetic and pharmacological targeting of activin receptor-like

kinase 1 impairs tumor growth and angiogenesis. The Journal of Experimental Medicine. 2010; 207(1):85-100.

30. Suzuki Y, Ohga N, Morishita Y, Hida K, Miyazono K and Watabe T. BMP-9 induces proliferation of multiple types of endothelial cells in vitro and in vivo. Journal of Cell Science. 2010; 123(10):1684-1692.
31. Kroon J, In 't Veld LS, Buijs JT, Cheung H, van der Horst G and van der Pluijm G. Glycogen synthase kinase-3beta inhibition depletes the population of prostate cancer stem/progenitor-like cells and attenuates metastatic growth. Oncotarget. 2014; 5(19):8986-8994.
32. Craft CS, Romero D, Vary CP and Bergan RC. Endoglin inhibits prostate cancer motility via activation of the ALK2-Smad1 pathway. Oncogene. 2007; 26(51):7240-7250.
33. Shi S, Hoogaars WM, de Gorter DJ, van Heiningen SH, Lin HY, Hong CC, Kemaladewi DU, Aartsma-Rus A, ten Dijke P and t Hoen PA. BMP antagonists enhance myogenic differentiation and ameliorate the dystrophic phenotype in a DMD mouse model. Neurobiology of disease. 2011; 41(2):353-360.
34. Cuny GD, Yu PB, Laha JK, Xing X, Liu JF, Lai CS, Deng DY, Sachidanandan C, Bloch KD and Peterson RT. Structure-activity relationship study of bone morphogenetic protein (BMP) signaling inhibitors. Bioorganic & medicinal chemistry letters. 2008; 18(15):4388-4392.
35. Borno ST, Fischer A, Kerick M, Falth M, Laible M, Brase JC, Kuner R, Dahl A, Grimm C, Sayanjali B, Isau M, Rohr C, Wunderlich A, Timmermann B, Claus R, Plass C, et al. Genome-wide DNA methylation events in TMPRSS2-ERG fusion-negative prostate cancers implicate an EZH2-dependent mechanism with miR-26a hypermethylation. Cancer discovery. 2012; 2(11):1024-1035.
36. Bacac M, Provero P, Mayran N, Stehle J-C, Fusco C and Stamenkovic I. A mouse stromal response to tumor invasion predicts prostate and breast cancer patient survival. PloS one. 2006; 1(1):e32.
37. Shou J, Ross S, Koeppen H, de Sauvage FJ and Gao WQ. Dynamics of notch expression during murine prostate development and tumorigenesis. Cancer research. 2001; 61(19):7291-7297.
38. Zhang Y, Wang Z, Ahmed F, Banerjee S, Li Y and Sarkar FH. Down-regulation of Jagged-1 induces cell growth inhibition and S phase arrest in prostate cancer cells. International journal of cancer Journal international du cancer. 2006; 119(9):2071-2077.
39. Leong KG and Gao WQ. The Notch pathway in prostate development and cancer. Differentiation. 2008; 76(6):699-716.
40. Bin Hafeez B, Adhami VM, Asim M, Siddiqui IA, Bhat KM, Zhong W, Saleem M, Din M, Setaluri V and Mukhtar H. Targeted knockdown of Notch1 inhibits invasion of human prostate cancer cells concomitant with inhibition of matrix metalloproteinase-9 and urokinase plasminogen activator. Clinical cancer research : an official journal of the American Association for Cancer Research. 2009; 15(2):452-459.
41. Larrivee B, Prahst C, Gordon E, del Toro R, Mathivet T, Duarte A, Simons M and Eichmann A. ALK1 signaling inhibits angiogenesis by cooperating with the Notch pathway. Dev Cell. 2012; 22(3):489-500.
42. David L, Mallet C, Mazerbourg S, Feige J-J and Bailly S. (2007). Identification of BMP9 and BMP10 as functional activators of the orphan activin receptor-like kinase 1 (ALK1) in endothelial cells.
43. Siegel PM and Massague J. Cytostatic and apoptotic actions of TGFβ in homeostasis and cancer. Nat Rev Cancer. 2003; 3(11):807-820.

44. Massagué J. TGFβ in Cancer. Cell. 2008; 134(2):215-230.
45. Wang K, Feng H, Ren W, Sun X, Luo J, Tang M, Zhou L, Weng Y, He TC and Zhang Y. BMP9 inhibits the proliferation and invasiveness of breast cancer cells MDA-MB-231. Journal of cancer research and clinical oncology. 2011; 137(11):1687-1696.
46. Ren W, Sun X, Wang K, Feng H, Liu Y, Fei C, Wan S, Wang W, Luo J, Shi Q, Tang M, Zuo G, Weng Y, He T and Zhang Y. BMP9 inhibits the bone metastasis of breast cancer cells by downregulating CCN2 (connective tissue growth factor, CTGF) expression. Molecular biology reports. 2014; 41(3):1373-1383.
47. Ren W, Liu Y, Wan S, Fei C, Wang W, Chen Y, Zhang Z, Wang T, Wang J, Zhou L, Weng Y, He T and Zhang Y. BMP9 inhibits proliferation and metastasis of HER2-positive SK-BR-3 breast cancer cells through ERK1/2 and PI3K/AKT pathways. PloS one. 2014; 9(5):e96816.
48. Bacac M, Provero P, Mayran N, Stehle JC, Fusco C and Stamenkovic I. A mouse stromal response to tumor invasion predicts prostate and breast cancer patient survival. PloS one. 2006; 1:e32.
49. Morikawa M, Koinuma D, Tsutsumi S, Vasilaki E, Kanki Y, Heldin CH, Aburatani H and Miyazono K. ChIP-seq reveals cell type-specific binding patterns of BMP-specific Smads and a novel binding motif. Nucleic acids research. 2011; 39(20):8712-8727.
50. Berridge MV, Herst PM and Tan AS. (2005). Tetrazolium dyes as tools in cell biology: new insights into their cellular reduction. Biotechnology Annual Review: Elsevier), pp. 127-152.
51. van der Pluijm G, Que I, Sijmons B, Buijs JT, Lowik CW, Wetterwald A, Thalmann GN, Papapoulos SE and Cecchini MG. Interference with the microenvironmental support impairs the de novo formation of bone metastases in vivo. Cancer Res. 2005; 65(17):7682-7690.
52. Karkampouna S, Kruithof BP, Kloen P, Obdeijn MC, van der Laan AM, Tanke HJ, Kemaladewi DU, Hoogaars WM, t Hoen PA, Aartsma-Rus A, Clark IM, Ten Dijke P, Goumans MJ and Kruithof-de Julio M. Novel ex vivo culture method for the study of Dupuytren's Disease: effects of TGFβ type 1 receptor modulation by antisense oligonucleotides. Molecular therapy Nucleic acids. 2014; 3:e142.
53. Guzman C, Bagga M, Kaur A, Westermarck J and Abankwa D. ColonyArea: an ImageJ plugin to automatically quantify colony formation in clonogenic assays. PLoS One. 2014; 9(3):e92444.

SUPPLEMENTARY DATA

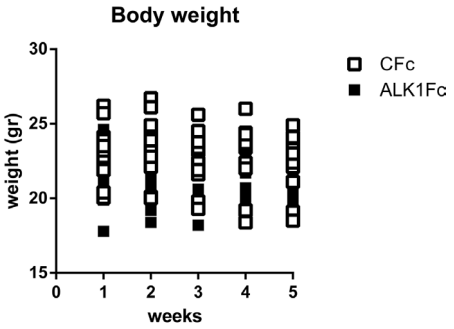

Suppl. Fig. 1 Body weight of animals used for *in vivo* experiment. Body weight (grams) of all the animals of treatment groups measured weekly during the course of treatment with either CFc (n=6) or ALK1Fc (n=7).

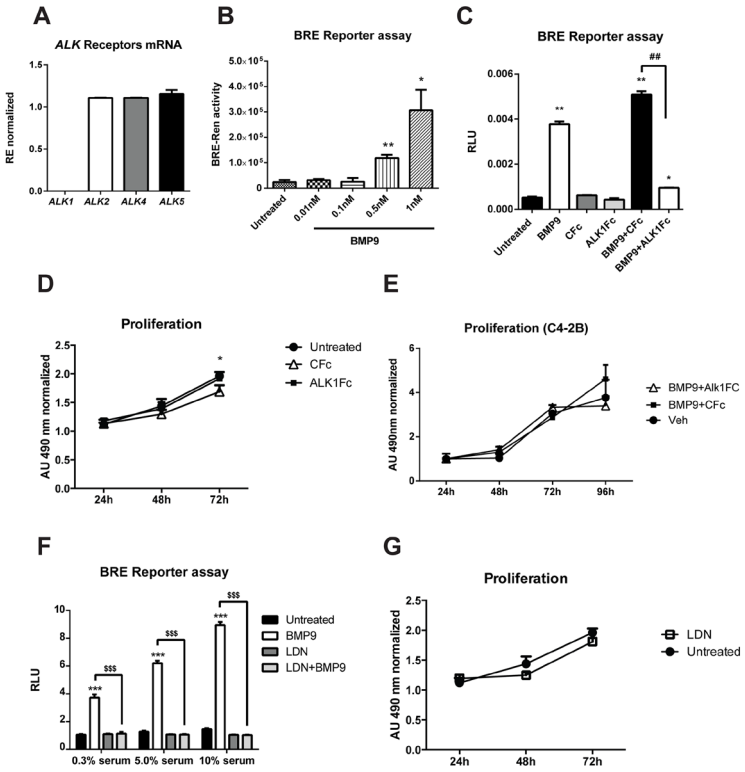

Suppl. Fig. 2 Characterization of dose response for BMP9 with luciferase reporter. **A**) Endogenous expression of *ALK1*, *ALK2*, *ALK4* and *ALK5* receptors in PC-3M-Pro4Luc2cells (mRNA level). Relative expression levels normalized to β-actin are shown. Error bars indicate +/-SD. **B**) Dose dependent response of PC-3M-Pro4Luc2 cells to recombinant BMP9 (0.01, 0.1, 0.5, 1 nM). Downstream activation of BMP signaling was tested by transfection of BRE-renilla construct and measured by reporter activity assay. Graph represents values from three independent experiments; error bars indicate ± SEM (n=3). P value < 0.05 (*) and P value < 0.01 (**). **C**) BRE reporter luciferase (BREluc) assay; Inhibitory concentration of ALK1Fc or CFc (10 ug/ml) was determined in cells stimulated with 1 nM BMP9. Graph represents values from two independent experiments; error bars indicate ± SEM (n=2). P value < 0.05 (*) and P value < 0.01 (**) compared to "untreated" control. P value < 0.01 (##) **D**) MTS assay (24, 48, 72 hours) was performed in PC-3M-Pro4-luc2 human prostate cancer cell line treated with recombinant ALK1Fc (10 ug/ml), CFc (10 ug/ml). Accumulation of MTS was measured based on absorbance at 490 nm. Values are normalized to the basal measurements at 24 hours after cell seeding and treatments. Graph represents values from two independent experiments (n=2). Error bars indicate ±SEM. **E**) MTS assay (24, 48, 72, 96 hours) was performed in C4-2B human prostate cancer cell lines stimulated with recombinant BMP9 (1 nM), BMP9 (1 nM)+ALK1Fc (10 ug/ml) or BMP9 (1 nM)+CFc (10 ug/ml). (n=3). **F**) BMP promoter assay (BRE-luciferase). PC-3M-Pro4 were seeded and, transfected with BRE-luc and renilla plasmid DNA. After 24 hours the medium was replaced with 0.3%, 5%, 10% FCII serum containing media and treated with BMP9 (1nM), LDN193189 (LDN, 120nM) and BMP9+LDN. Luc and Ren values were measured 24 hrs after treatment. RLU ratio values are shown (Luc/Ren). Error bars indicate ±SD. **G**) MTS assay (24, 48, 72

hours) was performed in PC-3M-Pro4-luc2 human prostate cancer cell line treated with LDN inhibitor (LDN193189, 120 nM). (n=2). Error bars indicate +/-SEM.

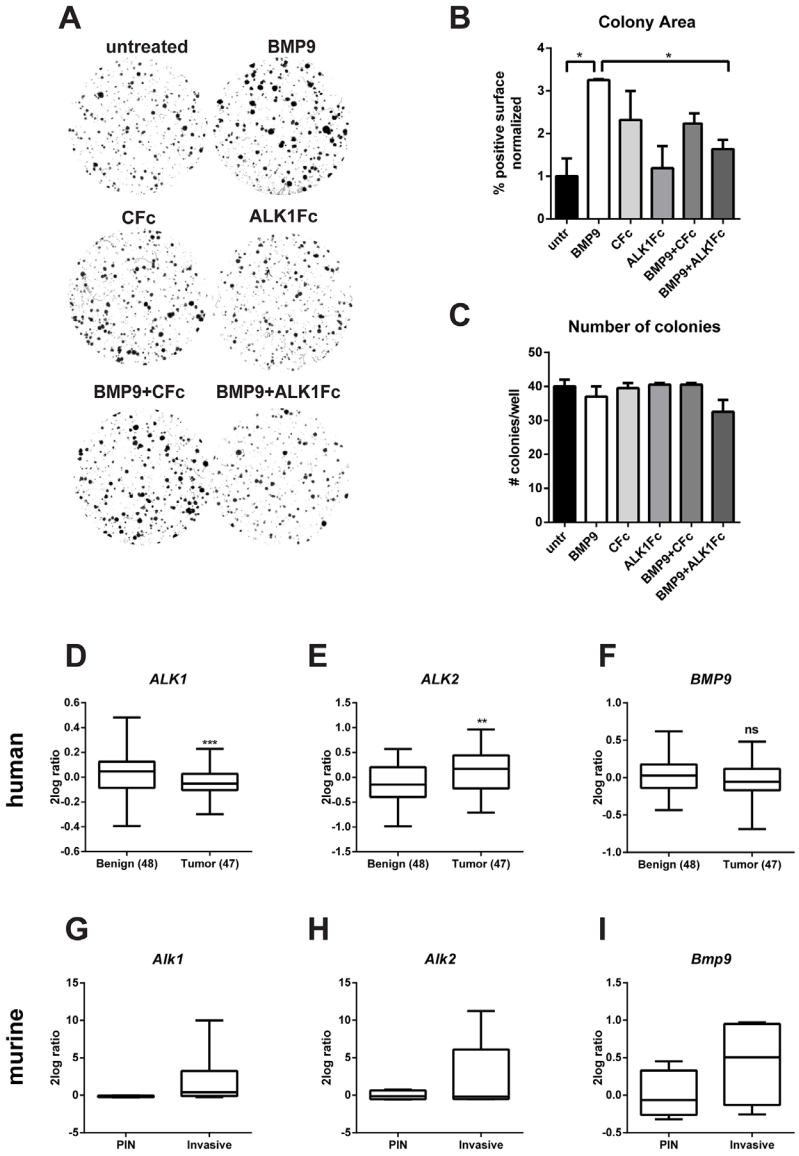

Suppl. Fig. 3 Effect of BMP9 and ALK1Fc on clonogenicity and ALK expression in human samples. A) Clonogenic assay of PC-3M-Pro4Luc2 cells. Low-density cultures (100 cells per well of 6well plate) were stimulated with BMP9, CFc, ALK1Fc, BMP9+CFc, BMP9+ALK1Fc. Colony formation was assessed after 10 days by crystal violet staining. Representative images are shown. **B-C**) Quantification of surface covered by crystal violet positive colonies (colony area) and colony number. Graph shows percentage of positive

surface normalized per condition (average of three independent experiments). P value < 0.05 (*). Error bars indicate SEM. **D-F**) Bioinformatics analysis of AMC OncoGenomics database (Sueltman transcript comparison) showing mRNA expression of *ALK1, ALK2* and *BMP9* in prostate tissues among benign prostate tissues (n=48) versus tumor tissues (n=47). Values are expressed as 2log ratio tumor/ benign. ns: non-significant. P value < 0.01 (**) **G-I**) Microarray cDNA analysis (adapted from *Bacac et al.,* (36) of *Alk1, Alk2* and *Bmp9* expression in microdissected murine stroma derived from two tumor stages; prostate intraepithelial neoplasia (PIN, n=4), and invasive tumors (n=6).

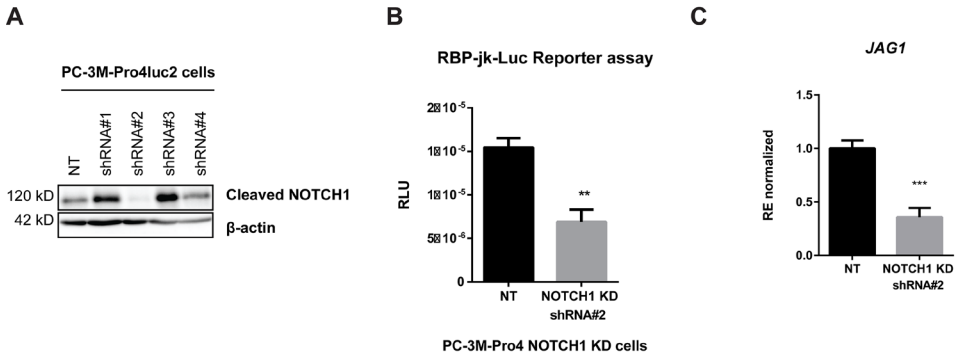

Suppl.Fig.4. Characterization of NOTCH1 knock-down. **A**) Western immunoblotting for NOTCH1 protein as validation of lentiviral shRNA-mediated knockdown of NOTCH1 intracellular domain (cleaved) in PC-3M-Pro4luc2 PCa cell line using five shRNA constrcuts. Based on the downregulation of cleaved NOTCH1 observed after lentiviral transduction and puromycin selection, the stable line expressing the shRNA #2 construct was selected for further experiments. NT; non-targeting shRNA lentiviral mediated transduction. B-actin was used as loading control. **B**) NOTCH transcription factor RBP-Jk-luciferase reporter assay in non-targeting (NT) and NOTCH1 (shRNA#2) knockdown (KD) PC-3M-Pro4Luc2 cells. RLU: relative luciferase units (signal of luciferase normalised to renilla values). n=3, P value < 0.01 (**) **C**) QPCR for *JAG1* mRNA levels in non-targeting (NT) and NOTCH1 (shRNA#2) knockdown (KD) PC-3M-Pro4Luc2 cells. Fold over the value of NT is represented. Error bars indicate ±SD. P value < 0.001 (***).

6

CRIPTO and its signaling partner GRP78 drive the metastatic phenotype in human osteotropic prostate cancer

Eugenio Zoni
Lanpeng Chen
Zoraide Granchi
Esther I. Verhoef
Sofia Karkampouna
Federico La Manna
Rob C. M. Pelger
Ewa Snaar-Jagalska
Geert J.L.H. van Leenders
Lijkele Beimers
Peter Kloen
Peter C. Gray
Gabri van der Pluijm
Marianna Kruithof-de Julio

Manuscript Provisionally Accepted

Abstract

Prostate cancer (PCa) is the most prevalent cancer in men and metastatic spread to bone is detected in up to 80% of patients with advanced disease at autopsy. PCa can progress from treatable androgen-dependent stage to castration-resistant stage with distant metastases for which novel therapeutic targets and strategies are urgently needed. Here we identify the cell surface/secreted oncoprotein Cripto as a potential target for the diagnosis and treatment of metastatic PCa. We show that high expression levels of Cripto correlate with poor survival in stratified risk groups of PCa patients and demonstrate that Cripto and its signalling partner Grp78 are highly expressed in PCa metastases. We find that Cripto and Grp78 are expressed at substantially higher levels in the metastatic $ALDH^{high}$ subpopulation of PC-3M-Pro4luc2 PCa cells compared to non-metastatic $ALDH^{low}$. In order to mimic the bone metastatic niche *in vitro,* we cultured the highly osteotropic PC-3M-Pro4luc2 PCa cells with differentiated primary human osteoblasts. This strongly induces Cripto and Grp78 expression in the PCa cells and increases the size of the $ALDH^{high}$ subpopulation relative to the $ALDH^{low}$ in PC-3M-Pro4luc2. Additionally, Cripto or Grp78 knockdown decreases cell proliferation, migration, clonogenicity and the size of the metastasis-initiating $ALDH^{high}$ subpopulation. Significantly, we find that Cripto knockdown reduces the dissemination and invasion of PC-3M-Pro4luc2 cells in a zebrafish model and strongly inhibits bone metastasis in a preclinical mouse model. Taken together, our findings highlight a functional role for Cripto and Grp78 in PCa metastasis and suggest that targeting Cripto/Grp78 signaling may have significant therapeutic potential.

Introduction

Prostate cancer (PCa) is the second most common cancer in men worldwide (1). While current treatments of primary tumors are initially very effective, these beneficial responses are often followed by tumor recurrence and incurable bone metastasis. Therefore, identifying molecular mediators of PCa relapse and metastasis will aid in the development of therapies for this deadly phase of the disease.

Cripto (TDGF1, Cripto-1) is a small, GPI-anchored/secreted foetal-oncoprotein that plays important roles in regulating stem cell differentiation, embryogenesis, tissue growth and remodeling (2). Cripto promotes transformation, migration, invasion and angiogenesis and its misregulation can contribute to cancer development and progression in multiple malignancies, including breast cancer and PCa, which are both characterized by osteotropism in their metastatic stage (3,4). Cripto modulates crucial pathways that regulate bone metastasis such as the TGF-β pathway (5) and functions as an obligatory co-receptor for Nodal, a TGF- β superfamily member that promotes epithelial to mesenchymal transition (EMT) in PCa (5-7). Glucose-regulated protein 78 (Grp78) was identified as a Cripto binding protein and essential mediator of Cripto signaling (8-10). Grp78 is well established as a key survival factor in development and cancer (8,9) and, notably, up-regulation of Grp78 has been associated with the development of castration resistant PCa (CRPC) (11). While Cripto was reported to impact primary human prostate adenocarcinomas (6), its role in driving CRPC and PCa bone metastasis remains unknown.

Here, we investigated the roles of Cripto and Grp78 in aggressive, metastatic human PCa cells both *in vitro* and *in vivo* using an embryonic zebrafish model and a pre-clinical mouse model of experimentally induced PCa bone metastasis. We find that Cripto and Grp78 are upregulated in clinical samples of PCa metastases from human patients and in the highly metastatic $ALDH^{high}$ stem/progenitor-like subpopulation of a human castration resistant PCa cell line (12,13). We further demonstrate that knockdown of Cripto or Grp78 in these cells decreases the size of the stem/progenitor-like subpopulation and also inhibits their extravasation following inoculation into zebrafish and their metastatic potential in a preclinical mouse model of bone metastasis *in vivo*. Together, these findings provide new evidence that Cripto and Grp78 may drive metastatic PCa and highlight the therapeutic potential of targeting the cell surface Cripto/Grp78 complex for the treatment of this deadly disease.

Materials and Methods

PCa Cell lines and culture conditions

Human osteotropic PCa PC-3M-Pro4luc2 cells were maintained in DMEM with 10% FCII, 0.8 mg/ml Neomycin (Santa Cruz, USA) and 1% Penicillin-Streptomycin (Life Technologies, USA). C4-2B cells were maintained in T-medium DMEM (Sigma-Aldrich, The Netherlands) with 20% F-12K nutrient mixture Kaighn's modification (GibcoBRL, USA), 10% FCS, 0.125 mg/ml biotin, 1% Insulin-Transferrin-Selenium, 6.825 ng/ml T3, 12.5 mg/ml adenine and 1% Penicillin/Streptomycin. Primary human osteoblasts were differentiated at confluence: ascorbic acid (50 mg/ml, MERCK, USA) was added in DMEM with 10% FCS, 1% Penicillin-Streptomycin and 1% MEM Non-essential Amino Acids (Gibco-Thermo Scientific, USA). Upon detection of nodules (day 11), medium was supplemented with β-glycerolphosphate (5mM, Sigma, the Netherlands) and 100 nM dexamethasone. After 3 weeks, cells were washed with phosphate buffered saline (PBS) and fixed with 4% paraformaldehyde (PFA). Culture was analyzed for osteogenesis with Alizarin Red staining (ICN Biomedicals, USA) (14). Cells were maintained at 37°C, 5% CO_2

Suppressing Cripto and Grp78 expression with shRNAs

Short hairpin RNAi constructs for Cripto1 (TDGF1 clone# TRCN004889, TRCN004890 and TRCN004891) and HSPA5 (Grp78 clone# TRCN231123, TRCN218611) were obtained from Sigma's MISSION library (Core Facility at LUMC). 500 µL of shRNA-lentiviral vector and 8 µg Polybrene (Sigma, USA) were added to PC-3M-Pro4Luc2 and PC-3M-Pro4Luc2_dTomato cells and incubated for 2 hours. Scrambled shRNA (SHC002, non-targeted, NT or control) with lack of homology for any mammalian mRNA sequence was used as negative control. Cells were selected using puromycin (1µg/ml, Sigma, USA).

Flow Cytometry and aldehyde dehydrogenase assay

PC-3M-Pro4Luc2 were fluorescently labelled with PKH26 Red Fluorescent Cell Linker Kit according to protocol (Sigma-Aldrich, MO, USA). 900.000 cells were seeded in a 10 cm petri dish on a layer of confluent and differentiated human osteoblast. After 48 hours cells were washed with PBS, 1mM EDTA and harvested using trypsin. Fluorescently labelled PC-3M-Pro4Luc2 cells were separated from osteoblast with BD FACS ARIA (BD Biosciences, USA). Non-labelled PC-3M-Pro4Luc2 cells; labelled PC-3M-Pro4Luc2 tumor only and osteoblast only cells were included as controls. Aldehyde dehydrogenase (ALDH) activity was measured using ALDEFLUOR kit (StemCell

Technologies, Durham, USA) (12). Data were analyzed with FCS Express (De Novo software).

Western Blot

Cells were washed with PBS and proteins were extracted with RIPA buffer. Proteins were quantified using Pierce Protein Quantification Assay (ThermoFisher scientific, USA) and 10µg of samples separated by 10% SDS-PAGE and transferred to a blotting membrane using standard techniques. Signal was detected after incubation with 1:1,000 primary antibody (anti-Cripto, #PBL6900, (15)) and with 1:10,000 secondary horseradish peroxidase (HRP) antibody (Promega, USA).

Cripto overexpression

Cripto construct was generated as previously described (16). PC-3M-Pro4Luc2 cells were transfected with Lipofectamine2000 (Life Technologies, USA) and C4-2B cells with Fugene HD (Promega, USA) according to supplier's protocol. Five hours after transfection, the culture medium was replaced. Before collection, cells were washed with PBS and RNA extracted using Trizol (Invitrogen, USA).

RNA isolation and real-time qPCR

After viable cell sorting with ALDEFLUOR Assay Kit (Stem Cell Technologies, USA) (12), total RNA was isolated with Trizol Reagent (Invitrogen, USA) and cDNA synthesized by reverse transcription (Promega, USA) according to protocol. qRT-PCR was performed with BioRad CFX96 (Biorad, The Netherlands). Gene expression was normalized to GAPDH, HPRT and Actin. Primers are listed in Supplementary Table 1.

Proliferation assay

Cells were seeded at density of 1,500 cells/well and allowed to grow for 24, 48, and 72 hours. Proliferation was assessed with 3-(4,5 dimethylthiazol- 2- yl)- 5 -(3 -carboxymethoxyphenyl)- 2 -(4 -sulfophenyl)- 2 H-tetrazolium after 2 hours incubation at 37°C. (CellTiter96 Aqueous assay, Promega, USA). Data were normalized for number of cells.

Transwell migration assay

Migration assays were performed using 24-well transwells (8 mm, Corning Life Sciences, The Netherlands) (13). For the experiments with conditioned medium from osteoblast, this was diluted in the lower chamber 1:2 with medium (50% condition) or administered un-diluted (100% condition).

Colony formation assay

Clonogenic assay was performed in 6 well-plate. 100 cells were seeded in 2mL of medium supplemented with 10% FCII. After 2 weeks, plates were washed with PBS, cells fixed with 4% PFA and colonies stained with 0.1% crystal violet (Sigma-Aldrich, The Netherlands). Plates were imaged before processing the data (17).

Zebrafish maintenance, embryo preparation and tumor cell inoculation

Tg(fli1:GFP)i114 zebrafish line (18,19) was handled and maintained according to local animal welfare regulations to standard protocols (www.ZFIN.org). 2 days-post fertilization (dpf) dechorionized zebrafish embryos were anaesthetized and injected with PC-3M-Pro4Luc2 cells fluorescently labelled as we previously described (13,20). Data are representative of at least two independent and blind experiments with equal or more than 30 embryos per group. Experiments with survival rate of control group lower than 80% were discarded.

Mice

Male 4-5 week-old athymic nude mice (Balb/c *nu/nu* n=10 per group) were purchased from Charles River (L'Arbresle, France). Animals were housed in individual ventilated cages under sterile condition, and sterile food and water provided *ad libitum*. Animal experiment has been approved by the local committee for animal health ethics and research of Leiden University (DEC #14226) and carried out in accordance with the European Communities Council Directive 86/609/EEC.

Intracardiac PCa cell injection and whole body bioluminescent imaging (BLI)

A single cell suspension ($1x10^5$ PC-3M-Pro4Luc2 Cripto knock-down (KD) or non-targeted (NT) control cells per 100 µl PBS) was injected into the left ventricle of anesthetized 5-week old male nude mice (Balb/c nu/nu). Tumor growth and metastasis formation was monitored weekly by bioluminescent reporter imaging (BLI) using IVIS100 Imaging System (Caliper LifeSciences, USA) (12). Analyses of images was performed and quantified with Living Image 4.2 (Caliper Life Sciences, USA).

Immunofluorescence

Immunofluorescence staining was performed on 5-µm paraffin embedded sections. For antigen retrieval, sections were boiled in antigen unmasking solution (Vector Labs, UK) and incubated in 3% H_2O_2 for sequestering endogenous peroxidase (21). Sections were stained with Cripto antibody (#PBL6900, (15)). After blocking with 1% bovine serum albumin (BSA)-PBS-0.1% Tween-20, sections were incubated with primary antibody (1:1000) overnight at 4°C. Detection of Cripto was enhanced using tyramide amplification (Invitrogen/Molecular Probes, USA) and by incubation of slides with horseradish peroxidase (HRP-conjugated secondary antibody (Invitrogen/Molecular Probes, USA), diluted 1:100), followed by incubation with tyramide-488 for 10 minutes (21). Nuclei were visualized by TO-PRO3 (Invitrogen/Molecular Probes, 1:1000 diluted in PBS-0.1% Tween-20) or DAPI. Images were acquired with Leica SP8 confocal (Leica, Germany).

Immunohistochemistry

5 µm formalin fixed, paraffin embedded (FFPE) sections were dewaxed and rehydrated using xylene and ethanol, and endogenous peroxidase was blocked for 20 minutes in 0.3% H_2O_2 in PBS. Heat-induced antigen retrieval was done in TRIS-EDTA buffer (pH=9, 4397-9001, Klinipath, The Netherlands) with a pressure cooker (1.2 bar). Antibodies (anti-Cripto, #PBL6900, 1:1,000 (15); Anti-Cytokeratin 18 (CK18) diluted 1:1,000, Clone DC10, Dako, USA) were diluted 1:1,000 in PBS-BSA 0.1% and incubated overnight at 4°C. Envision (K500711, DAKO, USA) was used to visualize the antibody, followed by counterstaining with hematoxylin.

Human Material

Clinical prostate cancer bone metastasis (10 patients) were collected, stored and issued by the Erasmus MC Tissuebank under ISO 15189:2007 standard operating procedures. Use of these materials for research purposes is regulated according to the Human Tissue and Medical Research: Code of conduct for responsible use (2011). Confirmation that the Medical Research Involving Human Subjects Act (WMO) does not apply to the present study was obtained by the local ethics committee since the research was performed on “waste material” (3 patients) collected from Academisch Medisch Centrum, Amsterdam.

Statistical analysis

Statistical analysis was performed with GraphPad Prism 6.0 (GraphPad software) using t-test or ANOVA for comparison between more groups. Data is presented as mean ± SEM. P-values ≤ 0.05 were considered to be statistically significant (* $P < 0.05$, ** $P < 0.01$, *** $P < 0.001$).

Results

Cripto is highly expressed in metastasis from human PCa patients and correlates with poor survival

Cripto and its signaling partner Grp78 have each been shown to play important roles in primary tumor development and bone metastasis (22). We investigated the correlation of survival with Cripto expression in two independent sets of publically available PCa datasets (GSE21032 and GSE10645 (23,24)). In both datasets Cripto expression was associated with poor prognosis (**Fig. 1 A and B** top; Hazard Ratio (HR)=1.87 and p=0.001 for GSE10645 and HR=2.2 and p=0.06 for GSE21032). Additionally, in both datasets, the expression of Cripto in stratified risk groups was significantly higher in the high vs. low risk group (**Fig. 1 A and B** Bottom; p=1.13e-103 for GSE10645 and p=3.68e-23 for GSE21032). We further investigated the expression of Cripto and Grp78 in the Ramaswamy Multi-cancer dataset from Oncomine™ (Compendia Bioscience), which compares PCa metastasis to primary sites in 76 samples (25) and found that Cripto and Grp78 are significantly upregulated in metastasis compared to primary sites in human PCa (**Fig. 1C**, p=7.15e-4 for Cripto and p=0.03 for Grp78; 1=primary site; 2=metastatic site). Given its expression in metastasis and its correlation with survival, we subsequently investigated the expression of Cripto in PCa bone metastasis by immunostaining of paraffin embedded sections of bone metastasis freshly isolated from patients. We detected significant expression of Cripto and co-localization of Cripto with cytokeratin-18 in serial sections from each of the 13 specimens analyzed (**Fig. 1D**). Moreover, immunostaining with the same antibody revealed that Cripto is also prominently expressed in experimentally induced bone metastasis tissue resulting from intracardiac injection of human castration resistant PC-3M-Pro4Luc2 PCa cells in mice **(Suppl. Fig 1).** Taken together, these data demonstrate that Cripto is selectively expressed in aggressive and metastatic PCa and that its expression correlates with poor prognosis.

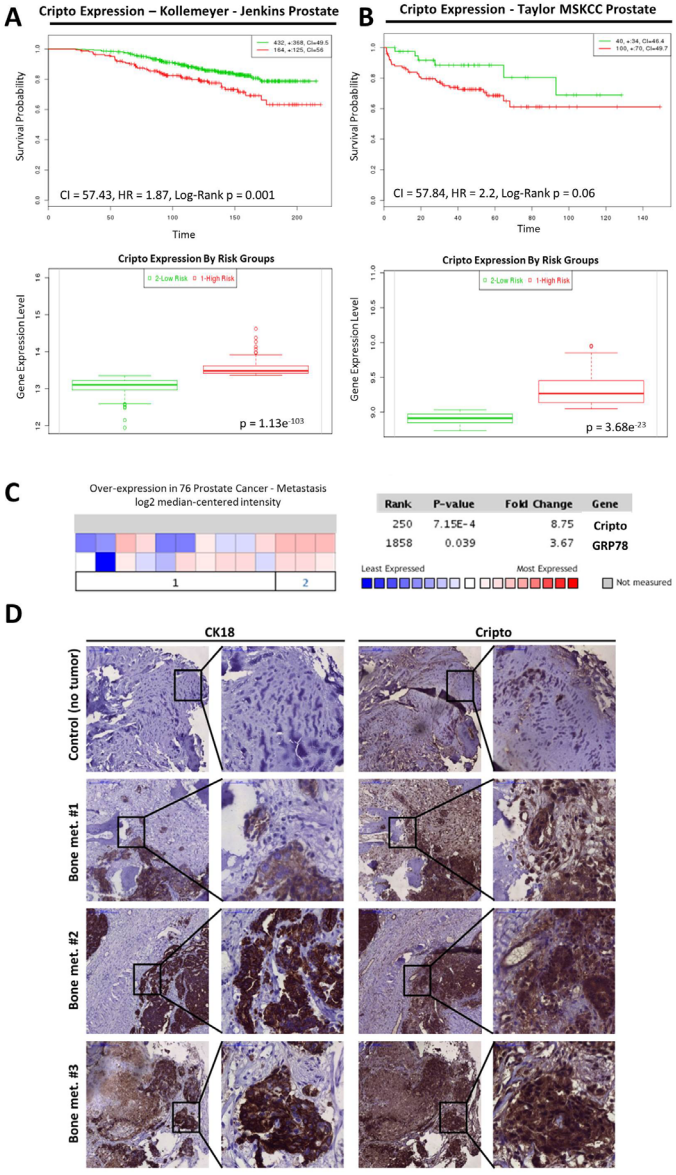

Figure 1. Cripto is expressed in PCa metastasis from human patients and correlates with poor patient prognosis. **A-B**) Top panels: Kaplan-Meier survival curves of censored Cox analysis in Kollemeyer-Jenkins prostate and Taylor-MSKCC prostate database stratified by maximized Cripto expression risk groups. Red = high expression; Green = low expression. Bottom panels: Cripto expression levels stratified by risk groups. Red = high Risk and high Cripto expression; Green = low risk and low Cripto expression **C**) Cripto and Grp78 are significantly up-regulated in PCa metastasis. The Ramaswamy Multi-cancer publicly available dataset (data accessed from www.oncomine.org) was used

for analysis. Colors are Z-score normalized and represent from lower (blue) to higher (red) expression. 1 = primary site; 2 = metastasis. **D**) Representative images of serial sections of PCa bone metastasis stained for CK18 and Cripto and counter stained with hematoxylin (N=13) at lower (10X) and higher (40X, see inserts) magnification.

Co-culture with primary human osteoblasts augments the size of the ALDH^{high} subpopulation, increases Cripto and Grp78 expression levels and promotes the metastatic phenotype of PCa cells

Human PCa cell lines (PC-3M-Pro4Luc2 and C4-2B cells) express detectable levels of Cripto and Grp78 mRNA (**Fig. 2A**). We previously reported that the ALDH^{high} subpopulation of PC-3M-Pro4Luc2 cells displays stem/progenitor-like properties and is highly metastatic relative to their ALDH^{low} counterpart (12). Cripto and Grp78 are expressed in human PCa cell lines (PC-3M-Pro4Luc2 and C4-2B cells) (**Fig. 2A**) and given their known roles in regulating stem cell function and tumor aggressiveness, we tested if Cripto and Grp78 are selectively expressed in the ALDH^{high} subpopulation. Indeed, qRT-PCR analysis on selected subpopulation of cells isolated after viable cell sorting, showed that both Cripto and Grp78 are highly expressed in ALDH^{high} vs. ALDH^{low} subpopulation ($p<0.01$ for Cripto) (**Fig. 2B**). This result is consistent with a role for Cripto and Grp78 in promoting PCa metastasis.

In PCa and other cancers, the osteoblastic microenvironment functions as premetastatic niche by attracting bone-metastasizing tumor cells (26-28). We developed a model of the bone metastatic niche in which primary human osteoblasts are co-cultured with PC-3M-Pro4Luc2 cells *in vitro*. Differentiation of the human osteoblasts was confirmed by Alizarin red staining (**Suppl. Fig 2A**). We find that in the presence of osteoblasts the size of PCa cell ALDH^{high} subpopulation was dramatically increased compared to the size of the ALDH^{high} subpopulation in PCa cells cultured alone (co-culture=60% vs. control=15%, $p<0.05$) **(Fig. 2C)**. Moreover, mRNA analysis after viable cell sorting of fluorescently labelled PC-3M-Pro4Luc2 cells (co-cultured cells compared to control), showed significant increase in Cripto ($p<0.05$) and Grp78 expression **(Fig. 2D)**. In addition, conditioned medium (CM) collected from osteoblasts positively influenced the migratory capability of PC-3M-Pro4Luc2 cells. The increase in migration was directly proportional to the concentration of the conditioned medium used in the experimental setting ($p<0.001$ for 50% CM + 50% not-CM vs. control; $p<0.001$ for 100% CM vs. control and $p<0.001$ for 100% CM vs. 50% CM) **(Fig 2E)**. In line with these observations, administration of osteoblast conditioned medium led to the acquisition of a motile, mesenchymal phenotype in PC-3M-Pro4Luc2 PCa cells as indicated by a decrease in the mRNA expression of the epithelial marker E-Cadherin ($p<0.05$), a

concomitant increase in the mesenchymal markers ZEB1 and ZEB2 ($p<0.05$ for both genes) **(Suppl. Fig. 2B)** and a significant reduction of the ratio E-Cadherin/Vimentin ($p<0.05$) and ratio E-Cadherin/N-Cadherin **(Fig. 2E)**. Together, these data indicate that co-culture with osteoblasts promotes the metastatic phenotype of PCa cells.

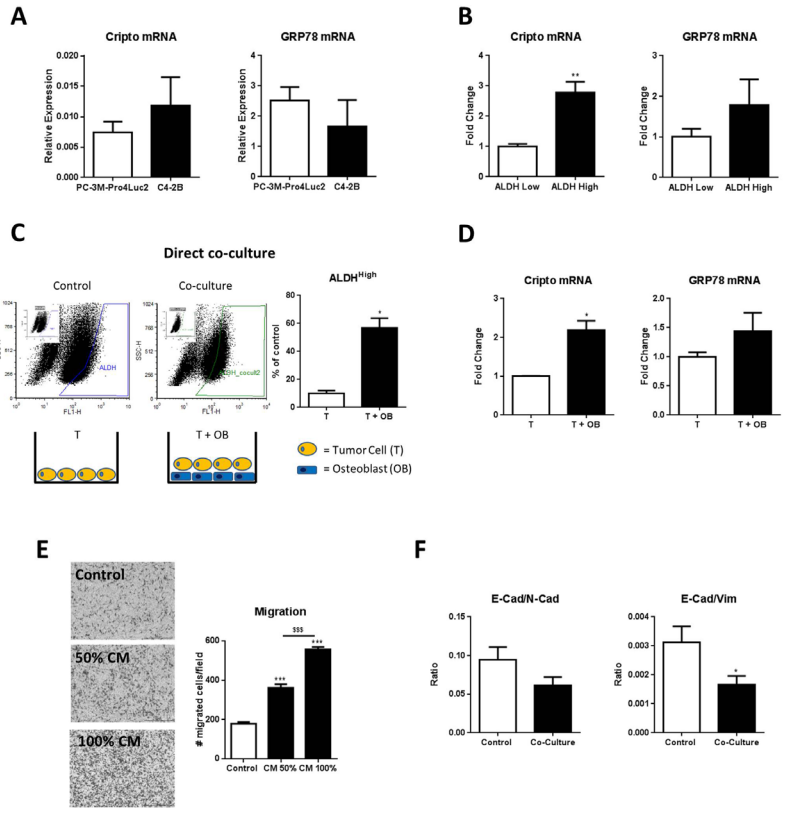

Figure 2. Co-culture with human osteoblasts increases expression of Cripto and Grp78 and cancer stem cell properties of human PCa cells. A) Cripto and Grp78 are expressed in PC-3M-Pro4Luc2 and C4-2B human PCa cell lines. Error bars ± SEM. **B**) Cripto and Grp78 are significantly up-regulated in highly metastatic subpopulation of ALDH^{high} PCa cells vs. low metastatic ALDH^{low} in PC-3M-Pro4Luc2 cells. Error Bars ± SEM **C**) Direct co-culture of fluorescently-labeled PC-3M-Pro4Luc2 human PCa cells (T) with differentiated human osteoblasts (OB) for 48h increases the size of the ALDH^{high} subpopulation in PCa cells. Error Bars ± SEM. **D**) mRNA analysis shows increased Cripto and Grp78 expression after co-culture. Error Bars ± SEM. **E**) Conditioned medium (CM) from human osteoblast enhances migration of PC-3M-Pro4Luc2 human PCa cells. Error Bars ± SEM. **F**) Co-culture of PC-3M-Pro4Luc2_dTomato PCa cells for 48h with human osteoblast induces a shift to mesenchymal phenotype as indicated by significant decrease in ratio E-Cad/Vim and E-Cad/N-Cad. Error Bars ± SEM. *, P<0,05; **, P<0,01; *** and $$$, P<0,001.

Cripto and Grp78 maintain stem cell-like properties of aggressive human PCa cells *in vitro*

In order to test the function of Cripto and Grp78 in human PCa cells, we generated stable knockdown lines in PC-3M-Pro4Luc2 and C4-2B cells and validated reduced expression of Cripto and Grp78 by Western Blot and qRT-PCR **(Fig. 3A, Suppl. Fig 3A and Suppl. Fig. 4A)**. As previously shown by others in PC3 cells and consistent with the extensive post-translational modification of Cripto, we detected two protein bands of approximately 17 and 25 kDa (5,29) **(Fig. 3A)**. Cripto knockdown lines (shRNA#2 and #3) both show decreased cell proliferation ($p<0.001$ at 24h for shRNA#2 and $p<0.001$ at 24, 45, 72h for shRNA#2 and shRNA#3) **(Fig. 3B).** No effect on cell proliferation was observed in the C4-2B Cripto knockdown cells **(Suppl. Fig. 3B).** The PC-3M-Pro4Luc2 Cripto knockdown cells also had a significantly reduced percentage of metastatic, stem cell-like $ALDH^{high}$ cells relative to non-targeted control cells ($p<0.05$ for shRNA#2 and p=ns for shRNA#3) **(Fig. 3C)**. Grp78 knockdown similarly displayed reduction of the size of $ALDH^{high}$ subpopulation of cells ($p<0.05$ for shRNA#1 and p=ns for shRNA#2) **(Suppl. Fig. 4B)**.

We previously reported that the $ALDH^{high}$ subpopulation of PC-3M-Pro4Luc2 is enriched for cells with increased clonogenicity and migratory properties relative to the $ALDH^{low}$ cell subpopulation (12). Here we show that PC-3M-Pro4Luc2 Cripto knockdown cells have significantly reduced clonogenicity relative to control cells as measured by the number and area of colonies produced ($p<0.05$) **(Fig. 3D)**. This effect appeared to be specific since transfection of a non-targetable Cripto expression construct resulted in significant rescue of the loss of clonogenicity caused by the Cripto shRNA ($p<0.001$ for colony number and $p<0.05$ for colony area) **(Fig. 3D).** Grp78 knockdown in PC-3M-Pro4Luc2 human PCa cells also resulted in a decrease in the number of colonies ($p<0.05$) and a similar trend was shown for colony area **(Suppl. Fig 4C)**. Finally, Cripto knockdown significantly reduced the migratory capability of both cell lines ($p<0.05$ and $p<0.01$ respectively, **Fig. 4A and B**). Complete (PC-3M-Pro4Luc2) or partial (C4-2B) rescue of the effects of shRNA knockdown could be again achieved by the non-targetable Cripto expression construct **(Fig. 4C and D)**. Grp78 knockdown in PC-3M-Pro4Luc2 cells also resulted in a significant reduction of migratory potential ($p<0.001$ for both shRNAs) (Suppl. Fig. 4D). Together, these data suggest that Cripto and Grp78 are required to maintain the stem cell-like phenotype of PC-3M-Pro4Luc2 cells.

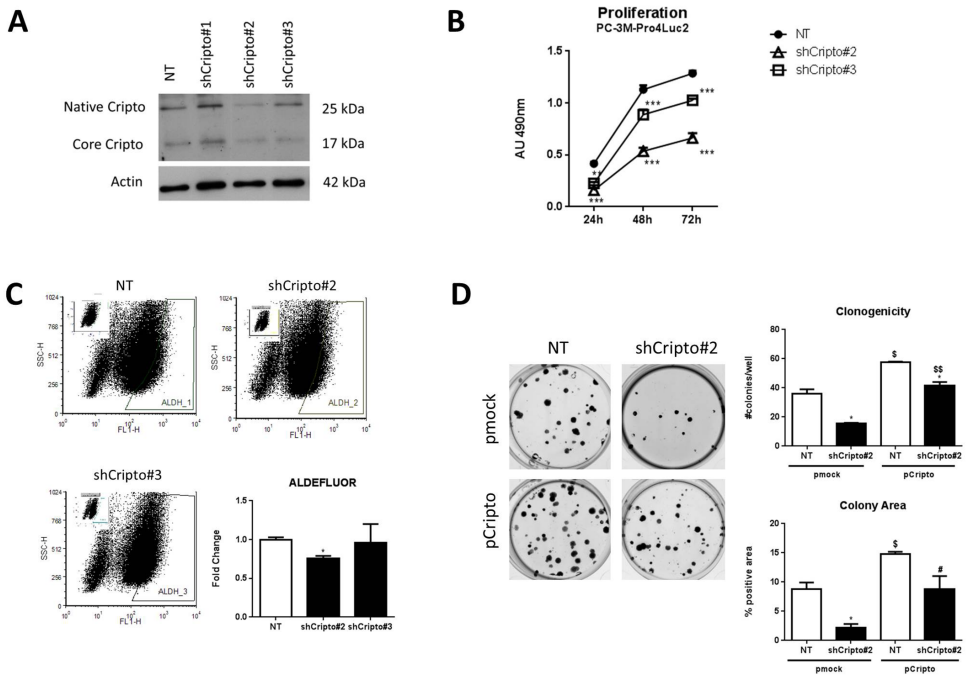

Figure 3. Cripto knock-down causes loss of the stem cell-like phenotype in PCa cells. **A**) Western Blot analysis of Cripto expression in control (scrambled shRNA, NT) PC-3M-Pro4Luc2 (first lane) and Cripto knock-down PC-3M-Pro4Luc2 cells with shCripto#1, #2, #3, derived from different shRNA constructs. Two bands of respectively 25 KDa (Native) and 17 KDa (Core) for Cripto are detected as previously shown (see Results). **B**) Knockdown of Cripto affects the proliferation in PC-3M-Pro4Luc2 . Error Bars ± SEM. **C**) Cripto knock-down leads to a decrease in the size of $ALDH^{high}$ subpopulation in PC-3M-Pro4Luc2 cells. Error Bars ± SEM. **D**) Cripto knockdown affects clonogenic ability and Cripto overexpression is capable of reversing this phenotype in PC-3M-Pro4Luc2. Error Bars ± SEM. * and $ and #, P<0,05; ** and $$, P<0,01; ***, P<0,001.

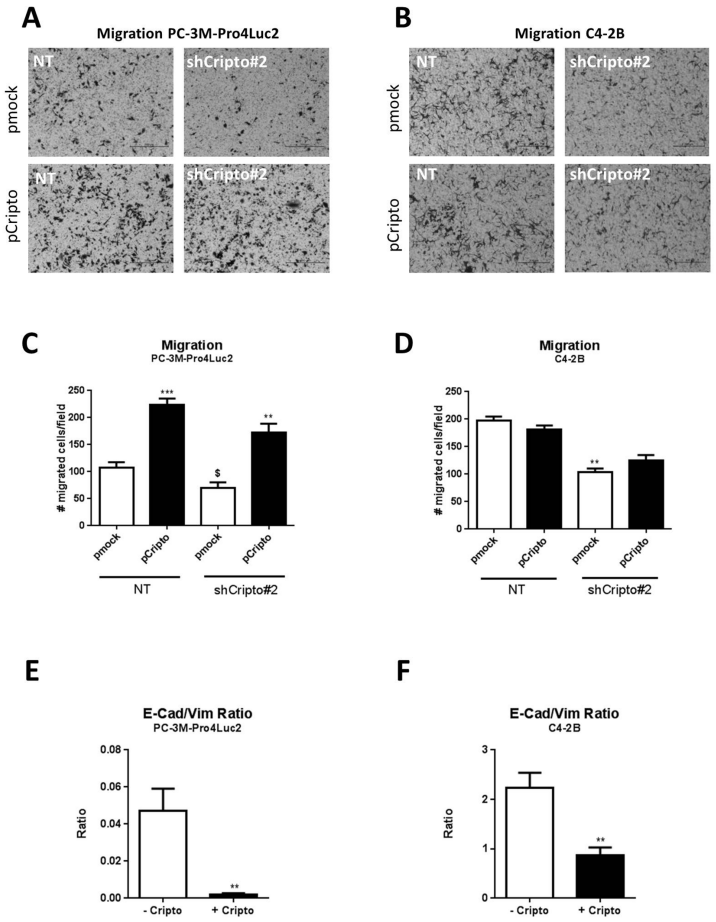

Figure 4. Cripto overexpression promotes PCa cell migration and rescues the Cripto knock-down phenotype. A-B) Cripto Knock-down significantly reduces cell migration in PC-3M-Pro4Luc2 and C4-2B cells and Cripto overexpression (**C-D**) is capable of rescuing completely (PC-3M-Pro4Luc2) or partially (C4-2B) the phenotype. Error Bars ± SEM. **E**) mRNA analysis in PC-3M-Pro4Luc2 cells and C4-2B (**F**) after 48h of Cripto overexpression shows decrease in E-Cad/Vim ratio supporting the switch towards a more mesenchymal phenotype. Error Bars ± SEM. $, P<0,05; **, P<0,01; ***, P<0,001.

Cripto promotes EMT and invasiveness of human PCa cells

EMT is strongly associated with tumor cell invasion and Cripto was recently reported to promote EMT in human PCa (6). Consistent with this study, we found that Cripto overexpression in PC-3M-Pro4Luc2 and C4-2B cells **(Suppl. 5A and B)** causes a strong and significant down-regulation of the epithelial marker E-Cadherin ($p<0.05$) at the mRNA level in both cell lines and an increase in the mesenchymal markers Vimentin, SNAIL2 and TWIST in PC-3M-Pro4Luc2 cells ($p<0.05$, $p<0.05$ and $p<0.01$ respectively) and ZEB1 in C4-2B cells **(Suppl. Fig 5C and D).** Cripto overexpression caused a strong and significant decrease in the ratio of E-Cadherin/Vimentin ($p<0.01$) in both PCa cell lines **(Fig. 4E and F)**. Together, these data support a role for Cripto in promoting EMT and the invasive phenotype in PC-3M-Pro4Luc2 and C4-2B cells.

We have previously shown that zebrafish can be used to effectively evaluate migration and invasion of human PCa cells and the interaction between PCa cells and the vasculature at the single cell level *in vivo* (13,30). Clear detection of extravasating tumor cells in this system is facilitated by the fact that the vascular system of zebrafish embryos is completely functional and the embryos are transparent (31). We tested the role of Cripto and Grp78 in PCa cell extravasation and metastasis by injecting fluorescently-labeled PC-3M-Pro4Luc2 cells with Cripto or Grp78 knocked down into the circulatory system of zebrafish embryos (13). In the first hours disseminated cells arrested in the host vasculature and then we observed extravasation from 12 hpi (hours post implantation) and perivascular tumor cells in multiple foci including the intersegmental vessels, the optic veins, the dorsal aorta and the caudal vein. The perivascular tumor cells invaded the neighboring tail fin exclusively at the posterior ventral end of the caudal hematopoietic tissue (CHT). At day 4 post-implantation (4 dpi), Cripto knockdown caused a significant reduction in extravasation and metastatic tumor growth compared to control cells with scrambled shRNA **(Fig. 5A, B and C)**. Similarly, Grp78 knockdown cells displayed a significant reduction in the tumor growth into the tail fin after invasion from CHT compared to control cells (**Suppl. Fig. 6A and B**). However, invasion was not significantly different in Grp78 knockdown cells compared to control **(Suppl. Fig. 6C)**. Taken together, these data support our *in vitro* findings and reinforce the hypothesis that Cripto/Grp78 signaling plays an important role in the maintenance of an invasive and aggressive phenotype in human PCa.

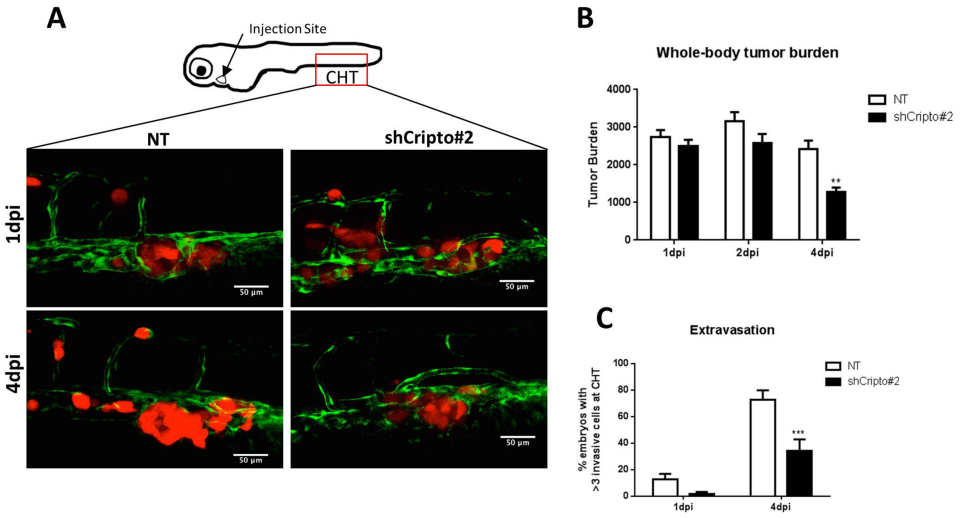

Figure 5. Cripto knockdown reduces invasion and tumor growth of human PCa cells *in vivo*. A) PC-3M-Pro4Luc2_dTomato human PCa cells with scrambled shRNA control (NT) and ShCripto#2 shRNAs have been injected in the duct of Cuvier to monitor extravasation and formation of distant metastasis in vivo. 30 embryos injected/group. **B**) Cripto knock-down reduces whole-body tumor burden at 4dpi (days post injection). Error Bars ± SEM. **C**) Cripto knock-down reduces number of extravasated cells at 1 and 4dpi at the caudal hematopoietic tissue (CHT). Error Bars ± SEM. **, P<0,01; *** P<0,001.

Cripto knockdown decreases metastasis formation *in vivo*

We previously demonstrated that intracardiac injection of luciferase-expressing PC-3M-Pro4Luc2 cells in mice results in bone metastasis (12). Here we used this preclinical mouse model to test the role of Cripto in mediating the metastatic activity of these PCa cells. Cripto knockdown cells or control cells with a scrambled shRNA were injected into the left cardiac ventricle of nude mice (Balb/c nu/nu) and bioluminescence, which reflects tumor size, was measured weekly for the course of the experiment. Quantification of bioluminescent images showed significant reduction in metastasis formation and the number of metastasis in mice inoculated with Cripto knockdown cells compared to mice injected with control cells (week 5, $p<0.05$) **(Fig. 6 A, B, C)**. This result is consistent with the other findings outlined above and suggests that Cripto is required for bone metastasis in a mouse model of human PCa.

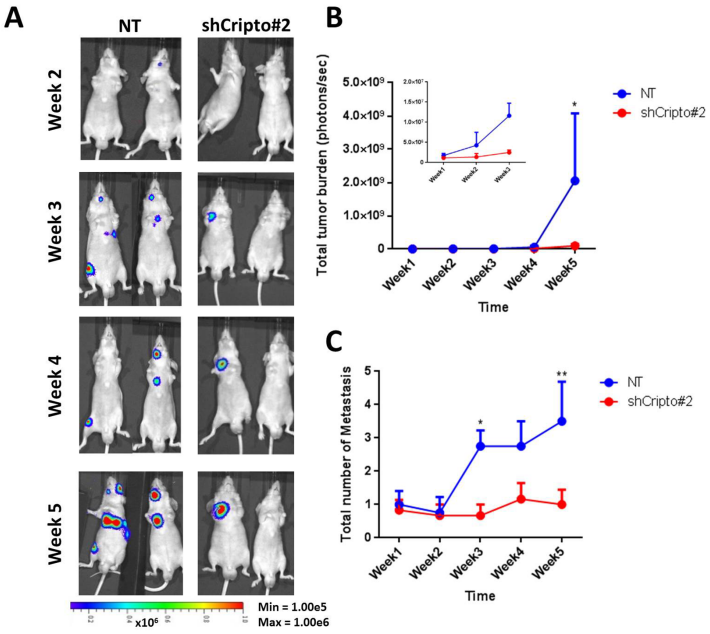

Figure 6. Cripto knockdown inhibits bone metastasis of human PCa cells *in vivo*. **A**) PC-3M-Pro4Luc2 human PCa cells with Cripto knock-down (ShCripto#2) and shRNA scrambled control (NT) have been injected in the left ventricle of nude mice. Formation of distant metastasis was monitored weekly with BLI measurements. Images are representative of 6 animals for Cripto Knock-down and 4 animals for non-targeted control. **B**) Quantification of BLI measurements. Difference is significant at week 5 ($p<0.05$ with two way ANOVA). Cripto knockdown is represented in red, non-targeted control is represented in blue. Error Bars ± SEM. **C**) Total number of metastasis per mouse in mice injected with either Cripto knock-down (ShCripto#2, red) or control (NT, blue) PC-3M-Pro4Luc2 cells, (*, $p<0.05$; **$p<0,01$; with two way ANOVA). Error Bars ± SEM.

Discussion

This study presents evidence supporting a role for Cripto and Grp78 in the regulation of the invasive program of PCa cells that maintains stem cell-like and aggressive phenotypes in human PCa. Cripto/Grp78 signaling is known to regulate stem cells and tumor cells (32) and our results suggest that this signaling may promote the acquisition of a metastatic phenotype in PCa. This phenotype includes the ability of PCa cells to invade the supportive stroma and neighboring tissues to allow subsequent formation of bone metastasis at distant sites (33). Cripto/Grp78 signaling may also play a specific role in metastasis by facilitating initial colonization of the bone by PCa cells.

Our demonstration that Cripto is strongly upregulated in high-risk patient groups compared to low risk groups and that it correlates with poor survival highlight the significance of these proteins in metastatic PCa. Importantly, the selective expression of Cripto and Grp78 in PCa metastasis was substantiated by analysis of publicly available datasets (25) and reinforced by our analysis on 13 samples of PCa bone metastasis derived from CRPC patients.

The $ALDH^{high}$ subpopulation of PC-3M-Pro4Luc2 cells is enriched for tumor initiating cells with metastatic potential and generally accounts for a small percentage of all tumor cells (12,13). Here we show that these highly metastatic $ALDH^{high}$ cells have higher levels of Cripto and Grp78 expression compared to non-stem cell-like, non-metastatic $ALDH^{low}$ cells. This finding supports our hypothesis that Cripto and its cell surface signaling partner Grp78 are restricted to a small subpopulation of cells characterized by high metastatic ability, similar to what was recently shown in breast cancer (15). Our results also support the notion that Cripto signaling promotes EMT (6,7) and the migratory and invasive phenotype in PCa cells associated with a switch from a sessile, epithelial state to a motile, mesenchymal phenotype. Indeed, transcriptional analysis following Cripto overexpression reveals the emergence of an “EMT signature” characterized by a marked reduction in the expression of the epithelial marker E-Cadherin paralleled by a significant increase in the expression of the mesenchymal markers Vimentin, Snail2 and Twist, again indicating the acquisition of the mesenchymal phenotype.

The activation of the bone stroma by metastatic cells alters the physiological balance between osteoblast-mediated bone formation and osteoclast-mediated bone resorption during bone metastatic colonization (34). Strikingly, we found that co-culture of PCa cells with human osteoblasts, important cellular constituents of the bone metastatic niche (34), induced a significant increase in Cripto and Grp78 mRNA

expression in the tumor cells. Osteoblasts have previously been reported to promote the aggressiveness of osteolytic human PCa cells *in vitro* (26). These findings, are in line with our data showing that osteoblasts promote the metastatic phenotype of PCa cells by causing expansion of the ALDH^{high} subpopulation, increasing tumor cell migration and inducing expression of Cripto and Grp78. In light of previous studies demonstrating that Cripto binds cell surface Grp78 and that this interaction is required for Cripto signaling, our results suggest that Cripto and Grp78 function cooperatively to regulate the interaction between tumor cells and osteoblasts within the bone microenvironment. However, given the complexity of the bone metastatic niche, we focused primarily on the role of Cripto and Grp78 in the maintenance of an aggressive and metastatic phenotype in PCa cells. Additional experiments are required to elucidate the interactions between PCa cells and the different components of the bone microenvironment in mechanistic detail.

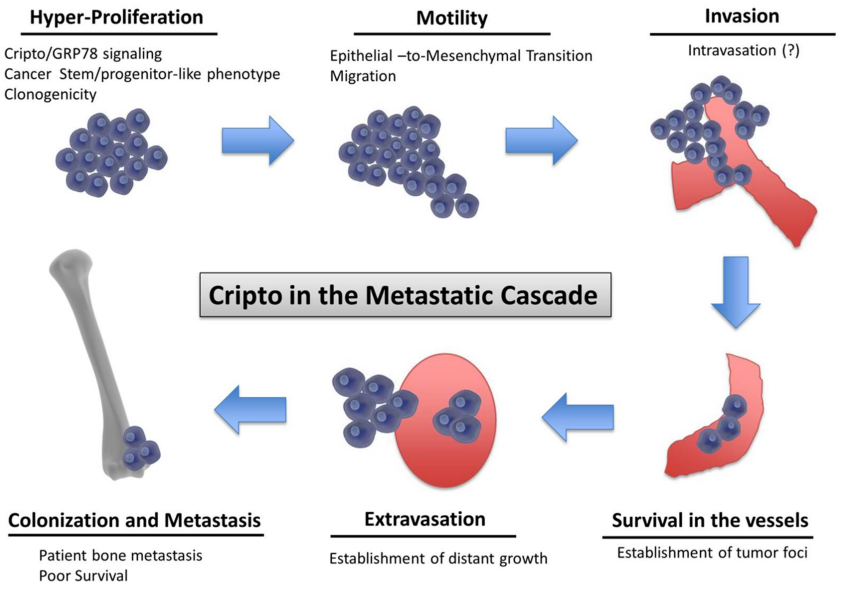

Figure 7. Schematic representation of the proposed role of Cripto in the metastatic cascade in human prostate cancer. Cripto and Grp78 influence cell proliferation and are highly expressed in a subpopulation of highly metastatic stem/progenitor-like cells (ALDH^{high}). Cripto and Grp78 knock-down impairs cell migration, suggesting a role of these genes in the acquisition of an invasive phenotype. Cripto- and Grp78-expressing cells are better adapted to surviving in the circulation and of forming distant metastases in zebrafish and mouse xenograft models.

In conclusion, we demonstrate that Cripto and it signalling mediator Grp78 may play pivotal, functional roles in the acquisition and maintenance of an invasive, metastatic phenotype in human prostate cancer (see schematic representation in **Fig. 7**). Therefore, from a therapeutic and diagnostic point of view, Cripto and Grp78 represent compelling molecules for targeting and monitoring of highly aggressive stem/progenitor-like prostate cancer cells in advanced human prostate cancer.

Acknowledgements

We would like to thank Sofia Karkampouna, Federico La Manna, Janine Melsen and Tim Rodenburg (Dept. of Urology, LUMC, The Netherlands) for discussion about this work and help. We thank Boudewijn Kruithof (Dept. of Molecular Cell Biology, LUMC, the Netherlands) for help and support during the acquisition of high-resolution images. We thank Guido de Roo from the Flow cytometry facility (Dept. of Hematology, LUMC, The Netherlands) for technical support and Jan Kroon (Dept. of Urology, LUMC, The Netherlands) for providing samples of experimental metastasis. We also would like to thank Chris van der Bent and Hetty Sips (Dept. of Endocrinology, LUMC, The Netherlands) for help and technical support.

Grant Support

The research leading to these results has received funding from the FP7 Marie Curie ITN under grant agreement n°264817 - BONE-NET (GP, EZ, ZG). This project receives also additional support from the Dutch Cancer Society under grant agreement UL2015-7599 KWF (MK, GP, PK) and UL2014-7058 - PROPER (GP, LC, ESJ), from Leiden University Fond (MK) and Clayton Foundation (PG). The authors disclose no potential conflicts of interest.

REFERENCES

1. Jemal A, Center MM, DeSantis C, Ward EM. Global patterns of cancer incidence and mortality rates and trends. Cancer Epidemiol Biomarkers Prev 2010;19(8):1893-907.
2. Klauzinska M, Castro NP, Rangel MC, Spike BT, Gray PC, Bertolette D, et al. The multifaceted role of the embryonic gene Cripto-1 in cancer, stem cells and epithelial-mesenchymal transition. Semin Cancer Biol 2014;29:51-8.
3. de Castro NP, Rangel MC, Nagaoka T, Salomon DS, Bianco C. Cripto-1: an embryonic gene that promotes tumorigenesis. Future Oncol 2010;6(7):1127-42.
4. Castro NP, Fedorova-Abrams ND, Merchant AS, Rangel MC, Nagaoka T, Karasawa H, et al. Cripto-1 as a novel therapeutic target for triple negative breast cancer. Oncotarget 2015;6(14):11910-29.
5. Lawrence MG, Margaryan NV, Loessner D, Collins A, Kerr KM, Turner M, et al. Reactivation of embryonic nodal signaling is associated with tumor progression and promotes the growth of prostate cancer cells. Prostate 2011;71(11):1198-209.
6. Terry S, El-Sayed IY, Destouches D, Maille P, Nicolaiew N, Ploussard G, et al. Cripto overexpression promotes mesenchymal differentiation in prostate carcinoma cells through parallel regulation of AKT and FGFR activities. Oncotarget 2014.
7. Pilli VS, Gupta K, Kotha BP, Aradhyam GK. Snail-mediated Cripto-1 repression regulates the cell cycle and epithelial-mesenchymal transition-related gene expression. FEBS Lett 2015;589(11):1249-56.
8. Shani G, Fischer WH, Justice NJ, Kelber JA, Vale W, Gray PC. Grp78 and Cripto form a complex at the cell surface and collaborate to inhibit transforming growth factor beta signaling and enhance cell growth. Mol Cell Biol 2008;28(2):666-77.
9. Lee AS. Grp78 induction in cancer: therapeutic and prognostic implications. Cancer Res 2007;67(8):3496-9.
10. Kelber JA, Panopoulos AD, Shani G, Booker EC, Belmonte JC, Vale WW, et al. Blockade of Cripto binding to cell surface Grp78 inhibits oncogenic Cripto signaling via MAPK/PI3K and Smad2/3 pathways. Oncogene 2009;28(24):2324-36.
11. Pootrakul L, Datar RH, Shi SR, Cai J, Hawes D, Groshen SG, et al. Expression of stress response protein Grp78 is associated with the development of castration-resistant prostate cancer. Clin Cancer Res 2006;12(20 Pt 1):5987-93.
12. van den Hoogen C, van der Horst G, Cheung H, Buijs JT, Lippitt JM, Guzman-Ramirez N, et al. High aldehyde dehydrogenase activity identifies tumor-initiating and metastasis-initiating cells in human prostate cancer. Cancer Res 2010;70(12):5163-73.
13. Zoni E, van der Horst G, van de Merbel AF, Chen L, Rane JK, Pelger RC, et al. miR-25 Modulates Invasiveness and Dissemination of Human Prostate Cancer Cells via Regulation of alphav- and alpha6-Integrin Expression. Cancer Res 2015;75(11):2326-36.
14. van der Horst G, Farih-Sips H, Lowik CW, Karperien M. Hedgehog stimulates only osteoblastic differentiation of undifferentiated KS483 cells. Bone 2003;33(6):899-910.
15. Spike BT, Kelber JA, Booker E, Kalathur M, Rodewald R, Lipianskaya J, et al. Cripto/Grp78 signaling maintains fetal and adult mammary stem cells ex vivo. Stem Cell Reports 2014;2(4):427-39.
16. Gray PC, Shani G, Aung K, Kelber J, Vale W. Cripto binds transforming growth factor beta (TGF-beta) and inhibits TGF-beta signaling. Mol Cell Biol 2006;26(24):9268-78.
17. Guzman C, Bagga M, Kaur A, Westermarck J, Abankwa D. ColonyArea: an ImageJ plugin to automatically quantify colony formation in clonogenic assays. PLoS One 2014;9(3):e92444.
18. Stoletov K, Montel V, Lester RD, Gonias SL, Klemke R. High-resolution imaging of the dynamic tumor cell vascular interface in transparent zebrafish. Proc Natl Acad Sci U S A 2007;104(44):17406-11.

19. Lawson ND, Weinstein BM. In vivo imaging of embryonic vascular development using transgenic zebrafish. Dev Biol 2002;248(2):307-18.
20. He S, Lamers GE, Beenakker JW, Cui C, Ghotra VP, Danen EH, et al. Neutrophil-mediated experimental metastasis is enhanced by VEGFR inhibition in a zebrafish xenograft model. J Pathol 2012;227(4):431-45.
21. Karkampouna S, Kruithof BP, Kloen P, Obdeijn MC, van der Laan AM, Tanke HJ, et al. Novel Ex Vivo Culture Method for the Study of Dupuytren's Disease: Effects of TGFbeta Type 1 Receptor Modulation by Antisense Oligonucleotides. Mol Ther Nucleic Acids 2014;3:e142.
22. Bianco C, Strizzi L, Normanno N, Khan N, Salomon DS. Cripto-1: an oncofetal gene with many faces. Curr Top Dev Biol 2005;67:85-133.
23. Taylor BS, Schultz N, Hieronymus H, Gopalan A, Xiao Y, Carver BS, et al. Integrative genomic profiling of human prostate cancer. Cancer Cell 2010;18(1):11-22.
24. Nakagawa T, Kollmeyer TM, Morlan BW, Anderson SK, Bergstralh EJ, Davis BJ, et al. A tissue biomarker panel predicting systemic progression after PSA recurrence post-definitive prostate cancer therapy. PLoS One 2008;3(5):e2318.
25. Ramaswamy S, Ross KN, Lander ES, Golub TR. A molecular signature of metastasis in primary solid tumors. Nat Genet 2003;33(1):49-54.
26. Morhayim J, van de Peppel J, Demmers JA, Kocer G, Nigg AL, van Driel M, et al. Proteomic signatures of extracellular vesicles secreted by nonmineralizing and mineralizing human osteoblasts and stimulation of tumor cell growth. FASEB J 2015;29(1):274-85.
27. Coleman RE. Clinical features of metastatic bone disease and risk of skeletal morbidity. Clin Cancer Res 2006;12(20 Pt 2):6243s-49s.
28. Shiozawa Y, Pedersen EA, Havens AM, Jung Y, Mishra A, Joseph J, et al. Human prostate cancer metastases target the hematopoietic stem cell niche to establish footholds in mouse bone marrow. J Clin Invest 2011;121(4):1298-312.
29. Saloman DS, Bianco C, Ebert AD, Khan NI, De Santis M, Normanno N, et al. The EGF-CFC family: novel epidermal growth factor-related proteins in development and cancer. Endocr Relat Cancer 2000;7(4):199-226.
30. Ghotra VP, He S, van der Horst G, Nijhoff S, de Bont H, Lekkerkerker A, et al. SYK is a candidate kinase target for the treatment of advanced prostate cancer. Cancer Res 2015;75(1):230-40.
31. Isogai S, Lawson ND, Torrealday S, Horiguchi M, Weinstein BM. Angiogenic network formation in the developing vertebrate trunk. Development 2003;130(21):5281-90.
32. Gray PC, Vale W. Cripto/Grp78 modulation of the TGF-beta pathway in development and oncogenesis. FEBS Lett 2012;586(14):1836-45.
33. van der Pluijm G. Epithelial plasticity, cancer stem cells and bone metastasis formation. Bone 2011;48(1):37-43.
34. Ozdemir BC, Hensel J, Secondini C, Wetterwald A, Schwaninger R, Fleischmann A, et al. The molecular signature of the stroma response in prostate cancer-induced osteoblastic bone metastasis highlights expansion of hematopoietic and prostate epithelial stem cell niches. PLoS One 2014;9(12):e114530.

SUPPLEMENTARY DATA

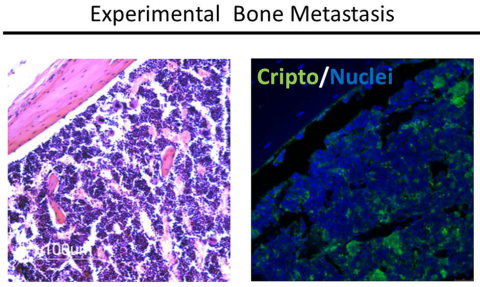

Suppl. Fig 1. Cripto expression in experimental bone metastasis. Cripto expression in experimental bone metastasis derived from intra cardiac inoculation of PC-3M-Pro4Luc2 human PCa cells in a preclinical mouse model of PCa bone metastasis.

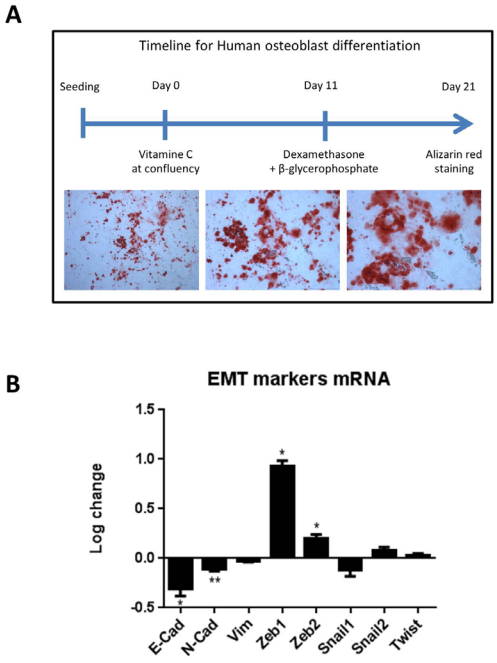

Suppl. Fig 2. Osteoblast differentiation and influence of direct co-culture of tumor cells with human osteoblast on EMT markers. A) Alizarin Red staining of differentiated osteoblast shows efficacy of the differentiation process (see materials and methods). **B**) Co-culture of PC-3M-Pro4Luc2 tumor cells with differentiated primary human osteoblast induces downregulation of E-Cad and strong upregulation of Zeb1 in PC-3M-Pro4Luc2 cells. Error Bars ± SEM. *, P<0,05; **, P<0,01.

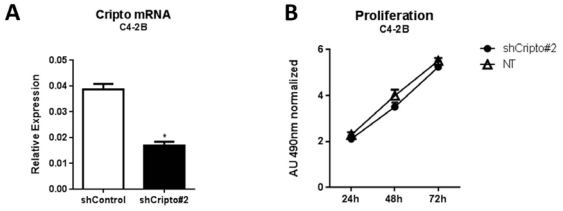

Suppl. Fig. 3. Cripto knock-down in C4-2B cells. A) C4-2B with Cripto knock-down show significanly lower Cripto expression compared to control cells. **B**) Cripto Knock-down does not affect C4-2B proliferation. Error Bars ± SEM. *, P<0,05.

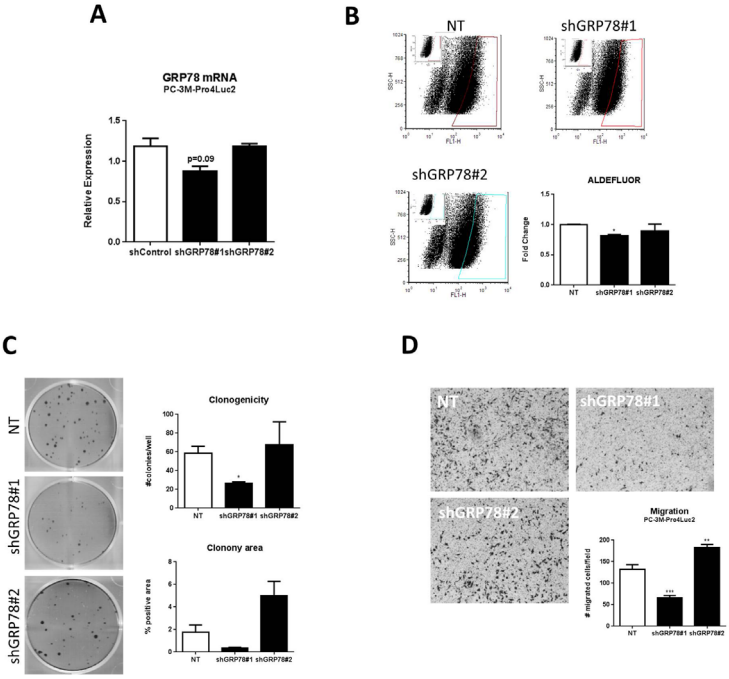

Suppl. Fig. 4. Grp78 Knock-down, functional study. **A**) PC-3M-Pro4Luc2 cells with Grp78 knock-down by two different shRNAs. Error Bars ± SEM. **B**) Grp78 KD reduces the size of ALDHhigh subpopulation of cells in PC-3M-Pro4Luc2 human prostate cancer cells. Error Bars ± SEM. **C-D**) Grp78 KD significanlty reduces clonogenicity and migration of PC-3M-Pro4Luc2 human prostate cancer cells. Error Bars ± SEM. *, P<0,05; **, P<0,01; ***, P<0,001.

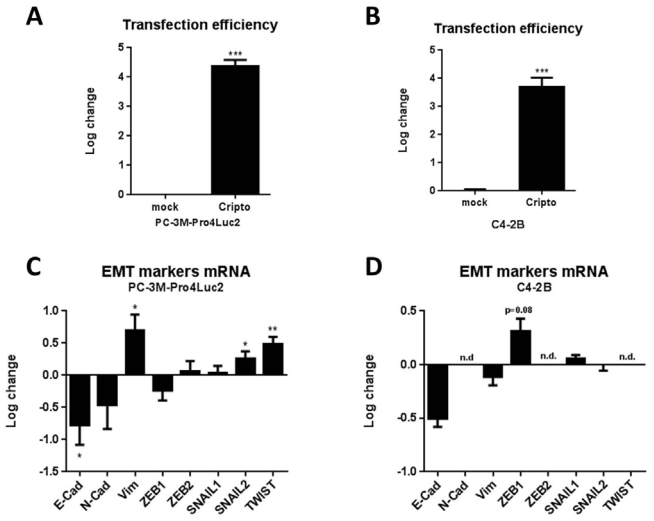

Suppl. Fig. 5. Cripto overexpression in two human prostate cancer cell lines. **A-B**) Tumor cells overexpressing Cripto show significanlty higher Cripto expression compared to mock transfected cells (control). Error Bars ± SEM. **C-D**) Cripto overexpresssion in PC-3M-Pro4Luc2 and C4-B cells induces significant decrease of E-Cad and upregulation of Vim in PC-3M-Pro4Luc2 cells. Error Bars ± SEM. *, P<0,05; **, P<0,01; ***, P<0,001.

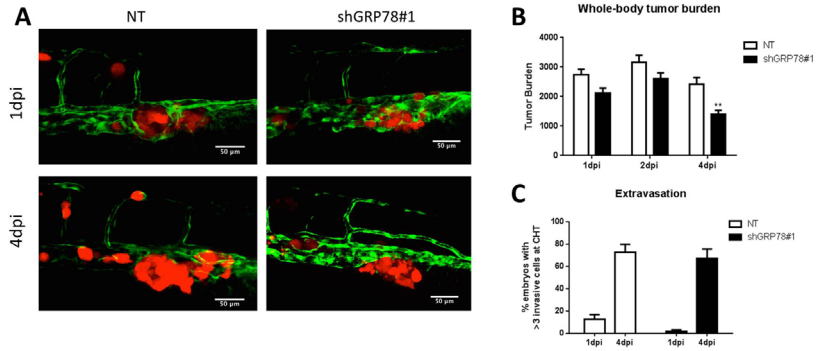

Suppl. Fig. 6. Grp78 KD reduces invasion and tumor growth *in vivo*. A) PC-3M-Pro4Luc2_dTomato human prostate cancer cells with Grp78 knock-down have been injected in the duct of Cuvier to monitor extravasation and formation of distant metastasis in vivo. 30 embryos injected per group. **B-C**) Grp78KD reduces extravasation and tumor growth significantly at 4dpi (days post injection) at the caudal hematopoietic tissue (CHT). No effect on tumor burden is observed. Error Bars ± SEM. (Blind observations). **, P<0,01.

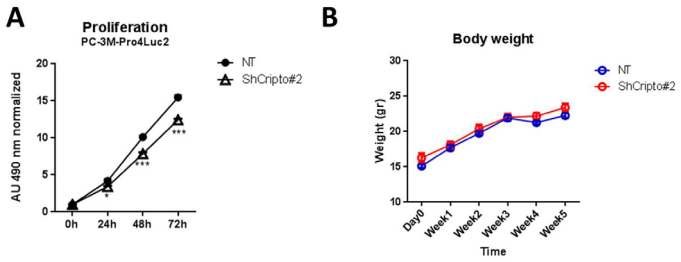

Suppl. Fig. 7. Cripto Knock-down effect on proliferation and measurment of weight of animal injected with matching cells *in vivo*. A) MTS performed on PC-3M-Pro4Luc2 cells with Cripto KD and NT control to confirm KD effect on proliferation prior to inoculation in animals. Experiment performed on same cells injected in vivo. Error Bars ± SEM. **B**) Body weight of animals (shCripto = 6 animals, NT = 4 animals). Error Bars ± SEM. *, P<0,05; ***, P<0,001.

7

General discussion and future perspectives

Adapted from:Oncoscience. 2015 Aug 24;2(8):663-4. eCollection 2015

Prostate cancer consist of heterogeneous epithelial cell subpopulations of which prostate cancer cells with stem/progenitor-like characteristics (CSCs) have been increasingly recognized as the “driver” cancer cell subpopulation in tumor initiation, local and distant relapse, hormone refractory disease, castration, metastasis and chemotherapy resistance (1-4). Therefore, unraveling the molecular properties of malignant subpopulation of CSCs may represent a promising strategy to identify new attractive targets for therapeutic intervention.

The work presented in this thesis covers two aspects of the molecular characteristics of CSCs: in the first part the identification of miRs as novel regulators of gene expression in CSCs are described; in the second part two studies are presented that focus on the identification of new potential markers and functional factors that are involved in prostate cancer pathogenesis, progression and bone metastasis. A schematic representation and graphic summary of our observations is depicted in **Fig. 1**.

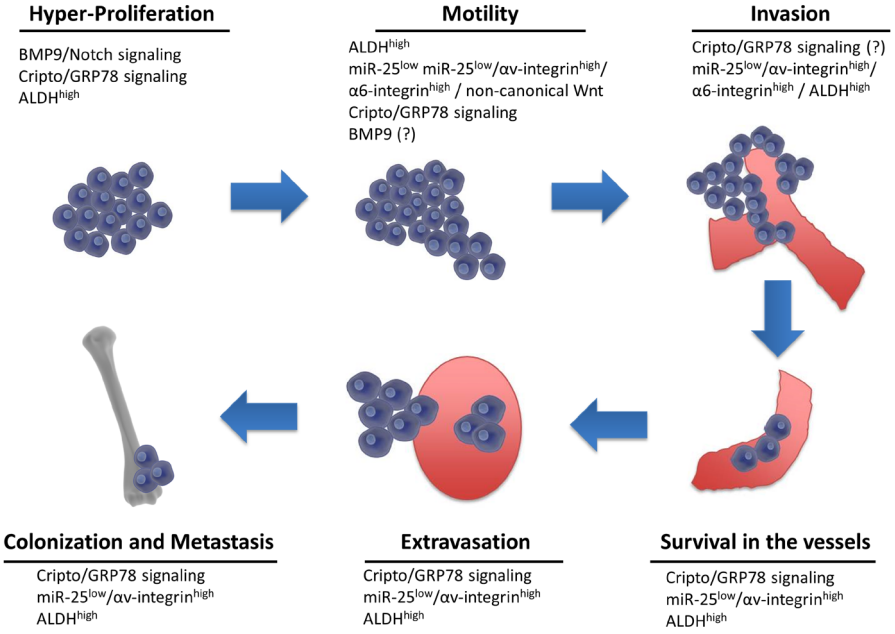

Figure 1. Schematic representation of the metastatic cascade. The involvement of miR-25, α_v, α_6 integrins, non-canonical Wnt signaling, ALDH, BMP9 and Cripto signaling pathways are highlighted in the different steps of the metastatic process.

Molecular characteristics of highly aggressive prostate cancer stem-like cells

Cellular heterogeneity is an important characteristic of many epithelial cancers, including prostate cancer. The major aim of this thesis was to identify the molecular properties of selected subpopulation of highly metastatic cancer stem/progenitor-like cells in human prostate cancer. In the first part of this thesis, we characterized the miR expression of two subpopulation of cells: the tumor- and metastasis-initiating $ALDH^{high}$ cancer stem/progenitor-like cells and the more differentiated, poorly tumorigenic/metastatic $ALDH^{low}$ cells (5). In the past 10 years, high aldehyde dehydrogenase activity has been progressively established as a maker to identify highly aggressive and metastatic prostate cancer stem cells (5-8) also in clinical studies (5,9). However, to the best of our knowledge, none of the previous studies have systematically investigated the molecular characteristics (e.g. miR expression) of $ALDH^{high}$ vs. $ALDH^{low}$ cells in human prostate cancer.

In **Chapter 3**, microRNA expression profiling of cultured $ALDH^{high}$ and $ALDH^{low}$ prostate cancer cells revealed a number of differentially expressed miRs (10). Our results are strengthened by clinical profiling data of a comparison of three subpopulations of transformed epithelial cells isolated from primary prostate tumors, namely: the stem-cell subpopulation, the $\alpha2\beta1^{hi}$ /$CD133^{-}$ transient-amplifying cells and the $\alpha2\beta1^{low}$ cells committed for terminal differentiation (11). Our study shows that miR-25 is low/absent in the $ALDH^{high}$ subpopulation isolated from prostate cancer cell lines and in the $\alpha2\beta1^{hi}$ /$CD133^{+}$ basal stem-cell subpopulation isolated from patients and steadily increases during differentiation to $\alpha2\beta1^{hi}$/$CD133^{-}$ transit amplifying cells and $\alpha2\beta1^{low}$ committed basal cells. miR-25 is part of the miR-106b-25 cluster (12). Consistent with our findings, the expression of the miR-106b-25 cluster appears to mediate neuronal differentiation of adult neural stem/progenitor cells and, interestingly, induction of miR-106b-25 in hypoxic conditions has been linked to increased expression of neuronal markers in prostate cancer cell lines (13,14). Moreover miR-25 has recently been identified in PC12 cells (15,16) as regulator of neuronal differentiation, supporting the involvement of this microRNA in differentiation processes (17).

The data of our study, highlight the limitations of molecular profiling approaches in cell cultures, heterogeneous cell lines and heterogeneous bulk clinical tissues. For example, it was found that the miR-106b-25 cluster was up-regulated in primary tumors and distant metastases from multiple solid cancers, including those of the human prostate (12,18-21). Importantly, none of this studies focus specifically on miR-25 expression but solely on the expression of the miR-106b-25 cluster. Additionally,

microRNAs within one cluster might be regulated differently by different transcription factors and miR-25 has been shown to be uncoupled from the MCM7 host gene (22,23). A likely explanation for these apparent contradictory observations is that cancer cell lines and bulk tumor tissues are not homogeneous and consist of a mixture of heterogeneous subpopulations of cells (24).

Therefore, we speculated that the increase in absolute expression levels of miR-25 in bulk tissues during prostate cancer progression may be indicative of an increase in the proportion of more differentiated, less invasive, "miR-25^{high}" more differentiated, "luminal" epithelial cells. This is reinforced by the fact that, forced miR-25 overexpression led to a decrease in α2-integrin and β1-integrin expression (**Chapter 3**), markers of epithelial basal stem cell (25). Our bioinformatic analysis revealed that αv-integrin and α6-integrin are target genes of miR-25. The identification of these genes confirmed the results of previous studies showing a significant higher expression αv-integrin and α6-integrin selectively in the ALDH^{high} subpopulation compared to ALDH^{low} in prostate cancer and in high-risk prostate cancer patients (26,27). Such studies also demonstrated that knockdown (26) or targeting of αv-integrin (28) significantly diminished the acquisition of a metastatic stem/progenitor cell phenotype and reduced the formation of prostate cancer bone metastasis in preclinical *in vivo* models. Consistent with these data, miR-25 overexpression significantly reduced the migratory potential of both bulk cell lines and selected ALDH^{high} subpopulation.

The induction of dramatic morphological changes after miR-25 overexpression prompted us to study the underlying mechanism(s) of these phenotypic alterations. Our analysis showed that overexpression of miR-25 dramatically impaired F-actin polymerization, thus reducing focal adhesion sites. Integrins provide a structural link between F-actin and the extracellular matrix and contribute to formation of these focal adhesion points (29). Additionally, integrins (αv-integrin in particular), are also involved in the activation of latent TGF-β which represents one of the major driver during EMT (30-32). As already discussed in **Chapter 3**, organization of F-actin is linked to activation of integrin-transmembrane receptors which regulates the activation of Rho-GTPases, RAC1 and CDC42 (33). Given the ability of miR-25 to target αv-integrin and α6-integrin it seems likely that regulation of these integrins by miR-25 has a major impact of the cellular phenotype. Interestingly, cells with a stellate, mesenchymal morphology like PC-3M-Pro4Luc2, often require activated RAC1 for migration (34). These observations are in line our findings that show reduced RAC1 mRNA upon forced miR-25 expression (10). Taken together, our functional and molecular profiling data highlight a pivotal role

of miR-25 as a non-coding RNA for the regulation of tumor aggressiveness by the regulation of cytoskeletal organization and motility.

In **Chapter 4** we describe a potential, other role for miR-25 in the modulation of the invasive program in human prostate cancer through modulation of canonical and non-canonical WNT signaling of which RAC1 is also a component (35,36). The WNT/PCP pathway is considered the β-catenin independent branch of WNT signaling. Beside the involvement of WNT signaling in the pathogenesis of prostate cancer and bone metastasis (reviewed in (37-41)), accumulating evidence revealed the role for non-canonical WNT/PCP signaling in prostate cancer progression, invasion and metastasis (36). Interestingly, canonical WNT signaling and non-canonical WNT/PCP signaling are part of a negative feedback-loop in which WNT/PCP negatively regulates canonical WNT signaling and *vice versa* (42). This led us to hypothesize that a possible differential basal level of canonical and non-canonical WNT signaling could maintain the mesenchymal and motile phenotype in PC-3M-Pro4Luc2 human prostate cancer cell line. Therefore, we speculated that the highly migratory phenotype in this cell line is due to a imbalance between canonical WNT and non-canonical WNT/PCP pathway. Indeed, in **Chapter 4** we describe that the non-Canonical WNT/PCP pathway is approximately 10-fold more active that the canonical counterpart in our model. Moreover, administration of TGF-β, a known inducer of EMT in prostate cancer, strongly increased non-canonical WNT/PCP signaling with a concomitant decrease in canonical WNT signaling. Using the Smad-3 dependent TGF-β reporter (CAGA-luciferase) we demonstrated that miR-25 can attenuate the activation of TGF-β signaling in human prostate cancer and is capable of blocking TGF-β-driven invasiveness. Overexpression of miR-25 also produced a significant increase in canonical WNT signaling, suggesting a modulation of the crosstalk between canonical and non-canonical WNT signaling pathway. Although additional experiments are warranted to confirm a specific and direct effect of miR-25 on non-canonical WNT/PCP signaling, we found that DACT1 knockdown recapitulated the induction of canonical WNT signaling on a bioluminescent reporter that we also detected upon miR-25 overexpression.

Taken together, the data described in this thesis support a key role of miR-25 in the regulation of motility invasiveness and epithelial differentiation in human prostate cancer. Furthermore, our data are in line with the literature concerning an intriguing contribution of non-canonical WNT signaling in prostate cancer progression and emphasize that targeting of this pathway might represent an interesting strategy to restrain EMT, invasion and metastasis.

In **Chapter 2**, we reviewed the established miR-gene interactions among TGF-β, Notch and Wnt signaling pathway and identified a miR signature that highlighted the crosstalk between these pathways. Beside the relevance of CREBBP and EP300 in EMT, which has already been addressed in **Chapter 2**, we wanted to test whether the list of genes identified could be linked to our findings about the role of miR-25 in aggressiveness of prostate cancer stem cells.
Interestingly, we found that CREB1 is identified as predicted target gene of miR-25 in two independent bioinformatics online available tools: TargetScan and microT-CDS. Although direct evidence is (still) lacking one can speculate that miR-25 may be involved in CREB1 downregulation and, as a result, would have a functional impact also on CREBBP (CREB-binding protein) and on the interaction with its signaling partner EP300.

The value of the signature identified in **Chapter 2**, is supported by multiple connections with pathways analyzed in other chapters of this thesis (e.g. Cripto and Notch signaling). In **Chapter 6** we have discussed the role of Cripto as emerging gene whose expression turns out to be involved in the formation of bone metastasis in prostate cancer. Interestingly, two miRs identified in our signature, (miR-15 and the miR-16) have been previously shown to directly interact with Cripto (43). Given the documented role of Cripto in EMT in prostate cancer (44), and its interaction with multiple TGF-β, Wnt and Notch signaling networks (45), this observation supports the involvement of the miRs signature during EMT. Moreover, in **Chapter 5** we show that the soluble chimeric protein ALK1Fc (ACE-041) (46) reduces BMP9 signaling and decreases proliferation of highly metastatic and tumor initiating human prostate cancer cells *in vitro* and *in vivo*. Interestingly miR-34a and miR-24, that were also identified in our miR signature, are shown to target BMP9 (GFD2) by TargetScan online predictive tool. Taken together, our observations emphasize the functional value of the miR signature and further strengthen the role of TGF-β family members and the Notch pathway in human prostate cancer.

As already discussed, EMT represents a crucial process that characterize the early phase of tumor invasion and generate the basis for the metastatic spread of the tumor. The role of CRIPTO during EMT in prostate cancer has already been described (44), however, to the best of our knowledge, the involvement of CRIPTO in the formation of bone metastasis by prostate cancer has not been reported.

Given the clinical problem of bone metastasis and the fact that Grp78 (i.e. Cripto signaling partner) has been associated with the development of castration resistance (47), in **Chapter 6** we tested whether we could register an involvement of Cripto in the onset of bone metastasis in prostate cancer.

Immunohistochemic analysis of clinical bone metastases collected shows that Cripto is strongly expressed and co-localize with cytokeratin-18 positive prostate epithelial cells. This support our hypothesis and suggest a functional involvement of Cripto in the formation of bone metastasis. Our *in vitro* experiments support the role of Cripto and Grp78 in the maintenance of aggressive characteristics in prostate cancer cell lines. The knock-down of Cripto and Grp78 induced a decrease in invasiveness and self-renewal properties in prostate cancer cell lines. Moreover, inoculation of Cripto and Grp78 knock-down cells in the circulation of zebrafish embryos via the duct of Cuvier (10,48), resulted in formation of significantly lower number of experimental metastasis compared to control cells. Finally, we demonstrated that Cripto knockdown significantly reduced the metastatic outgrowth in a preclinical mouse model of prostate cancer bone metastasis.

Our results suggest that Cripto and Grp78 might represent novel markers that could predict the formation of bone metastasis and be indicative of the initiation of invasiveness. This could therefore be of great value for the identification of new therapeutic targets.

miR-25 and Cripto in the landscape of new markers for prostate cancer monitoring and prediction

Although the progress in the molecular diagnostic research for prostate cancer in the last years, there is still a urgent need for the identification of novel additional predictive markers for prostate cancer monitoring and progression.
In this context, the AR has represented the major target for studies focused on prostate cancer treatment. Such studies have addressed the status of the AR and its modification in response to drugs (e.g. abiraterone and enzalutamide both resulted in increased expression of certain AR variants (49,50)). Given the fact that the distant relapse represents the lethal phase of the cancer progression, other approaches have focused on the identification of novel molecules involved in the interaction between the supportive stroma and the tumor cells (51). However, the identification of reliable, predictive markers for the castration resistant phase is still challenging.

In the landscape of the emerging molecular markers for CRPC, recent studies have highlighted the role of small non-coding RNA miR-1247-5p and of its target gene myc-binding protein 2 (MYCBP2) (52). Other recent work has revealed that the tri- and tetra-antennary N-glycan might be associated with the castration resistant status, therefore representing a potential predictive biomarker for castration-resistant prostate cancer (53). Moreover, the TMPRSS2-ERG fusion gene is currently in clinical testing for its

diagnostic and prognostic value, however ERG fusions have been reported to be positive or negative for clinical outcome (54). The data described in **Chapter 3** and **Chapter 6** of this thesis suggest that new approaches and new molecules respectively might contribute to the identification of new markers of interest in CRPC. In **Chapter 3**, we have identified miR-25 as novel microRNA downregulated in the stem-cell compartments isolated from CRPC patients (10) and our results presented in **Chapter 6** show that high expression of Cripto is associated with poor survival in prostate cancer and that Cripto is highly expressed in prostate cancer bone metastasis collected from CRPC patients.

Many studies have already successfully measured proteins and noncoding RNAs in blood or urine collected from prostate cancer patients (reviewed in (55)). However, the findings presented in this thesis highlight the difference of analyzing miRs and gene expression in bulk tissues compared to selected subpopulation of cells. The manipulation of selected targets in specific subpopulation of cells introduce additional layers of complexity linked to the development of targeting strategies that can selectively hit those highly metastatic cluster of cells dispersed within the tumor.

In other words, we prove here that miR-25 is crucial for prostate cancer cell migration and invasion, but we show that miR-25 is downregulated in aggressive prostate cancer subpopulation of cells which makes it a “negative marker”, thus difficult to apply in the clinical practice. However, our molecular studies could contribute to the identification of novel target genes, to be employed as therapeutic targets. This notion is supported by the fact that αv-integrin, that we prove here to be targeted by miR-25, has already been shown as interesting therapeutic target involved in the formation of bone metastasis in human prostate cancer (28).

We believe that the discovery of specific molecules, selectively expressed on highly malignant clones might help in the development of new targeting strategies, especially if those malignant clones and cells are spread and under-represented in the bulk tumor mass (only few aggressive cancer stem/progenitor-like cells are detected (11,56)). From this perspective, the membrane-bound nature of Cripto makes it an interesting target for the development of new molecules capable of targeting highly metastatic cells for diagnostic and therapy purposes. Additionally, this strategy could also be employed in the development of probes capable of revealing the localization of Cripto expressing cells during surgical intervention. Moreover, the soluble nature of Cripto, makes it an interesting molecule for the development of diagnostic and prognostic test to monitor the progression of prostate cancer in patients. Soluble Cripto could be detected in the blood collected from prostate cancer patients by ELISA kits

already available for research purposes. Interestingly, manipulation of Cripto signaling has already been shown to be successful in the modulation of the maintenance of mammary stem cells in breast cancer (57).

Clinical relevance, possible therapeutic opportunities and future perspectives

The study presented in **Chapter 5**, supports the role of BMP9 as a tumor-promoting factor in human prostate cancer cells *in vitro* and *in vivo,* acting on the Notch signaling pathway. To our knowledge, our study represents the first functional evidence for a role of BMP9 and the functional evidence of its targeting in human prostate cancer. Several approaches have been described for therapeutic targeting of the Notch signaling pathway in various diseases, but the majority of these clinical studies failed due to significant adverse effects (58,59). Interestingly, current options to interfere with Notch signaling originate from Alzheimer's disease research where γ-secretase inhibitors (GSI) are employed to prevent the accumulation of amyloid-β peptides (60). The γ-secretases enzymes contribute to the cleavage of the transmembrane portion of the Notch receptor and represent crucial players in the activation of the Notch signaling pathway. Unfortunately, animal and human safety trials revealed a significant toxicity involving gastrointestinal bleeding and immunosuppression following the administration of GSI applied to T-cell acute lymphoblastic leukemia (T-ALL) (58,59). Interestingly, promising results have been achieved in preclinical studies by combining GSIs with conventional chemotherapeutic agents (61) with minimal toxicity. In prostate cancer, administration of GSIs blocks tumor angiogenesis and enhances the docetaxel-mediated antitumor response, indicating a causal role of Notch signaling in mediating therapy resistance in human prostate cancer (61).

Our data in **Chapter 5** suggest that ALK1Fc might impact on cellular proliferation via an indirect effect on Notch signaling pathway. Therefore, this indicates that ALK1Fc might represent an interesting molecule to contain prostate tumor growth. Given the combinatorial effect of GSIs and current therapies, these results support the development of studies to investigate whether employment of ALK1Fc could contribute to sensitize prostate cancer cells to current treatment. Given the fact that ALK1Fc has recently been shown to be well tolerated by patients with advanced refractory cancer (62), showing promising antitumor activity, this might represent a promising and alternative strategy to circumvent the toxic side effects produced by GSIs. Additionally, ALK1Fc has been shown to reduce the vascular density in various solid tumors (63). Considering that angiogenesis is a crucial process coupled to osteogenesis (51,64) in osteoblastic bone metastasis (such those originated from prostate cancer), the testing

of ALK1Fc in preclinical bone metastatic models might be promising. Moreover, the recent experimental evidence that endothelial Notch activity promotes angiogenesis and osteogenesis in bone (65), reinforces the application of ALK1Fc in a metastatic setting (ALK1Fc interferes with Notch signaling see **Chapter 5**). However, a limitation of the animal models employed in the metastatic setting, is that osteoblast progenitors and hematopoietic stem cells (HSCs), responsible for the bone remodeling are tightly associated with "type H", $CD31^{high}$ vessels (64). These vessels are at their highest peak in young 4-week-old animals compared to old 11-week-old mice (64). Thus, a possible strategy to evaluate the efficacy of ALK1Fc in a metastatic setting in murine models, could combine the treatment with ALK1Fc together with the stimulation of the bone growth.

The results presented in **Chapter 6** suggest that Cripto and its signaling partner Grp78 could be employed as novel target genes to identify selectively metastatic prostate cancer cells. Interestingly, Grp78 has been shown to be involved in therapy resistance (66) and Grp78-targeted nanotherapy has already been tested in human prostate cancer (67). Additionally, the development of new molecules capable of targeting Cripto has already been shown to be effective in breast cancer (57). Moreover, the availability of monoclonal antibody specifically targeting Grp78 support the developing of strategies targeting the Cripto/grp78 pathway (68,69). These together support the development of preclinical studies to investigate the application and the relevance of such molecules in prostate cancer treatment.

The results in **Chapter 3**, support that the identification of new putative (up-regulated) miR-25 predicted target genes, could help in the identification of new factors involved in the maintenance of the aggressiveness in prostate cancer. Such research could then be exploited to identify novel small molecules capable to target these factors.

A direct translation of our direct findings would consist of an overexpression of miR-25 selectively in those highly migratory and invasive aggressive clones. Obviously this imply the application of selected targeting of specific cells which, up to date, is still under testing and development (2). Such targeting would require knowledge of the differences between normal and cancer stem cells. The latest developments in targeted therapy comprise the design of novel siRNA, miRNA, and antisense nucleotide therapy against CSCs. In this context, miR-25 could represent an interesting target for this type of new therapies and for nanotherapeutic approaches that have already investigated the application of such strategy to target both genes active in CSCs and the CSCs niche (2,70).

The targeting of CSCs might be achieved by four approaches: targeting component of the CSCs niche, targeting resistance mechanisms, inhibition of self-renewal signaling pathways and elimination therapy (2). The last one involve the eradication of CSCs based on specific characteristics of these cells for example the expression of specific molecules/antigens. In this context, the identification of new specific markers for these cells would be of great value and help.

REFERENCES

1. Maitland NJ, Collins A. A tumour stem cell hypothesis for the origins of prostate cancer. BJU Int 2005;96(9):1219-23.
2. Ismail F, Winkler DA. Getting to the source: selective drug targeting of cancer stem cells. ChemMedChem 2014;9(5):885-98.
3. Kreso A, Dick JE. Evolution of the cancer stem cell model. Cell Stem Cell 2014;14(3):275-91.
4. Zoni E, Kruithof-de Julio M, van der Pluijm G. miR-25, integrin and cancer invasiveness. Oncoscience 2015;2(8):663-4.
5. van den Hoogen C, van der Horst G, Cheung H, Buijs JT, Lippitt JM, Guzman-Ramirez N, et al. High aldehyde dehydrogenase activity identifies tumor-initiating and metastasis-initiating cells in human prostate cancer. Cancer Res 2010;70(12):5163-73.
6. Burger PE, Gupta R, Xiong X, Ontiveros CS, Salm SN, Moscatelli D, et al. High aldehyde dehydrogenase activity: a novel functional marker of murine prostate stem/progenitor cells. Stem Cells 2009;27(9):2220-8.
7. van den Hoogen C, van der Horst G, Cheung H, Buijs JT, Pelger RC, van der Pluijm G. The aldehyde dehydrogenase enzyme 7A1 is functionally involved in prostate cancer bone metastasis. Clin Exp Metastasis 2011;28(7):615-25.
8. Doherty RE, Haywood-Small SL, Sisley K, Cross NA. Aldehyde dehydrogenase activity selects for the holoclone phenotype in prostate cancer cells. Biochem Biophys Res Commun 2011;414(4):801-7.
9. Le Magnen C, Bubendorf L, Rentsch CA, Mengus C, Gsponer J, Zellweger T, et al. Characterization and clinical relevance of ALDHbright populations in prostate cancer. Clin Cancer Res 2013;19(19):5361-71.
10. Zoni E, van der Horst G, van de Merbel AF, Chen L, Rane JK, Pelger RC, et al. miR-25 Modulates Invasiveness and Dissemination of Human Prostate Cancer Cells via Regulation of alphav- and alpha6-Integrin Expression. Cancer Res 2015;75(11):2326-36.
11. Rane JK, Scaravilli M, Ylipaa A, Pellacani D, Mann VM, Simms MS, et al. MicroRNA expression profile of primary prostate cancer stem cells as a source of biomarkers and therapeutic targets. Eur Urol 2015;67(1):7-10.
12. Poliseno L, Salmena L, Riccardi L, Fornari A, Song MS, Hobbs RM, et al. Identification of the miR-106b~25 microRNA cluster as a proto-oncogenic PTEN-targeting intron that cooperates with its host gene MCM7 in transformation. Sci Signal 2010;3(117):ra29.
13. Liang H, Studach L, Hullinger RL, Xie J, Andrisani OM. Down-regulation of RE-1 silencing transcription factor (REST) in advanced prostate cancer by hypoxia-induced miR-106b~25. Exp Cell Res 2014;320(2):188-99.
14. Brett JO, Renault VM, Rafalski VA, Webb AE, Brunet A. The microRNA cluster miR-106b~25 regulates adult neural stem/progenitor cell proliferation and neuronal differentiation. Aging (Albany NY) 2011;3(2):108-24.
15. Westerink RH, Ewing AG. The PC12 cell as model for neurosecretion. Acta Physiol (Oxf) 2008;192(2):273-85.
16. Greene LA, Tischler AS. Establishment of a noradrenergic clonal line of rat adrenal pheochromocytoma cells which respond to nerve growth factor. Proc Natl Acad Sci U S A 1976;73(7):2424-8.
17. Yu Y, Lu X, Ding F. microRNA regulatory mechanism by which PLLA aligned nanofibers influence PC12 cell differentiation. J Neural Eng 2015;12(4):046010.
18. Hudson RS, Yi M, Esposito D, Glynn SA, Starks AM, Yang Y, et al. MicroRNA-106b-25 cluster expression is associated with early disease recurrence and targets caspase-7 and focal adhesion in human prostate cancer. Oncogene 2013;32(35):4139-47.

19. Ambs S, Prueitt RL, Yi M, Hudson RS, Howe TM, Petrocca F, et al. Genomic profiling of microRNA and messenger RNA reveals deregulated microRNA expression in prostate cancer. Cancer research 2008;68(15):6162-70.
20. Szczyrba J, Loprich E, Wach S, Jung V, Unteregger G, Barth S, et al. The microRNA profile of prostate carcinoma obtained by deep sequencing. Mol Cancer Res 2010;8(4):529-38.
21. Martens-Uzunova ES, Jalava SE, Dits NF, van Leenders GJ, Moller S, Trapman J, et al. Diagnostic and prognostic signatures from the small non-coding RNA transcriptome in prostate cancer. Oncogene 2012;31(8):978-91.
22. Song G, Wang L. Transcriptional mechanism for the paired miR-433 and miR-127 genes by nuclear receptors SHP and ERRgamma. Nucleic Acids Res 2008;36(18):5727-35.
23. Wu HL, Heneidi S, Chuang TY, Diamond MP, Layman LC, Azziz R, et al. The expression of the miR-25/93/106b family of micro-RNAs in the adipose tissue of women with polycystic ovary syndrome. J Clin Endocrinol Metab 2014;99(12):E2754-61.
24. Shackleton M, Quintana E, Fearon ER, Morrison SJ. Heterogeneity in cancer: cancer stem cells versus clonal evolution. Cell 2009;138(5):822-9.
25. Collins AT, Habib FK, Maitland NJ, Neal DE. Identification and isolation of human prostate epithelial stem cells based on alpha(2)beta(1)-integrin expression. J Cell Sci 2001;114(Pt 21):3865-72.
26. van den Hoogen C, van der Horst G, Cheung H, Buijs JT, Pelger RC, van der Pluijm G. Integrin alphav expression is required for the acquisition of a metastatic stem/progenitor cell phenotype in human prostate cancer. Am J Pathol 2011;179(5):2559-68.
27. Colombel M, Eaton CL, Hamdy F, Ricci E, van der Pluijm G, Cecchini M, et al. Increased expression of putative cancer stem cell markers in primary prostate cancer is associated with progression of bone metastases. Prostate 2012;72(7):713-20.
28. van der Horst G, van den Hoogen C, Buijs JT, Cheung H, Bloys H, Pelger RC, et al. Targeting of alpha(v)-integrins in stem/progenitor cells and supportive microenvironment impairs bone metastasis in human prostate cancer. Neoplasia 2011;13(6):516-25.
29. Cluzel C, Saltel F, Lussi J, Paulhe F, Imhof BA, Wehrle-Haller B. The mechanisms and dynamics of (alpha)v(beta)3 integrin clustering in living cells. J Cell Biol 2005;171(2):383-92.
30. Buijs JT, Henriquez NV, van Overveld PG, van der Horst G, ten Dijke P, van der Pluijm G. TGF-beta and BMP7 interactions in tumour progression and bone metastasis. Clin Exp Metastasis 2007;24(8):609-17.
31. Worthington JJ, Klementowicz JE, Travis MA. TGFbeta: a sleeping giant awoken by integrins. Trends Biochem Sci 2011;36(1):47-54.
32. Wipff PJ, Hinz B. Integrins and the activation of latent transforming growth factor beta1 - an intimate relationship. Eur J Cell Biol 2008;87(8-9):601-15.
33. Huveneers S, Danen EH. Adhesion signaling - crosstalk between integrins, Src and Rho. J Cell Sci 2009;122(Pt 8):1059-69.
34. Bid HK, Roberts RD, Manchanda PK, Houghton PJ. RAC1: an emerging therapeutic option for targeting cancer angiogenesis and metastasis. Mol Cancer Ther 2013;12(10):1925-34.
35. Fukukawa C, Nagayama S, Tsunoda T, Toguchida J, Nakamura Y, Katagiri T. Activation of the non-canonical Dvl-Rac1-JNK pathway by Frizzled homologue 10 in human synovial sarcoma. Oncogene 2009;28(8):1110-20.
36. Wang Y. Wnt/Planar cell polarity signaling: a new paradigm for cancer therapy. Mol Cancer Ther 2009;8(8):2103-9.
37. Kypta RM, Waxman J. Wnt/beta-catenin signalling in prostate cancer. Nat Rev Urol 2012;9(8):418-28.
38. Kharaishvili G, Simkova D, Makharoblidze E, Trtkova K, Kolar Z, Bouchal J. Wnt signaling in prostate development and carcinogenesis. Biomed Pap Med Fac Univ Palacky Olomouc Czech Repub 2011;155(1):11-8.

39. Verras M, Sun Z. Roles and regulation of Wnt signaling and beta-catenin in prostate cancer. Cancer Lett 2006;237(1):22-32.
40. Rucci N, Teti A. Osteomimicry: how tumor cells try to deceive the bone. Front Biosci (Schol Ed) 2010;2:907-15.
41. Hall CL, Kang S, MacDougald OA, Keller ET. Role of Wnts in prostate cancer bone metastases. J Cell Biochem 2006;97(4):661-72.
42. Veeman MT, Axelrod JD, Moon RT. A second canon. Functions and mechanisms of beta-catenin-independent Wnt signaling. Dev Cell 2003;5(3):367-77.
43. Chen F, Hou SK, Fan HJ, Liu YF. MiR-15a-16 represses Cripto and inhibits NSCLC cell progression. Mol Cell Biochem 2014;391(1-2):11-9.
44. Terry S, El-Sayed IY, Destouches D, Maille P, Nicolaiew N, Ploussard G, et al. CRIPTO overexpression promotes mesenchymal differentiation in prostate carcinoma cells through parallel regulation of AKT and FGFR activities. Oncotarget 2015;6(14):11994-2008.
45. Klauzinska M, Castro NP, Rangel MC, Spike BT, Gray PC, Bertolette D, et al. The multifaceted role of the embryonic gene Cripto-1 in cancer, stem cells and epithelial-mesenchymal transition. Semin Cancer Biol 2014;29:51-8.
46. Seehra J, Knopf J, Pearsall RS, Grinberg A, Kumar R. Antagonists of bmp9, bmp10, alk1 and other alk1 ligands, and uses thereof. Google Patents; 2009.
47. Pootrakul L, Datar RH, Shi SR, Cai J, Hawes D, Groshen SG, et al. Expression of stress response protein Grp78 is associated with the development of castration-resistant prostate cancer. Clin Cancer Res 2006;12(20 Pt 1):5987-93.
48. Ghotra VP, He S, van der Horst G, Nijhoff S, de Bont H, Lekkerkerker A, et al. SYK is a candidate kinase target for the treatment of advanced prostate cancer. Cancer Res 2015;75(1):230-40.
49. Sprenger CC, Plymate SR. The link between androgen receptor splice variants and castration-resistant prostate cancer. Horm Cancer 2014;5(4):207-17.
50. Antonarakis ES, Lu C, Wang H, Luber B, Nakazawa M, Roeser JC, et al. AR-V7 and resistance to enzalutamide and abiraterone in prostate cancer. N Engl J Med 2014;371(11):1028-38.
51. Ozdemir BC, Hensel J, Secondini C, Wetterwald A, Schwaninger R, Fleischmann A, et al. The molecular signature of the stroma response in prostate cancer-induced osteoblastic bone metastasis highlights expansion of hematopoietic and prostate epithelial stem cell niches. PLoS One 2014;9(12):e114530.
52. Scaravilli M, Porkka KP, Brofeldt A, Annala M, Tammela TL, Jenster GW, et al. MiR-1247-5p is overexpressed in castration resistant prostate cancer and targets MYCBP2. Prostate 2015;75(8):798-805.
53. Ishibashi Y, Tobisawa Y, Hatakeyama S, Ohashi T, Tanaka M, Narita S, et al. Serum tri- and tetra-antennary N-glycan is a potential predictive biomarker for castration-resistant prostate cancer. Prostate 2014;74(15):1521-9.
54. Shen MM, Abate-Shen C. Molecular genetics of prostate cancer: new prospects for old challenges. Genes Dev 2010;24(18):1967-2000.
55. Ronnau CG, Verhaegh GW, Luna-Velez MV, Schalken JA. Noncoding RNAs as novel biomarkers in prostate cancer. Biomed Res Int 2014;2014:591703.
56. Malanchi I, Santamaria-Martinez A, Susanto E, Peng H, Lehr HA, Delaloye JF, et al. Interactions between cancer stem cells and their niche govern metastatic colonization. Nature 2012;481(7379):85-9.
57. Spike BT, Kelber JA, Booker E, Kalathur M, Rodewald R, Lipianskaya J, et al. CRIPTO/GRP78 signaling maintains fetal and adult mammary stem cells ex vivo. Stem Cell Reports 2014;2(4):427-39.
58. Golde TE, Schneider LS, Koo EH. Anti-abeta therapeutics in Alzheimer's disease: the need for a paradigm shift. Neuron 2011;69(2):203-13.
59. Karran E, Mercken M, De Strooper B. The amyloid cascade hypothesis for Alzheimer's disease: an appraisal for the development of therapeutics. Nat Rev Drug Discov 2011;10(9):698-712.

60. Groth C, Fortini ME. Therapeutic approaches to modulating Notch signaling: current challenges and future prospects. Semin Cell Dev Biol 2012;23(4):465-72.
61. Cui D, Dai J, Keller JM, Mizokami A, Xia S, Keller ET. Notch Pathway Inhibition Using PF-03084014, a gamma-Secretase Inhibitor (GSI), Enhances the Antitumor Effect of Docetaxel in Prostate Cancer. Clin Cancer Res 2015;21(20):4619-29.
62. Bendell JC, Gordon MS, Hurwitz HI, Jones SF, Mendelson DS, Blobe GC, et al. Safety, pharmacokinetics, pharmacodynamics, and antitumor activity of dalantercept, an activin receptor-like kinase-1 ligand trap, in patients with advanced cancer. Clin Cancer Res 2014;20(2):480-9.
63. Hawinkels LJ, de Vinuesa AG, Paauwe M, Kruithof-de Julio M, Wiercinska E, Pardali E, et al. Activin Receptor-like Kinase 1 Ligand Trap Reduces Microvascular Density and Improves Chemotherapy Efficiency to Various Solid Tumors. Clin Cancer Res 2016;22(1):96-106.
64. Kusumbe AP, Ramasamy SK, Adams RH. Coupling of angiogenesis and osteogenesis by a specific vessel subtype in bone. Nature 2014;507(7492):323-8.
65. Ramasamy SK, Kusumbe AP, Wang L, Adams RH. Endothelial Notch activity promotes angiogenesis and osteogenesis in bone. Nature 2014;507(7492):376-80.
66. Zhang Y, Tseng CC, Tsai YL, Fu X, Schiff R, Lee AS. Cancer cells resistant to therapy promote cell surface relocalization of GRP78 which complexes with PI3K and enhances PI(3,4,5)P3 production. PLoS One 2013;8(11):e80071.
67. Delie F, Petignat P, Cohen M. GRP78-targeted nanotherapy against castrate-resistant prostate cancer cells expressing membrane GRP78. Target Oncol 2013;8(4):225-30.
68. Gray PC, Vale W. Cripto/GRP78 modulation of the TGF-beta pathway in development and oncogenesis. FEBS Lett 2012;586(14):1836-45.
69. Jakobsen CG, Rasmussen N, Laenkholm AV, Ditzel HJ. Phage display derived human monoclonal antibodies isolated by binding to the surface of live primary breast cancer cells recognize GRP78. Cancer Res 2007;67(19):9507-17.
70. Vinogradov S, Wei X. Cancer stem cells and drug resistance: the potential of nanomedicine. Nanomedicine (Lond) 2012;7(4):597-615.

8

SUMMARY

In the past decade it became increasingly clear that tumor heterogeneity represents one of the major problems for cancer treatment, also in prostate cancer. The identification of the molecular properties of these highly aggressive cells (Cancer Stem Cells, CSCs) dispersed within the tumor represents a challenge for the identification of new efficient therapies. In most of the cases, current treatments are indeed successful in eradicating the primary tumor. However, the clinical evidence of relapse and the occurrence of therapy resistance, suggest the presence of subpopulation of cells within the tumor, that can survive such treatments and can perpetuate the cancer.

In **Chapter 1** we provide an overview of the general properties of cancer, with particular attention at the tumor heterogeneity. In this chapter we discuss the problem of prostate cancer and uncover specific aspects of tumor initiation and progression. The current diagnostic strategies are discussed and current therapeutic options for both localized and advanced disease are also addressed. Additionally we provide an overview about the molecular properties of prostate cancer stem cells and discuss the molecular pathways involved in prostate cancer progression and bone metastasis formation, with particular focus on the role of microRNAs (miR).

In **Chapter 2** we investigated the reciprocal established miR/gene interactions among the Notch, Wnt and TGF-β signaling pathways. With this approach, we identified a validated miR signature that is common to these three key signaling pathways in prostate cancer progression and bone metastasis formation. Our analysis support the cross-talk between TGF-β, Wnt and Notch signaling and their regulatory role during the process of epithelial to mesenchymal transition (EMT).

In **Chapter 3**, miR-25 was identified as a key regulator of invasion and metastasis in human prostate cancer stem cells in vitro and in vivo. The expression of miR-25 steadily and consistently increases during epithelial differentiation in the human benign prostate hyperplasia (BPH) and prostate cancers. Forced miR-25 expression in the $ALDH^{high}$ subpopulation of highly tumorigenic and metastatic prostate cancer cells strongly reduced their invasive ability. Our research led to the identification of αv- and α6-integrins as direct target genes of miR-25. Furthermore, we found that forced miR-25 overexpression in osteotropic human prostate cancer cells attenuated extravasation and subsequent metastatic colonization in vivo.

In **Chapter 4** we provide a follow-up study about the role of miR-25 in the maintenance of aggressive behaviour of prostate cancer cells. The acquisition of an invasive phenotype is key to cancer progression and characterized by enhanced motility and migration. In prostate cancer, a mesenchymal and migratory phenotype is induced by TGF-β. We found that overexpression of miR-25 abolished the TGF-β-induced migration.

In addition, we identified DACT1 as a putative miR-25 target gene. DACT1 appears to modulate the reciprocal interaction of canonical and non-canonical WNT/PCP signaling that represents one of the key regulatory pathways involved in the acquisition and maintenance of a migratory phenotype.

As previously discussed, one of the key signaling pathways involved in prostate cancer is the Notch signaling network. Notch signaling is a developmental pathway that has been shown to be involved in both prostate cancer initiation and progression, as well as in bone metastasis formation.

In **Chapter 5** we found that BMP9 supports the growth of prostate cancer and induces indirectly Notch signaling pathway activity. BMP9 expression correlates with poor prognosis and BMP9 signaling can be inhibited by administration of soluble chimeric protein (ALK1Fc), which is capable of retarding tumor growth in an orthotopic prostate cancer model in vivo.

Together these findings suggest that ALK1Fc might represent an interesting molecule for prostate cancer treatment.

Finally, in **Chapter 6**, Cripto and Grp78 have been identified as novel proteins that are involved in the formation of prostate cancer bone metastases. Knockdown of Cripto and Grp78 in human prostate cancer cells reduced extravasation of these cells when inoculated into the circulation of zebrafish embryos. Moreover, Cripto knock-down diminished bone metastasis formation in a preclinical mouse xenograft model. In line with these observations elevated Cripto expression was detected in clinical bone metastasis samples isolated from Castration Resistant Prostate Cancer (CRPC) patients.

The results of this thesis are discussed in **Chapter 7**, where we evaluated and analysed the clinical relevance and the possible therapeutic opportunities of our findings. Collectively, the studies described in this thesis have increased our insights into the molecular properties of highly metastatic and tumorigenic $ALDH^{high}$ prostate cancer stem-like cells and provided new targets for possible diagnostic and therapeutic applications.

NEDERLANDSE SAMENVATTING

De laatste jaren is duidelijk geworden, dat tumor heterogeniteit één van de grootste problemen vormt bij de behandeling tegen kanker, waaronder ook prostaatkanker. De huidige behandelingen zijn meestal succesvol in het vernietigen van de primaire tumor, echter terugkeer van de tumor en therapie resistentie zijn veelvoorkomende problemen. Deze klinische resultaten duiden op de aanwezigheid van een subpopulatie van cellen die de behandeling kunnen overleven en de tumor in stand kunnen houden. Deze zeer agressieve kankercellen, ook wel kanker stamcellen genoemd, liggen verspreid over het tumorweefsel en bemoeilijken de ontwikkeling van nieuwe efficiënte therapieën.

Hoofdstuk 1 beschrijft de algemene kenmerken van prostaatkanker en het klinische probleem van de heterogeniteit. We bespreken de totstandkoming en progressie van de tumor en bespreken de huidige diagnostische strategieën en behandelopties voor prostaatkanker in een begin- en vergevorderd stadium. Bovendien wordt een overzicht gegeven van de moleculaire eigenschappen van prostaatkanker stamcellen. Daarnaast bespreken we de signaalroutes die betrokken zijn bij de progressie van prostaatkanker en uitzaaiingen (metastasen) naar het bot- en beenmerg, met daarbij specifieke aandacht voor microRNA's (miRs).

In **hoofdstuk 2** is de wisselwerking tussen miRs en genen van de Notch, Wnt and TGF-β signaalroutes onderzocht. Hierbij hebben we een gemeenschappelijk signatuur van miRs geïdentificeerd die de progressie en metastasering van prostaatkanker beïnvloeden. Onze resultaten ondersteunen eerdere waarnemingen dat diverse interacties voorkomen tussen TGF-β, Wnt en Notch en tonen aan de mIRs een regulatoire rol vervullen in het verkrijgen van agressieve eigenschappen door het proces van een epitheliale naar een mesenchymale transitie (EMT).

In **hoofdstuk 3** is miR-25 geïdentificeerd als een belangrijke regulator van de invasie en metastasering van humane prostaatkanker stamcellen *in vitro* en in *vivo*. De expressie van miR-25 stijgt gestaag en consequent gedurende de epitheliale differentiatie van zowel niet-getransformeerde menselijke prostaatcellen (benigne prostaat hyperplasie, BPH) als prostaatkanker. Geforceerde miR-25 expressie in de $ALDH^{high}$ subpopulatie van agressieve prostaatkanker cellen resulteerde in sterk verminderde invasie. Ons onderzoek heeft geleid tot de identificatie van αv- en α6-integrines als directe doelwit genen van miR-25. Bovendien hebben we ontdekt dat overexpressie van miR-25 door humane prostaatkanker cellen de uittreding uit bloedvaten (extravasatie) en opeenvolgende metastasering sterkt remt in een intact organisme.

In **hoofdstuk 4** hebben we de rol van miR-25 bij het in standhouden van het agressieve gedrag van prostaatkanker cellen verder onderzocht. Het verkrijgen van agressieve eigenschappen (invasief fenotype) is geassocieerd met mesenchymale en migratoire

karakteristieken en essentieel voor kanker progressie (uitzaaiing). Bij prostaatkanker kan dit proces (epitheliale-mesenchymale transitie of EMT) geïnduceerd worden door TGF-β. Onze bevindingen laten zien dat overexpressie van miR-25 de migratie, die geïnduceerd wordt door TGF-β, kan opheffen. Daarnaast hebben we vastgesteld dat DACT1 als doelwitgen fungeert van miR-25. DACT1 moduleert de wisselwerking tussen twee belangrijke manieren waarop wnt signalering plaatsvindt, t.w. “canonical” vs “non-canonical” wnt signalering, en speelt een belangrijke rol bij het verkrijgen van migratoire eigenschappen via “non-canocical” wnt signalering.
De Notch signaleringsroute is in hoge mate betrokken bij de initiatie, progressie en metastasering van prostaatkanker.
In **hoofdstuk 5** laten we zien, dat BMP9 de groei van prostaatkanker stimuleert en indirect de Notch signalering induceert. BMP9 expressie correleert met een slechte prognose en kan geremd worden door het oplosbaar chimeer eiwit ALK1Fc (bindt en vangt BMP9 weg) dat de tumorgroei kan vertragen in een orthotoop prostaatkanker model *in vivo*. Deze resultaten laten zien dat ALK1Fc een potentieel interessant molecuul is voor de behandeling van prostaatkanker.
In **hoofdstuk 6** wordt het onderzoek beschreven over de rol van de signaaltransductie eiwitten Cripto en Grp78 bij invasief gedrag en skeletmetastasering van prostaatkanker. Knockdown van Cripto en Grp78 in humane prostaakanker cellen remt de uittreding (extravasatie) van tumorcellen na inoculatie in de bloedcirculatie van zebravissen. Bovendien resulteerde Cripto knockdown in verminderde botmetastasering in een model van botmetastasering in vivo (muis xenograft model). Onze bevindingen worden verder ondersteund, omdat Cripto verhoogd tot expressie komt in botmetastasen bij patiënten met gevorderd, castratie resistent prostaatkanker (bestaande klinische mRNA gegevensbestanden).

De onderzoeksresultaten, de mogelijke klinische relevantie en therapeutische implicaties worden besproken in **hoofdstuk 7**. De onderzoeksresultaten, die beschreven zijn in dit proefschrift, hebben ons een beter inzicht gegeven in de moleculaire eigenschappen die ten grondslag liggen aan het agressieve gedrag van prostaatkanker stam/progenitor cellen en hebben bovendien geleid tot identificatie van potentiële nieuwe doelwitgenen voor diagnostische en therapeutische toepassingen.

LIST OF PUBLICATIONS

1. **Zoni E**., van der Pluijm G., The Role of microRNAs in Bone Metastases. Journal of Bone Oncology. *Provisionally Accepted*.

2. **Zoni E**., Melsen J., van de Merbel M., Pelger R. C. M., van der Pluijm G., miR-25 modulates the crosstalk between canonical and non-canonical Wnt signaling. *Manuscript in Preparation*.

3. **Zoni E**., Chen L., Granchi Z., Verhoef E.I., Pelger R.C.M., Snaar-Jagalska E., van Leenders G., Beimers L., Kloen P., Gray P.C., van der Pluijm P.C., Kruithof-de Julio M., CRIPTO and its signalling partner GRP78 drive the metastatic phenotype in human osteotropic prostate cancer. *Provisionally Accepted*.

4. **Zoni E.***, Karkampouna S.*****, Gray P., Goumans MJ., Hawinkels L., van der Pluijm G., ten Dijke P., Kruithof-de Julio M. ALK1Fc suppresses tumor growth by impairing angiogenesis and proliferation of human prostate cancer cells in vivo. ***** Equally contributed. *Submitted*.

5. **Zoni E**., Kruithof-de Julio M., van der Pluijm G., miR-25, integrin and cancer invasivenss. *Oncoscience. 2015 Aug 24;2(8):663-4. eCollection 2015.*

6. Sokolova V., Fiorino A., **Zoni E**., Reid JF., Pierotti MA., Gariboldi M., The effects of miR-20a on p21: two mechanisms blocking growth arrest in TGF-β responsive colon carcinoma. *J Cell Physiol. 2015 May 26. doi: 10.1002/jcp.25051.*

7. **Zoni E**., van der horst G., van de Merbel A.F., Chen L., Rane J., Pelger R.C.M., Visakorpi T., Maitland N., Snaar-Jagalska B.E., van der Pluijm G., miR-25 modulates invasiveness and dissemination of human prostate cancer cells via regulation of αv- and α6-integrin expression. *Cancer Research. 2015 Apr 9 doi: 10.1158/0008-5472.CAN-14-2155.*

8. **Zoni E.**, van der Pluijm G., Gray P.C., Kruithof-de Julio M., "Epithelial Plasticity in Cancer: Unmasking a MicroRNA Network for TGF-β-, Notch-, and Wnt-Mediated EMT," *Journal of Oncology, doi: 10.1155/2015/198967.*

9. Reid JF., Sokolova V., **Zoni E.**, Lampis A., Pizzamiglio S., Bertan C., Zanutto S., Perrone F., Camerini T., Gallino G., Verderio P., Leo E., Pilotti S., Gariboldi M., Pierotti MA., miRNA Profiling in Colorectal Cancer Highlights miR-1 Involvement in MET-Dependent Proliferation. *Mol Cancer Res. 2012 Apr;10(4):504-15.*

CURRICULUM VITAE

Eugenio Zoni was born on 14 May, 1986 in Monza, Italy. In 2005 he obtained the high school diploma (Classical Studies) at Liceo Classico Statale B. Zucchi in Monza, Italy. In the same year he started to study Biotechnology at the University of Milan-Bicocca, Milan, Italy where he obtained a Bachelor diploma in 2009 with a dissertation prepared at the Laboratory of Cellular and Molecular Immunology headed by Dr. Francesca Granucci. After his Bachelor diploma, Eugenio started an internship at the Cancer Genomic Group at the FIRC Institute of Molecular Oncology Foundation (IFOM), Milan, Italy where he worked with Dr. Elisabetta Crippa in Dr. Manuela Gariboldi's group on a project focused on the role of microRNA in Breast Cancer. During 2009-2011 Eugenio followed the MSc program of Medical Biotechnology at the University of Milan-Bicocca, Milan, Italy. In 2011 he obtained his Master diploma Cum Laude, with a thesis focused on the analysis of miRNA/gene interactions in the TGF-β pathway in Colorectal Cancer. This experimental work was prepared under the supervision of Dr. Viktorija Sokolova and Prof. Dr. Roberto Perego in Manuela Gariboldi's group at IFOM, Milan, Italy.
In January 2012 Eugenio started his PhD studies at the Urology Research Group headed by Dr. Gabri van der Pluijm at the Department of Urology in Leiden University Medical Center, Leiden, The Netherlands. During his PhD studies, Eugenio took part of the BONE-NET Marie Curie FP7 PhD Program and was awarded with a Travel Award from the European Association for Urological Research in 2012; an ISEH travel grant and an IBMS travel grant from the International Bone and Mineral Society in 2012 and 2013 respectively; and an ENA travel grant and Oral Presentation Award at the 2nd International Symposium ACTC in Crete, Greece in 2014. The work presented in this thesis is the result of the research that Eugenio has conducted from January 2012 to December 2015 at the Urology Research Group, where he is currently appointed.

ACKNOWLEDGEMENTS

The work presented in this thesis would have not been possible without the contribution, the help and the support of many people. These are the elements that make the difference, and even if you don't always see them or they act "behind the scenes", they kept me going and carrying on during these four years. I first want to thank all the people working in J3 and in particular my promotor, Prof. Pelger. Dear **Rob**, thank you for your support and for discussion and chat, also about non-scientific books which in the end I bought and I am reading! Second, I want to thank my co-promotor, Dr. van der Pluijm. Beste **Gabri**, thank you for the possibility you gave me to be in the Netherlands and to be part of your group. Thank you for your time, for your help (not only scientific), for your always positive attitude and for your support. **Marianna**, I don't know whether I should place you in the Molecular Cell Biology lab, in the Urology lab or in your new lab in Bern; what I know is that, despite the location, you have been a constant presence during these years and without your help it would have been much more difficult.
A special thanks goes to all the members of the Urology Research Lab. **Jan**, we started our PhD together and you have been a transparent, honest and always correct mate. I wish you all the best for your life and for your career and hope that we will keep in touch! **Jeroen**, you have also been far from home for a bit of time in your life and you probably know that being abroad can be "fancy" but can be also difficult. Thank you for your help at the beginning and for bringing me to IKEA! **Federico**, you arrived in the Netherlands almost at the end of my PhD and brought a "rainbow" (in any sense) in our windowless office! **Sofia**, we met during the animal course and then we started to work together; thanks for standing me, especially in critical moments and for sharing the good, the bad and the ugly times that we encountered during these years. **Maaike**, thank you for your help with the mice and for talking about life and "Flipje". Thanks also to **Henry**, **Kasia** and **Geertje**.
A separate thanks goes to my two students. I can say that I learned a lot from both of you and hope that I managed to transmit to you something: **Marjan**, you have been my first student and I am happy that now you are part of the group; **Janine**, thank you for your great help on different projects and for translating my Dutch summary!

I want also to thank the collaborators and colleagues from different institutions and departments: **Lanpeng** thank you for all your efforts, for your time and great help and for being enthusiast every time for new ideas, I wish you all the best for your PhD and career. **Zoraide**, thanks for the help with the "Fluidigm" and for discussion about science and not only science! I would like to thank the members of my thesis committee

and also Dr. **Ewa Snaar-Jagalska**, Prof. **Norman Maitland**, Dr. **Jayant Rane**, **Esther** and Dr. **Arno van Leenders**, Prof. **Guido Jenster**, Dr. **Marco Cecchini**, Dr. **Peter Kloen**, Dr. **Andre van Wijen** and Dr. **Gerald Verhaegh** for your help and always constructive discussions. A separate thanks goes to Dr. **Peter Gray**: thank you Peter for bringing always an important contribution and great ideas to our work from far away.
Thanks also to all the members of the BONE-NET consortium and the ENDO-, the CARDIO- and the RADI-lab for the help and the time we had together, in particular to: **Sander**, **Monique**, **Leonard**, **Mieke**, **Edwin**, **Andrea**, **Rosa**, **Eline**, **Patrick**, **Onno**, **Isabel**, **Geerte**, **Lisa** and **Lisa**, **Trea**, **Jimmy**, **Padmini, Twan**, **Iolanda**, **Luana**, **Laura**, **Lancy** and **Ivo**, I wish you all the best.
A special thanks goes to **Hetty** and **Chris**: you have always been there, ready to help and to spend time to guide me through the labyrinth of the D4-lab. I would like also to say thanks to **Guido** and **Sabrina** from the flow-cytometry facility, for your help and discussion about life and motorcycles during the long waiting for the sorting.
Then, despite the geographical distance, in these four years I learned that there are people who I can count on and who kept on supporting me, even from far away: **Gully**, **Lollo**, **Ari**&**Jack**, **Elisa**, **Geko**, **Juri**&**Laura**, **Laura Mora**, **Drea** and **Gabri** (also from far away). Thank you for visiting me in Leiden, for being there and for our Skype sessions!

Finally, I want to say thanks to my family and my parents **Elisabetta** and **Ulisse**; this thesis is for you. Thank you for everything you did for me since year 0. Thank you for giving me the possibility to study and for “letting me go”, far away, four years ago. **Edo** and **Ila**, thank you for being always there when I need you.

Monika, you are the simplest person I know and I learned with you that life is easy, but we, somehow, make it very complicated. However, as you always tell me, if we make a list, then it will be easy to do all the things! “Terima Kasih” for making me strong and for being with me.